T-3307

THE PHASE BEHAVIOR OF THE BINARY SYSTEMS OF M-CRESOL, QUINOLINE, AND TETRALIN AT TEMPERATURES UP TO 600 K.

by

Vicki Gene Niesen

A thesis submitted to the Faculty and the Board of Trustees of the Colorado School of Mines in partial fulfillment of the requirements for the degree of Doctor of Philosophy (Chemical and Petroleum-Refining Engineering).

Golden, Colorado

Date 10/5/86

Signed: [signature]

Vicki Gene Niesen

Approved: [signature]

Victor F. Yesavage,
Thesis Advisor

Golden, Colorado

Date 10/6/86

[signature]

Arthur J. Kidnay,
Professor and Head
Chemical Engineering
and Petroleum Refining

ABSTRACT

An experimental method was developed and evaluated for obtaining phase behavior data at temperatures up to 350°C and at pressures up to 10 MPa. In addition, unique binary vapor-liquid equilibria were generated for the binary systems of m-cresol, quinoline, and tetralin at 250, 275, 300, and 325°C. These compounds are of interest because they are highly non-ideal and are also accepted models for coal liquids. A low boiling azeotrope was observed for the m-cresol/tetralin system that moved toward higher m-cresol concentrations and eventually disappeared as the temperature increased. The m-cresol /quinoline data indicated a high boiling azeotrope at very low m-cresol concentrations that disappeared at higher temperatures. No azeotrope was present in the tetralin /quinoline system. Due to hydrogen bonding, both m-cresol and quinoline are quite hygroscopic. Water was found to be the major impurity and had very large effects on the vapor pressures even at extremely low concentrations.

The data obtained were used to evaluate recently proposed models including two equations of state and five mixing rules. The equations of state were the Soave-Redlich-Kwong and a recent modification which extended it to polar compounds. The mixing rules ranged from a simple

interaction parameter to more complex rules involving temperature and volume dependencies. A sophisticated statistical program based on the maximum likelihood method was developed to determine interaction parameters for the models. The maximum likelihood method was modified to allow the use of implicit constraints which greatly facilitates phase behavior modeling.

While the modified Soave-Redlich-Kwong equation of state modeled the vapor pressures of the polar compounds better over wide temperature regions, the Soave-Redlich-Kwong equation of state performed better in the temperature region where the data from this investigation were located. For these systems, at temperatures between 250 and 325°C, temperature or volume functional dependencies were found not to significantly affect the performance of the mixing rule. The major contributing factor to the modeling capabilities of a mixing rule was found to be the addition of a third fitting parameter. A mixing rule with three parameters was capable of not only modeling the experimental data but also attempted to correct for poor vapor pressure predictions by the equation of state. The three parameter mixing rule was shown not to predict phase behavior as well as a simple interaction parameter when extrapolated to lower temperatures and compared to experimental data. The simple interaction model performed well qualitatively; however, poor vapor pressure predictions by the equation of state prevented more quantitative results. Further equation of state developments are needed to provide better pure fluid vapor pressure predictions for polar compounds.

TABLE OF CONTENTS

TABLE OF CONTENTS (cont.)

LIST OF TABLES

LIST OF TABLES (cont.)

LIST OF FIGURES

LIST OF FIGURES (cont.)

ACKNOWLEDGEMENTS

The author gratefully acknowledges the financial support of the United States Department of Energy, Office of Fossil Energy through Grant #DE-FG22-80PC30230 and Grant No. DE-FG22-84PC70006. In addition, the author wishes to thank her advisor for the guidance and encouragement.

INTRODUCTION

The primary goal of this research was to advance the understanding of phase behavior of non-ideal fluids at elevated temperatures and pressures. This area of thermodynamic research is particularly important due to its wide industrial applications. Phase behavior data are required for any process where a phase change occurs, for example in distillation columns or flash tanks. Development of new processes such as synfuel processing or high temperature/pressure distillation are restricted by the lack of knowledge of thermodynamic properties including phase behavior. The economic feasibility of a process is often dependent upon optimal designs which are in turn dependent upon correlations that can accurately predict thermodynamic properties. These correlations must be developed and tested over a wide range of conditions and compounds. Currently there is a severe lack of phase behavior data at elevated conditions (Gmehling et al. (1982)), which has greatly hindered the development of satisfactory models. In addition, the phase behavior of non-ideal compounds is not well known at any conditions. The areas of research of most importance in this field are best stated by Prausnitz (1986), "To increase our knowledge, we require on the one hand new results from theoretical molecular physics and on the other, more accurate experimental data for equilibrium properties of dense mixtures, especially for those containing one or more polar components."

To help meet the needs of phase behavior research, an experimental program was developed to generate phase behavior data at elevated conditions. A flow vapor-liquid equilibrium (VLE) apparatus was redesigned to generate high quality phase behavior data at temperatures up to 350°C and pressures up to 10 MPa. A flow system requires stable operation for relatively long periods of time to ensure constant compositions throughout the system. The equipment was modified to allow operation at equilibrium for up to thirty minutes. The major improvements were in temperature control, phase boundary control and the development of operating and safety procedures.

This experimental program was not limited to the development of a single VLE experimental apparatus. The production of high quality data is equally dependent upon the sample quality as well as an accurate analysis of the VLE samples produced. Consequently, techniques had to be developed for purifying samples, monitoring and maintaining sample purity during physical measurements as well as the analysis of the vapor and liquid samples by gas chromatography. The importance and difficulty of these procedures cannot be overstated.

The experimental program was evaluated by comparison of binary VLE data with literature data. VLE data were obtained for the methanol/ethanol system at two isotherms, 100 and 140°C and compared to data published by Butcher et al. (1966). The two data sets compared well at 100°C but discrepancies were found at 140°C. It was discovered that Butcher's data were inconsistent with published vapor pressure measurements at 140°C; therefore, it was felt that the data from this investigation more accurately represented the phase behavior at 140°C.

Once the experimental program had been developed and evaluated against literature data, unique VLE data were generated for the binary systems of m-cresol, quinoline, and tetralin (1,2,3,4 tetrahydronaphthalene) at four isotherms, 250, 275, 300, and 325°C. The compounds studied are of significant interest because they are highly non-ideal and are also accepted models for coal liquids. Therefore the data generated in this thesis can be used not only for basic thermodynamic research but also will provide needed information for more practical applications.

Since the type of VLE data generated in this investigation is extremely rare, the next logical step was to evaluate some current models using the data. Two equations of state (EOS) were chosen, the Soave-Redlich-Kwong (SRK) as a base case and a recently proposed modification to the SRK that attempts to extend the SRK to more polar compounds, Yesavage (1986). The mixing rules chosen were some of the most recently proposed methods for predicting strong interactions between unlike molecules. Five mixing rules were studied in this research ranging from a simple interaction parameter to newly proposed density dependent mixing rules, Luedecke et al. (1985) and Holder et al. (1986).

To determine the interaction parameters in the mixing rules, a sophisticated statistical program was written. The maximum likelihood algorithm as described by Anderson et al. (1978) was extended to permit the use of implicit constraints. This method performs a true statistical fit of the data by using all of the experimental data including estimates of the experimental errors. In addition, it provides useful information for statistically comparing models.

To achieve the primary goal of this research an experimental program was developed for measuring VLE behavior at elevated conditions; unique binary VLE data were generated; and recently proposed methods for modeling highly non-ideal systems were tested using the VLE data.

SCOPE OF EXPERIMENTAL PROGRAM

The main emphasis of this research was to develop an experimental method capable of producing accurate phase behavior data at elevated temperatures and pressures on a routine basis. This experimental method is multifaceted and equally dependent upon each part of the program to obtain accurate phase behavior data. The experimental program consists of three areas.

1. Physical Measurements
2. Analytical Techniques
3. Sample Purification

The experimental VLE measurements were generated on an equilibrium flash vaporization flow system. This equipment had been previously built, Niesen (1981); however, the equipment had only been developed to the stage where it was capable of measuring vapor pressures of pure components. The equipment could not be operated at the conditions required for VLE measurements. A limited amount of VLE data on the ethanol/water system was taken on the equipment before this research began. These data were taken with great difficulty by Palavra (see Niesen et al. (1986)) and required a significant amount of time.

A significant portion of this thesis research was devoted to extending the VLE apparatus to operate stably over reasonably long periods of time. The operation of a flow system is much more difficult than a batch or recirculation scheme. The main difference is that the flow system must run at both steady state and equilibrium conditions for relatively long periods of time to ensure that the vapor and liquid compositions are not changing. This requires good temperature and flow rate control, both of which were totally lacking in the original design. However, a flow system has certain advantages such as large sample sizes and lower concentrations of decomposition products. In addition, this equipment operates at relatively high temperatures and pressures which can lead to a number of possible safety hazards. The operation of the equipment required a thorough understanding of the physical processes to eliminate any unsafe operating conditions.

The final design of the equipment is capable of maintaining equilibrium conditions for a period of up to 30 minutes. In this time period, the entire contents of the system can be replaced five to six times. Specifically, the temperature can be maintained within +/- 0.1 K at a flow rate of 100 mls/min and two phases can be maintained inside the equilibrium cell. The final operating procedure for binary VLE measurements was used successfully for over a year without any hazardous situations.

The development of the analytical methods required as much time as the development of the VLE apparatus and at times proved to be the primary roadblock in the research program. An Hewlett-Packard model 5710A gas chromatograph was used to analyze the VLE samples. Previously, this equipment was used for simulated distillations. This was the first time that it was used for quantitative analyses.

Numerous problems were encountered in developing procedures for the gas chromatograph that would attain the desired accuracy of +/- 0.001 mole fraction. The two major problems were nonreproducibility and nonlinearity of the relative responses of the different compounds. These problems were partly overcome by a tedious method requiring that all samples be bracketed by two known standards. The remaining difficulty was that the GC was not reproducible from one run to the next. Since many aspects of the GC could cause this problem, it was extremely difficult to pinpoint the source. In fact, it was found that several factors contributed to the problem. Variables, such as gas flow rates, sample concentration, and sample size contributed to the nonreproducibility. It was learned that the results of an analysis are totally dependent upon the skill and knowledge of the operator. Without accurate and reproducible analytical techniques, the entire research project was inoperative.

The need for sample purity may appear to be obvious; yet there are many examples in the literature where the physical measurements may have been quite good, but the fluids studied were of inferior quality. Consequently, the data obtained are not accurate and of only limited use. One good example of this problem is discussed in the section titled "Sample Purification" in this thesis. Precise vapor pressure measurements were obtained on impure m-cresol which resulted in erroneous values, Nasir and Kobayashi (1980).

The initial purity is not the only concern, many compounds (such as methanol or tetralin) may decompose at high temperatures and pressures. Also, hygroscopic compounds may absorb water from the atmosphere. Consequently, the samples must be carefully monitored while the physical measurements are being made. An understanding of the chemistry of the compounds being studied is quite necessary to alert the experimentalist of possible problems. Procedures were established to provide the highest purity samples possible ($> 99.9\%$) and the samples were monitored to ensure sample integrity during the physical measurements. The importance of this phase of the program cannot be overemphasized.

PHYSICAL MEASUREMENTS

Before describing the redesign of the existing equipment, it is best if the overall final flow system is presented first. This will allow the reader to follow the subsequent discussion more fully. A complete literature survey for the VLE equipment is presented by Niesen (1981).

Description of the Vapor Liquid Equilibria Apparatus

An equilibrium flash vaporization flow system has been developed which can generate vapor-liquid equilibrium data at temperatures up to 350°C and pressures up to 10 MPa. The system was designed to study the phase behavior of coal derived liquids and model compound mixtures, at conditions similar to the extreme conditions at which coal liquids are produced and processed.

An equilibrium flash vaporization flow system was chosen since substantial quantities of the vapor and liquid streams may be required for characterization (for example, distillation cuts for coal liquids). In addition, it has been found that the flow system has other advantages. When working with a compound that decomposes, such as methanol, the decomposition products do not accumulate as in a batch system but are flushed from the cell and kept at a low level. The flow system also allows the sample to be degassed as it heats up since any noncondensable gas will exit in the vapor stream, accumulate in the vapor condenser, and not be recirculated.

The overall flow diagram for the equilibrium flash vaporization flow apparatus is presented in Figure 1. The flow system was designed for use with corrosive, relatively unstable compounds (such as coal liquids) and for running with the relatively small samples (one liter). For virtually all of the system, 0.635 cm o.d. 316 SS tubing was used. The possibility of two-phase flow developing in the sample line required a constant downward movement of the stream once the heating process began, to prevent trapping of the liquid in a low spot of the system.

The sample is pumped from the surge tank to a preheater using a diaphragm metering pump. To minimize sample decomposition, the test fluid is preheated gradually using a 6 m preheater coil in a fluidized bed sand bath. The preheated fluid then flows downward past an in-line bayonet heater used for adjustment of the temperature. The sample fluid then flows through a final heat exchanger coil and into an equilibrium cell, both of which are located in an air bath with temperature regulation within +/- 0.1°C.

Inside the equilibrium cell, the vapor and liquid separate. The vapor is removed from the top of the cell and

FIGURE 1

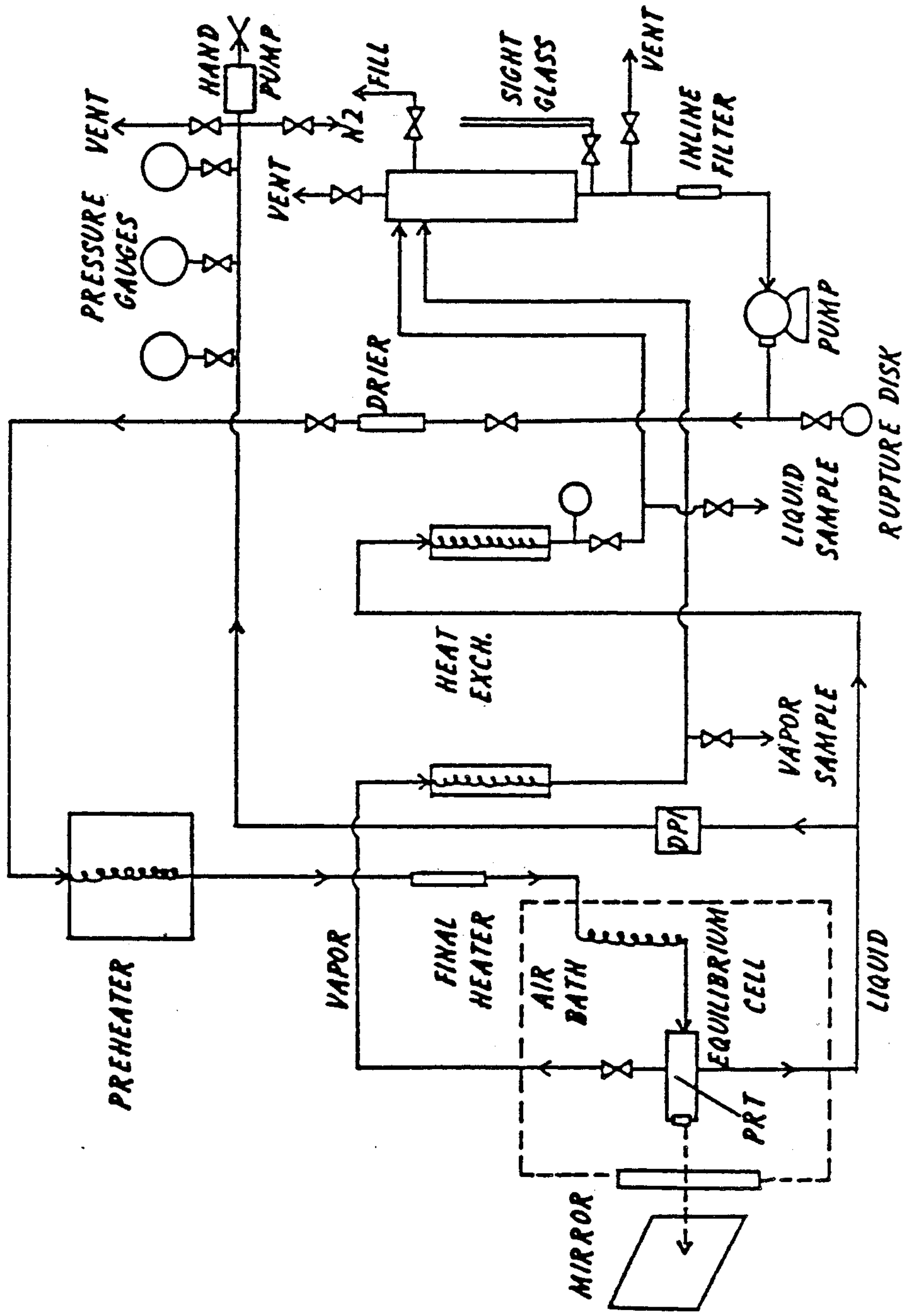

VAPOR LIQUID EQUILIBRIA APPARATUS

the liquid from the bottom. The vapor passes through a micrometering valve which sets the vapor flow rate and reduces the pressure of the gas stream to atmospheric; the gas is then cooled and condensed in an heat exchanger. The liquid is held under pressure as it passes through a heat exchanger to prevent flash vaporization. The liquid is then reduced to atmospheric pressure through a micrometering valve which regulates the system pressure. The liquid and condensed gas streams are sampled before the two streams are returned to the surge tank.

A windowed equilibrium cell is required for visual liquid level control since most corrosive liquids will affect other liquid level control devices. Originally the cell was a windowed, stainless steel Jerguson gage. The window was made of borosilicate glass with an asbestos gasket on each side of the glass. This performed adequately for nontoxic mixtures, but some leakage occurred around the window. Efforts to seal the original cell over the large temperature cycles required proved ineffective. Thus, a new cell was designed and constructed which would maintain the seal between the cell and the sight glass over many temperature cycles. This cell resembles a design by Lin et al. (1985).

Figure 2 is a drawing of the new cell, showing the

FIGURE 2

EQUILIBRIUM CELL

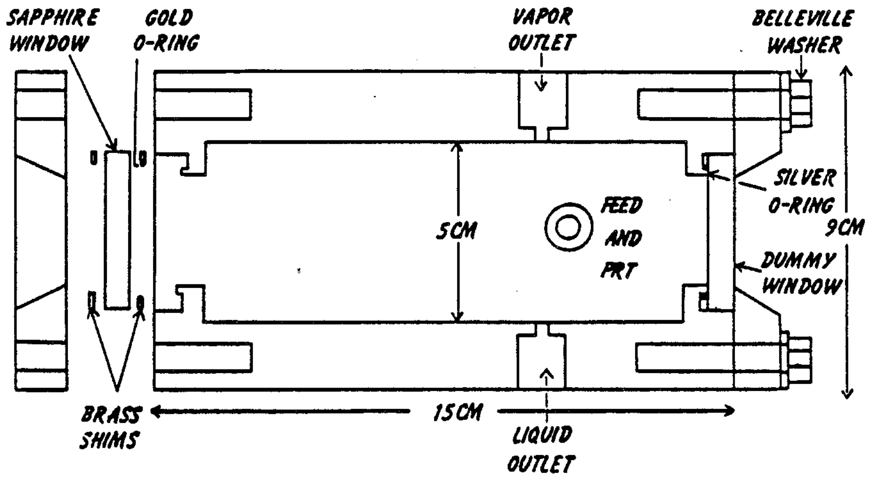

location of the major components. The cell body, end-caps, and 0.952 cm bolts are made of 316 stainless steel. The view port is a 4.445 cm diameter by 0.635 cm thick sapphire window. A 0.101 cm diameter, 24 K gold o-ring seals the sapphire window. The gold flows under pressure from the bolts to form a tight seal. The opposite end of the cell has a dummy window which is made of 316 stainless steel, the side facing into the cell has been polished to a shiny matte surface. A 99.9% silver o-ring seals the dummy window. Brass backup shims are used to hold the o-rings in place and to evenly distribute the sealing force around the outer edge of the windows. Belleville washers are used to counteract thermal expansion effects. The new design was quite successful and seals up to 10 MPa.

Temperature measurements consist of an in-line Omega 100 ohm platinum resistance thermometer, initially located at the feed entrance to the cell. The PRT has recently been moved inside the equilibrium cell for more precise temperature measurements. The PRT has four leads to eliminate the resistance of the leads and is encased in a 316 SS sheath to allow it to be placed in the process line. The platinum resistance thermometer was calibrated, over the temperature range of interest, against a calibrated Leeds and Northrup model 8163-B platinum resistance thermometer.

The resistance is measured with a Keithley 5 1/2 digit multimeter. The calibration of the digital multimeter is periodically checked against Leeds and Northrup standard resistors over the range of interest.

The pressure measuring system consists of a Ruska differential pressure indicator (DPI), null indicator, and a series of Heise bourdon tube gauges. Once the liquid has left the air bath, a static line is taken off which runs to the lower chamber of the DPI cell. The upper chamber of the DPI cell is in communication with the Heise gauges. Gas pressure is applied to the upper chamber of the DPI cell until the liquid and gas pressures are equalized. The gas pressure is then read on the pressure gauges which is equal to the system pressure. The advantages of this arrangement are that the process fluid does not enter the Heise gauges which eliminates corrosion and cleaning; the process fluid may exceed the maximum temperature for which the Heise gauges are compensated; and a long static line would be required if the process fluid ran directly to the gauges. This last advantage prevents compositional changes in the flowing liquid line.

Precise temperature control is vital in the operation of the equipment. An Omega Model D921 controller with a solid state relay controls the fluidized sand bath, and a

Bayley Model 124 controller controls the bayonet heater. These controllers allow temperature control of the equipment to within +/- 0.1°C.

Redesign of the Vapor Liquid Equilibria Equipment

It is important to understand that for VLE measurements it is inherently more difficult to operate a flow system in contrast to a static system. The equilibrium state required for the measurements must be achieved and maintained in a dynamic system in contrast to a more stable batch system. For example, the temperature of a bath is much easier to control than the temperature of a fluid flowing at 100 mls/min. Consequently, system control, particularly temperature control, was the major equipment flaw needing to be solved.

For a binary system there are two degrees of freedom. Additionally, there is the obvious requirement that two phases be maintained at all times. For this equipment, the temperature and vapor/liquid split are controlled requiring the pressure to be fixed. The vapor/liquid split is controlled by setting the flow rates of the two phases.

Initially, it was decided that for precise measurements the equilibrium state would have to be maintained for a period of approximately 30 minutes. This time length was based on a flow rate on the order of 100 mls/min. and a system volume of approximately 500-750 mls. In this length of time, the entire system would be completely recycled 5-6 times. This time period would allow the vapor and liquid line to be flushed so that the compositions would be constant. In fact, tests were made to show that the 30 minutes was indeed more than an adequate time period.

Once a time length was calculated that would ensure equilibrium conditions throughout the entire system, the problem was to design the control systems needed. Specifically the goals were to control temperature to within +/- 0.1 K and to maintain a constant phase boundary level in the equilibrium cell.

As stated previously, it is very difficult to control the temperature of a fluid flowing at 100 mls/min. through a 1/4" (0.634 cm) tube to within +/- 0.1 K. The initial design had only the bare minimum for control devices because it was erroneously believed that a system in the two phase region would be more stable than a single phase. The first improvement was the addition of an Omega Model D921 temperature controller with a solid state relay to regulate the fluidized sand bath. This increased the level of control from +/- 2 K to almost +/- 0.1 K; however, this still required the operator to manually adjust the inline bayonet heater with a rheostat on an almost continuous basis.

A search was made for another controller which could control the inline bayonet heater. Most off-the-shelf controllers were incapable of either the control specifications required in the flow system or controlling at temperatures up to 350°C. An excellent controller was purchased from Bayley (model 124). This controller has a simple design, yet can control a bath to +/- 0.001 K. With the new controller, the ease of operation was drastically increased while maintaining +/- 0.1 K control.

Many methods were tried in an attempt to control the flow rates of the two phases. A micrometering valve on the vapor line inside the air bath provides a pressure drop that sets the vapor flow rate relative to the total system pressure. It was found from experience that for operational ease and safety it was best that this valve remain at a constant setting (this may not be possible for ternary VLE measurements) for the following reasons. Firstly, since this valve is located inside the oven it would freeze in one position due to thermal cycling and possible coking. Secondly, if the valve was inadvertently closed, the pressure of the system built up and ruptured the pressure relief disk. All of the hazardous situations occurred when this valve was closed. Thirdly, the valve has a fine needle that can be broken off if the valve is closed too tightly, causing the valve to remain plugged when the operator believed that it was open. This again has resulted in a potential safety hazard. Fourthly, by changing the valve setting, the vapor flow rate was changed. If the valve was opened, more heat was required to vaporize the extra fluid. This affected the performance of the temperature control system. Lastly, if the vapor flow rate was too high, the fluidized sand bath was not able to provide the heat required to vaporize high boiling compounds, especially at the upper temperatures near 350°C.

The primary method of regulating the vapor/liquid split is a micrometering valve located on the liquid line after the fluid has been cooled. Many attempts were made to control the liquid flow rate with a back pressure regulator and in all cases this proved unsatisfactory. The regulators tested did not have fine enough control to give a stable operation.

The final design incorporated a micrometering valve which had a spring loaded needle to prevent damaging the valve. Problems were encountered with small particles (possibly coke) plugging the valve. Therefore, a 100 mesh strainer was placed inline above the valve. If a smaller mesh filter was used, it created a high pressure drop that prevented the vaporization of high boiling compounds near atmospheric conditions. The 100 mesh strainer became plugged rather easily and affected the overall stability of the system by creating large pressure fluctuations. Since a larger 100 mesh strainer was used, it was still possible to get a fine particle into the micrometering valve. This problem created an inability to control the liquid line despite radical changes in the valve setting. This problem occurred on an infrequent basis and required that the valve be cleaned.

Finally, it should not be assumed that the addition of two controllers and two micrometering valves solved the operational problems of this equipment. The overall stability of the system is tied to many variables, such as the total flow rate, vapor flow rate, temperature control, pressure fluctuations, phase boundary level and the compounds being studied. All of these variables and their interrelationships must be viewed as a whole to operate the equipment properly. The modifications occurred over a period of time. For example, the first system, m-cresol/quinoline, required more than six months to obtain four isotherms. The second system, m-cresol/tetralin, required approximately four months and the last system, tetralin/quinoline, only required one month. This is a clear indication of the length of time required for the program development and also the level to which the program was finally developed. Some of the causes and effects discovered during this investigation are discussed in the Troubleshooting Procedures in Appendix A. Also in Appendix A are the Operating Procedures, Shutdown Procedures and the Safety Precautions.

Evaluation of Vapor Liquid Equilibria Apparatus

Previously, the VLE apparatus had been evaluated (Niesen (1981)) by measuring the vapor pressure of water. Also, ethanol/water binary measurements had been made on the equipment by Palavra (see Niesen et al. (1986)). These measurements were compared to literature data and found to compare well with data reported by Gmehling et al. (1986) but differed from that of Barr-David et al. (1959) near the azeotrope. In fact, it was shown that the data of Barr-David were thermodynamically inconsistent near the azeotrope, Niesen et al. (1986).

The ethanol/water measurements were difficult and tedious. The analysis of the VLE samples required very accurate density measurements since the gas chromatograph available for the project could not analyze for water. It was decided to attempt to reproduce another system available in the literature for several reasons:

1. The system was in the process of being redesigned and had to be reevaluated.

2. The VLE samples from the ethanol/water system could not be analyzed on the gas chromatograph (GC) since water cannot be detected on an flame ionization detector. Since the GC was to be an important part of the project, a system was needed that could be analyzed with the available GC.

3. A system was needed that was relatively nontoxic, inexpensive and available at high purities to be used in the development of the VLE program.

The system chosen was methanol/ethanol. Literature data by Butcher et al. (1966) were available over three isotherms at 100, 140, and 160°C. This investigation attempted to reproduce Butcher's data at 100 and 140°C. The methanol was purchased from J. T. Baker. The analysis provided by the manufacturer showed a purity of 100.00% methanol with 0.009% water by Karl Fischer titration. The ethanol was purchased from Midwest Solvent Company and Aaper Chemical Company, both were documented to be 200 proof.

The analysis of the VLE samples was performed on the Hewlett-Packard model 5710A gas chromatograph. A packed column (GP 80/100 Carbopack C/0.1% SP-1000) was purchased from Supelco, Inc. to separate low boiling alcohols.

The data obtained during this investigation are presented in Tables 1 and 2. The data taken compared well with Butcher's at 100°C as can be seen in Figure 3. However, at 140°C, the data in this thesis were consistently shifted to the left of Butcher's data, Figure 4. Initially, it was assumed that there was a problem with the data from this thesis. Much time was spent in trying to isolate the problem; for example, the temperature calibration was checked to ensure that it was not off at the higher temperature. In addition, the pressure measuring system was tested against a dead weight tester and shown to be within the errors of the pressure gauges.

In an attempt to locate the discrepancy, the vapor pressures of both ethanol and methanol were measured. This eliminated any errors due to the GC analyses. These vapor pressures were then compared to Butcher's as well as vapor pressure data published by Ambrose et al. (1975) and Skaates et al. (1964). All of the vapor pressure data are presented in Table 2. For methanol, it can be seen that Butcher's data are significantly lower than the data from this research and the other two sets. The data from this research are lower than those of both Ambrose and Skaates. However, at these pressures and temperatures, the measurements from this investigations are comparable to theirs given the degree of uncertainty in our pressure and

TABLE 1

METHANOL ETHANOL VAPOR LIQUID EQUILIBRIA DATA AT 100°C

X (methanol)	Y	PRESSURE (KPa)
0.161	0.225	246.5
0.428	0.529	278.2
0.591	0.691	301.6
0.828	0.878	331.8
0.948	0.967	346.9

METHANOL ETHANOL VAPOR LIQUID EQUILIBRIA DATA AT 140°C

X (methanol)	Y	PRESSURE (KPa)
0.420	0.502	887.7
0.580	0.646	941.3
0.829	0.865	1028.9
0.950	0.959	1066.4

TABLE 2

METHANOL VAPOR PRESSURE

Temp. (°C)	Ambrose (KPa)	Skaates (KPa)	Butcher (KPa)	This Inves. (KPa)
100	353.4	----	351.6	353.0
140	1089.3	1088.0	1077.0	1083.6
160	1755.0	1759.6	1735.5	1748.1

ETHANOL VAPOR PRESSURES

Temp. (°C)	Ambrose (KPa)	Butcher (KPa)	This Investigation (KPa)
140	755.1	751.5	760.2
160	1251.6	1255.6	1253.9

FIGURE 3

VAPOR LIQUID EQUILIBRIA FOR METHANOL/ETHANOL AT 100°C

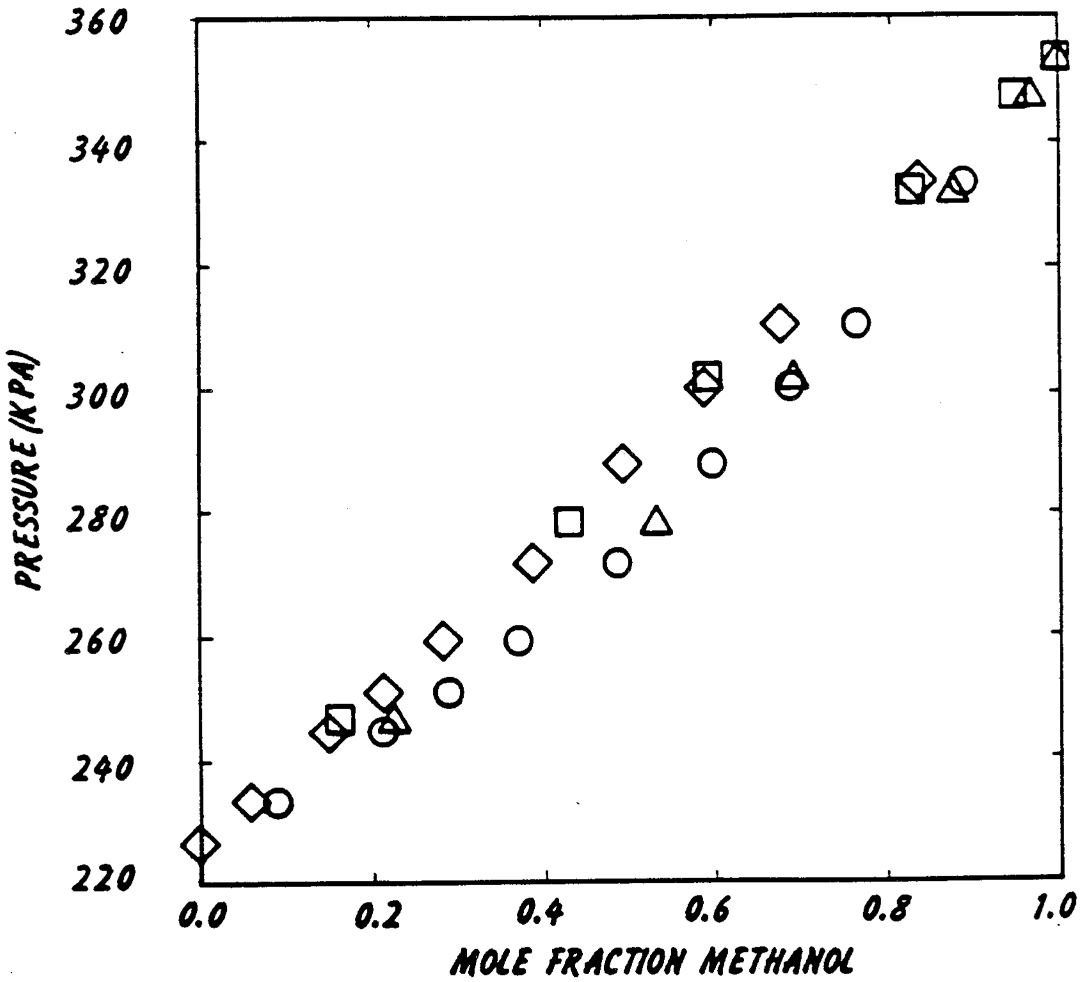

Vapor Liquid Equilibria from Methanol/Ethanol at 100°C
□Liquid and△vapor, this investigation.
◇Liquid and○vapor, Butcher, et al. (1966).

FIGURE 4

VAPOR LIQUID EQUILIBRIA FOR METHANOL/ETHANOL AT 140°C

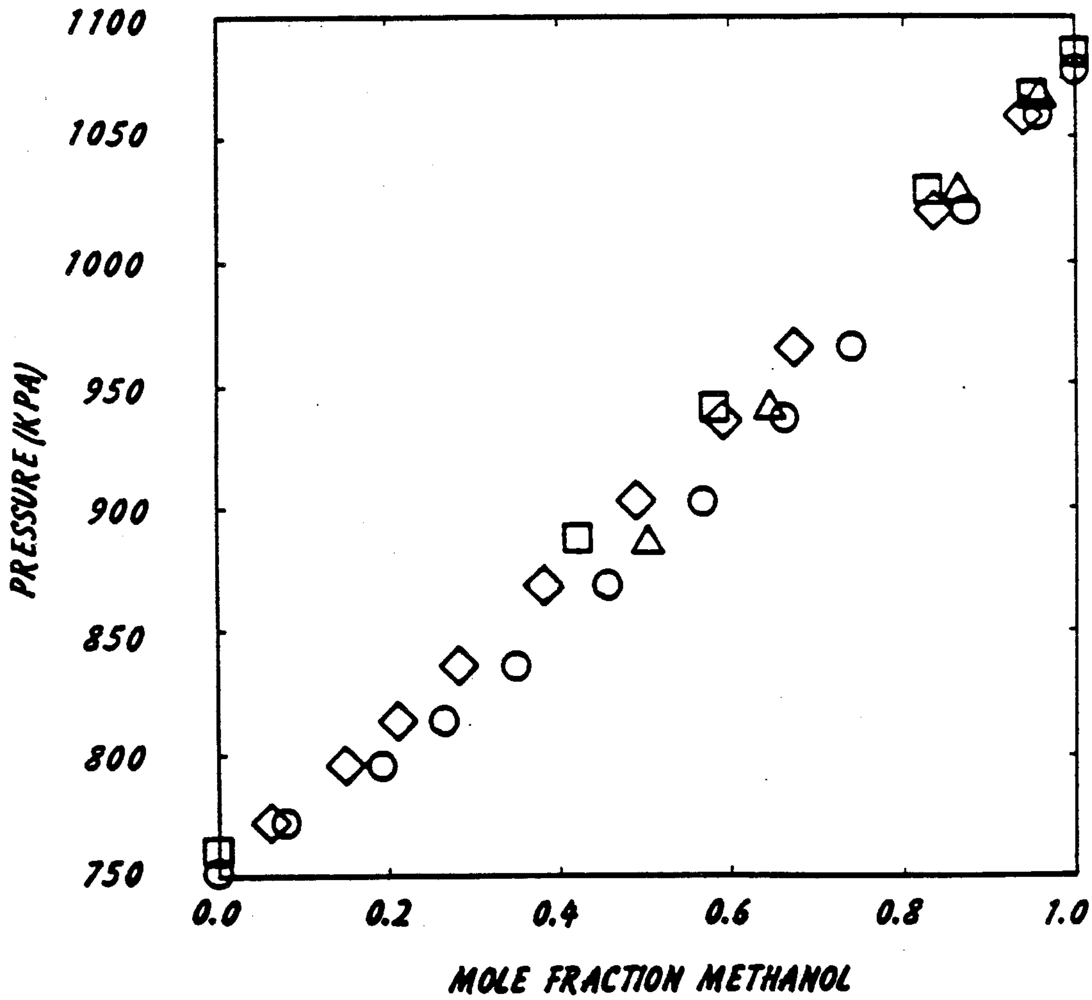

Vapor Liquid Equilibria for Methanol/Ethanol at 140°C
□Liquid and △vapor, this investigation.
◇Liquid and ○vapor, Butcher, et al. (1966).

temperature measurements (.7 kPa for pressures lower than 689.5 kPa and 3.45 kPa for the higher pressures as well as +/- 0.1 K). In the case of ethanol, the data from this research are somewhat higher than the other investigators, but still within experimental error.

It was discovered that the discrepancies with the vapor pressures and the VLE measurements were most likely due to impurities. Both methanol and ethanol are hygroscopic. In the case of methanol, the water will lower the vapor pressure and for ethanol, water will elevate the vapor pressure. In addition, methanol is subject to decomposition at higher temperatures. The decomposition products are more volatile than methanol and contribute to higher methanol vapor pressures.

Due to Butcher's methanol vapor pressure data being significantly lower than all other data, it is believed that the VLE data from this research more accurately reflects the behavior at 140°C. It may be significant that two very common systems (methanol/ethanol and ethanol/water) have been found to have discrepancies in the literature. VLE data at elevated temperatures and pressures may be difficult to obtain and the effects of impurities may be more pronounced at these conditions.

ANALYTICAL TECHNIQUES

The quality of the analyses of the samples was critical to the project's viability. The analyses were performed on an Hewlett-Packard model 5710A GC with a flame ionization detector (FID). The column chosen was an Hewlett-Packard series 530 19095S #100 which has a 2.65 micrometer coating of methyl silicone. The column performed well because it is slightly polar and therefore separates tetralin, quinoline, and m-cresol. The column was a hybrid of a packed and a capillary column which allowed the column to give sharp peaks as would be seen with a capillary column, but did not require that the sample be split as with the capillary column.

Since the samples were all liquid, they were manually injected into the injection port with a Hamilton 1 microliter syringe. Shooting the compounds "neat" (pure) caused the FID to become oversaturated, so the samples were diluted with methyl ethyl ketone (MEK) at the ratio of 1 part sample to 20 parts MEK. The MEK came off the column quite rapidly and was not included in the area integration.

Due to problems discussed below, each sample was bracketed by two standards so that a relative response factor could be calculated for the sample. With good technique, the accuracy of the analyses was shown to be +/-

0.001 mole fraction. This accuracy was determined by analyzing samples whose concentrations were known by weight.

There were three major problems in trying to obtain GC analyses to the desired accuracy of +/- 0.001 mole fraction. First, an FID operates by forming primarily CHO^+ ions from the carbon atoms in the molecules and primarily these ions are counted. Therefore, a molecule with 10 carbon atoms will produce more CHO^+ ions than a molecule with 6 carbon atoms. Consequently, the 10 carbon molecule will produce a larger area count (or FID response) for the same concentration in molar units as the 6 carbon atom. This effect was not difficult to account for, a relative response factor (RRF) was calculated based on samples with known concentrations. The major difficulty was that the RRF changes with the ratio of the compounds being studied and the change is nonlinear. The reason for this is that not all of the carbon atoms are formed into CHO^+ ions. The number of CHO^+ ions formed is influenced by many factors such as the flame temperature, kinetics of the ionization reaction, the presence of other heteroatoms, etc. One way to account for these factors was to use a series of standards for the compounds being studied across the entire concentration range. When an unknown sample was analyzed, the RRF was calculated from two surrounding standards assuming that the RRF was linear between the two standards. This process became quite tedious since for a liquid and vapor sample, four standards were required.

The second problem was the nonreproducibility of the GC. After the previous discussion it is easy to see that the amount of O_2 or H_2 present affects the responses. If the air or hydrogen flow rates were not set precisely at the same point from day to day, the response for the same sample varied. Mechanically, it was difficult to set the same flow rates. In addition, the pressure regulators on the tanks varied during the day. The variations in responses were corrected for by analyzing the same set of standards each day the GC was used. In fact, when the GC was used in the morning and then again later in the afternoon, the standards were again reanalyzed to account for variation of the air flow rate during the day.

The third problem was the most difficult to solve. The FID responses were intermittently nonreproducible. Variations were as high as 1 mole percent for multiple injections of the same sample. Many factors could cause this problem such as electronic failures, leaks, dirty FID, leaking septa, clogged injection ports, impure gases, or nonreproducible injection sizes. From experience, it was found that:

1.) Nothing was ever found wrong with the electronics of the GC.

2.) While the FID did need to be cleaned, this did not appear to solve the problem.

3.) There did not appear to be any leaks in the system.

4.) A leaking septum definitely caused errors. Normally the area counts would suddenly decrease, since part of the sample was lost. The manufacturer suggested replacing the septums after every 10 injections. If a fine needle was used, then the septum lasted longer.

5.) Pieces of the septum invariably broke off and lodged in the injection port. This problem created peak tailing. The injection port has a glass liner that had to be replaced periodically. If the problem was not solved, the entire injection port was removed and cleaned. In addition, several centimeters of the column were cut off to remove any septum pieces lodged in the column.

6.) Only ultra high purity helium was used as the carrier gas to eliminate any contamination problems. A drying tube was placed on the air line; but this did not seem to have any effect on the performance of the GC.

7.) The most surprising problem was the syringe. Since all of the samples were liquid, the samples were manually injected. The response was directly tied to the sample size. If the sample size varied, then the response was not reproducible. Several times the syringe partially lost suction and varying amounts of samples were drawn up. This problem was particularly difficult to spot since the syringe appeared to be working and the injection sizes were so small that the variations were not visible to the naked eye. The symptom of this problem was erratic area counts for seemingly equal sample sizes.

Overall, all of the problems encountered were related to air flow rate or the physical injection of the sample onto the column. Accurate GC analyses were more dependent upon the operator's techniques than the equipment.

SAMPLE PURIFICATION

During the initial evaluation of the equipment, it was discovered that the purity of the samples was quite important. As was discussed previously under "Evaluation of the VLE Equipment," the methanol/ethanol system was affected not only by contaminants but also by decomposition products. While it became clear early on that this problem existed, the severity of the problem was not fully understood until much later.

All of the compounds used were purchased at the highest quality affordable; however, further purification was required in all cases. A spinning band distillation column was used to purify the samples to > 99.9%. Products from the distillation column were checked by GC analysis.

The m-cresol was purchased from Sigma Chemical Co. with a stated purity of 99%; by GC analysis it was typically found to be 99.8%. However, the water content could not be determined. All of the m-cresol was distilled in the distillation column to remove the water to the lowest level possible.

Synthetic quinoline was purchased from J.T. Baker and Alfa Products at a purity level of 99%. Synthetic quinoline was required since other sources of quinoline had significant quantities of isoquinoline as a contaminant. The quinoline was distilled to raise the purity to 99.9% and to eliminate water.

Tetralin was purchased from Aldrich Chemical Co. at a purity of 99%. Tetralin had a low boiling contaminant that was difficult to remove and required slow takeoff rates on the distillation column. Again, the final product was shown to be 99.9%$^+$ pure by GC analysis.

Even though the samples were initially purified to 99.9%, the integrity of the samples was monitored while the physical measurements were being made. If decomposition products increased to a level above 0.1 area percent, the sample was removed from the system. Also, if the pressure measurements appeared to be high, the sample was removed and redistilled to remove water.

In trying to obtain the VLE data for these compounds a major problem was identified. Initially, the VLE data had a high degree of scatter that could only be attributed to error in the pressure measurements. After carefully checking the actual pressure measurement system and finding no error, the problem was narrowed down to the actual samples. It was found that both quinoline and m-cresol, due to their hygroscopic natures, contain water as purchased even though the purity was 99+ mole percent. It was also found that if these compounds were exposed to the atmosphere, the water content would increase. Since water has a drastically different vapor pressure than do the compounds of interest, a small amount of water could result in a severe error in the pressure measurements. As discussed below, an attempt was made to estimate effects of trace amounts of water in the samples. It was found that even minute traces had surprisingly significant effects.

Water is a more volatile impurity and will affect the VLE measurements by increasing the measured pressures. The easiest and most accurate way to determine the error due to water on the measurements was to use actual experimental data to determine the effects of water on the vapor pressures of the pure compounds. Published data were found for the quinoline/water binary data at atmospheric pressure, Maczynski et al. (1965). While suitable data were not found for the m-cresol/water system, phenol/water binary data were also found at atmospheric pressure, Brusset et al. (1953). Since m-cresol and phenol are similar in molecular structure and chemistry this was a reasonable substitution. Tetralin is not hygroscopic and not miscible with water, therefore there should be no problem with water being an impurity.

Using the binary VLE data, an infinite dilution activity coefficient was estimated to be 0.24 for water in quinoline and 4.71 for water in phenol at atmospheric pressure (see Appendix B for the calculations). Assuming that the activity coefficient was independent of temperature (not necessarily a good assumption, but the best that can be done with a limited amount of data) the effects of trace amounts of water on the vapor pressures of quinoline and phenol were estimated. The results of these calculations are shown in Table 3. As can be seen, the effects of water on these compounds can be very significant. Assuming a purity of 99.9 weight percent quinoline (with the remainder assumed to be water), the error in the pressure measurement ranges from 4.4% (6 kPa) at 250°C to 3.3% (17.3 kPa) at 325°C and for 99.99 weight percent quinoline the error is 0.43% (.6 kPa) at 250°C and 0.33% (1.7 kPa) at 325°C. For 99.9 weight percent m-cresol (using water phenol data) the error is much greater, 58% (175 kPa) at 250°C to 42% (476.1 kPa) at 325°C. In fact, for m-cresol, the error was so large that the estimated m-cresol purity level was increased to 99.99 weight percent. At 99.99 weight percent m-cresol a 3.7% (11.5 kPa) error occurs at 250°C and a 3% (34.4 kPa) error at 325°C. These results were quite surprising but completely explained the error in data from this investiga-

TABLE 3

ERROR IN PRESSURE MEASUREMENT
DUE TO WATER CONTAMINATION

Quinoline

	99.9%[1]	99.99%
250°C	4.4% (6.0 kPa)	0.43% (0.6 kPa)
275°C	4.0% (8.8)	0.39% (0.8)
300°C	3.6% (12.5)	0.35% (1.2)
325°C	3.3% (17.3)	0.33% (1.7)

M-Cresol (Phenol)

	99.9%	99.99%
250°C	58.0% (175.5 kPa)	3.7% (11.5 kPa)
275°C	51.0% (250.7)	3.4% (17.1)
300°C	45.8% (349.4)	3.2% (24.6)
325°C	41.7% (476.1)	3.0% (34.4)

1. weight percent

tion and the error in literature values for the pure component vapor pressures of quinoline and m-cresol.

Figure 5 shows a plot of m-cresol vapor pressures. The data reported by Nasir et al. (1980) are consistently higher than the rest of the data. As stated in their article, the m-cresol was used as purchased from Aldrich with no further purification. The Nasir data are approximately 50 kPa higher than the rest of the data at 325°C, this error may result from a trace amount of water. A water concentration as low as 0.02 weight percent could be the reason for this significant error.

It can be seen that when dealing with compounds that are capable of hydrogen bonding and consequently are hygroscopic, a tremendous effort must be made to not only purify the samples but also to isolate them from the atmosphere before and during the actual physical measurements.

FIGURE 5

M-CRESOL VAPOR PRESSURE COMPARISON

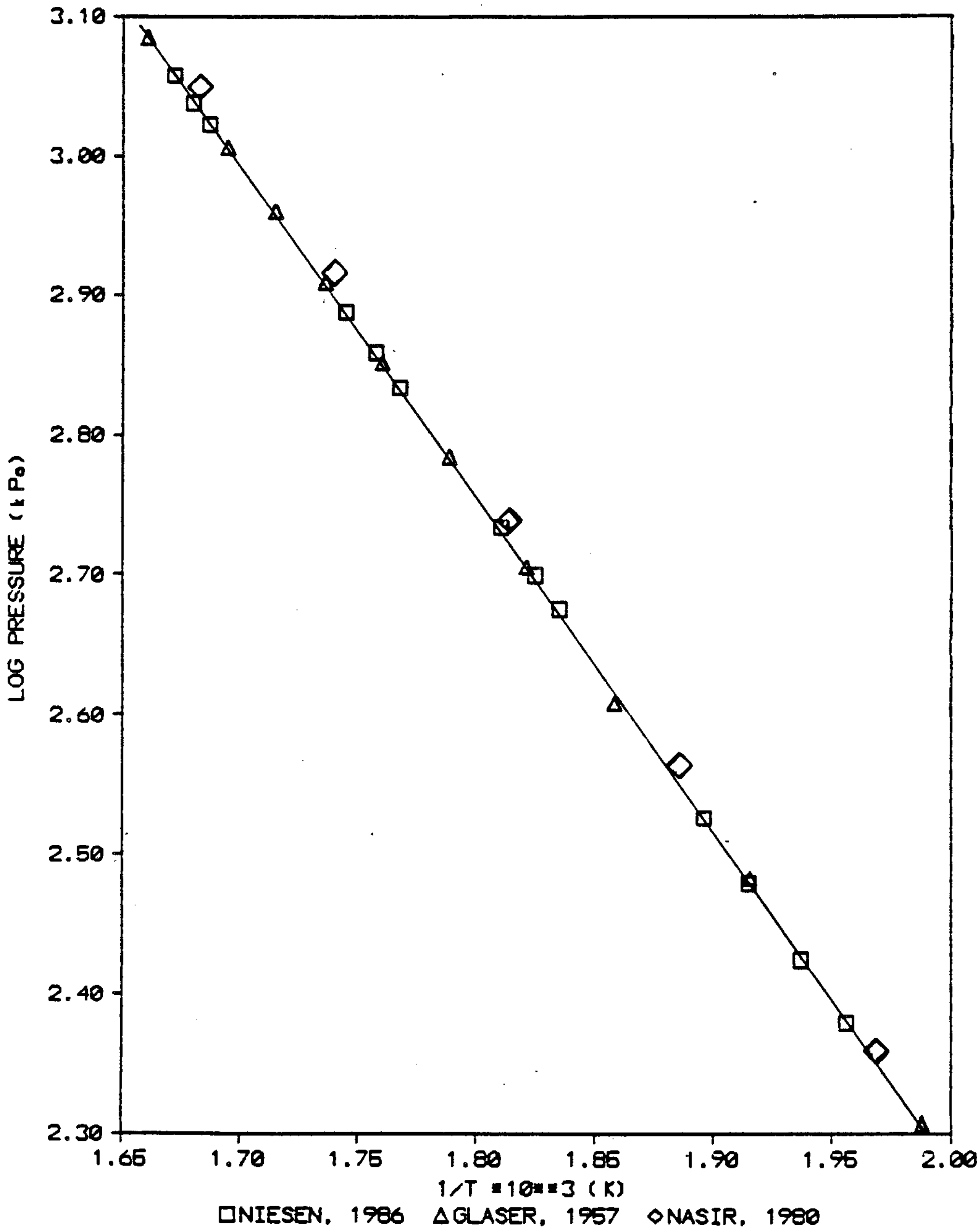

EXPERIMENTAL RESULTS

Once the experimental program had been developed and evaluated against literature data, new VLE data were generated for the binary systems of m-cresol, quinoline, and tetralin at four isotherms, 250, 275, 300, and 325°C. The compounds studied are of significant interest for two reasons. Firstly, two of the compounds are polar and exhibit association. Thermodynamic research of highly non-ideal compounds has been left virtually untouched especially at high temperatures and pressures. Without actual data, proposed equations of state and mixing rules for non-ideal systems cannot be tested. Secondly, it has been found that the modeling of coal liquids with traditional Kesler-Lee type petroleum correlations gives unpredictable results. It has been proposed that the failure of the petroleum correlations for the coal liquids is due to the presence of polar associating compounds in the coal liquids, Sharma (1978). The compounds selected for this work have been generally accepted by the research community as "model" compounds for coal liquids, Yesavage (1984). Therefore, the data generated in this thesis can be used not only for basic thermodynamic research but also will provide needed information for more practical applications.

M-cresol is a polar compound capable of hydrogen bonding through the hydroxyl group. Based on titration calorimetry data and apparent molecular weight determinations, it has been proposed that m-cresol molecules associate with each other in both the dimer and the trimer form, Eatough (1984) and Sandarusi (1984). The trimer form consists of a six membered ring of oxygens and hydrogens. This compound is quite hygroscopic due to its hydrogen bonding capabilities.

Quinoline is also polar and capable of hydrogen bonding due to the pair of nonbonded electrons on the nitrogen. However, unlike m-cresol, quinoline molecules do not associate to any significant degree with each other since the hydrogens on the molecule are not sufficiently acidic to interact with the nitrogen. Like m-cresol, quinoline is hygroscopic because of the capability to form hydrogen bonds with water.

Tetralin (1,2,3,4 tetrahydronaphthalene) is nonpolar and is not hygroscopic. It does not associate with other tetralin molecules.

These three compounds form three binaries with very different interactions. One binary, m-cresol/quinoline, has a strong polar- polar interaction. Hydrogen bonding occurs between quinoline and m-cresol as well as between m-cresol molecules. The second binary, m-cresol/tetralin, has the polar m-cresol molecules and nonpolar tetralin molecules. There are no hydrogens acidic enough on the tetralin molecule to hydrogen bond with m-cresol; however, m-cresol still will hydrogen bond with other m-cresol molecules. The third binary, quinoline/tetralin, is more of an ideal mixture since neither the tetralin or quinoline molecules have acidic hydrogens that can form hydrogen bonds with the nitrogen. Thus, the binaries of these three compounds provide a wide range of intermolecular interactions.

Vapor Pressure Measurements

Vapor pressure measurements were generated for m-cresol, quinoline, and tetralin over the temperature range of 250-325 °C. These measurements are presented in Tables 4-6. In Figures 6-8, the data from this research are compared with published data and data also generated at the Colorado School of Mines on a flow calorimeter, Flanigan (1986).

As can be seen, there are some discrepancies in some of the literature data. This is most likely due to trace amounts of impurities as discussed previously under "Sample Purification". The data from this investigation agree well with a large percentage of the published data and agree very

TABLE 4

M-CRESOL VAPOR PRESSURES

Temp (K)	Pressure (kPa)
511.2	239.2
516.2	265.8
522.2	301.3
527.4	336.1
545.1	473.3
548.2	500.5
552.4	541.6
565.8	680.8
569.1	722.2
573.2	771.5
592.8	1051.4
595.2	1090.4
598.1	1141.1

TABLE 5

QUINOLINE VAPOR PRESSURES

Temp (K)	Pressures (kPa)
535.8	175.0
536.0	176.0
545.0	209.1
548.3	223.6
556.0	256.7
573.7	350.5
575.8	362.2
589.8	454.9
597.6	515.6
598.2	520.1
598.6	523.1
603.2	562.4
606.5	592.7
610.0	622.4
612.7	649.6
614.4	664.5
618.4	709.3
619.7	721.4

TABLE 6

TETRALIN VAPOR PRESSURES

Temp (K)	Pressure (kPa)
506.6	175.8
514.8	207.5
528.7	274.8
539.0	331.3
553.2	420.9
556.2	445.4
573.1	583.4
578.4	632.0
587.9	731.0
595.3	809.2
603.5	908.5
613.3	1029.9

FIGURE 6

M-CRESOL VAPOR PRESSURES

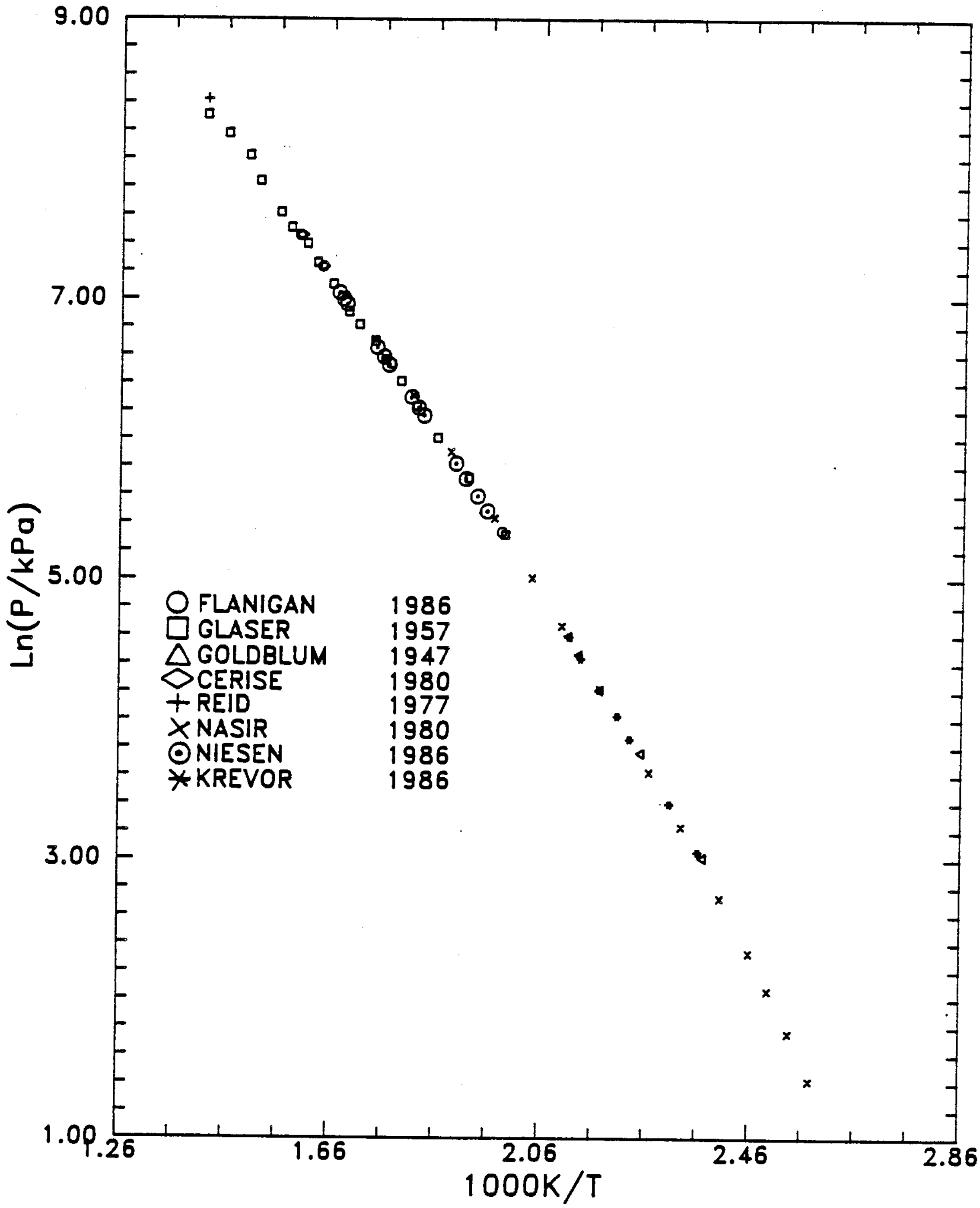

FIGURE 7
QUINOLINE VAPOR PRESSURES

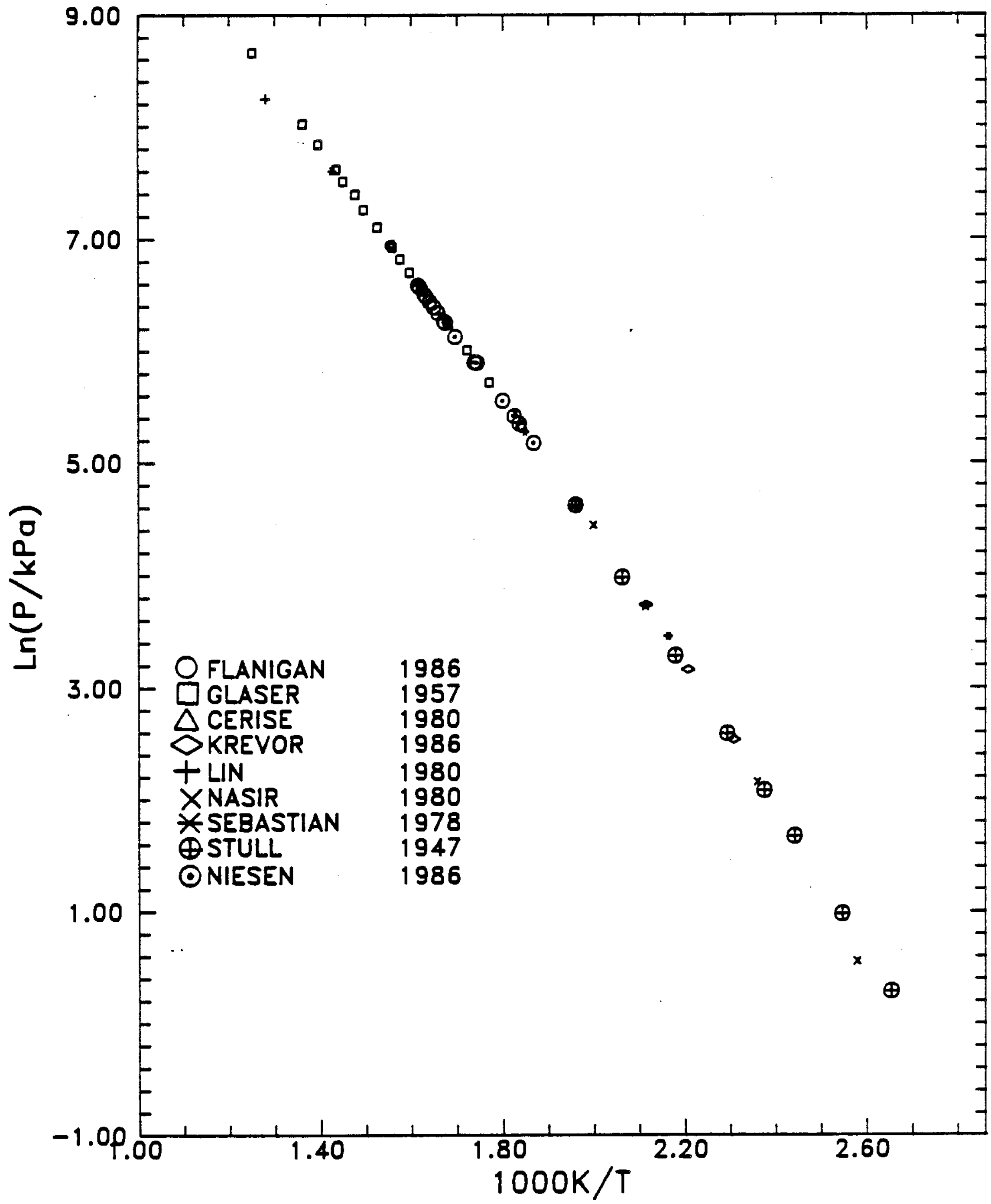

FIGURE 8
TETRALIN VAPOR PRESSURES

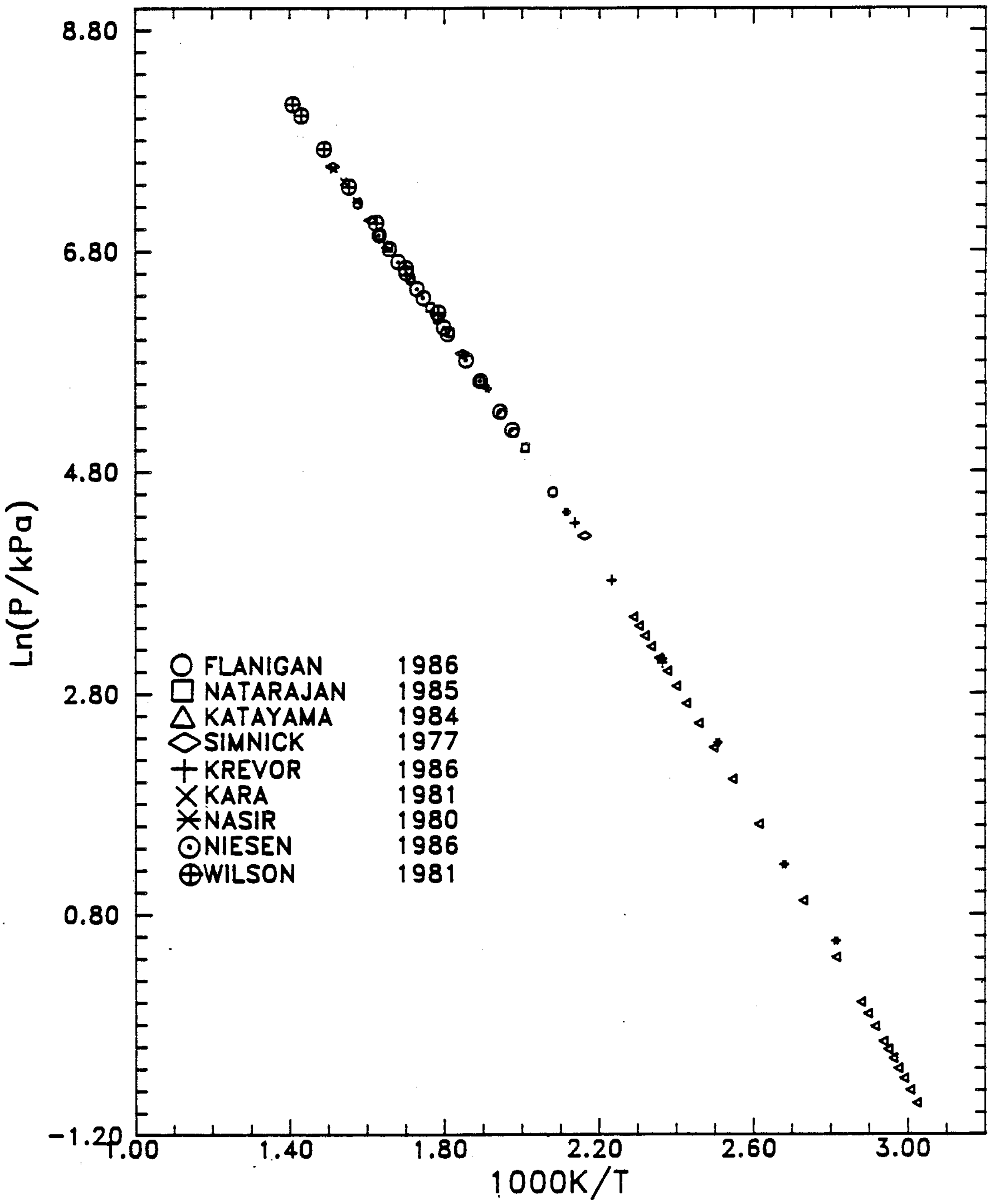

well with the vapor pressure data from the flow calorimeter at the Colorado School of Mines. It can also be seen that there are discrepancies in some of the critical points. These discrepancies are discussed later.

Vapor Liquid Equilibria Measurements

Listed in Tables 7 and 8 and shown in Figures 9 and 10 are the binary VLE data for the m-cresol/quinoline system at four isotherms, 250, 275, 300 and 325°C. At the lowest isotherm, 250°C, a high boiling azeotrope may be present at a low m-cresol concentration. Due to difficulties with water contamination it is difficult to determine exactly where the azeotrope occurs. Literature data, Lekhova (1971) and Krevor (1986) indicate the presence of an azeotrope at temperatures between 160 and 200°C that occurs at increasingly lower concentrations of m-cresol as the temperature increases.

A small degree of scatter in the data is present. In Figures 11-14 the x-y data are plotted for these isotherms. It can be seen that a smooth curve is formed by the x-y data. This indicates that steady state was obtained and since varying flow rates were used, it also indicates that equilibrium was obtained. Since equilibrium was obtained the scatter in the data is either due to errors in the

TABLE 7

VLE MEASUREMENTS FOR M-CRESOL/QUINOLINE

	Pressure (kPa)	X (mole percent m-cresol)	Y (mole percent m-cresol)
250°C	134.6*	0.0	0.0
	136.2	4.9	5.8
	137.9	12.3	14.3
	137.8	14.5	17.4
	150.0	32.5	43.5
	151.6	33.9	45.9
	161.1	41.2	56.3
	170.7	47.1	63.9
	171.0	47.1	64.8
	186.1	56.0	76.2
	195.1	59.5	78.6
	207.0	64.3	83.1
	216.2	66.8	85.8
	223.3	70.3	88.0
	248.4	79.1	92.7
	256.1	81.1	94.3
	293.3	94.6	98.7
	301.0	96.9	99.5
	308.3	100.0	100.0
275°C	221.9	0.0	0.0
	225.1	4.7	5.8
	228.9	11.8	14.8
	230.4	13.9	17.9
	248.6	28.9	39.3
	255.3	32.6	44.6
	265.9	37.1	51.7
	269.0	39.2	53.9
	282.1	44.8	61.5
	287.9	45.8	63.0
	317.1	55.7	74.8
	332.3	60.6	78.8
	340.5	63.0	80.8
	366.4	70.0	86.7
	389.6	74.7	89.5
	405.1	78.3	91.4
	419.0	80.9	92.9
	477.1	94.3	98.1
	486.1	97.2	99.2
	500.5	100.0	100.0

* interpolated value

TABLE 8

VLE MEASUREMENTS FOR M-CRESOL/QUINOLINE

	Pressure (kPa)	X (mole percent m-cresol)	Y (mole percent m-cresol)
300°C	346.2	0.0	0.0
	353.0	4.4	5.8
	363.4	13.2	17.8
	397.2	26.7	37.5
	406.0	31.6	43.4
	421.4	36.6	50.6
	429.4	38.7	52.5
	494.6	54.7	70.8
	517.4	59.0	75.5
	538.8	63.3	79.5
	581.2	70.3	84.3
	606.8	74.3	88.2
	640.8	80.2	91.3
	738.4	96.2	98.2
	738.4	96.2	98.1
	771.5	100.0	100.0
325°C	520.4	0.0	0.0
	529.2	4.2	5.8
	545.3	10.6	14.4
	548.6	12.4	18.1
	604.3	28.9	39.3
	643.2	35.8	49.1
	647.6	37.1	51.3
	679.8	43.1	58.3
	747.0	53.9	69.2
	827.0	66.3	80.7
	839.5	67.6	81.8
	858.4	69.6	83.5
	870.7	70.5	84.4
	908.4	75.3	87.5
	943.9	80.2	90.6
	1117.1	97.0	99.0
	1141.1	100.0	100.0

FIGURE 9

M-CRESOL/QUINOLINE VLE DATA AT 250-275°C

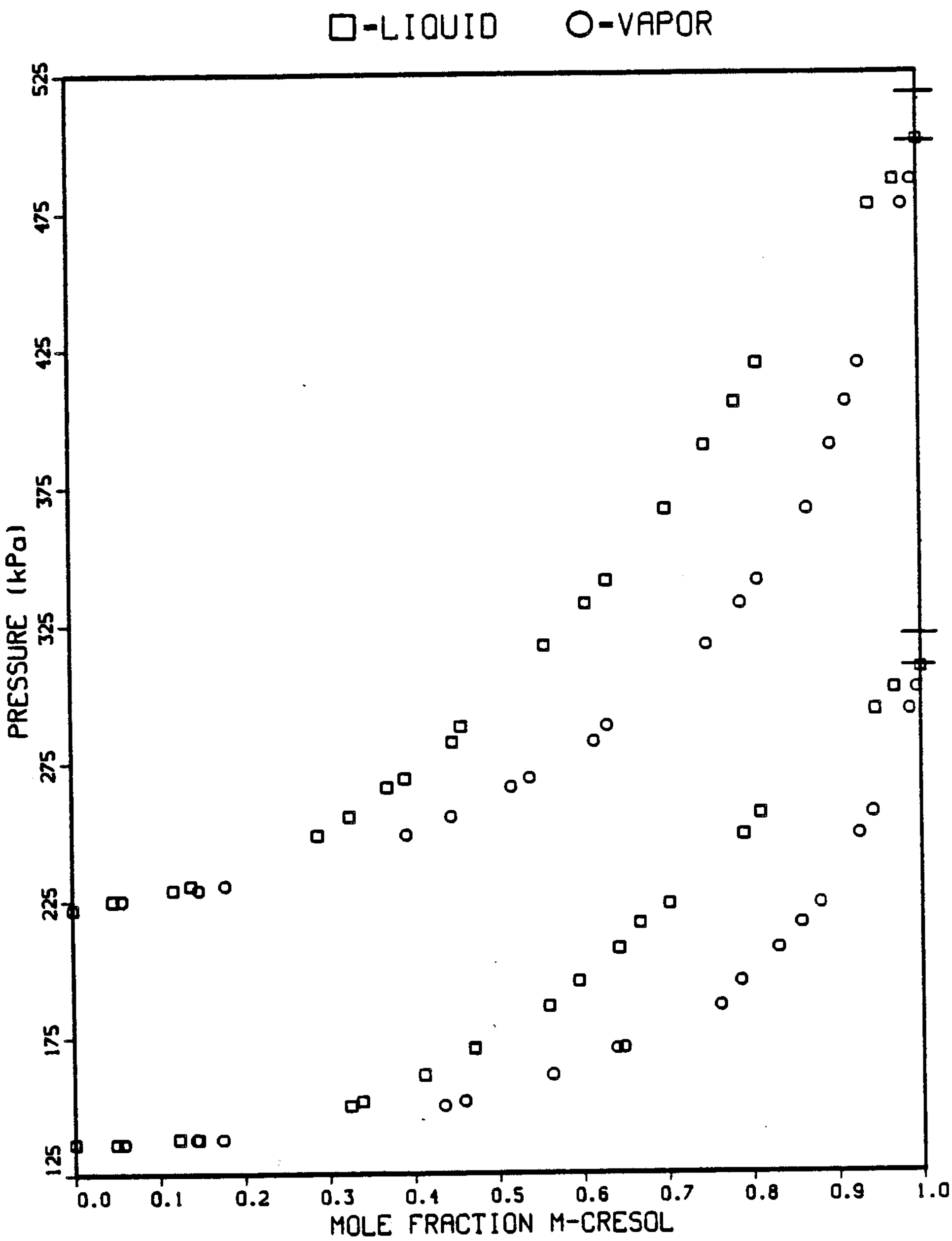

FIGURE 10

M-CRESOL/QUINOLINE VLE DATA AT 300-325°C

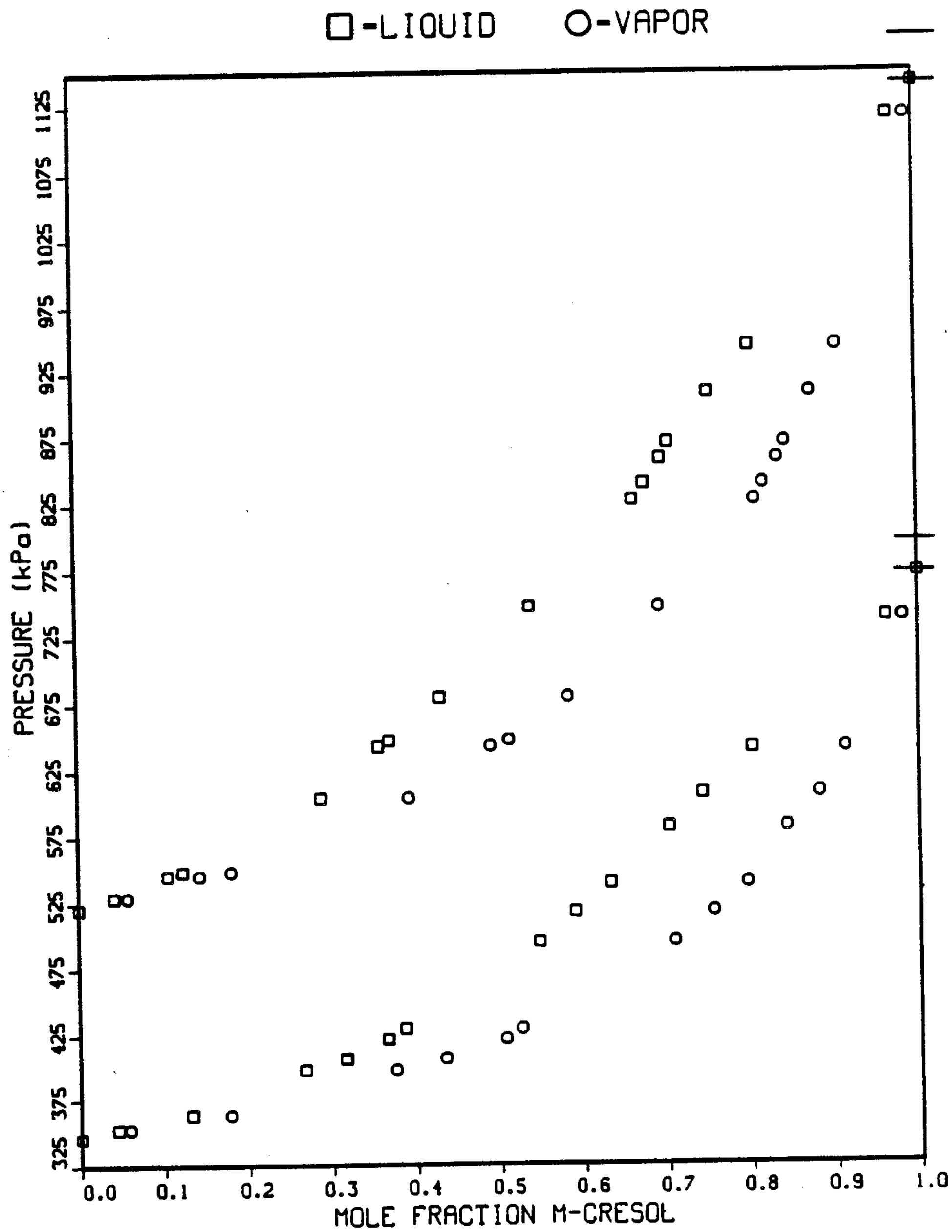

FIGURE 11

XY PLOT FOR M-CRESOL/QUINOLINE AT 250°C

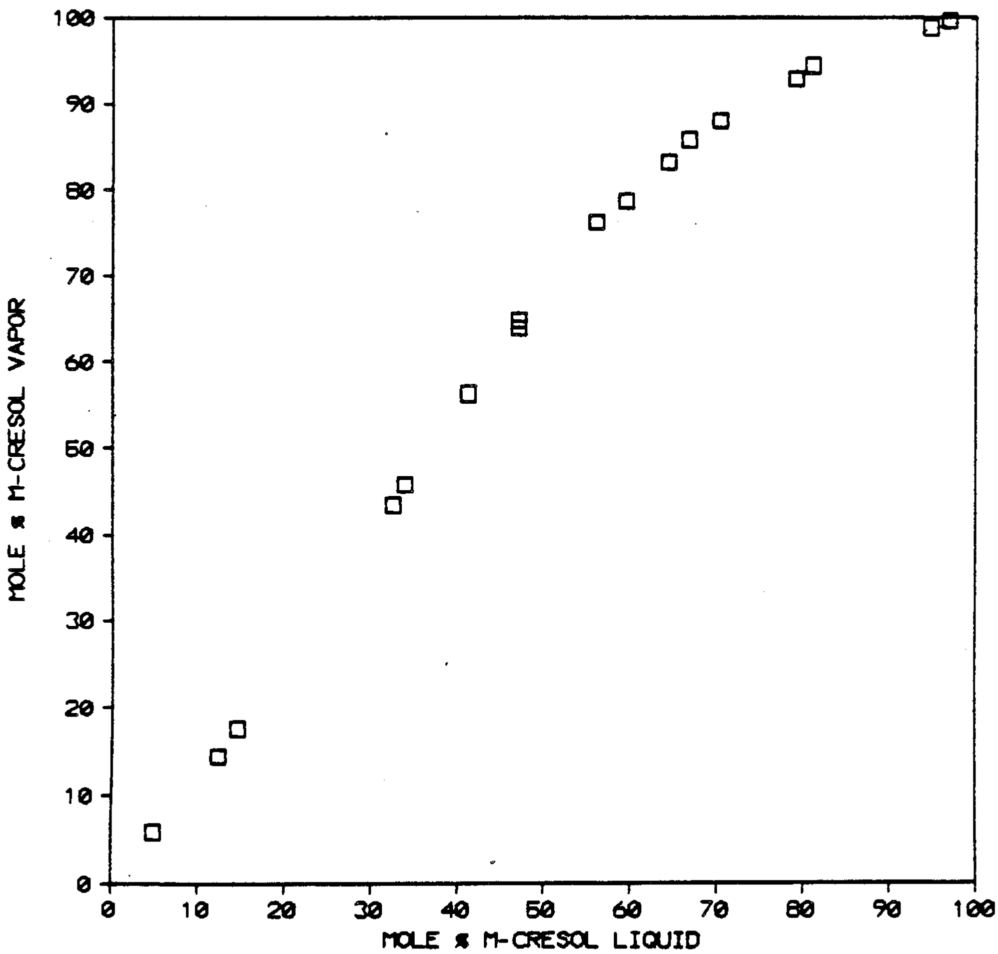

FIGURE 12

XY PLOT FOR M-CRESOL/QUINOLINE AT 275°C

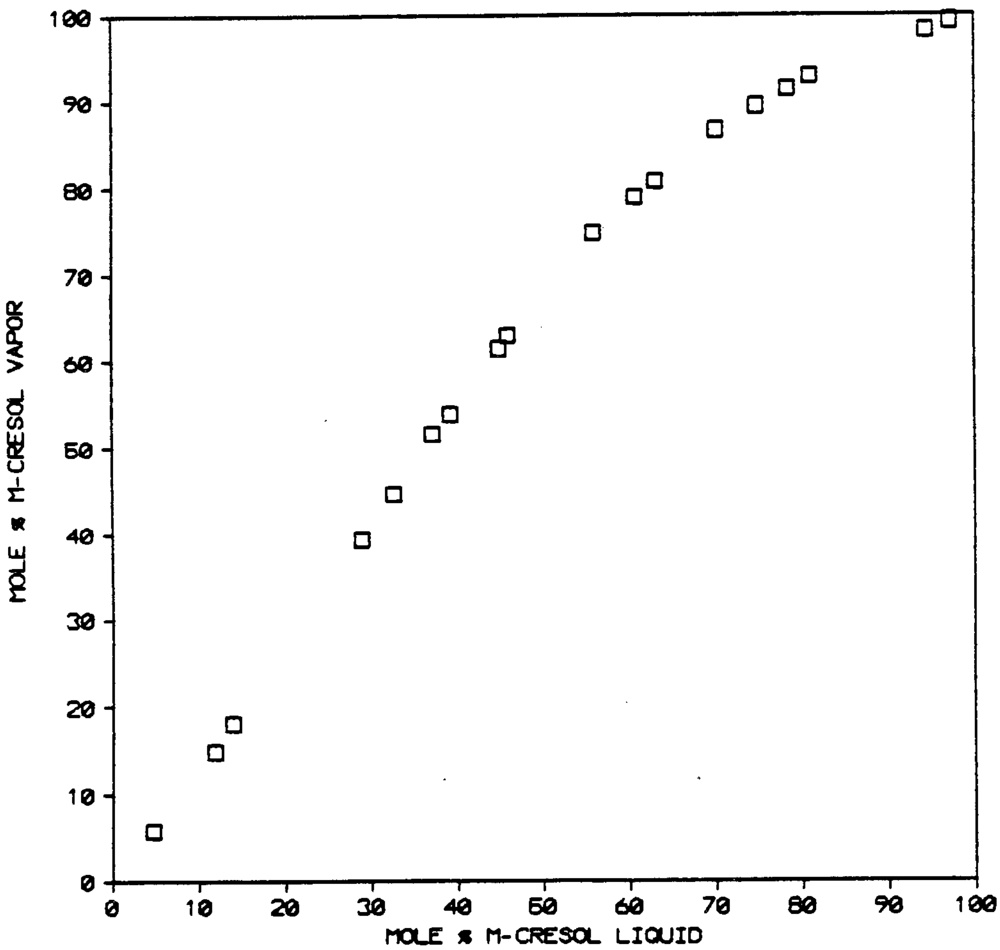

FIGURE 13

XY PLOT FOR M-CRESOL/QUINOLINE AT 300°C

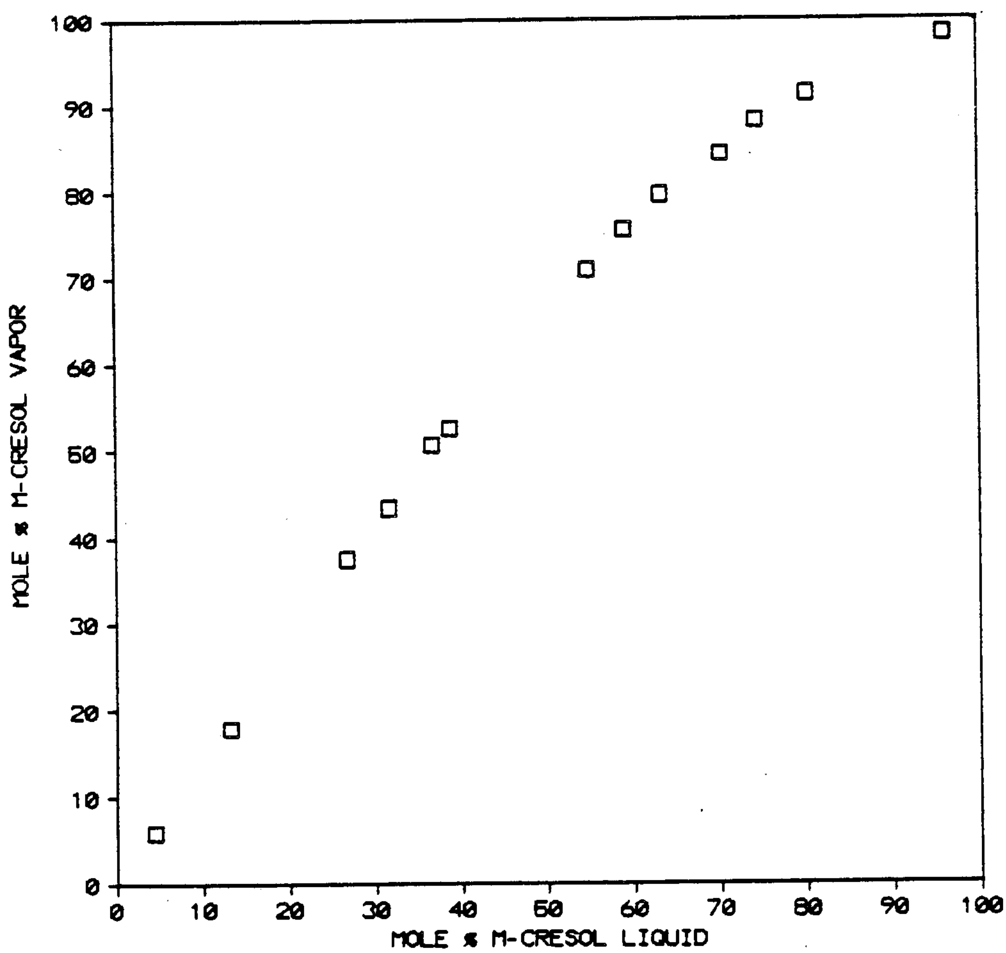

FIGURE 14

XY PLOT FOR M-CRESOL/QUINOLINE AT 325°C

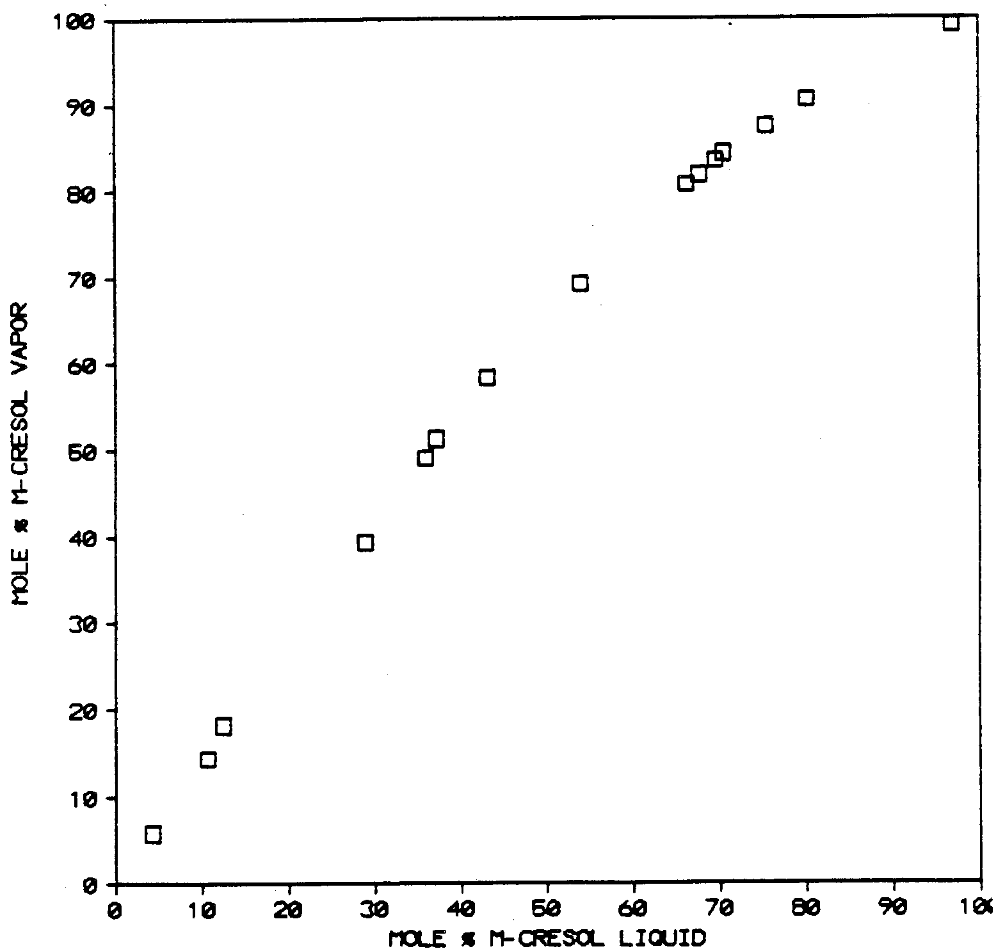

temperature or pressure measurements. Because of the water contamination problem, it is believed that the scatter is due to trace amounts of water. Figures 9 and 10 have two marks at 100% m-cresol for each isotherm. The distance between the two marks is the error that would result by a 0.01 weight percent water contamination as presented in Table 3. It is obvious that the error due to water contamination is significant.

VLE data for the m-cresol/tetralin system are tabulated in Tables 9 and 10 and shown in Figures 15 and 16. This system has polar interactions between m-cresol molecules that are disrupted by the relatively non-polar tetralin molecules, resulting in a low boiling azeotrope. This azeotrope moves, with increasing temperature, towards high m-cresol concentrations and at some temperature would disappear altogether. Recently published data by Krevor et al. (1986) indicate similar azeotropic behavior at temperatures between 150 and 195°C.

Figures 15 and 16 again have two marks at 100% m-cresol to indicate the error that is possible if the water contamination were 0.01 weight percent. Figures 17-20 are x-y plots for these data. The smooth curves indicate that equilibrium was obtained and that any scatter in the data is most likely due to trace water contamination resulting in

TABLE 9

VLE MEASUREMENTS FOR M-CRESOL/TETRALIN

	Pressure (kPa)	X (mole percent m-cresol)	Y (mole percent m-cresol)
250°C	246.0	0.0	0.0
	254.1	2.2	4.0
	261.9	5.0	8.5
	265.1	6.1	10.2
	270.8	8.7	13.8
	285.0	17.6	25.0
	289.0	20.5	28.5
	300.8	30.7	38.1
	306.8	42.5	49.3
	313.7	55.4	59.3
	315.3	60.6	63.2
	318.8	67.0	68.5
	318.8	72.5	72.9
	318.4	77.9	77.5
	317.4	81.7	80.7
	316.4	84.5	83.4
	314.7	88.9	87.5
	312.6	91.8	90.8
	311.4	95.8	95.0
	308.3	99.4	99.0
	308.3	100.0	100.0
275°C	386.6	0.0	0.0
	398.2	2.2	3.8
	410.5	5.0	8.3
	414.4	6.1	10.0
	428.5	10.4	15.7
	439.2	15.9	23.3
	460.6	26.3	34.4
	462.7	28.8	36.7
	474.0	34.9	42.1
	497.3	54.5	59.2
	505.5	62.2	65.4
	506.2	67.8	69.8
	506.9	72.6	73.9
	508.2	75.6	76.4
	509.2	84.3	84.0
	507.0	88.4	87.9
	505.3	92.7	91.9
	505.1	95.6	95.1
	500.3	100.0	100.0

TABLE 10

VLE MEASUREMENTS FOR M-CRESOL/TETRALIN

	Pressure (kPa)	X (mole percent m-cresol)	Y (mole percent m-cresol)
300°C	583.4	0.0	0.0
	599.5	2.5	4.3
	615.1	5.6	8.9
	633.6	9.2	14.0
	657.3	15.9	22.7
	687.1	25.8	33.9
	707.5	32.9	40.4
	708.0	33.3	41.1
	718.1	37.0	44.3
	729.5	42.9	49.8
	741.2	48.6	54.4
	765.1	64.6	67.8
	769.5	68.7	71.0
	772.1	74.1	75.6
	775.7	84.1	84.4
	777.0	88.1	88.6
	773.9	93.3	93.0
	772.3	95.6	95.3
	771.5	100.0	100.0
325°C	842.8	0.0	0.0
	855.0	2.1	4.3
	877.2	4.8	7.5
	888.2	6.8	10.3
	939.0	15.3	21.4
	986.0	25.3	32.7
	1017.0	33.1	40.0
	1061.7	43.2	50.0
	1079.9	50.9	56.6
	1102.6	59.7	64.1
	1119.0	68.3	71.2
	1130.6	74.0	75.8
	1130.4	81.1	81.9
	1133.9	83.9	84.6
	1134.2	88.4	88.4
	1140.0	93.3	93.2
	1139.3	95.4	95.4
	1141.1	100.0	100.0

FIGURE 15

M-CRESOL/TETRALIN VLE DATA 250-275°C

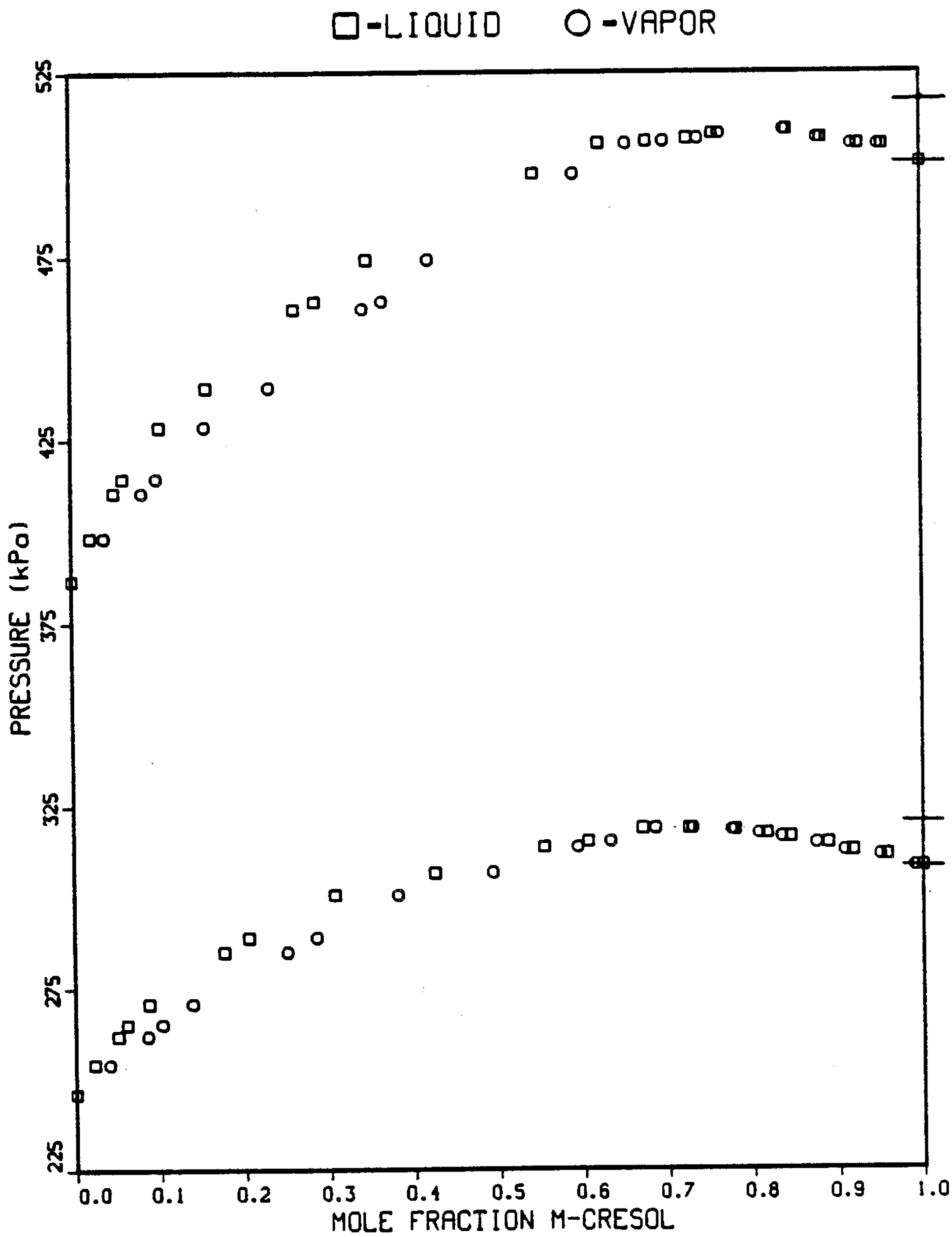

FIGURE 16

M-CRESOL/TETRALIN VLE DATA 300-325°C

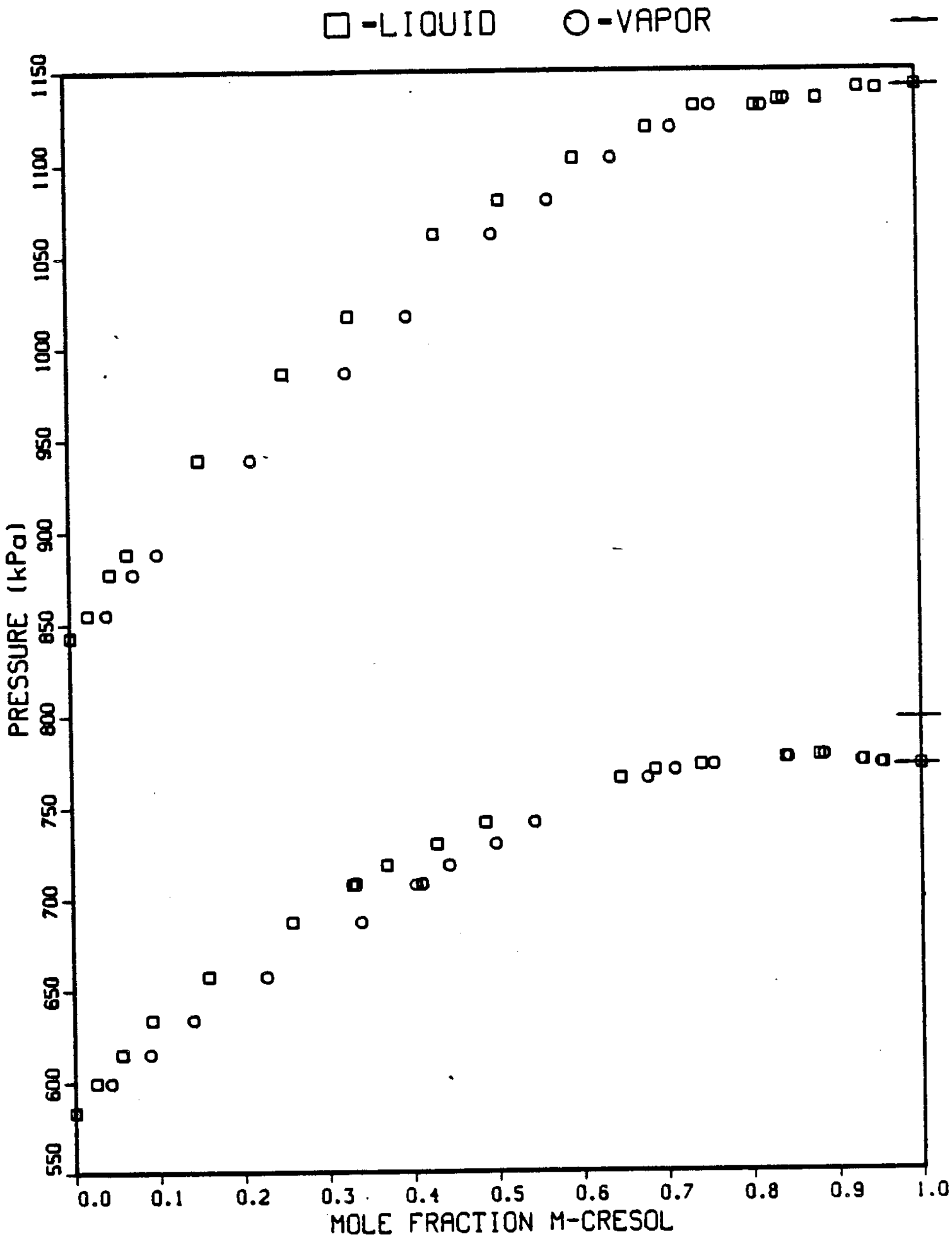

FIGURE 17

XY PLOT FOR M-CRESOL/TETRALIN AT 250°C

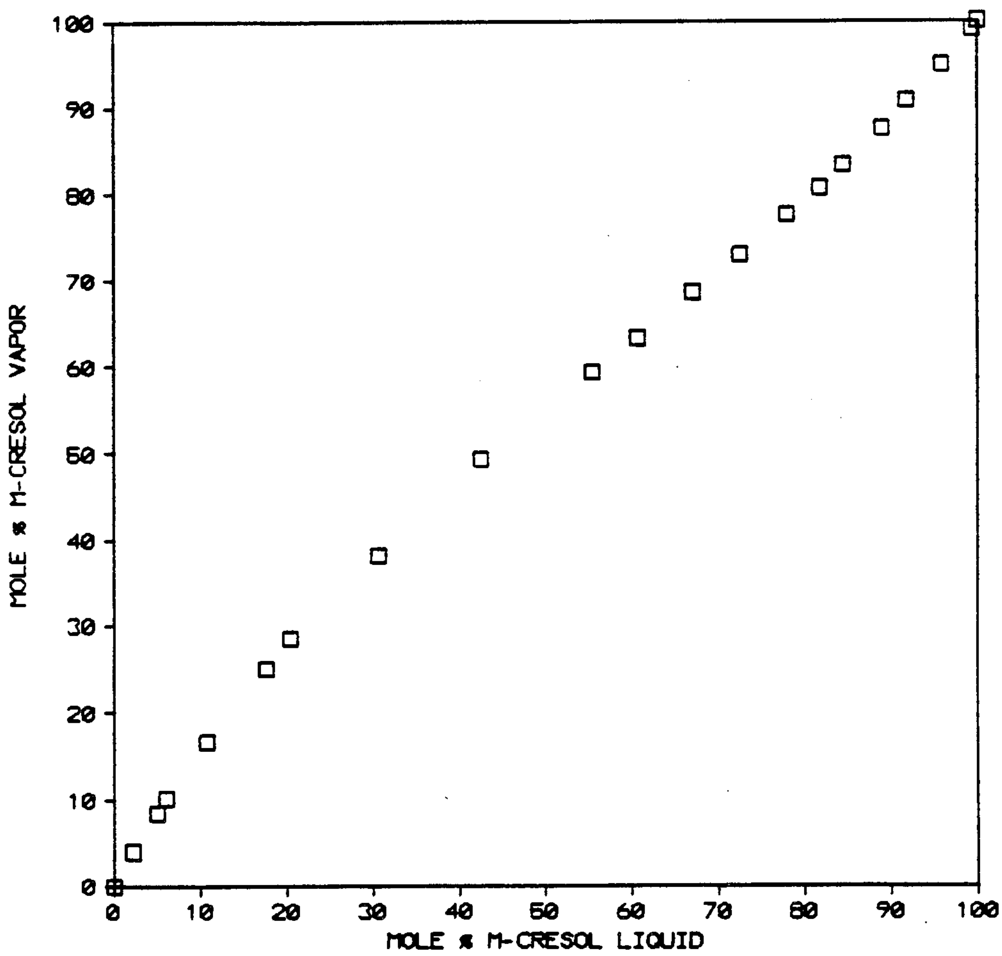

FIGURE 18

XY PLOT FOR M-CRESOL/TETRALIN AT 275°C

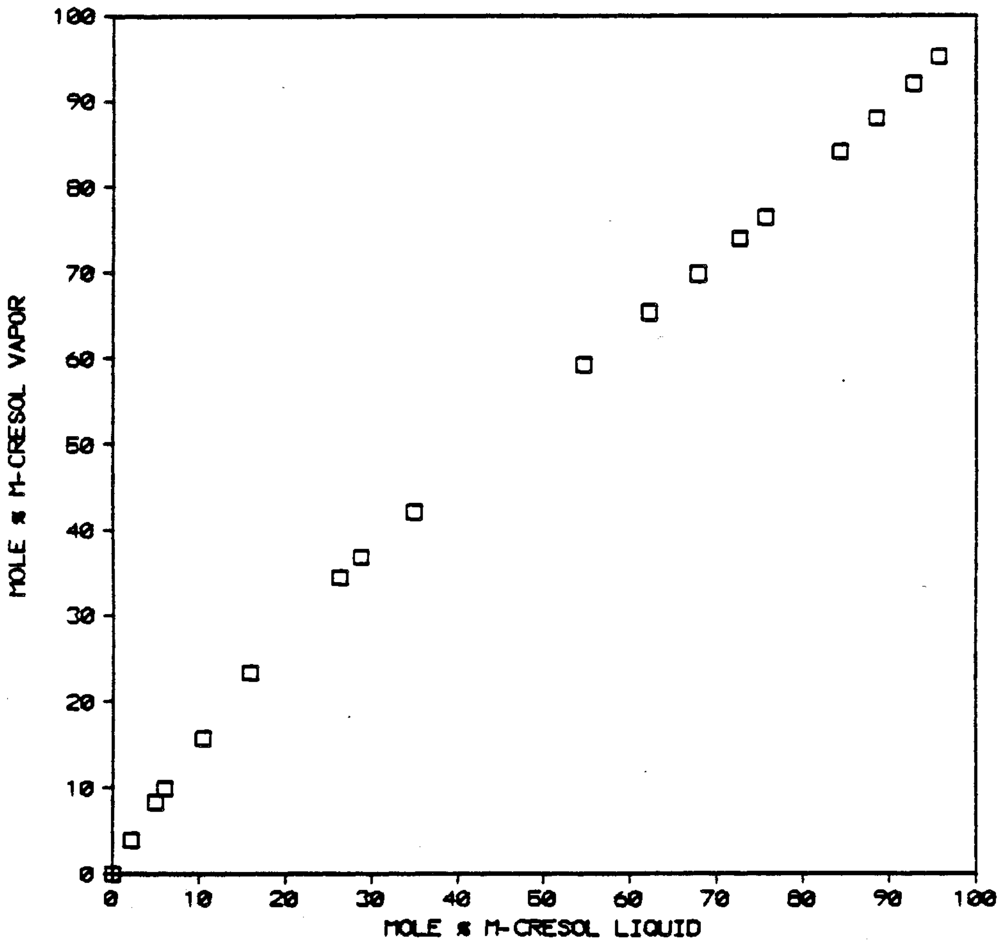

FIGURE 19

XY PLOT FOR M-CRESOL/TETRALIN AT 300°C

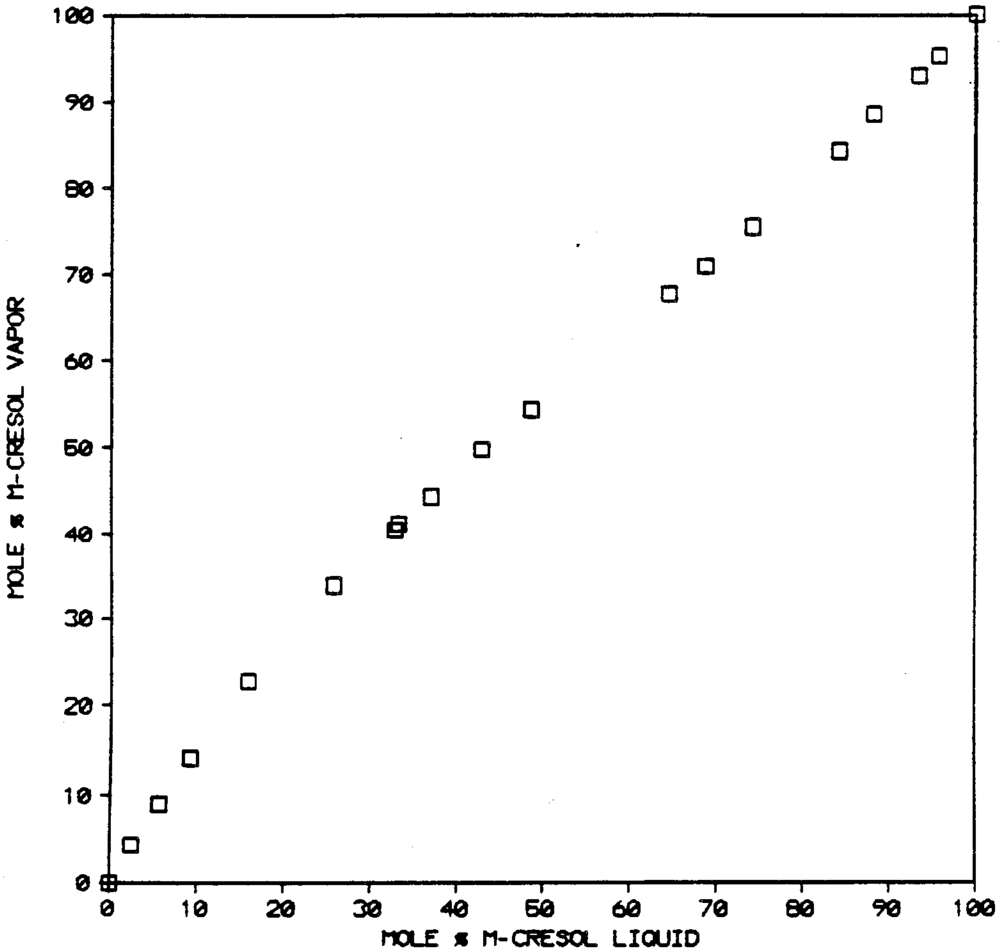

FIGURE 20

XY PLOT FOR M-CRESOL/TETRALIN AT 325°C

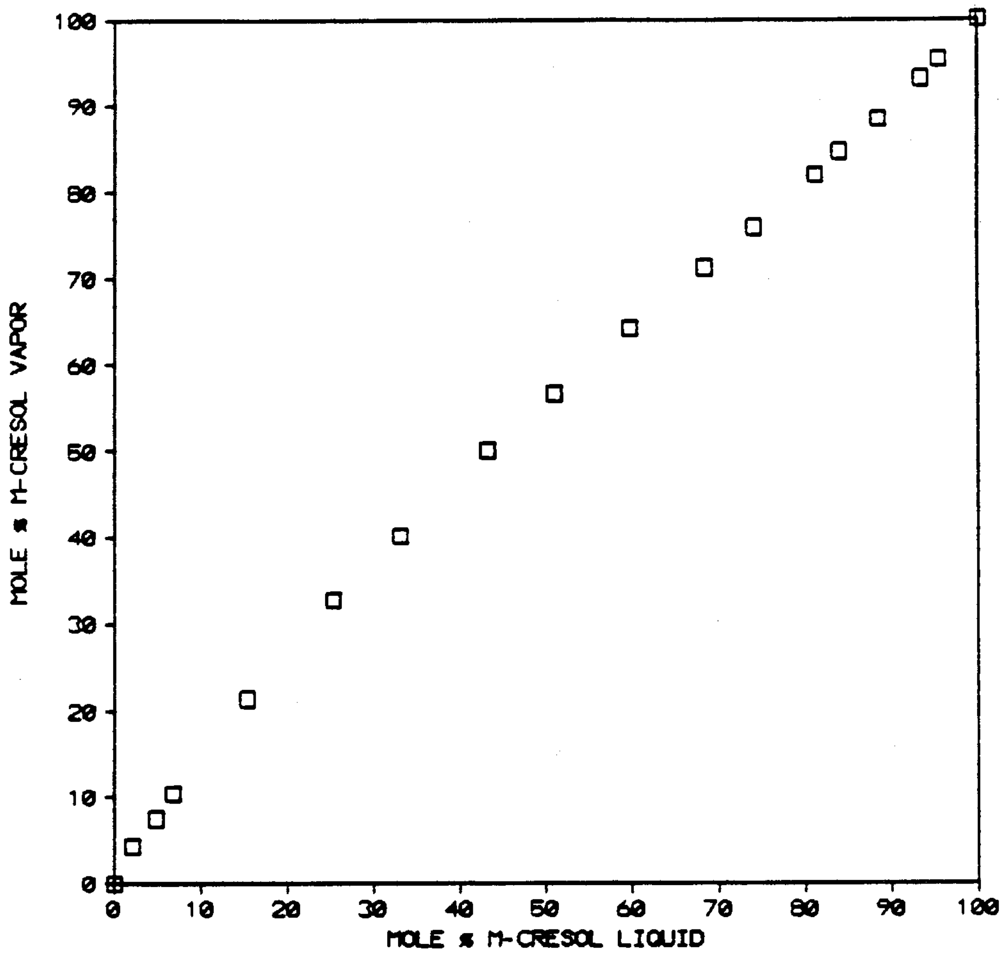

slightly higher pressures.

Figures 21 and 22 and Tables 11 and 12 show the VLE data obtained for the system tetralin/quinoline. Since tetralin is relatively nonpolar and there is not an acidic hydrogen to associate with quinoline, the system is relatively ideal. As discussed previously, the effect of water is far less substantial for quinoline than for m-cresol; consequently, there were few problems with error due to water contamination. Figures 23-26 are the x-y plots for this set of data.

TABLE 11

VLE MEASUREMENTS FOR TETRALIN/QUINOLINE

	Pressure (kPa)	X (mole percent tetralin)	Y (mole percent tetralin)
250°C	134.6*	0.0	0.0
	140.7	4.1	8.7
	151.0	10.2	18.8
	161.3	18.0	30.4
	182.6	32.6	46.9
	198.6	45.7	59.0
	213.8	58.9	70.4
	223.5	69.1	78.5
	235.6	82.6	87.9
	238.8	88.8	92.4
	246.0	100.0	100.0
275°C	221.9	0.0	0.0
	229.6	3.6	7.4
	243.4	9.9	17.7
	264.7	18.7	30.4
	286.0	30.5	44.2
	313.8	44.7	58.0
	337.2	58.3	69.2
	353.4	68.9	77.9
	369.7	81.7	87.2
	379.8	90.5	93.2
	386.6	100.0	100.0

* interpolated value

TABLE 12

VLE MEASUREMENTS FOR TETRALIN/QUINOLINE

	Pressure (kPa)	X (mole percent tetralin)	Y (mole percent tetralin)
300°C	346.2	0.0	0.0
	355.4	3.2	5.6
	373.1	7.9	13.7
	393.9	14.6	23.6
	416.7	22.0	33.1
	447.9	33.2	45.4
	474.7	43.7	54.6
	501.7	55.1	66.2
	522.6	65.4	74.1
	544.4	76.0	82.1
	571.5	91.3	93.6
	583.4	100.0	100.0
325°C	520.4	0.0	0.0
	553.4	7.5	12.3
	584.2	14.3	22.4
	616.3	22.2	31.9
	656.8	32.8	44.2
	691.8	43.0	53.9
	723.5	53.7	63.3
	762.6	65.6	73.3
	789.8	75.9	81.5
	826.6	91.6	93.6
	842.8	100.0	100.0

FIGURE 21

TETRALIN/QUINOLINE VLE DATA 250-275°C

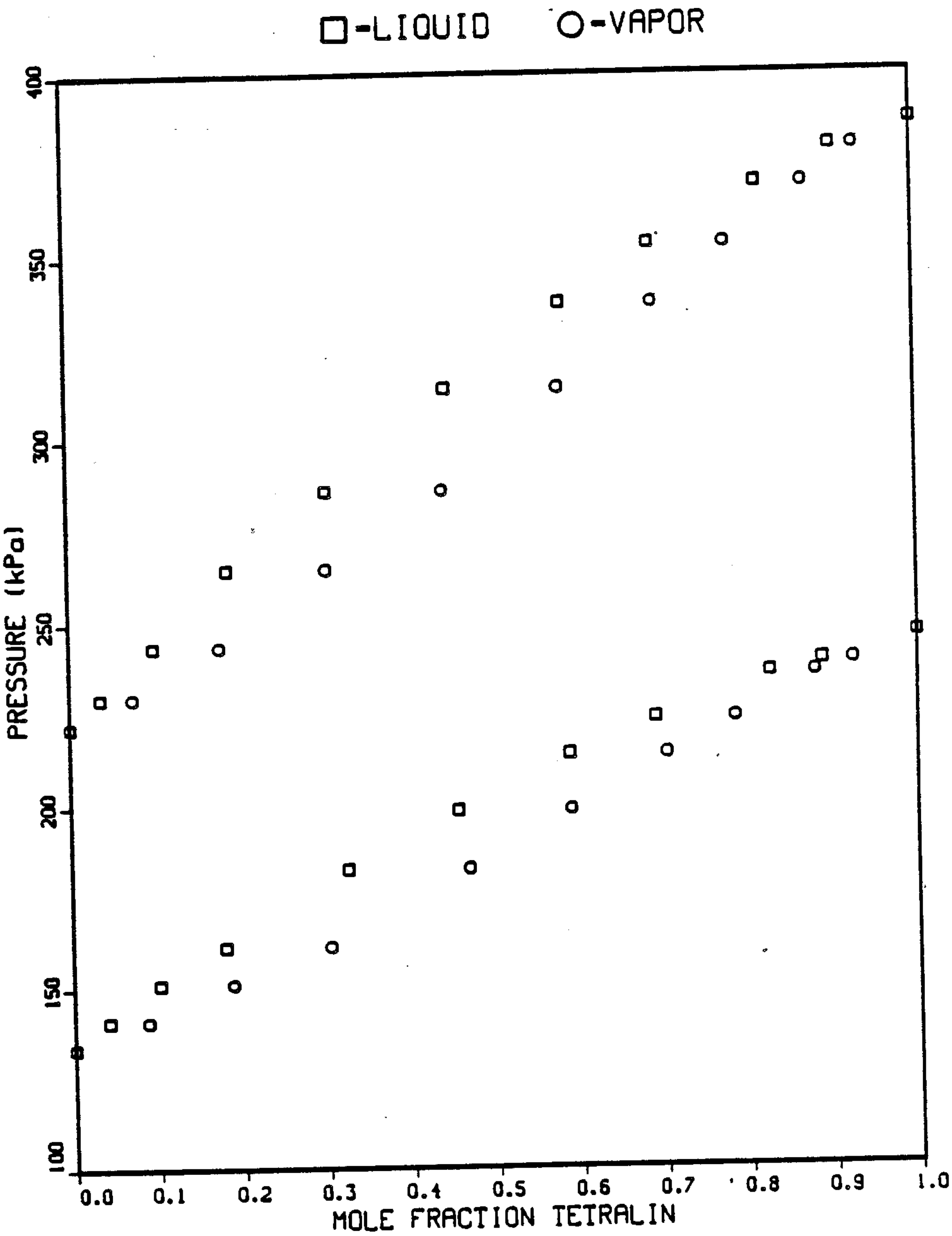

FIGURE 22

TETRALIN/QUINOLINE VLE DATA 300-325°C

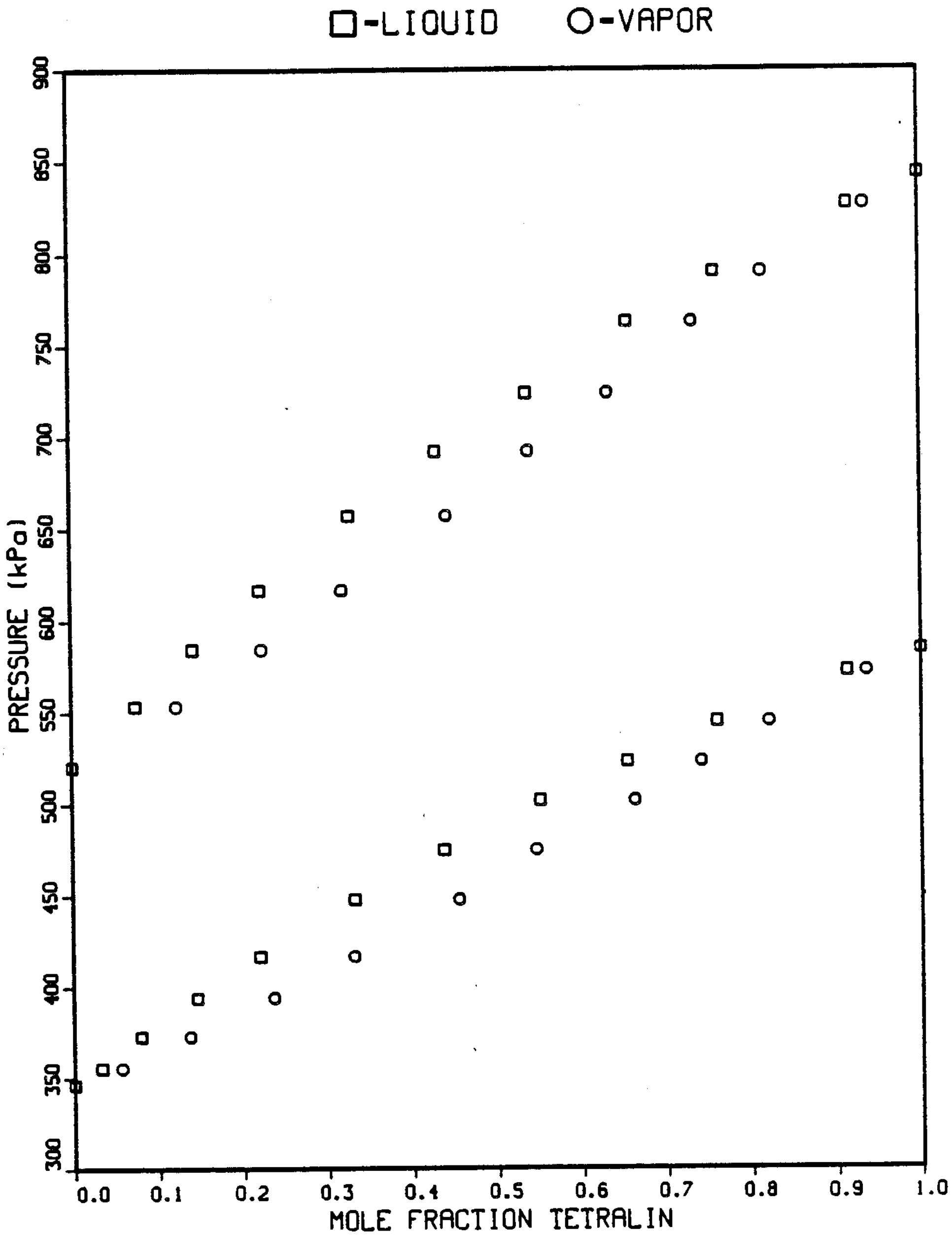

FIGURE 23

XY PLOT FOR TETRALIN/QUINOLINE AT 250°C

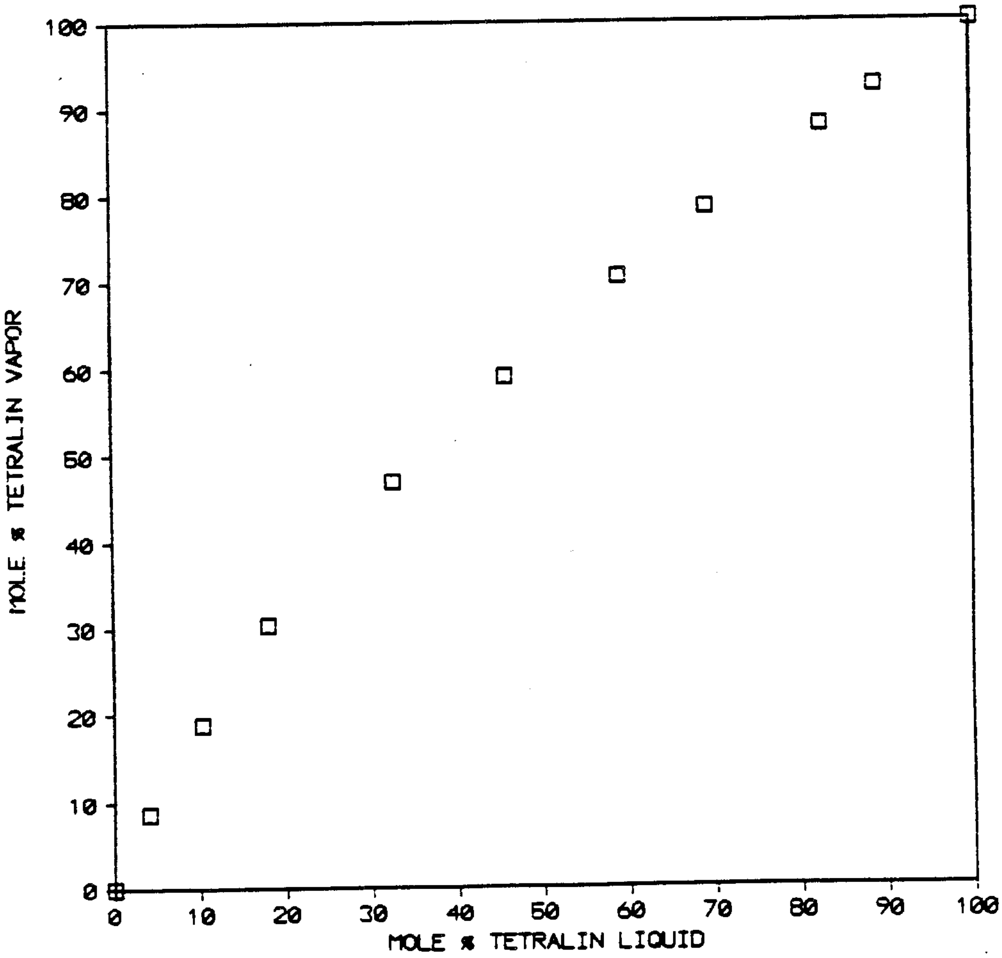

FIGURE 24

XY PLOT FOR TETRALIN/QUINOLINE AT 275°C

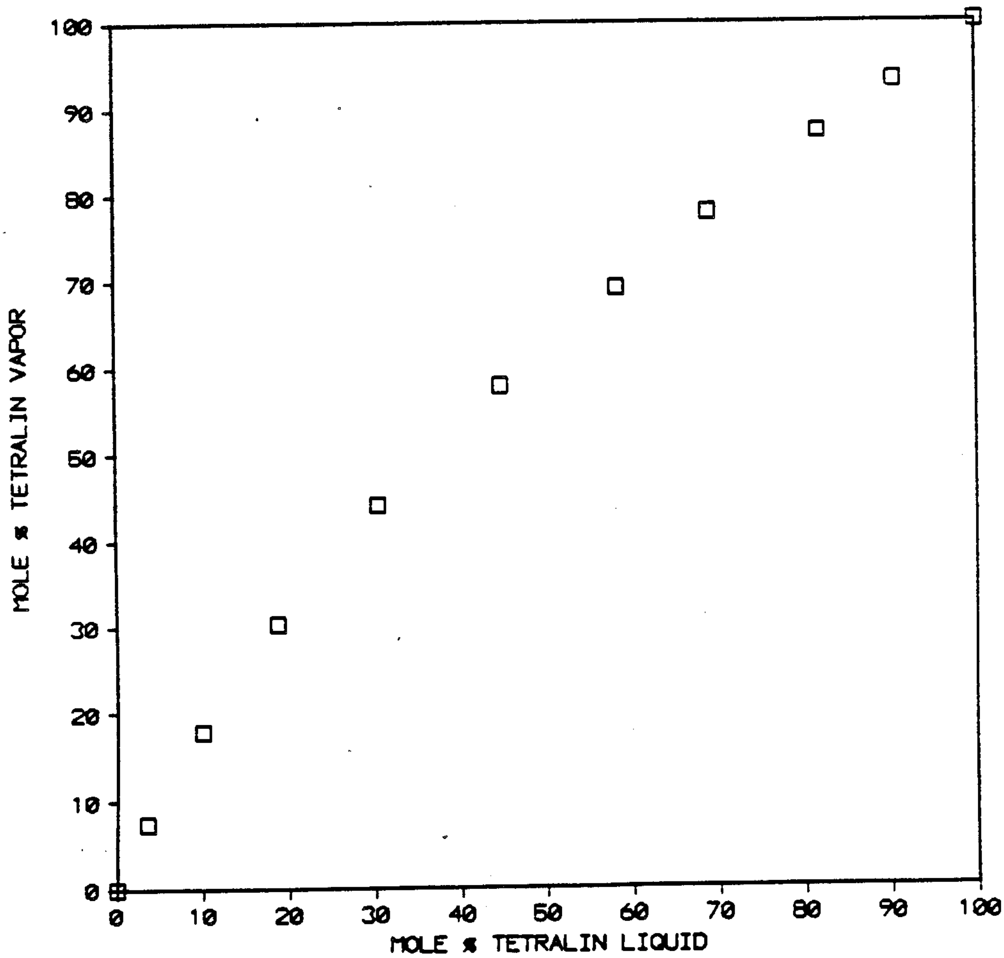

FIGURE 25
XY PLOT FOR TETRALIN/QUINOLINE AT 300°C

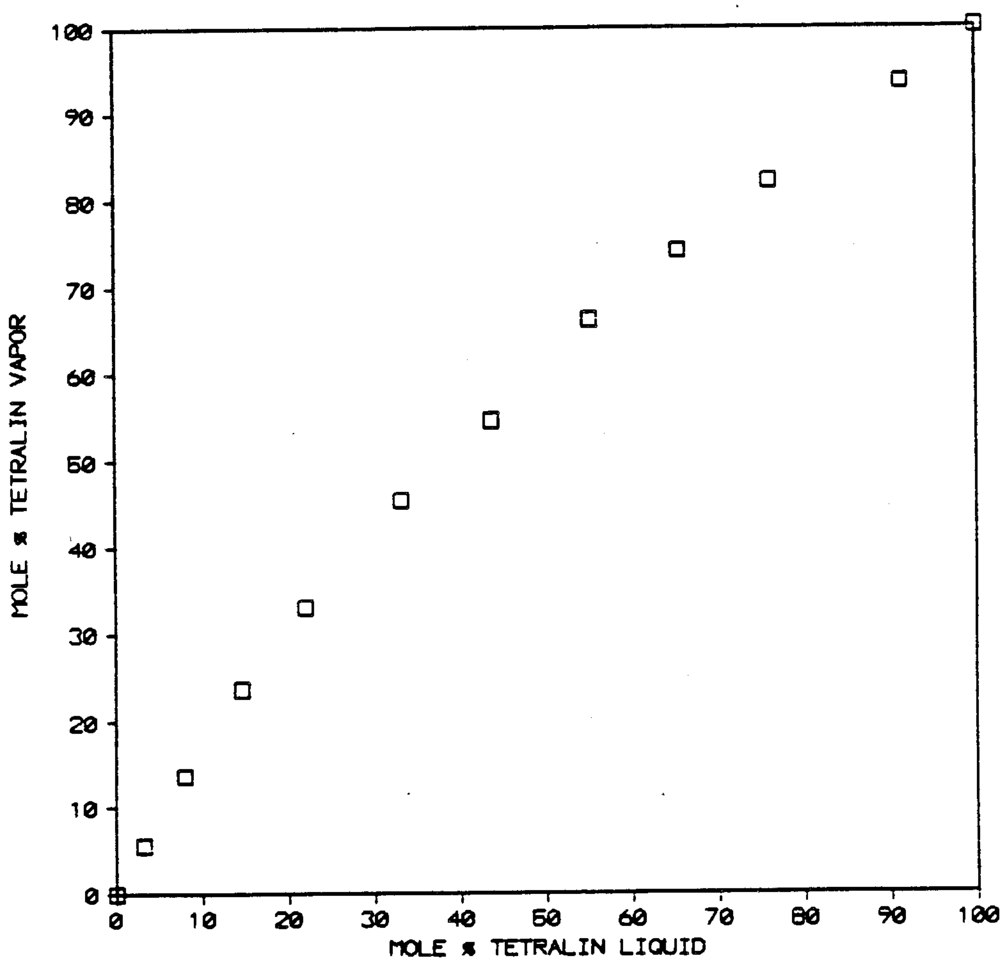

FIGURE 26

XY PLOT FOR TETRALIN/QUINOLINE AT 325°C

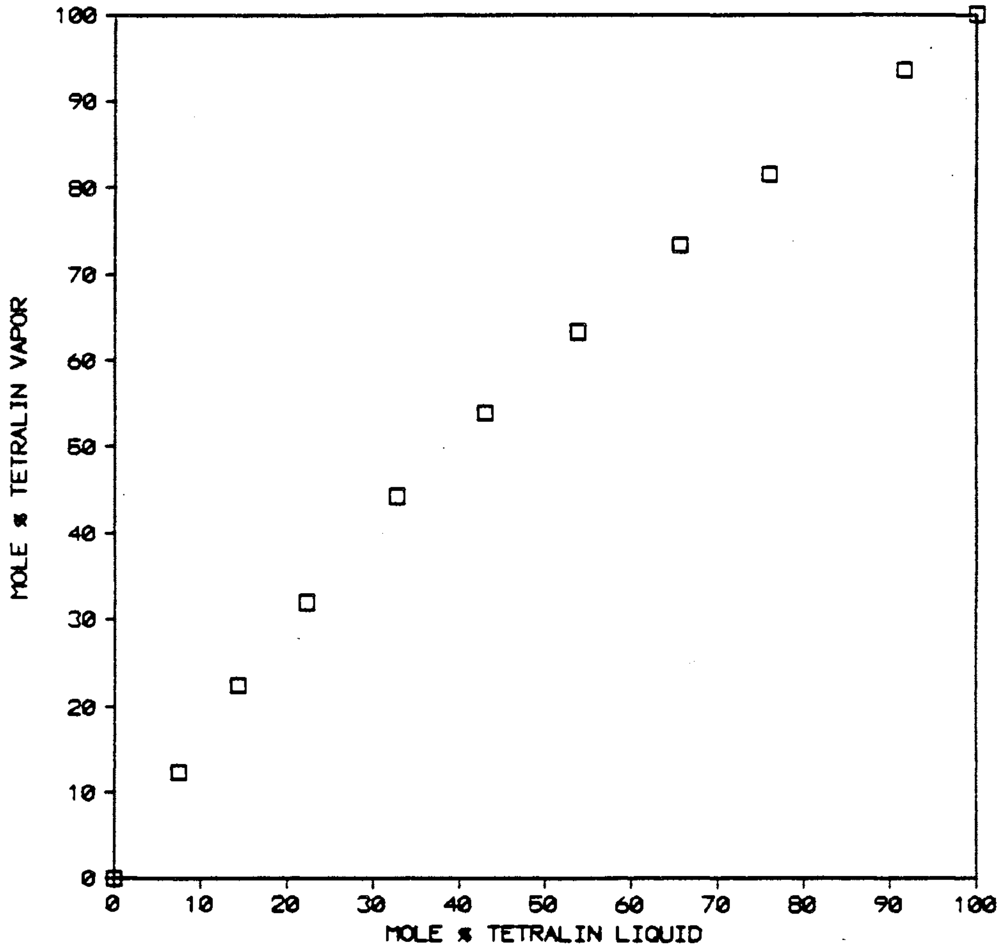

CORRELATIONAL METHODS

Development of thermodynamic models for highly non-ideal compounds, especially at high temperatures and pressures, has received little attention until recently. There is scarce data with which to test the applicability of currently proposed models. Because the data generated in this research are rare, the opportunity was taken to test some of the proposed models.

There are two important points in modeling VLE data; (1) the equation of state (EOS) needs to model the intermolecular interactions of a pure compound and (2) the mixing rules needed to model the intermolecular interactions between unlike molecules. In this research, two equations of state were studied as well as five mixing rules. In addition, even though the data from this investigation were not at extremely high pressures, fugacity coefficients were used in each phase rather than using an activity coefficient in the liquid phase. Current research trends are directed away from using activity coefficients in the liquid phase (Prausnitz et al. (1986)). It is not only inconvenient to have a separate model for each phase, but at higher pressures the activity coefficient models begin to fail. Obviously, at the critical point only one model can be used for both phases.

Fitting parameters to complex models has often been controversial. In this research, a sophisticated statistical algorithm was modified for direct application to fitting VLE data. The following discussions present the models studied as well as the method used for fitting parameters.

Equations of State

An equation of state (EOS) must be able to accurately reproduce the vapor pressures of fluids before attempting to model phase behavior data. For simple molecules (those with a high degree of symmetry) a two parameter EOS will suffice since the potential energy is a function of only the distance of separation and not the relative orientation between two molecules. However, when the molecules are no longer simple, a third parameter is required to account for the nonsymmetric forces; the acentric factor was introduced as the third parameter.

The three parameter EOS models asymmetric, nonpolar compounds well; however, the equation still lacks the ability to model polar compounds. For polar compounds the acentric factor is required to account not only for forces due to asymmetry but also for strong polar forces.

Two equations of state (EOS) were studied in this research, the Soave-Redlich-Kwong (SRK) equation as described by Soave (1971) and a recent modification to the SRK as proposed by Yesavage (1986). The SRK equation was chosen because it performs well for nonpolar compounds while remaining a simple, three parameter, cubic EOS. Cubic equations of this form have been used extensively in industrial applications, but are generally applicable only to non-polar fluids. The SRK equation was designed specifically to fit the vapor pressure curve of a pure, nonpolar fluid. The "a" term is temperature dependent and its temperature dependency is fixed so as to follow the vapor pressure curve. The acentric factor is calculated from vapor pressure data at $T_r = 0.7$; therefore, around $T_r = 0.7$, the SRK does a very good job at predicting vapor pressures. The SRK equation for a pure compound is given as:

$$P = RT/(v-b) - a(T)/v(v+b) \qquad (1)$$

where

$$b = 0.08664\ RT_c/P_c$$

$$a = (0.42747\ R^2T_c^2/P_c)\alpha$$

$$\alpha = (1 + m(1-(T_r)^{0.5}))^2$$

$$m = 0.48 + 1.574\omega - 0.176\omega^2$$

ω = acentric factor of the compound
T_c = critical temperature of compound
P_c = critical pressure of compound
T_r = T/T_c

For a mixture, mixing rules must be chosen to combine the "a" and "b" parameters. The form of the SRK equation for mixtures is dependent upon the mixing rules chosen. A discussion of the SRK equation for mixtures will be presented later.

As shown in Figure 27, a plot of $\alpha^{1/2}$ versus $1-T_r^{1/2}$ shows a linear relationship for pure nonpolar compounds. However, for the polar compounds shown in Figure 27, the relationship is not linear due to molecular association that occurs between polar molecules. This nonlinearity cannot be represented by the SRK equation; therefore, attempts have been made to modify the SRK, or other simple cubic EOS, so that vapor pressures of polar compounds can be predicted with reasonable accuracy. One such modification has recently been proposed by Yesavage (1986). Yesavage attempts to modify cubic equations of state while still using only three parameters. Other attempts have resulted in a fourth parameter whose magnitude may or may not have a relationship to the polarity of the fluid.

Yesavage's modification to the SRK (YSRK) is given as:

$$P = RT/(v-b) - a(T_c)\alpha_n\alpha_p/v(v+b) \qquad (2)$$

FIGURE 27

EFFECTS OF POLARITY[1]

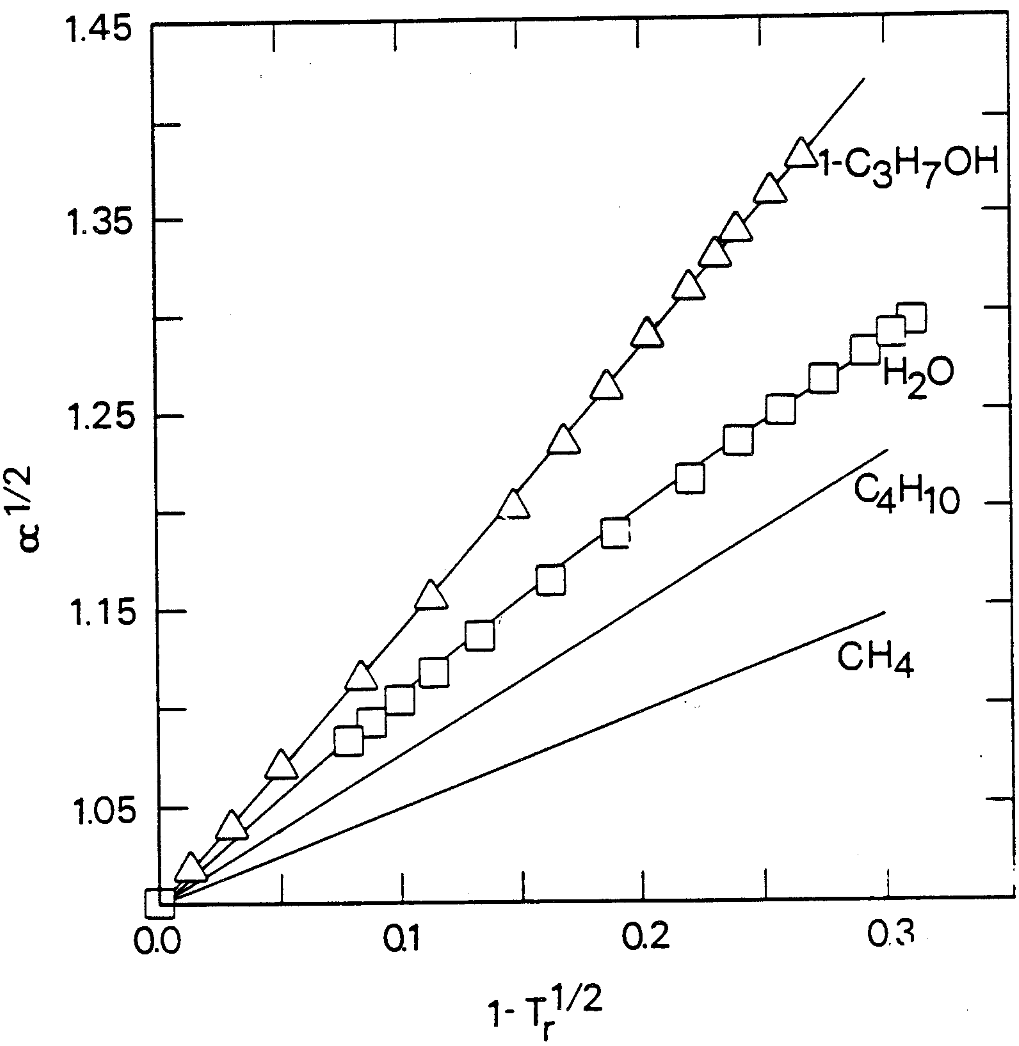

[1]Yesavage (1986)

where

$$b = 0.08664\ RT_c/P_c$$

$$a(T_c) = 0.42747\ R^2T_c^2/P_c$$

$$\alpha_n = (1.0 + m(1-T_r^{0.5}))^2$$

$$\alpha_p = 1 + R_p\ \exp(-R_p)^e - R_p\ \exp(-(R_p/T_r)^e)$$

$$m = 0.480 + 1.574\omega_n - 0.176\omega_n^2$$

R_p = polar parameter fit to VP data of polar parameter
T_c = critical temperature of the polar compound
P_c = critical pressure of the polar compound
e = 0.45
ω_n = acentric factor for nonpolar homomorph

Yesavage's modification to the SRK attempts to clearly separate the effects of shape from the effects of polarity. To accomplish this, Yesavage divides the "a" component of the SRK into three pieces. The $a(T_c)$ is the original term that models the symmetric forces that are present in simple molecules. The α_n term accounts for the intermolecular forces due to asymmetry. The term uses the acentric factor of a nonpolar homomorph to approximate the shape of the polar compound. The third term, α_p, is a new addition to the SRK that attempts to account only for the polar forces due to hydrogen bonding, dipole or quadrupole moments, etc. The expression for this third term is obtained from the effective intermolecular attractive potential and includes a new polar parameter, R_p, which is determined from vapor pressure data. When $R_p = 0$, indicating no polarity effects, the equation reduces to the SRK.

The Yesavage modification to the SRK is a function of the parameters a, b, ω_n, and R_p. Since ω_n is the acentric factor of a nonpolar homomorph, the equation of state remains essentially a three parameter EOS. A most encouraging aspect of the modification is that R_p appears to be related to the expected strength of polar interactions for different compounds. As can be seen in Table 13, the alcohol series shows a decreasing polar parameter with increasing molecular weight. This is a major improvement over other attempts to extend an EOS to polar compounds, Soave (1979); Soave (1980); and Mathias (1983).

Mixing Rules

While the importance of mixing rules has been neglected in the past, current research recognizes that mixing rules are the only method of introducing the effect of the forces between unlike molecules into the EOS. For simple, symmetric molecules, simple mixing rules will suffice; however, when the intermolecular forces between unlike molecules may include hydrogen bonding or forces due to dipole or quadrupole moments the mixing rules must be more sophisticated.

TABLE 13

POLAR PARAMETERS FOR ALCOHOL SERIES[1]

Compound	Polar Parameter, R_p
Water	29.58
Methanol	20.77
Ethanol	18.00
n-Propanol	4.64
n-Butanol	3.99

1 Yesavage (1986)

Originally, mixing rules for mixtures were proposed as simple arithmetic or geometric means of the parameters "a" and "b" as shown below, Prausnitz et al. (1986).

$$b = \sum x_i b_i \qquad (3)$$

$$a = \sum \sum x_i x_j a_{ij} \qquad (4)$$

Where x_i is the vapor or liquid composition of component i. Recent literature has suggested the necessity of a density dependency to properly model the interactions of highly non-ideal systems, Luedecke et al. (1985).

In this research, several forms of mixing rules were studied. All of these mixing rules modify only the original geometric mean mixing rule for the attractive term "a". The simple arithmetic mean mixing rule for the repulsive term "b" was not modified. The first mixing rule (Model 1) was a single, simple interaction parameter (k_{ij}) that was fit to all of the isotherms of each binary. This method is the simplest extension of the geometric mixing rule and for a binary is of the form:

$$a = x_1^2 a_1 + x_2^2 a_2 + 2x_1 x_2 (a_1 a_2)^{0.5}(1-k_{ij}) \qquad (5)$$

In combination with the EOS, this mixing rule leads to the following fugacity coefficient equation:

$$\ln\phi = \frac{b_i b}{RT(Z-D)} - \frac{b_i E}{b(Z+D)} + \frac{\ln(Z+D)}{Z}\left[\frac{Eb}{Db_i} - (2a_i x_i + 2*x_j(a_i a_j(1-k_{ij}))/bRT\right] - \ln(Z-D) \quad (6)$$

where $D = bP/RT$ and $E = aP/(RT)^2$ and all symbols are listed in Appendix D. This mixing rule was used as a base case from which all of the other models were compared.

Intermolecular interactions should decrease as the temperature rises due to the increase in the kinetic energies of the molecules. When the kinetic energies exceed the energies of association, the intermolecular associations will begin to break. Logic would dictate that the interaction parameter should decrease as the temperature rises. For this reason, the second mixing rule (Model 2) was a temperature dependent interaction parameter of the form, $k_{ij} = A + B/T$. The resulting fugacity coefficient equation is:

$$\ln\phi = \frac{b_i P}{RT(Z-D)} - \frac{b_i E}{b(Z+D)} + \frac{\ln(Z+D)}{Z}\left[\frac{Eb}{Db_i} - (2a_i x_i + 2*x_j(a_i a_j(1-A-B/T))/bRT^2\right] - \ln(Z-D) \quad (7)$$

where $D = bP/RT$ and $E = aP/(RT)^2$

The remaining mixing rules were different forms of density dependent interaction parameters. The reasoning behind the density dependent interaction parameters is that the intermolecular interactions should be significantly different between the liquid phase and the vapor phase, primarily due to the difference in molecular spacing. Volume is a function of composition, temperature and pressure; therefore, when volume dependency is incorporated into the mixing rule, in actuality the temperature, pressure and compositional dependencies of the mixing rule are changed. In order to have an equation of state which can be solved explicity, the density dependency can only be of the first order.

The density (or volume) dependency results in an equation of state that is quartic in volume. This requires little extra computational effort over the original cubic form. The algorithm for the solution of the quartic equation can be found in any mathematical handbook. The algorithm requires that a resultant cubic equation be solved. Any real root of the cubic equation can be used to solve for the quartic roots. The roots of the quartic equation corresponding to the vapor and liquid volumes are selected in the same manner as with a cubic equation. The largest real root is the vapor volume and the smallest real root that is greater than "b" is the liquid volume.

Three forms of density dependent mixing rules were studied. The first of these (as proposed by Holder et al. (1986)) is given as, $k_{ij} = A - B/v$ (Model 3). The corresponding fugacity coefficient equation is:

$$\ln\phi = \frac{b_i P}{RT(Z-D)} - \frac{b_i E}{b(Z+D)} + \frac{b_i F(D+2Z)}{bDZ(Z+D)} - \frac{F(1+x_i)}{DZx_i}$$

$$+ \frac{\ln(Z+D)}{Z}\left[\frac{Eb}{Db_i} - (2a_i x_i + 2*x_j(a_i a_j(1-A))/bRT - \frac{2b_i F}{bD^2}\right.$$

$$\left. + \frac{F(1+x_i)}{D^2 x_i}\right] - \ln(Z-D) \qquad (8)$$

where $D = bP/RT$

$E = (x_1^2 a_1 + x_2^2 a_2 + 2x_1 x_2 (a_1 a_2)^{0.5}(1-A))P/(RT)^2$

$F = 2x_1 x_2 \ (a_1 a_2)^{0.5} BP^2/(RT)^4$

The second density dependent mixing rule is a modification of the Holder mixing rule which incorporates a further temperature dependency (Model 4). The form of the interaction parameters is k_{ij}=(A - B/vRT) and the fugacity coefficient equation is the same as for the previous mixing rules with the temperature dependency included.

The final mixing rule was proposed by Luedecke, et al., (1985) (Model 5) and is also density dependent. However, the mixing rule is different in that it has a cubic compositional dependency. and has three parameters. The mixing rule (abbreviated as A+C's) for a binary system is given as:

$$a = x_1^2 a_1 + x_2^2 a_2 + 2x_1 x_2 (a_1 a_2)^{0.5}(1-A) \\ + 2x_1 x_2 (1/vRT)(x_1 c_{12} + x_2 c_{21}) \qquad (9)$$

The resulting fugacity coefficient equation is:

$$\ln\phi = \frac{b_i P}{RT(Z-D)} - \frac{b_i E}{b(Z+D)} + \frac{b_i F(D+2Z)}{bDZ(Z+D)} - \left(\frac{F}{x_i} + \frac{2x_i x_j c_{ij} P^2}{(RT)^4}\right)(1/ZD)$$

$$+ \frac{\ln(Z+D)}{Z}\left[\frac{Eb}{Db_i} - (2a_i x_i + 2*x_j(a_i a_j(1-A))/bRT - \frac{2b_i F}{bD^2}\right.$$

$$\left. + \frac{F}{D^2 x_i} + \frac{2x_i x_j c_{ij}}{b^2(RT)^2}\right] - \ln(Z-D) \qquad (10)$$

where $D = bP/RT$

$E = (x_1^2 a_1 + x_2^2 a_2 + 2x_1 x_2 (a_1 a_2)^{0.5}(1-A))P/(RT)^2$

$F = 2x_1 x_2 (x_1 c_{12} + x_2 c_{21})P^2/(RT)^4$

Several other modifications of the above mixing rules were studied briefly; these will be discussed in the analysis of the models.

Parameter Estimation

The estimation of parameters in mathematical models from experimental data can range from using very simple, to very sophisticated methods. The complexity of the method chosen is based upon the desired statistical accuracy of the fit. Typically, in a simple method, a least squares criterion is used; that is, the best estimates of the parameters are those which minimize the weighted sum of the squared deviations of the observed values from their calculated values. In this method the variables are divided into two groups, independent and dependent variables. A very basic assumption in the least squares method is that the values of the independent variables are true values. This assumption does not take into account the experimental errors associated with the independent variables and therefore inherently cannot give the best possible statistical estimation of the parameters.

When fitting VLE data to a mathematical model, the temperature (T) and the liquid composition (x) may be chosen as the independent variables while the pressure (P) and the vapor composition (y) are the dependent variables. One typical criterion used as the basis for estimating the best fit parameters is to minimize the difference between the measured and calculated bubble point pressures, Holder

(1986) and Mansoori (1986). In this case the following function is minimized:

$$S = \sum_{i}^{N} (P^{calc} - P^{meas})^2/(P^{meas})^2 \qquad (11)$$

"N" is the number of experimental data points. This method neglects experimental error in both T and x and does not use the vapor composition (y) at all.

A much more sophisticated model utilitzes all experimental data and the associated errors to obtain the best statistical estimates of the parameters. One such method, and the one used in this research, is known as the "maximum likelihood" method as described by Anderson et al. (1978). In the case of evaluating parameters from VLE data, the parameters are chosen so as to minimize the following function:

$$S = \sum_{i}^{N} \left[(P^{calc} - P^{meas})^2/\sigma_p^2 + (y^{calc} - y^{meas})^2/\sigma_y^2 + (T^{calc} - T^{meas})^2/\sigma_t^2 + (x^{calc} - x^{meas})^2/\sigma_x^2 \right] \qquad (12)$$

where σ_p, σ_y, σ_t, σ_x are the statistical variances associated with the measured variables and "N" is the number of data points. Essentially, the method allows all experimental values to float within prescribed variances, thereby giving the best possible fit of the VLE data.

Anderson's development of the maximum likelihood method requires that the dependent variables be written explicitly in terms of the independent variables and parameters. In the case of VLE data, to determine two of the variables explicitly requires certain approximations. If fugacity coefficients are used in each phase, then the vapor phase is considered not a strong function of pressure and vapor composition. In the liquid phase it is assumed that the fugacity is fairly independent of the pressure, so that the following equations can be written.

$$P = P^r(\phi_2^l(1-x_1)\phi_1^v + \phi_2^v\phi_1^l x_1)/\phi_1^v\phi_2^v \tag{13}$$

$$y_1 = \phi_2^v\phi_1^l x_1/(\phi_2^l(1-x_1)\phi_1^v + \phi_2^v\phi_1^l x_1) \tag{14}$$

$$\phi_i^v = f(T,P^r,y_1^r) \text{ and } \phi_i^l = f(T,P^r,x_1) \tag{15}$$

r = previous iteration

These approximations may or may not be good depending upon the fluids and the region of interest. It was suggested that the method could be developed using the implicit relationships between the variables. The following derivation presents a development of the maximum likelihood method for implicit relationships between the variables for two constraints.

Development of the Maximum Likelihood Method

It is assumed that there are N experimental observations consisting of the measured variables X, Y, and Z. K variables are chosen to be the independent variables with the remaining 2 variables being dependent. X is a vector that consists of the true values of the chosen independent variables and is of length NK. Y and Z are each a vector of one dependent variable and both are of length N.

Since there are two dependent variables, two equations (or constraints) will be required to relate the dependent variables to the independent variables and parameters. These are written as:

$$F\ (X,\ Y,\ Z,\ \Theta) = 0 \tag{16}$$

$$G\ (X,\ Y,\ Z,\ \Theta) = 0 \tag{17}$$

Θ is a vector of L undetermined parameters, and F and G are vectors of length N (one equation for each data point).

The criterion for convergence is chosen as the minimization of the following function:

$$S = (X-X^m)^T\lambda(X-X^m) + (Y-Y^m)^T\gamma(Y-Y^m) + (Z-Z^m)^T\delta(Z-Z^m) \tag{18a}$$

The superscript m indicates a measured value. λ is a diagonal matrix of size (NK,NK) whose diagonal elements are the squared reciprocals of the variances for the independent variables. γ and δ are diagonal matrices of size (N,N) whose diagonal elements are the squared reciprocals of the variances of the dependent variables Y and Z respectively. If Y and Z can be eliminated from equation (18a) based on the constraints 16 and 17, then the above function can be minimized in the following manner.

$$\partial S/\partial X = 0 \quad \text{and} \quad \partial S/\partial \Theta = 0 \qquad (19\ \&\ 20)$$

To eliminate Y and Z from equation (18a), they must be written in terms of X and Θ. To accomplish this substitution, the constraint equations are linearized by a first order Taylor series expansion about the most recent estimates of the parameters and the true values of the independent variables.

$$F \simeq F^r + F_x(X-X^r) + F_y(Y-Y^r) + F_z(Z-Z^r) + F_\theta(\Theta-\Theta^r) \qquad (21)$$

$$G \simeq G^r + G_x(X-X^r) + G_y(Y-Y^r) + G_z(Z-Z^r) + G_\theta(\Theta-\Theta^r) \qquad (22)$$

The superscript r indicates the previous iteration. By definition of the constraint equations, F and G equal zero. F^r and G^r are vectors of length N containing the values of F and G at the previous iteration. F_x and G_x are the derivatives of F and G with respect to the independent variables in vector X and are sparse matrices of size (N,NK). F_y, F_z, G_y, and G_z are derivatives of F and G with respect to the dependent variables Y and Z and are diagonal matrices of size (N,N). F_θ and G_θ are the derivatives of F and G with respect to each parameter in vector Θ and are matrices of size (N,L).

These two equations (21 and 22) can be solved for $Y-Y^r$ and $Z-Z^r$ in terms of X, Θ, and the previous values of F and G.

$$\begin{aligned} Z - Z^r = -(G_z - G_y F_y^{-1} F_z)^{-1}((G^r - G_y F_y^{-1} F^r) \\ +(G_x - G_y F_y^{-1} F_x)(X - X^r) \\ +(G_\theta - G_y F_y^{-1} F_\theta)(\Theta - \Theta^r)) \end{aligned} \tag{23}$$

$$\begin{aligned} Y - Y^r = -(G_y - G_z F_z^{-1} F_y)^{-1}((G^r - G_z F_z^{-1} F^r) \\ +(G_x - G_z F_z^{-1} F_x)(X - X^r) \\ +(G_\theta - G_z F_z^{-1} F_\theta)(\Theta - \Theta^r)) \end{aligned} \tag{24}$$

These equations can be substituted into equation 18a to give the function to minimized in terms of F^r, G^r, Θ, Y^r, Y^m, Z^r, Z^m, and X.

$$
\begin{aligned}
S = \; & (X - X^m)^T \lambda (X - X^m) \\
& + (Y^r - Y^m - (G_y - G_z F_z^{-1} F_y)^{-1} \\
& *((G^r - G_z F_z^{-1} F^r) + (G_x - G_z F_z^{-1} F_x)(X - X^r) + (G_\theta - G_z F_z^{-1} F_\theta)(\Theta - \Theta^r)))^T \\
& *\gamma \; (Y^r - Y^m - (G_y - G_z F_z^{-1} F_y)^{-1} \\
& * \; ((G^r - G_z F_z^{-1} F^r) + (G_x - G_z F_z^{-1} F_x)(X - X^r) + (G_\theta - G_z F_z^{-1} F_\theta)(\Theta - \Theta^r))) \\
& + (Z^r - Z^m - (G_z - G_y F_y^{-1} F_z)^{-1} \\
& *((G^r - G_y F_y^{-1} F^r) + (G_x - G_y F_y^{-1} F_x)(X - X^r) + (G_\theta - G_y F_y^{-1} F_\theta)(\Theta - \Theta^r)))^T \\
& *\delta \; (Z^r - Z^m - (G_z - G_y F_y^{-1} F_z)^{-1} \\
& *((G^r - G_y F_y^{-1} F^r) + (G_x - G_y F_y^{-1} F_x)(X - X^r) + (G_\theta - G_y F_y^{-1} F_\theta)(\Theta - \Theta^r)))
\end{aligned}
\tag{18b}
$$

The following quantities are redefined:

$$f^r = Y^r - (G_y - G_z F_z^{-1} F_y)^{-1} (G^r - G_z F_z^{-1} F^r) \tag{25a}$$

$$f_x = \; - (G_y - G_z F_z^{-1} F_y)^{-1} (G_x - G_z F_z^{-1} F_x) \tag{25b}$$

$$f_\theta = \; - (G_y - G_z F_z^{-1} F_y)^{-1} (G_\theta - G_z F_z^{-1} F_\theta) \tag{25c}$$

$$g^r = Z^r - (G_z - G_y F_y^{-1} F_z)^{-1} (G^r - G_y F_y^{-1} F^r) \tag{25d}$$

$$g_x = \; - (G_z - G_y F_y^{-1} F_z)^{-1} (G_x - G_y F_y^{-1} F_x) \tag{25e}$$

$$g_\theta = \; - (G_z - G_y F_y^{-1} F_z)^{-1} (G_\theta - G_y F_y^{-1} F_\theta) \tag{25f}$$

So that,

$$
\begin{aligned}
S = \; & (X - X^m)^T \lambda (X - X^m) + [f^r - Y^m + f_x (X - X^r) + f_\theta (\Theta - \Theta^r)]^T \gamma \\
& *[f^r - Y^m + f_x (X - X^r) + f_\theta (\Theta - \Theta^r)] \\
& + [g^r - Z^m + g_x (X - X^r) + g_\theta (\Theta - \Theta^r)]^T \delta \\
& *[g^r - Z^m + g_x (X - X^r) + g_\theta (\Theta - \Theta^r)]
\end{aligned}
\tag{18c}
$$

By redefining variables in equations 25a-25f the resulting equation 18c has the same form as equation 11 in Anderson et al. (1978). Thus from this point on, the implicit method developed here is exactly the same as the explicit method as described by Anderson. Following their development the two minimizing conditions (equations 19 and 20) are applied to 18c to obtain:

$$\Delta\Theta = \Theta^{r+1} - \Theta^{r} = -[T - R^{T}D^{-1}R]^{-1}[U - R^{T}D^{-1}Q] \qquad (26)$$

and

$$\Delta X = X^{r+1} - X^{r} = -D^{-1}[Q + R\Delta\Theta] \qquad (27)$$

where the following matrices as defined as:

$$D = \lambda + f_x^T\gamma f_x + g_x^T\delta g_x \qquad (28a)$$

$$R = f_x^T\gamma f_\theta + g_x^T\delta g_\theta \qquad (28b)$$

$$T = f_\theta^T\gamma f_\theta + g_\theta^T\delta g_\theta \qquad (28c)$$

$$U = f_\theta^T\gamma\Delta Y^m + g_\theta^T\delta\Delta Z^m \qquad (28d)$$

$$Q = \lambda\Delta X^m + f_x^T\gamma\Delta Y^m + g_x^T\delta\Delta Z^m \qquad (28e)$$

$$\Delta X^m = X^r - X^m \qquad (28f)$$

$$\Delta Y^m = Y^r - Y^m \qquad (28g)$$

$$\Delta Z^m = Z^r - Z^m \qquad (28h)$$

Equations 26 and 27 are the basis for the maximum likelihood method and correspond to Anderson's equations 12 and 13. θ^{r+1} are the new guesses for the parameters and X^{r+1} are the new estimates for the "true values" of the independent variables. Equations 23 and 24 are solved to give the new estimates of the dependent variables. The value of S (SN) is then calculated from equation 18c and compared to the last value of S. Convergence is achieved when (SN - S)/SN is below the criterion level.

Computationally, the algorithm is not difficult. Most matrices are either diagonal or symmetric for which inversion algorithms can be easily written. The largest symmetric matrix to be inverted is (NK,NK); therefore, the computational time involved is related to the number of experimental data points and the number of independent variables.

Maximum Likelihood Method for VLE Data

The preceding derivation can be used to fit almost any type of thermodynamic data as well as many other types of data. When the maximum likelihood equation is applied to VLE data, the following equations are used.

For binary phase behavior, the Gibb's phase rule indicates that there are two degrees of freedom. Therefore, if the variables are temperature (T), pressure (P), liquid composition (x), and vapor composition (y) then fixing any two of the variables will determine the other two, based upon two equilibria requirements:

$$f_1^v = f_1^l \text{ and } f_2^v = f_2^l \tag{29}$$

These equations can be written in terms of the compositions and the fugacity coefficients.

$$\phi_1^v y_1 = \phi_1^l x_1 \qquad \phi_2^v y_2 = \phi_2^l x_2 \qquad (30\ \&\ 31)$$

where $$y_1 + y_2 = 1 \quad \text{and} \quad x_1 + x_2 = 1 \qquad (32\ \&\ 33)$$

The two constraint equations for the maximum likelihood method are give as:

$$F(X,Y,Z,\Theta) = \phi_1^v y_1 - \phi_1^l x_1 = 0 \tag{34}$$

$$G(X,Y,Z,\Theta) = \phi_2^v y_2 - \phi_2^l x_2 = 0 \tag{35}$$

If T and x are chosen as the independent variables, then the vector X will consist of N sets of T and x and will be 2N long. Vector Y will consist of N values of P as a dependent variable and vector Z will consist of N values of y as the other dependent variable. Θ is the vector containing L interaction parameters for the mixing rule.

The function to be minimized is:

$$S = \sum_{i}^{N}\Big[(P^{calc} - P^{meas})^2/\sigma_p^2 + (T^{calc} - T^{meas})^2/\sigma_t^2 + (x^{calc} - x^{meas})^2/\sigma_x^2 + (y^{calc} - y^{meas})^2/\sigma_y^2\Big] \quad (36)$$

σ_p, σ_t, σ_x, and σ_y are the variances of the measured values P, T, x, and y. These variances are estimated as the experimental errors in the variables and are based on experience with the experimental apparatus used to obtain the data. For all of the VLE fits, the variances were estimated to be:

$$\begin{aligned} \sigma_p &= 0.7 \text{ kPa below } 689.5 \text{ kPa} \\ &= 3.5 \text{ kPa between } 689.5\text{-}\ 3500 \text{ kPa} \\ &= 13.79 \text{ kPa above } 3500 \text{ kPa} \\ \sigma_t &= 0.1 \text{ K} \\ \sigma_x,\ \sigma_y &= 0.002 \text{ mole fraction} \end{aligned}$$

The derivatives F_x, G_x, F_θ, G_θ, F_y, G_y, F_z and G_z as given in equation 18b can either be calculated analytically or numerically. The analytic expressions for the derivatives were quite cumbersome. A much easier method was to calculate the derivatives numerically; using a five point central difference formula, Abramowitz et al. (1965).

This maximum likelihood algorithm was independent of the equation of state. To change to a different EOS, only the subroutine that calculated the fugacity coefficients needed to be changed. To change the number of parameters used in the model, a derivative was calculated for each function (F and G) with respect to each parameter.

Maximum Likelihood Method for Vapor Pressure Data

To derive the maximum likelihood method for fitting vapor pressure data, the same derivation as presented previously applies except that only one constraint is now required. That constraint is:

$$F(X,Y,\Theta) = \phi^{v} - \phi^{l} = 0 \tag{37}$$

Consequently, to apply the previous derivation to one constraint, eliminate the function G as well as the dependent variable Z and all of their derivatives. The remaining equations will only be a function of F, Y, X, and Θ. The algorithm is the same as before; however, Anderson does offer a slightly modified version of equations 26 and 27 that allows for less computational effort. The function being minimized in this case is:

$$S = \sum_{i}^{N}\left[(P^{calc}-P^{meas})^2/\sigma_p^2 + (T^{calc}-T^{meas})^2/\sigma_t^2\right] \quad (38)$$

DISCUSSION OF CORRELATIONAL RESULTS

The correlational methods discussed in the previous section were applied to the phase behavior data reported in this thesis. An analysis of the correlational work is presented in this section. All computer programs developed for this work are presented in Appendix C.

Vapor Pressures

The initial step was to predict the vapor pressure of m-cresol, quinoline and tetralin using the original SRK equation of state. Listed in Table 14 are the critical properties and acentric factors of the compounds from Reid et al. (1977) and Lin et al. (1980). In all cases some discrepancies exist in the reported critical properties. Since the critical properties are quite high for these compounds, they are difficult to measure. In addition, it is documented (Simnick et al. (1977)) that tetralin decomposes rapidly at temperatures above 700 K which hinders the physical measurements. The predictive capabilities of any EOS are substantially diminished when incorrect critical properties are used; therefore, the correlational work in this thesis is subject to this error. The critical values ultimately chosen to be used in this research were selected based on a ln P versus 1/T plot of the vapor pressures. The

TABLE 14

CRITICAL PROPERTIES AND ACENTRIC FACTORS

Compound	T_c(K)	P_c (kPa)	ω
M-Cresol	705.8	4560	0.452
Quinoline	800.2	5775	0.316
Tetralin	719.2	3515	0.327

TABLE 15

HOMOMORPH ACENTRIC FACTORS AND POLAR PARAMETERS

Compound	ω_n	R_p
M-Cresol	0.326	0.909
Quinoline	0.303	0.0268
Tetralin	0.327	0.0

published values of the critical properties that best coincided with vapor pressure data were chosen.

The results of the vapor predictions are shown in Figures 28-30. Since the SRK equation fits the acentric factor at T_r=0.7, the predictions should be the best at this point. For all three compounds, an acentric factor was calculated from vapor pressure data at T_r=0.7. The only major difference in the calculated acentric factors and the published acentric factors was for tetralin. From Figure 28 it can be seen that the SRK prediction using the published acentric factor (.303) is quite bad even at a reduced temperature of T_r = 0.7. The new acentric factor was calculated to be 0.327 and, as can be seen in Figure 28, the SRK prediction is significantly better.

Yesavage's modification of the SRK equation uses an acentric factor for a nonpolar homomorph and a polar parameter, R_p, which is obtained from vapor pressure data. The acentric factors and polar parameters used in this work are listed in Table 15. Since tetralin is nonpolar, the polar parameter was zero.

The polar parameters were obtained by the regression of vapor pressure data using the maximum likelihood method. It was noted that when fitting data to determine the polar parameter, the data needed to be evenly spaced so as not to

FIGURE 28

TETRALIN VAPOR PRESSURE PREDICTIONS

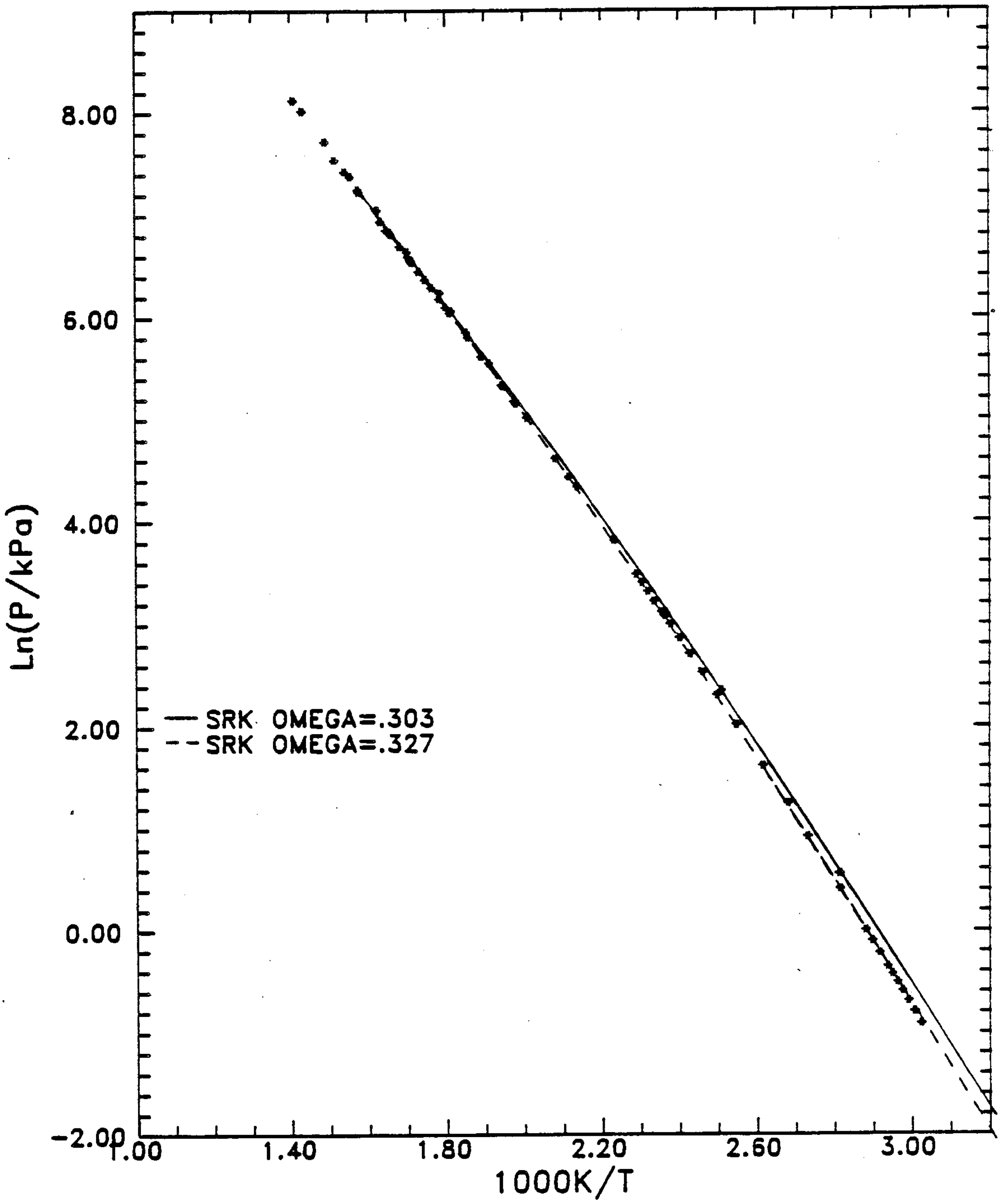

FIGURE 29
M-CRESOL VAPOR PRESSURE PREDICTIONS

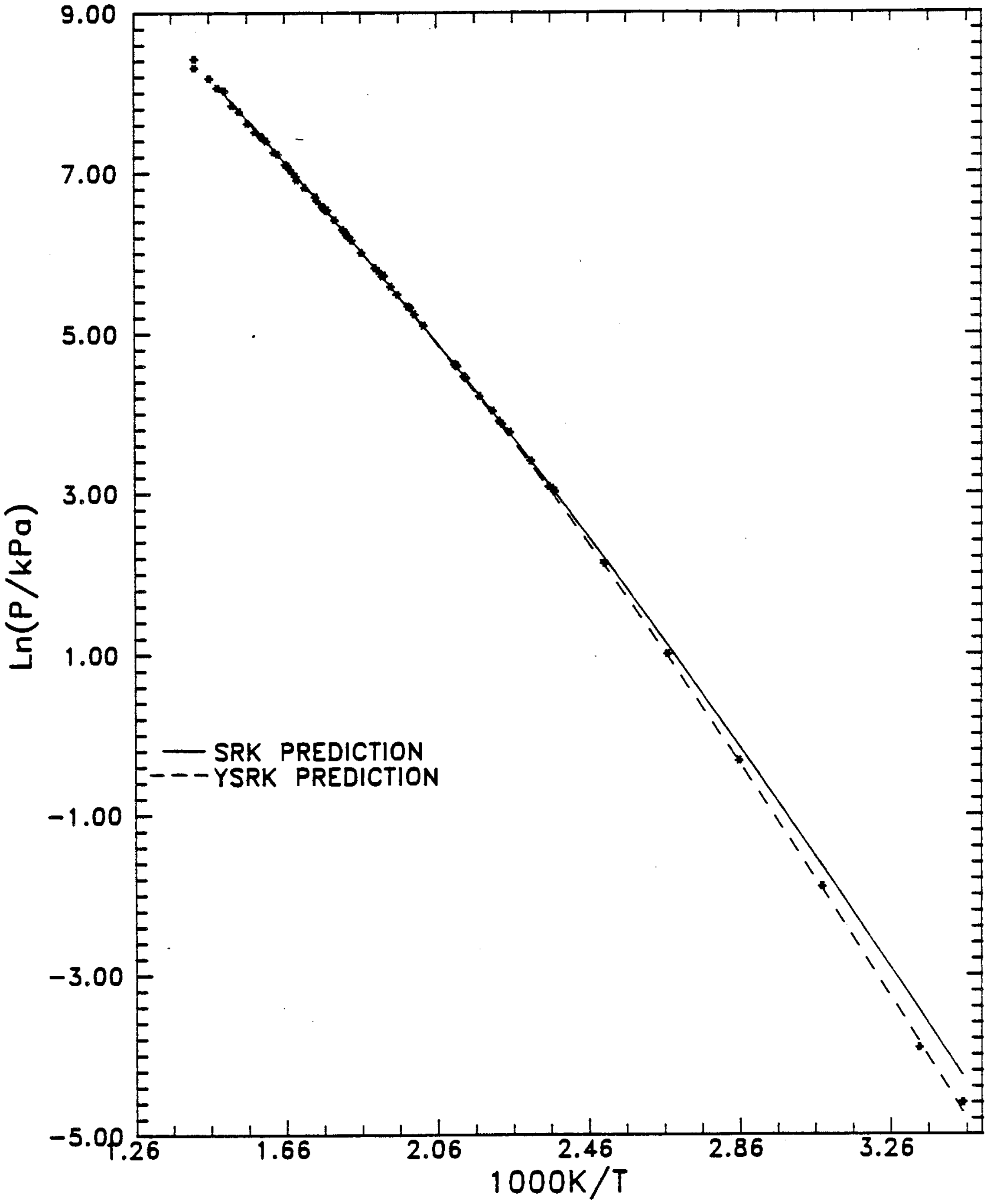

FIGURE 30
QUINOLINE VAPOR PRESSURE PREDICTIONS

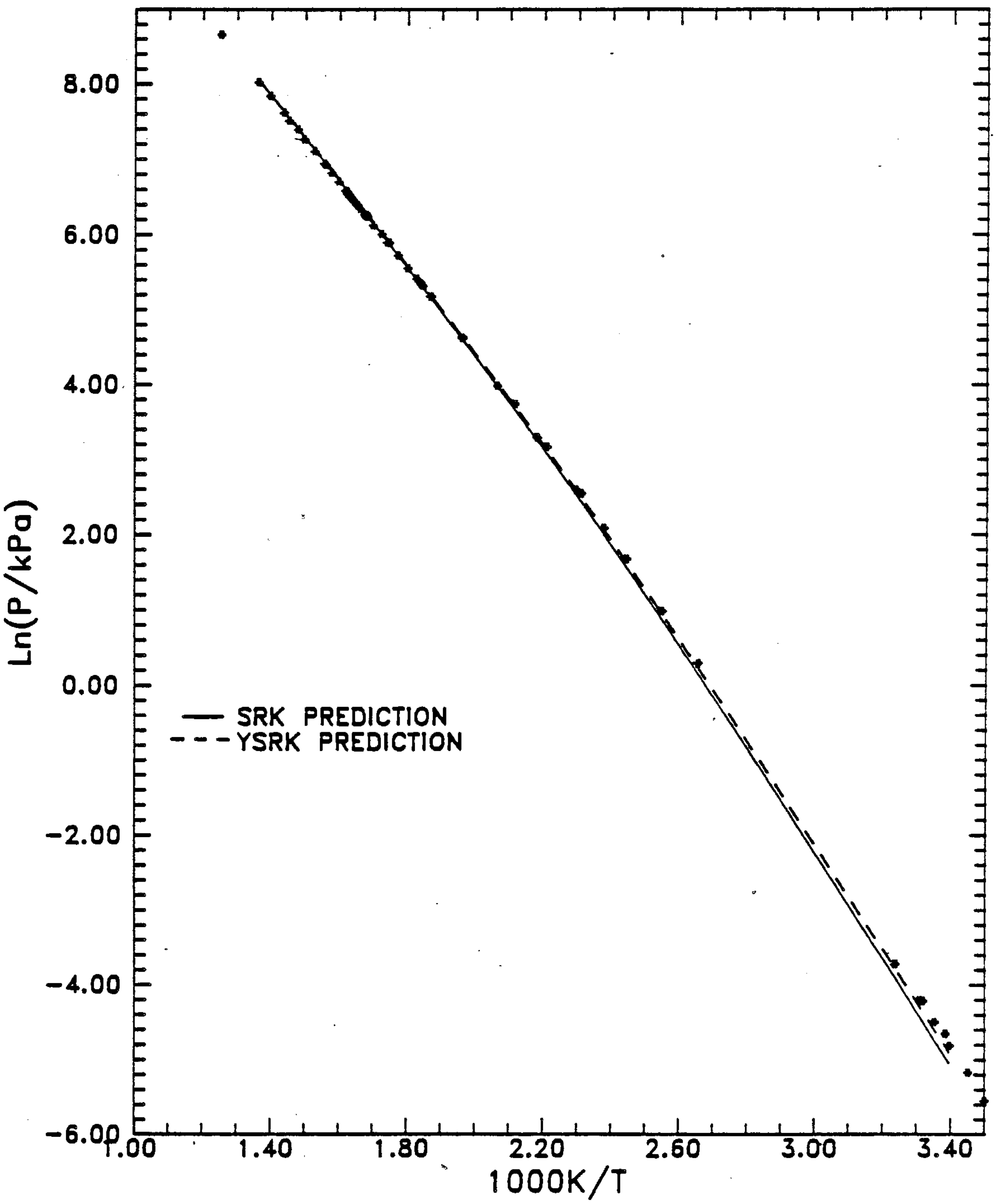

bias the fit in one particular region; therefore, vapor pressure data chosen for each compound were over the widest possible temperature range and as evenly spaced as possible. In the case of m-cresol, the vapor pressure data used were generated from a vapor pressure fit as given by Chao et al. (1983). This fit was documented as having an average percent deviation of 0.5% over a temperature range of 278 - 705.8 K. The vapor pressure data chosen for quinoline covered a temperature range of 294-735 K and were obtained from several sources: Glaser et al. (1957), Krevor et al. (1986), Van de Rostyne et al. (1983), Stull et al. (1947), and data from this and other research at the Colorado School of Mines. It was especially important to use vapor pressure data at the lower temperatures since the intermolecular interactions are more significant in this region.

The vapor pressures of m-cresol and quinoline predicted by Yesavage's modification are also shown in Figures 29-30. Yesavage's modification performs significantly better than the SRK at the very low temperatures where the SRK is in gross error. However, the SRK typically performs slightly better in the middle temperature range. This is not evident in Figures 29-30 due to the scale required to present the entire temperature range. For enthalpy measurements that require the calculation of a reference enthalpy departure at low temperatures or for low temperature phase behavior data, Yesavage's modification would perform better. The VLE data obtained in this research are in the reduced temperature ranges of 0.75 - 0.85; consequently, the SRK will give more accurate predictions than Yesavage's. If these VLE data were used to predict enthalpies, then Yesavage's modification may perform better than the SRK even though it may not fit the VLE data as accurately.

Vapor Liquid Equilibria

Using the maximum likelihood fitting routine, interaction parameters of the various mixing rules were fit to the phase behavior data. The fitting routine was found to work very well and rapid convergence (less than 10 iterations) was possible for all mixing rules. The logical initial guess for an interaction parameter was zero, this was computationally impossible only because of the alogorithm used for calculating the numerical derivatives. An initial guess for all of the parameters was a small positive number (.0001).

To determine which model better represented a data set, a simple statistical test was performed. A value of s^2 (as defined by Anderson (1978)) was calculated for each model.

$$s^2 = S/(N-L) \quad (39)$$

S = minimizing function (Equation 3)
N = number of data points
L = number of parameters

A value of F was calculated as the ratio of the s^2 values for two models.

$$F = s_1^2/s_2^2 \quad (40)$$

1 = model 1 and 2 = model 2

At a confidence level α, the value of F was compared to tabulated $F(\alpha:\nu_1,\nu_2)$ values. ν_1 and ν_2 are the degrees of freedom for the two models and are calculated as the number of data points minus the number of parameters, (N-L). If F was greater than $F(\alpha:\nu_1,\nu_2)$ then the two models were considered statistically different at a confidence level of α.

It is also possible to use the same statistical test to compare how well a single model represents two different sets of VLE data. However, it must be pointed out that the model consists of two separate parts; the EOS and the mixing rules. One must realize that a statistical difference between two models may be due to the inability of the EOS to predict pure component properties rather than the predictive capabilities of the mixing rule.

Results of the phase behavior modeling attempted in this research are tabulated in Tables 16, 18, 20. In these tables, the results of the F test are used to compare models. α_{ij} is the level of confidence to which it can be stated that models i and j are statistically different. In addition, a more conventional measure of comparison is also presented. The variables, temperature (T) and liquid composition (x) were held constant and the variables pressure (P) and vapor composition (y) were calculated. The average absolute percent deviations between measured values of P and y and predicted values were calculated and are presented as ΔP and Δy. Initially an overview will concentrate on the methods used for comparing the different models. A more indepth analysis will then be presented on the evaluation of the individual models.

Table 16 presents the modeling results for the tetralin/quinoline system and Table 17 presents the interaction parameters for the models. In comparing the models, F tests were performed to determine if one model statistically represented the data better than another. The best statistical model was model 5 (Luedecke et al. (1985)) using the SRK equation. This model was shown to be better than all of the other models by at least a confidence level of 90%.

TABLE 16

COMPARISON OF THERMODYNAMIC MODELS

TETRALIN/QUINOLINE AT 250-325°C

i	EOS	Model	s^2	α_{i1}	α_{i2}	α_{i3}	α_{i4}	α_{i5}	ΔP(%)	Δy(%)
1	SRK	k_{ij}	43.0	---					1.35	1.38
2	SRK	A+B/T	30.0	<90	---				1.11	2.37
3	SRK	A-B/v	33.0	<90	ns	---			1.20	1.62
4	SRK	A-B/vRT	41.0	ns	<90	<90	---		1.37	1.23
5	SRK	A+C's	19.0	99	90-95	95	99	---	0.49	2.26
6	YSRK	A+C's	31.0	---	---	---	---	90-95	0.54	4.14

1 = simple interaction parameter
2 = temperature dependent interaction parameter
3 = Holder et al. (1986)
4 = modification of Holder mixing rule
5 = Luedecke et al. (1985)

ns = significantly less than a 90% confidence level

TABLE 17

INTERACTION PARAMETERS

TETRALIN/QUINOLINE

EOS	Model	Parameters		
SRK	k_{ij}	A = -1.52E-2		
SRK	A+B/T	A = -.1355	B = 67.791	
SRK	A-B/v	A = 2.53E-2	B = 14.657	
SRK	A-B/vRT	A = 3.13E-3	B = 31083465	
SRK	A+C's	A = -.1356	C_{12} = -7.18E-2	C_{21} = -6.66E-2
YSRK	A+C's	A = -.1331	C_{12} = -7.08E-2	C_{21} = -5.69E-2

The values of C_{12} and C_{21} are normalized by $a_i(Tc)^2$

When comparing the models using the more conventional means of ΔP and Δy, the choice of the best model is much more obscure. Model 5 has a significantly lower average absolute percent deviation in pressure than all of the other SRK models; however, the average absolute percent deviation of y is one of the largest of all of the models. This is a clear indication of the problem that exists with a conventional technique of comparing models. In this case, one might be lead to choose one of the other models which did not predict pressure quite as well, but predicted vapor composition better. Since the physical values of pressure and vapor composition are different orders of magnitudes and have different experimental errors, it becomes quite difficult to weigh the relative values of one variable over another.

To resolve the discrepancies between the two methods of comparison, graphs of each model at the 250 and 325°C isotherms are presented in Figures 31 - 42. It can be clearly seen that the model that best represents the data is the Luedecke mixing rules (model 5) as predicted by the F test.

As will be shown with the other two data sets, the statistical F test predicts the correct ranking of the models. The ease with which this method can be applied greatly facilitates the evaluation of thermodynamic models.

FIGURE 31

TETRALIN/QUINOLINE 250°C ISOTHERM
PRED=SRK, SIMPLE

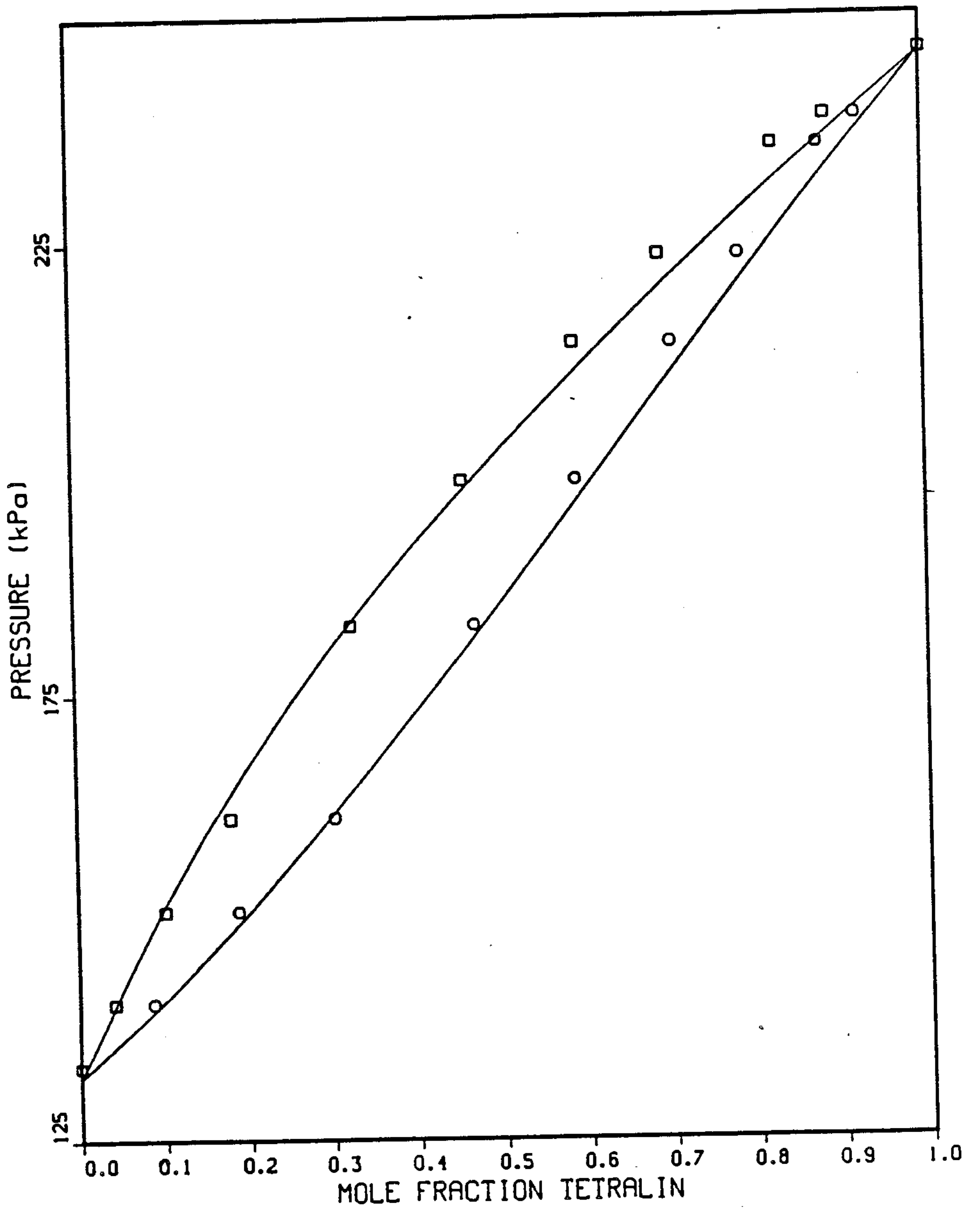

FIGURE 32

TETRALIN/QUINOLINE 325°C ISOTHERM
PRED=SRK, SIMPLE

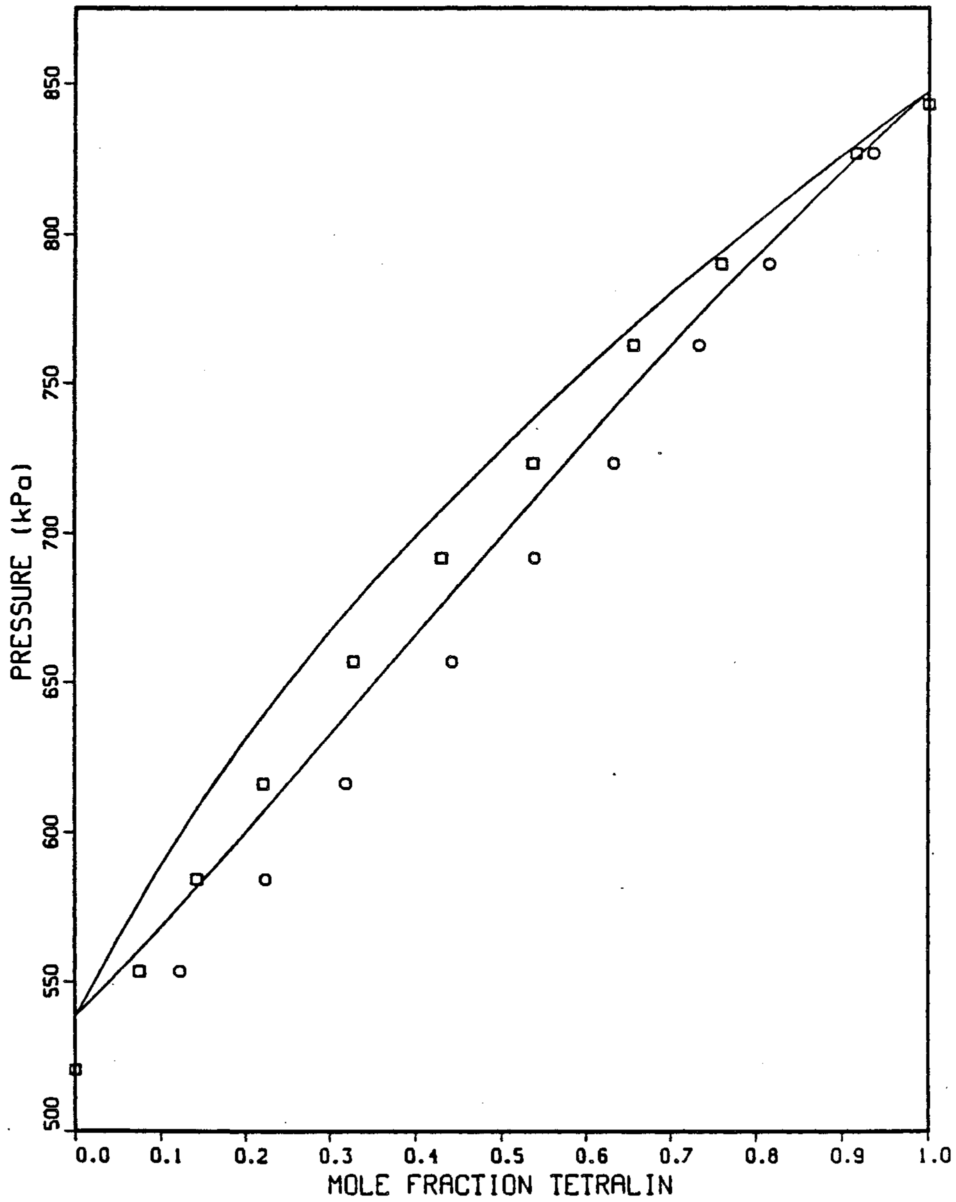

FIGURE 33

TETRALIN/QUINOLINE 250°C ISOTHERM
PRED=SRK, (A+B/T)

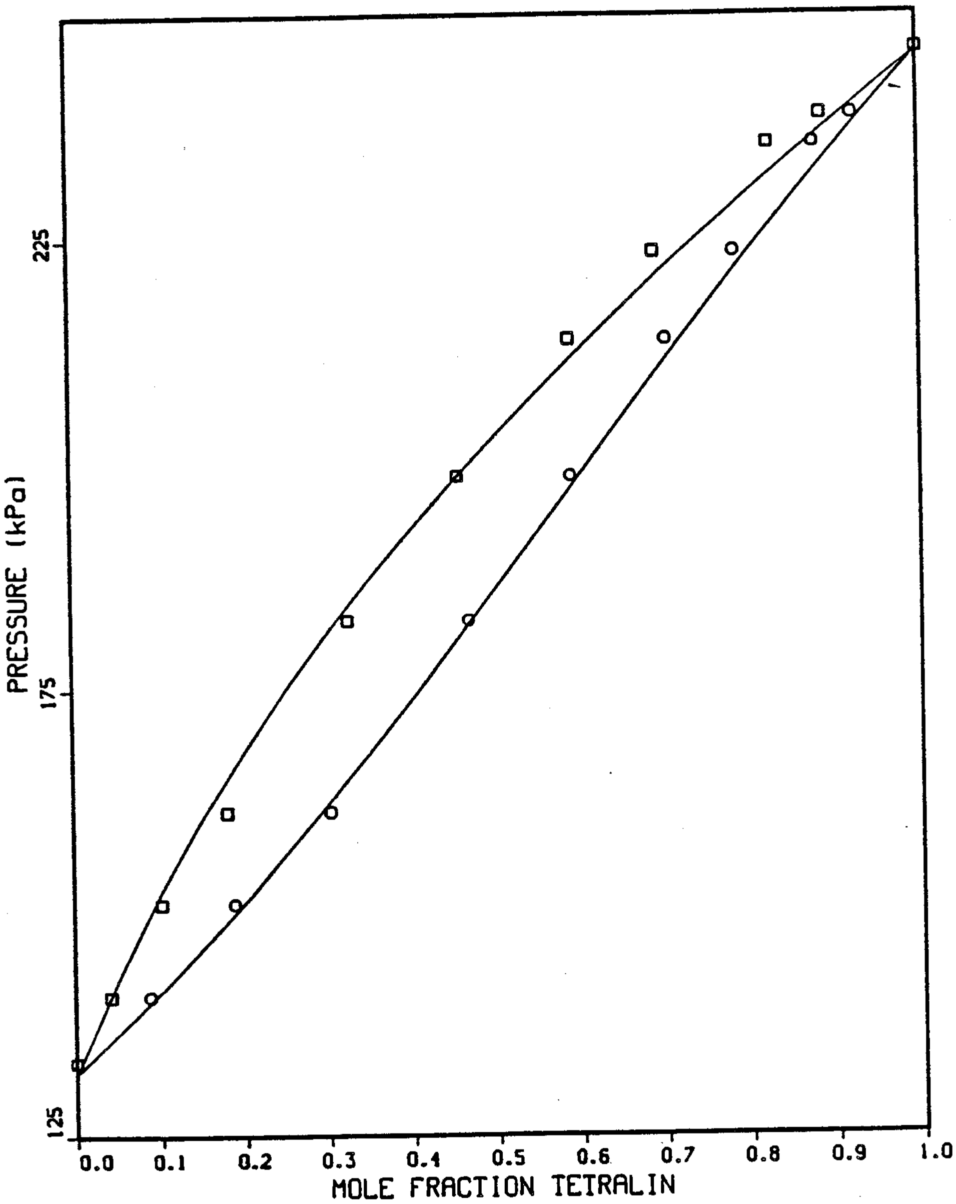

FIGURE 34
TETRALIN/QUINOLINE 325°C ISOTHERM
PRED=SRK, (A+B/T)

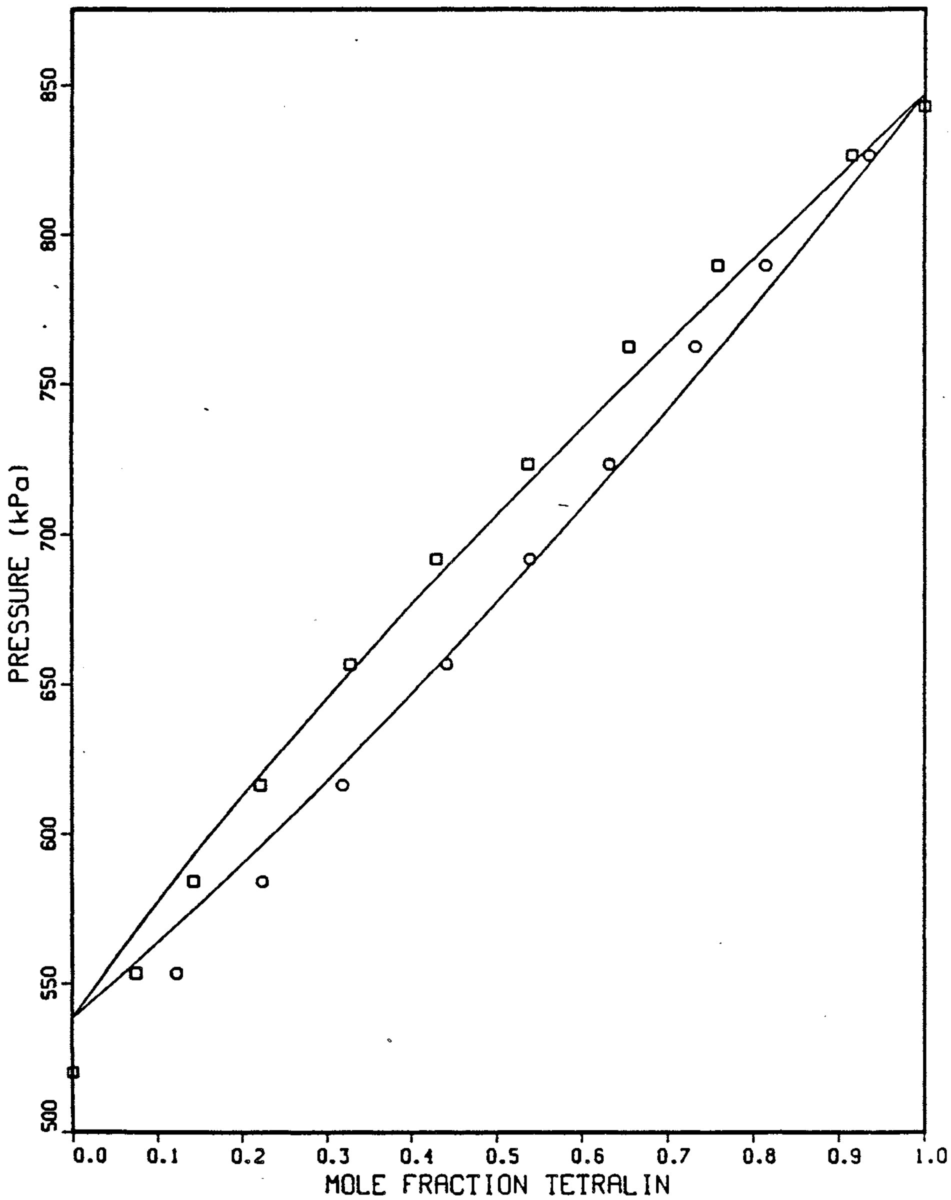

FIGURE 35
TETRALIN/QUINOLINE 250°C ISOTHERM
PRED=SRK, (A-B/V)

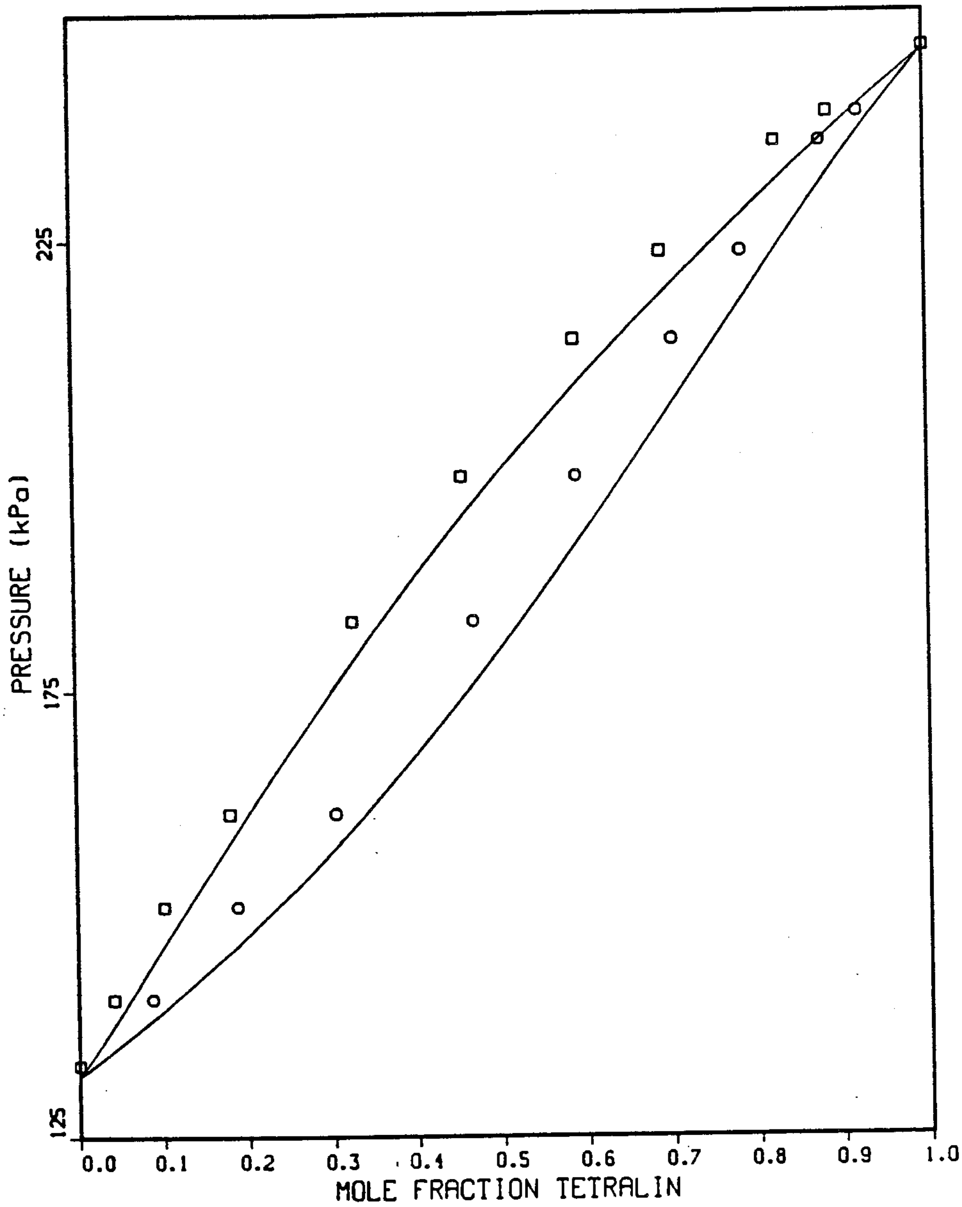

FIGURE 36
TETRALIN/QUINOLINE 325°C ISOTHERM
PRED=SRK, (A-B/V)

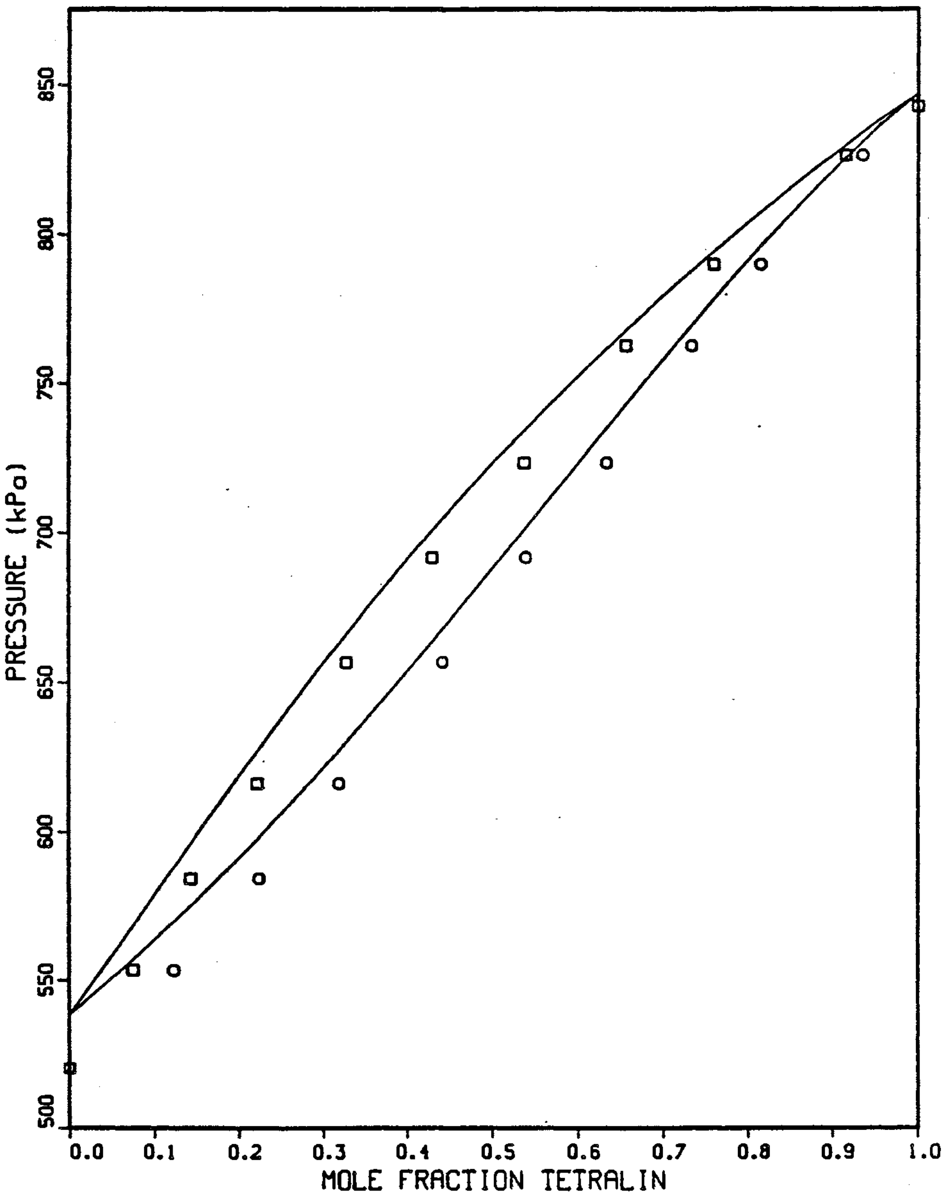

FIGURE 37

TETRALIN/QUINOLINE 250°C ISOTHERM
PRED=SRK, (A-B/VRT)

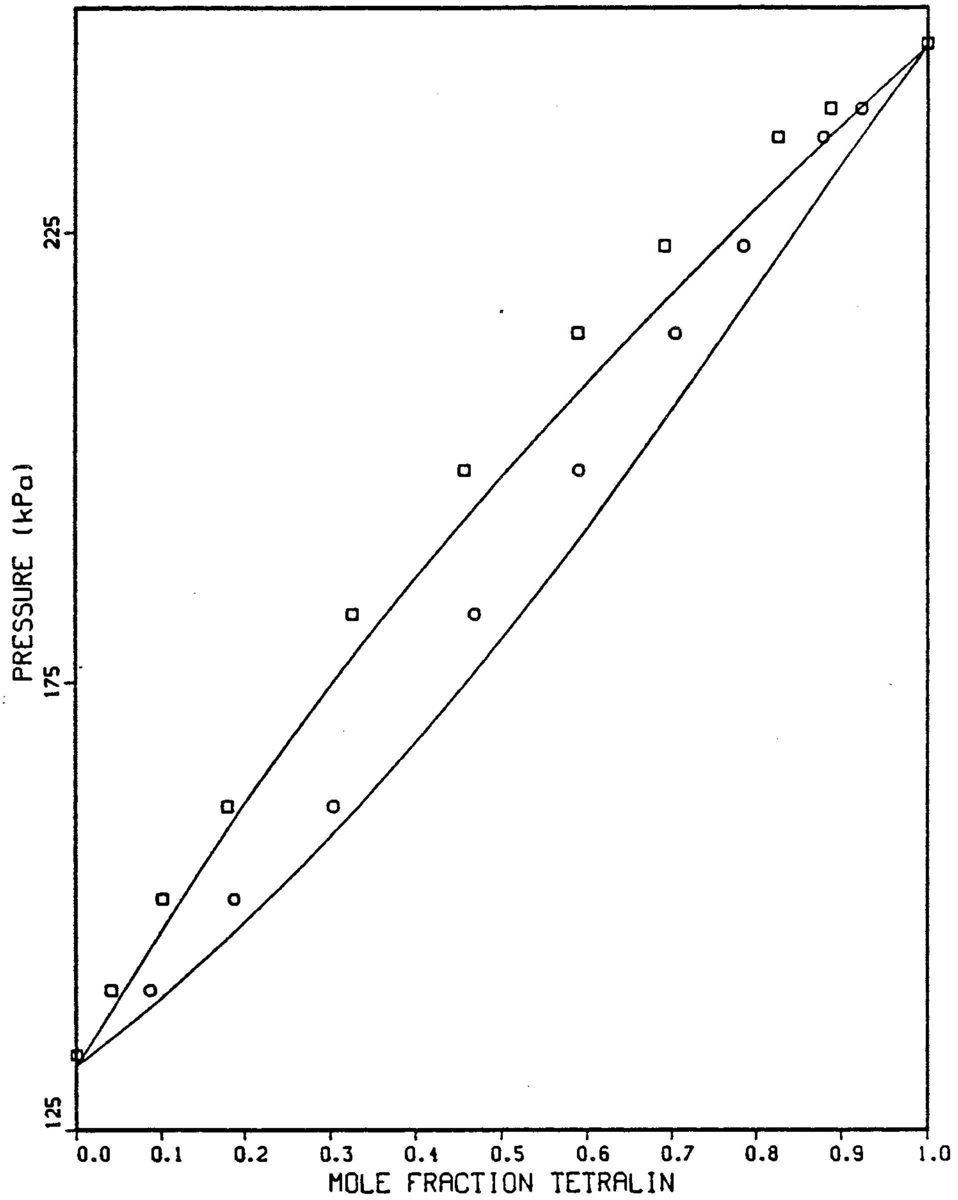

FIGURE 38

TETRALIN/QUINOLINE 325°C ISOTHERM
PRED=SRK, (A-B/VRT)

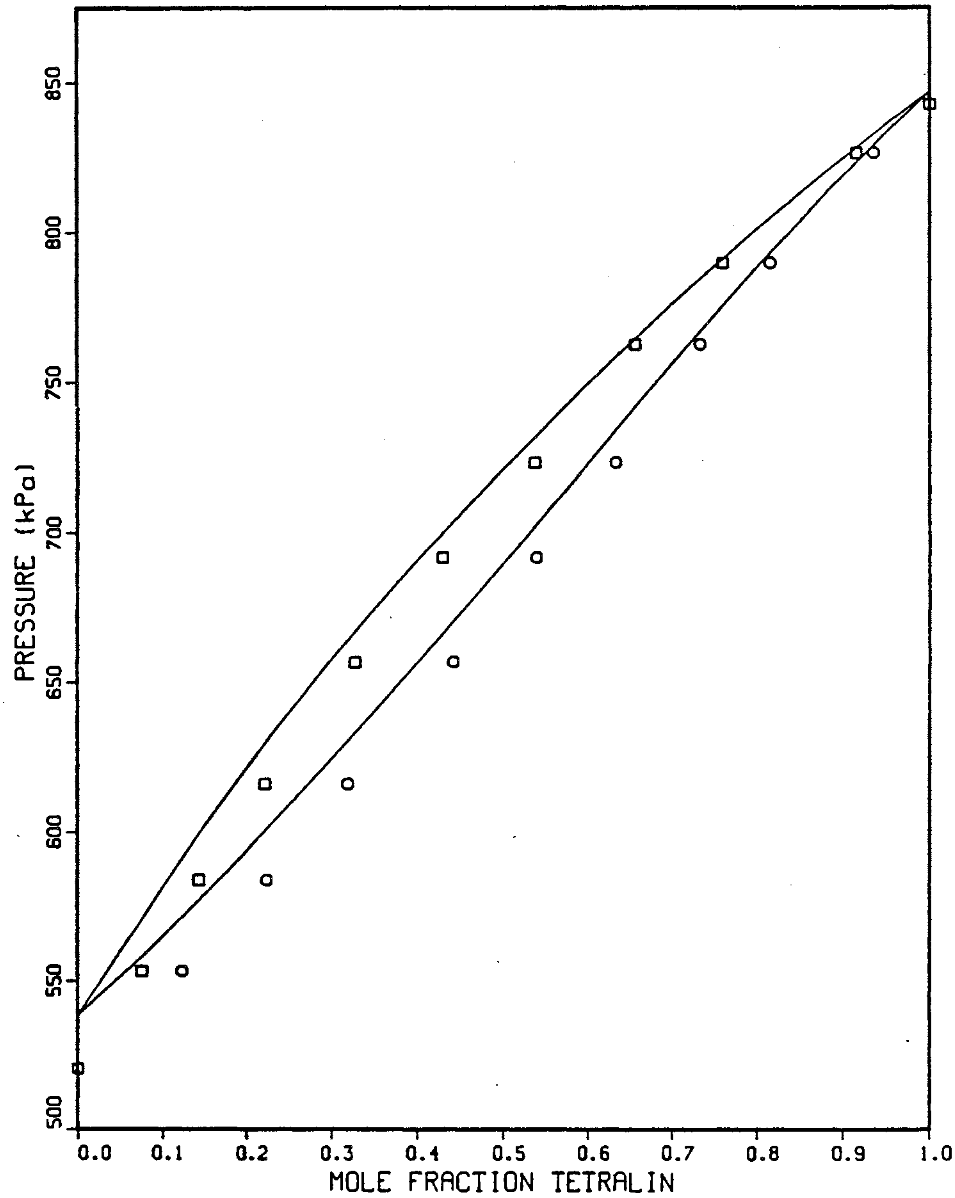

FIGURE 39
TETRALIN/QUINOLINE 250°C ISOTHERM
PRED=SRK, (A+C's)

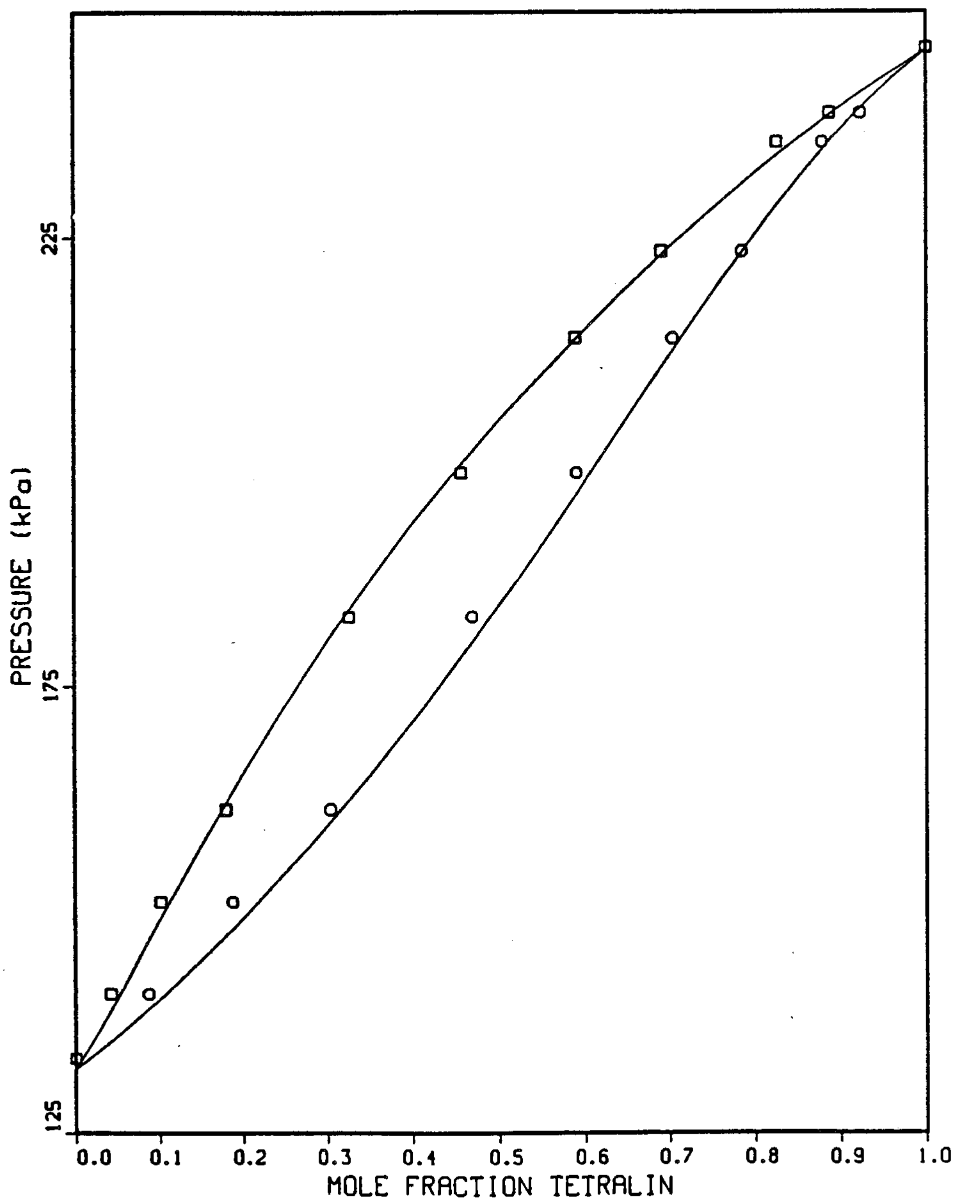

FIGURE 40
TETRALIN/QUINOLINE 325°C ISOTHERM
PRED=SRK, (A+C's)

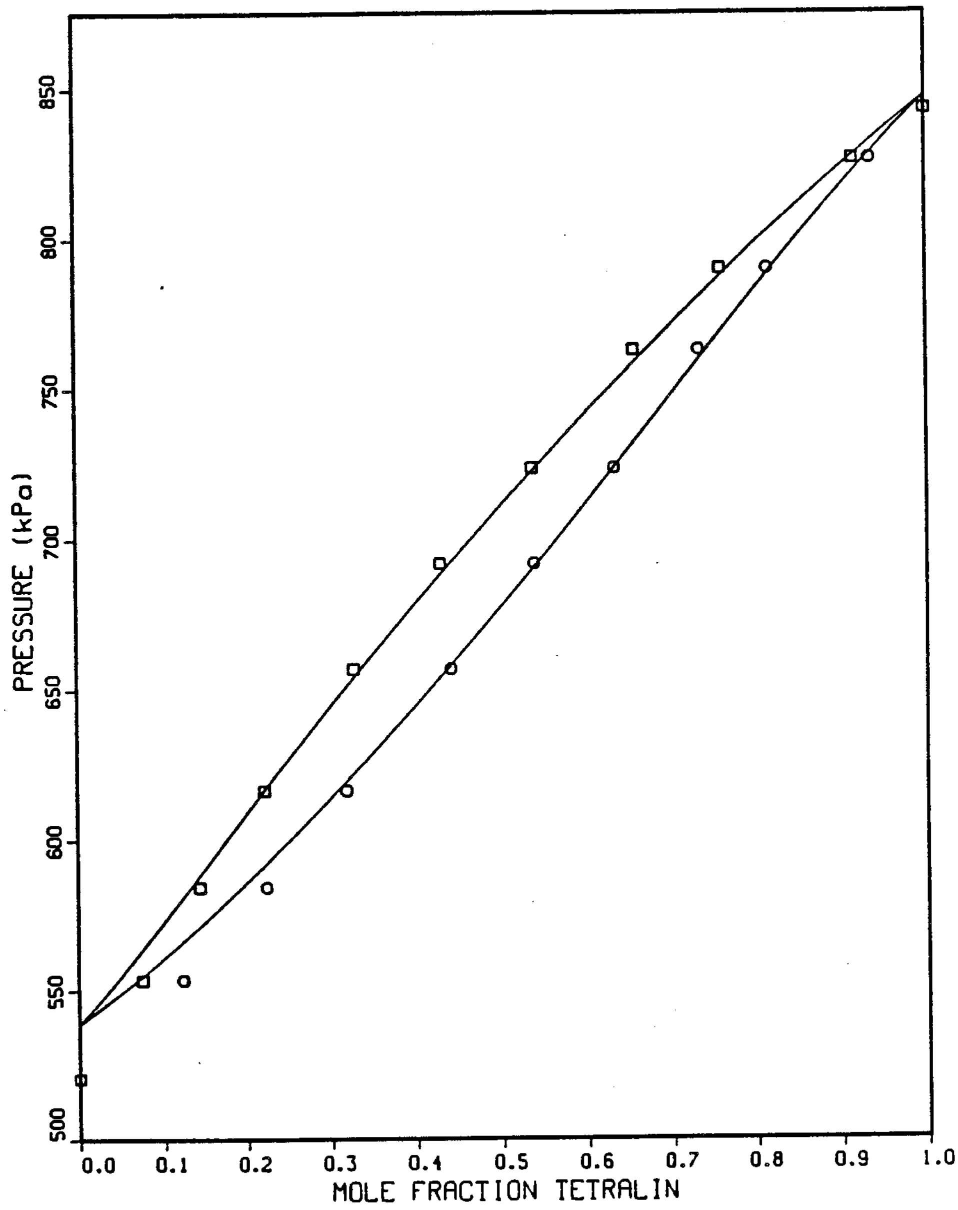

FIGURE 41
TETRALIN/QUINOLINE 250°C ISOTHERM
PRED=YSRK, (A+C's)

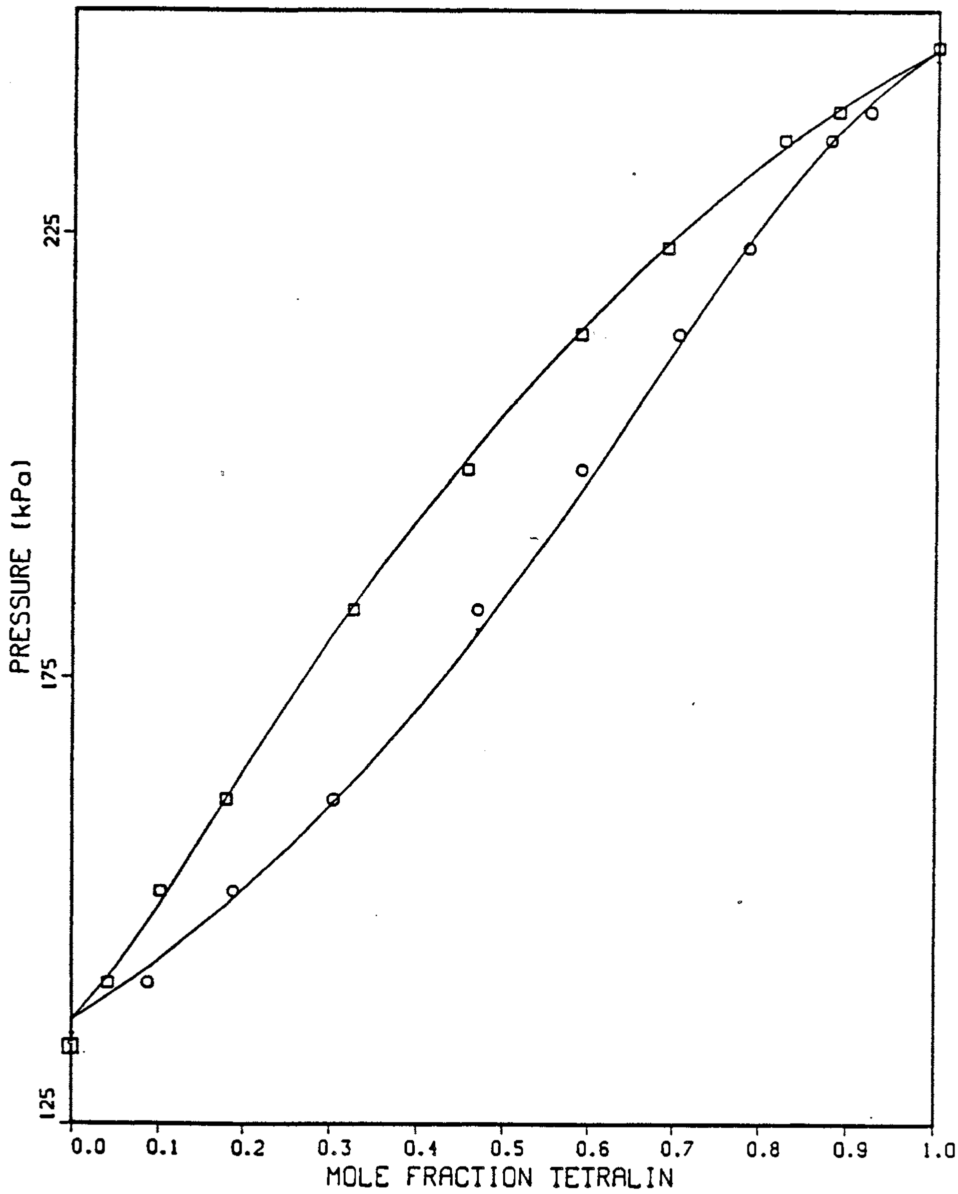

FIGURE 42
TETRALIN/QUINOLINE 325°C ISOTHERM
PRED=YSRK, (A+C's)

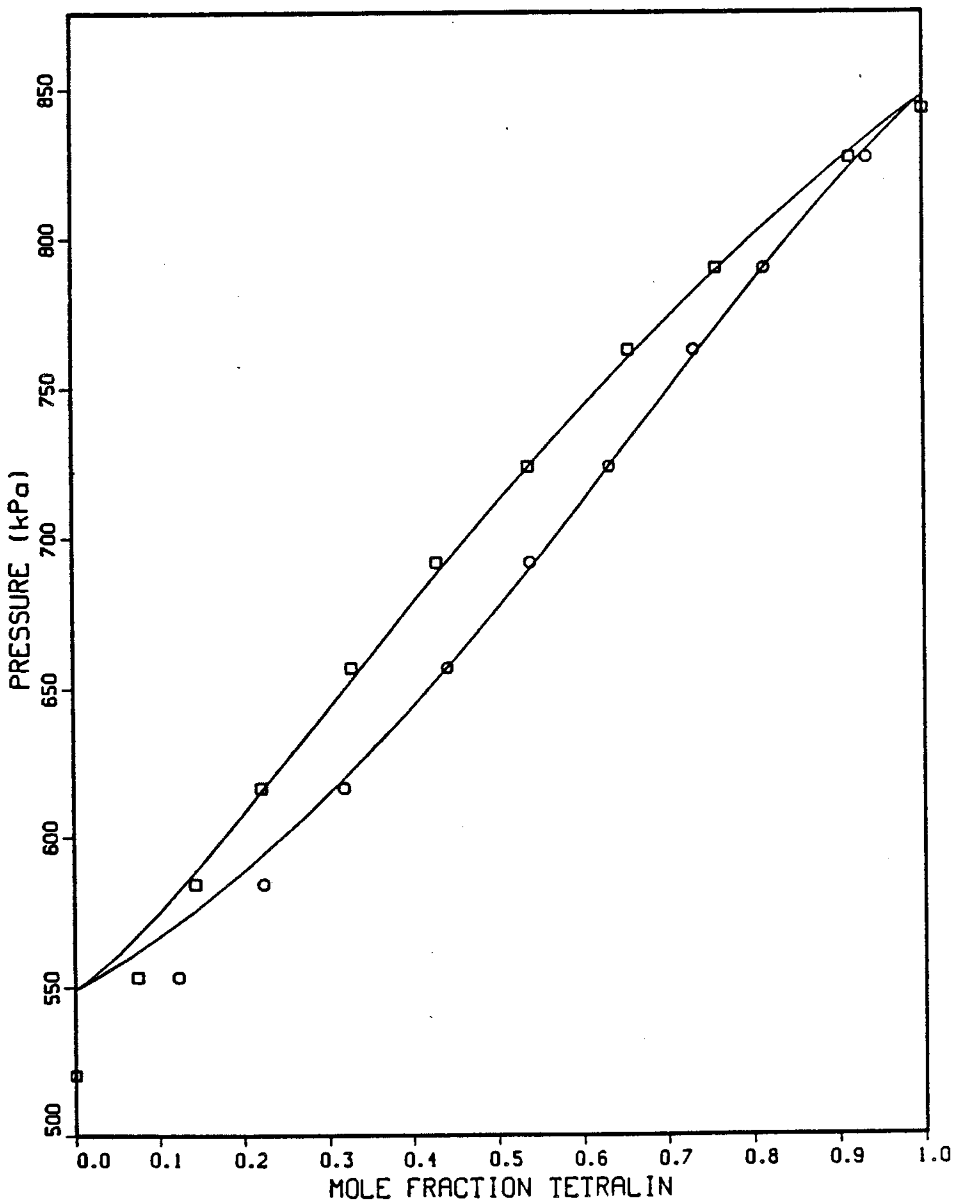

Table 18 presents the results of the modeling of the m-cresol/tetralin system; the corresponding interaction parameters are presented in Table 19. In this particular case, there was little statistical difference between models 1-4 but model 5 showed superior performance over all other models at a confidence level of 99% or better. Comparisons of the absolute standard deviation of pressure and vapor composition (ΔP and Δy) show that model 5 again has the lowest deviation in pressure and the largest deviation in y. As with the previous system, Figures 43-54 graphically confirm the superiority of the Luedecke mixing rule (model 5).

Table 20 presents the results for the m-cresol/quinoline system. The corresponding interaction parameters are presented in Table 21. In this case, the difference between all of the models is much less clear cut. Models 1-4 have little statistical difference and the superiority of model 5 is not as great. The absolute percent standard deviations in pressure and composition indicate that model 5 is superior in predicting both P and y. Again, there is some disagreement between the two methods of comparison. Figures 55-66 graphically show that all of the models predict this system rather well. Little difference can be discerned between models, but upon close examination model 5 can be seen to follow the data slightly better.

TABLE 18

COMPARISON OF THERMODYNAMIC MODELS

M-CRESOL/TETRALIN AT 250-325°C

i	EOS	Model	s^2	α_{i1}	α_{i2}	α_{i3}	α_{i4}	α_{i5}	ΔP(%)	Δy(%)
1	SRK	k_{ij}	21.8	---					1.00	1.29
2	SRK	A+B/T	19.6	ns	---				0.90	1.42
3	SRK	A-B/v	17.3	<90	ns	---			1.02	1.27
4	SRK	A-B/vRT	21.0	ns	ns	<90	---		1.06	1.19
5	SRK	A+C's	8.7	99.9	99.9	99.5	99.9	---	0.46	1.75
6	YSRK	A+C's	9.6	---	---	---	---	ns	0.51	1.84

1 = simple interaction parameter
2 = temperature dependent interaction parameter
3 = Holder et al. (1986)
4 = modification of Holder mixing rule
5 = Luedecke et al. (1985)

ns = significantly less than a 90% confidence level

TABLE 19

INTERACTION PARAMETERS

M-CRESOL/TETRALIN

EOS	Model	Parameters		
SRK	k_{ij}	A = 3.83E-2		
SRK	A+B/T	A = -1.99E-2	B = 31.973	
SRK	A-B/v	A = 8.59E-2	B = 18.475	
SRK	A-B/vRT	A = 5.36E-2	B = 27259270	
SRK	A+C's	A = -5.17E-2	C_{12} = -5.71E-2	C_{21} = -5.29E-2
YSRK	A+C's	A = -7.28E-2	C_{12} = -7.03E-2	C_{21} = -6.37E-2

The values of C_{12} and C_{21} are normalized by $a_i(Tc)^2$

TABLE 20

COMPARISON OF THERMODYNAMIC MODELS

M-CRESOL/QUINOLINE AT 250-325°C

i	EOS	Model	s^2	α_{i1}	α_{i2}	α_{i3}	α_{i4}	α_{i5}	ΔP(%)	Δy(%)
1	SRK	k_{ij}	21.5	---					1.15	2.36
2	SRK	A+B/T	21.4	ns	---				1.13	2.28
3	SRK	A-B/v	18.3	ns	ns	---			0.95	2.09
4	SRK	A-B/vRT	21.2	ns	ns	ns	---		1.13	2.30
5	SRK	A+C's	16.6	<90	<90	ns	<90	---	0.81	1.80
6	YSRK	A+C's	30.0	---	---	---	---	97.5	1.00	3.07

1 = simple interaction parameter
2 = temperature dependent interaction parameter
3 = Holder et al. (1986)
4 = modification of Holder mixing rule
5 = Luedecke et al. (1985)

ns = significantly less than a 90% confidence level

TABLE 21

INTERACTION PARAMETERS

M-CRESOL/QUINOLINE

EOS	Model	Parameters		
SRK	k_{ij}	A = -8.00E-2		
SRK	A+B/T	A = -5.58E-2	B = -13.652	
SRK	A-B/v	A = -.1389	B = -18.516	
SRK	A-B/vRT	A = -9.68E-2	B = -24613426	
SRK	A+C's	A = -7.57E-2	C_{12} = 7.09E-3	C_{21} = -2.16E-3
YSRK	A+C's	A = -.1063	C_{12} = -1.15E-2	C_{21} = -1.17E-2

The values of C_{12} and C_{21} are normalized by $a_i(Tc)^2$

FIGURE 43

M-CRESOL/TETRALIN 250°C ISOTHERM
PRED=SRK, SIMPLE

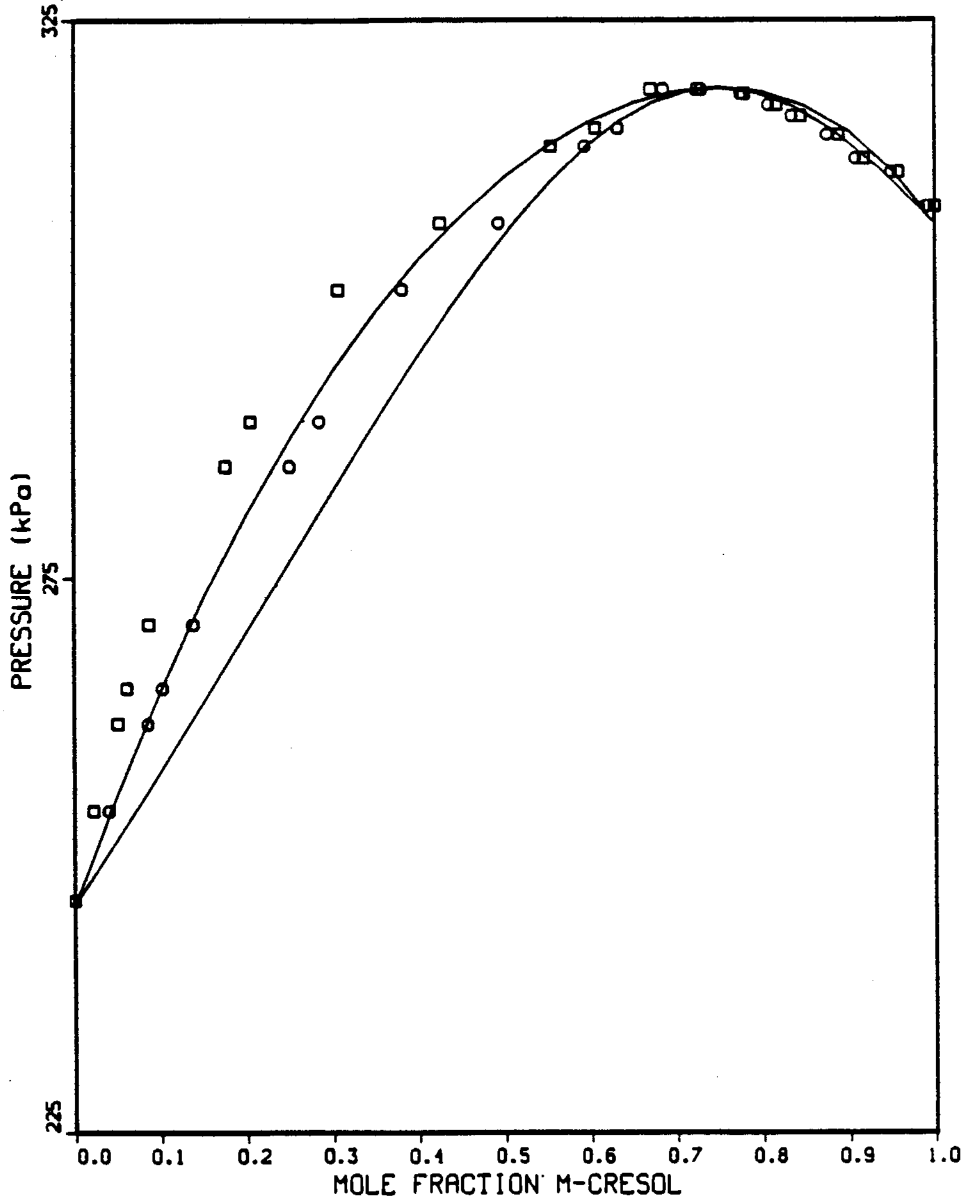

FIGURE 44

M-CRESOL/TETRALIN 325°C ISOTHERM
PRED=SRK, SIMPLE

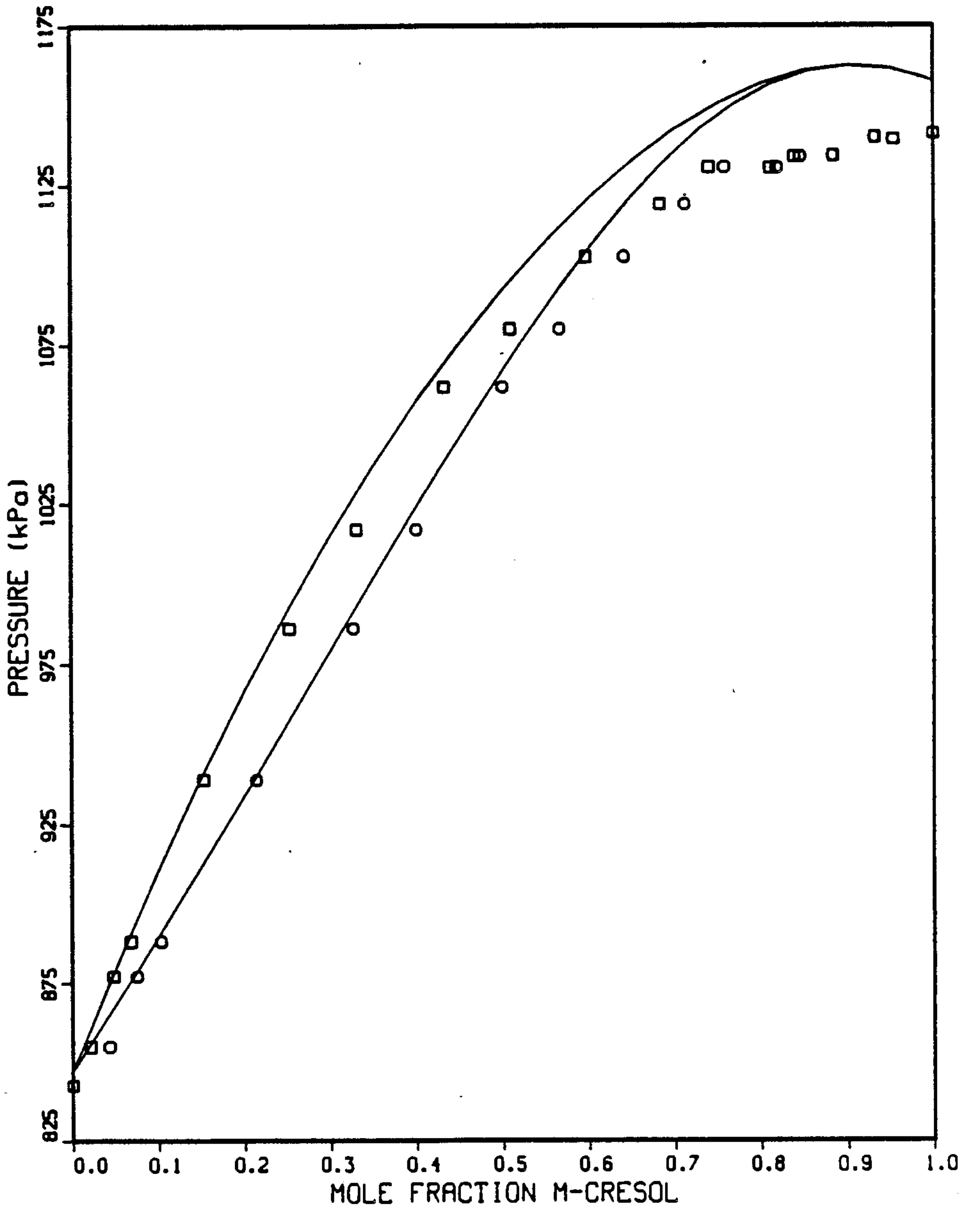

FIGURE 45

M-CRESOL/TETRALIN 250°C ISOTHERM
PRED=SRK, (A+B/T)

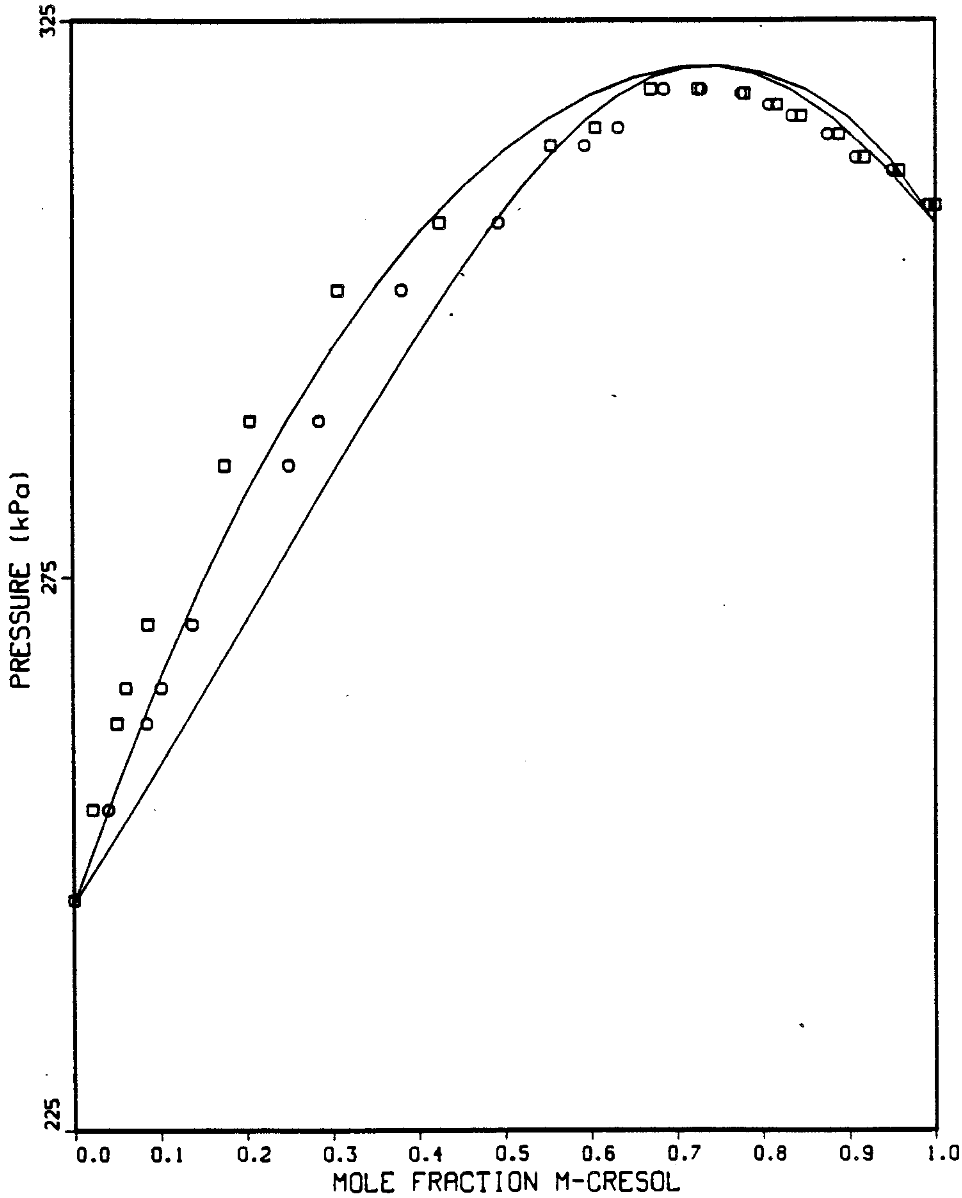

FIGURE 46
M-CRESOL/TETRALIN 325°C ISOTHERM
PRED=SRK, (A+B/T)

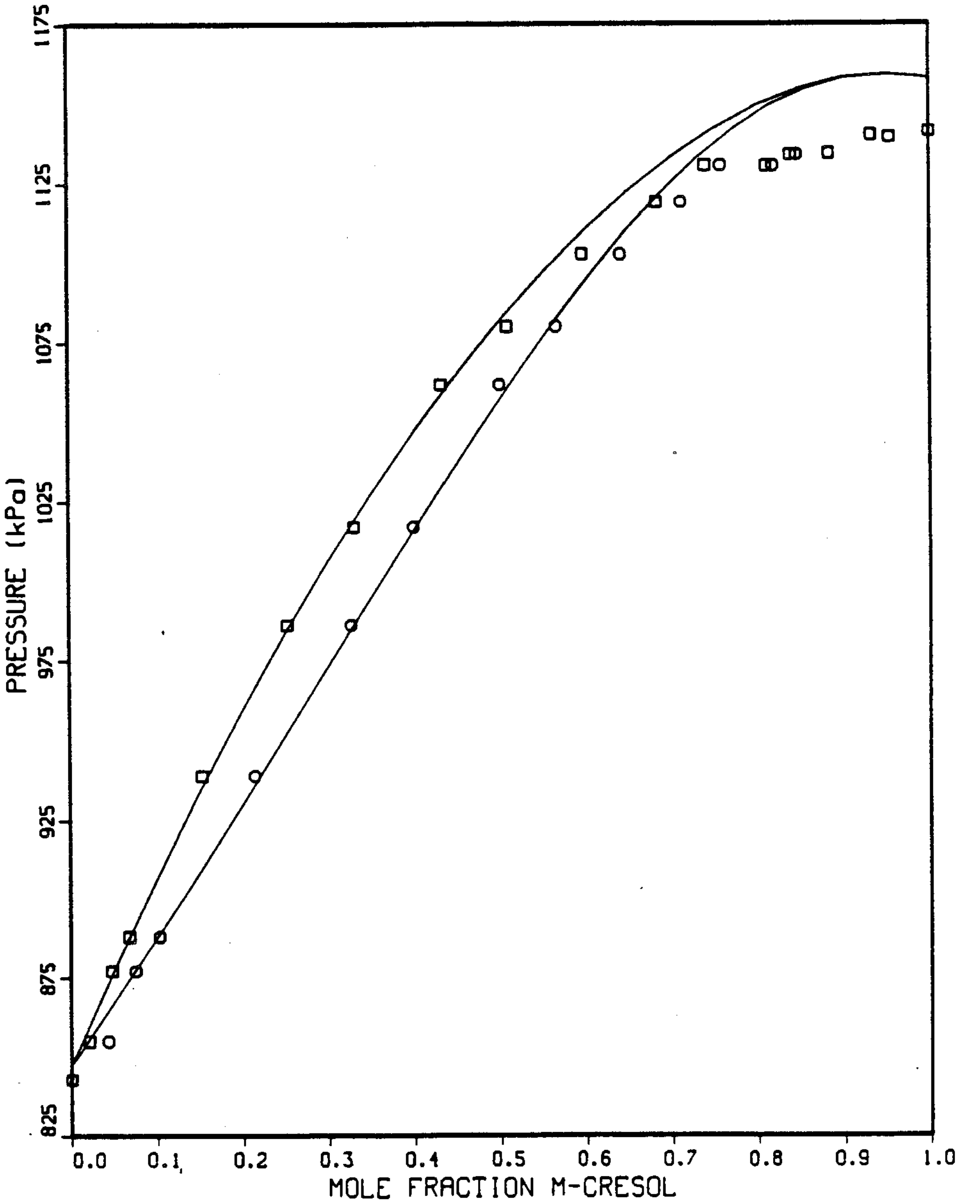

FIGURE 47
M-CRESOL/TETRALIN 250°C ISOTHERM
PRED=SRK, (A-B/V)

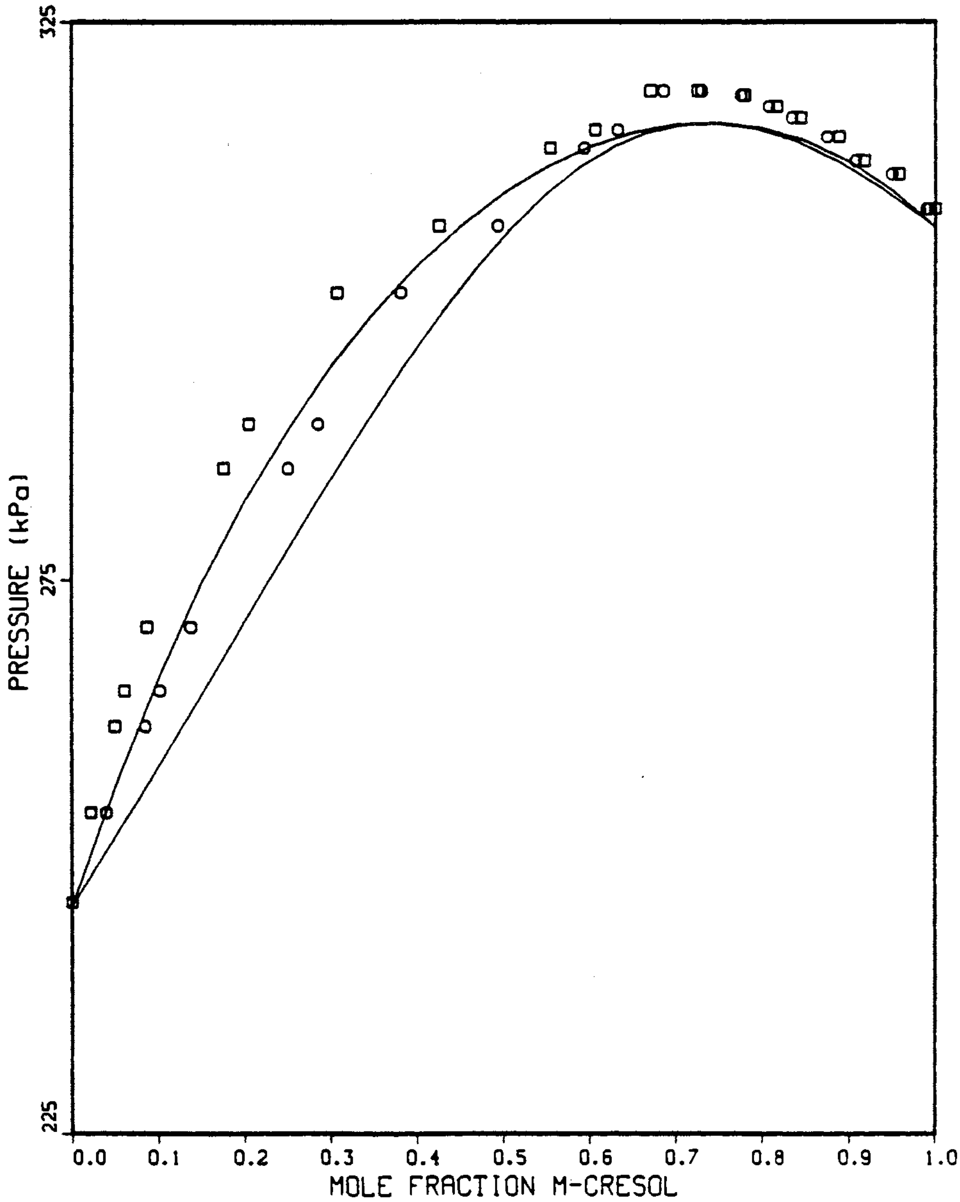

FIGURE 48
M-CRESOL/TETRALIN 325°C ISOTHERM
PRED=SRK, (A-B/V)

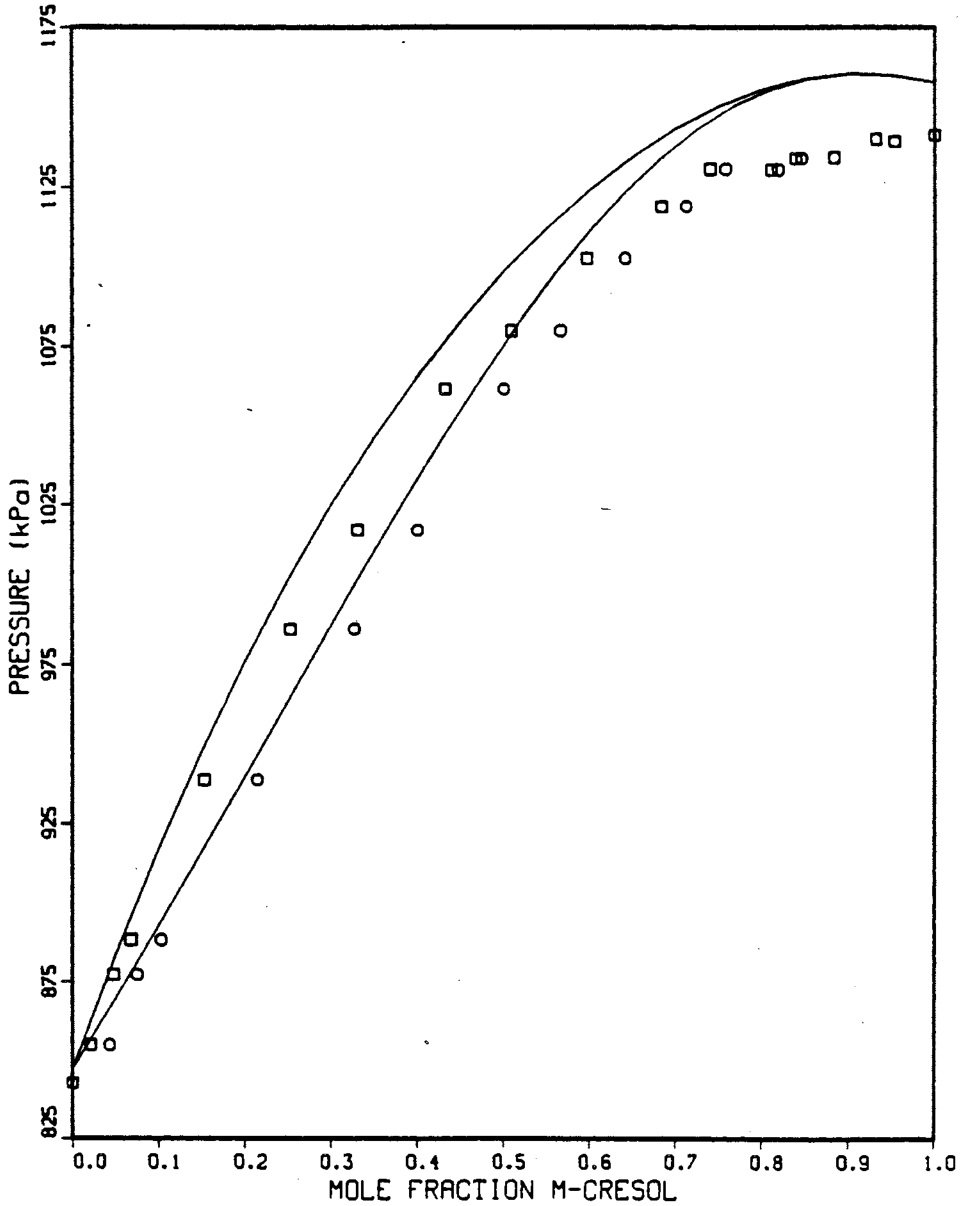

FIGURE 49
M-CRESOL/TETRALIN 250°C ISOTHERM
PRED=SRK, (A-B/VRT)

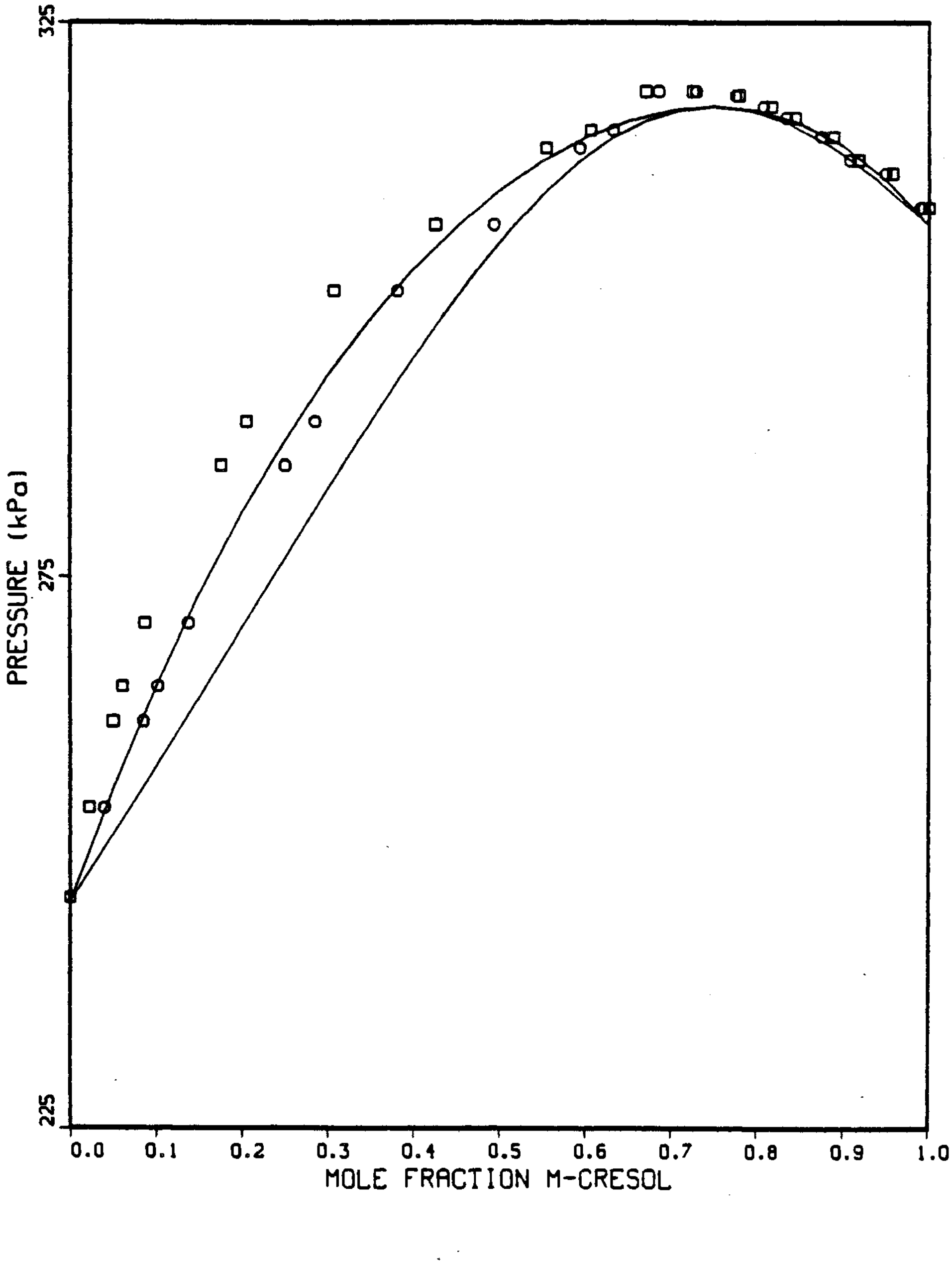

FIGURE 50
M-CRESOL/TETRALIN 325°C ISOTHERM
PRED=SRK, (A-B/VRT)

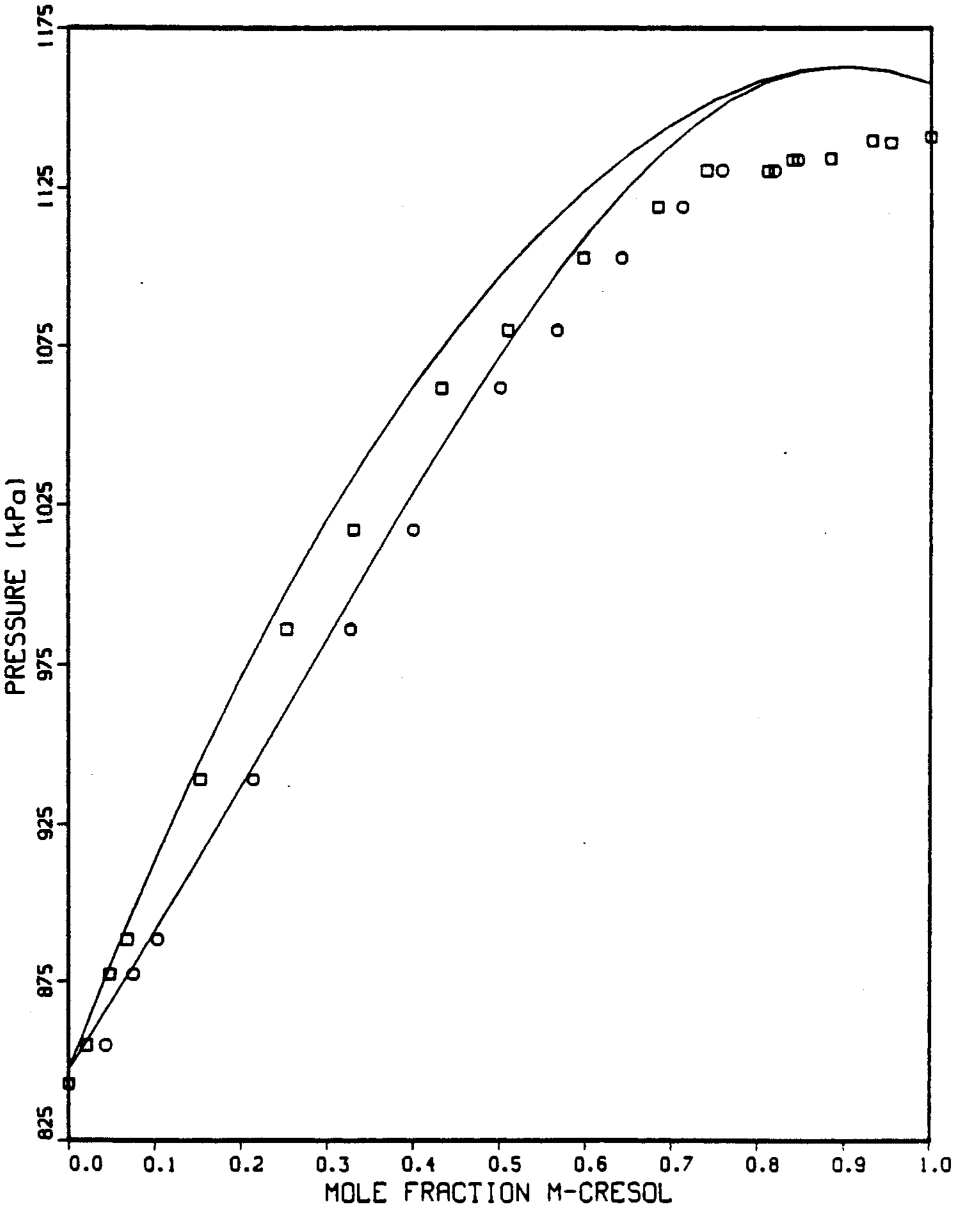

FIGURE 51
M-CRESOL/TETRALIN 250°C ISOTHERM
PRED=SRK, (A+C's)

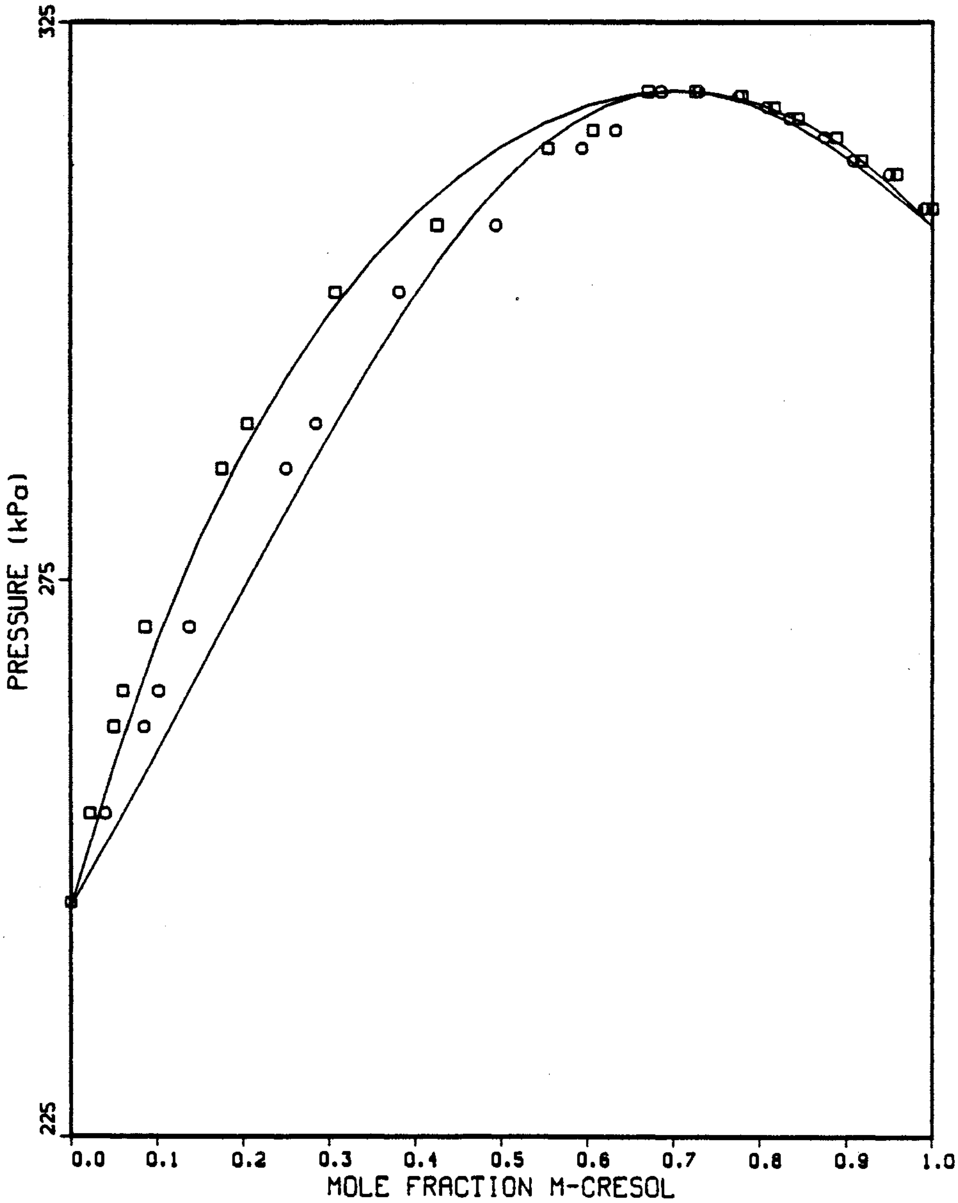

FIGURE 52
M-CRESOL/TETRALIN 325°C ISOTHERM
PRED=SRK, (A+C's)

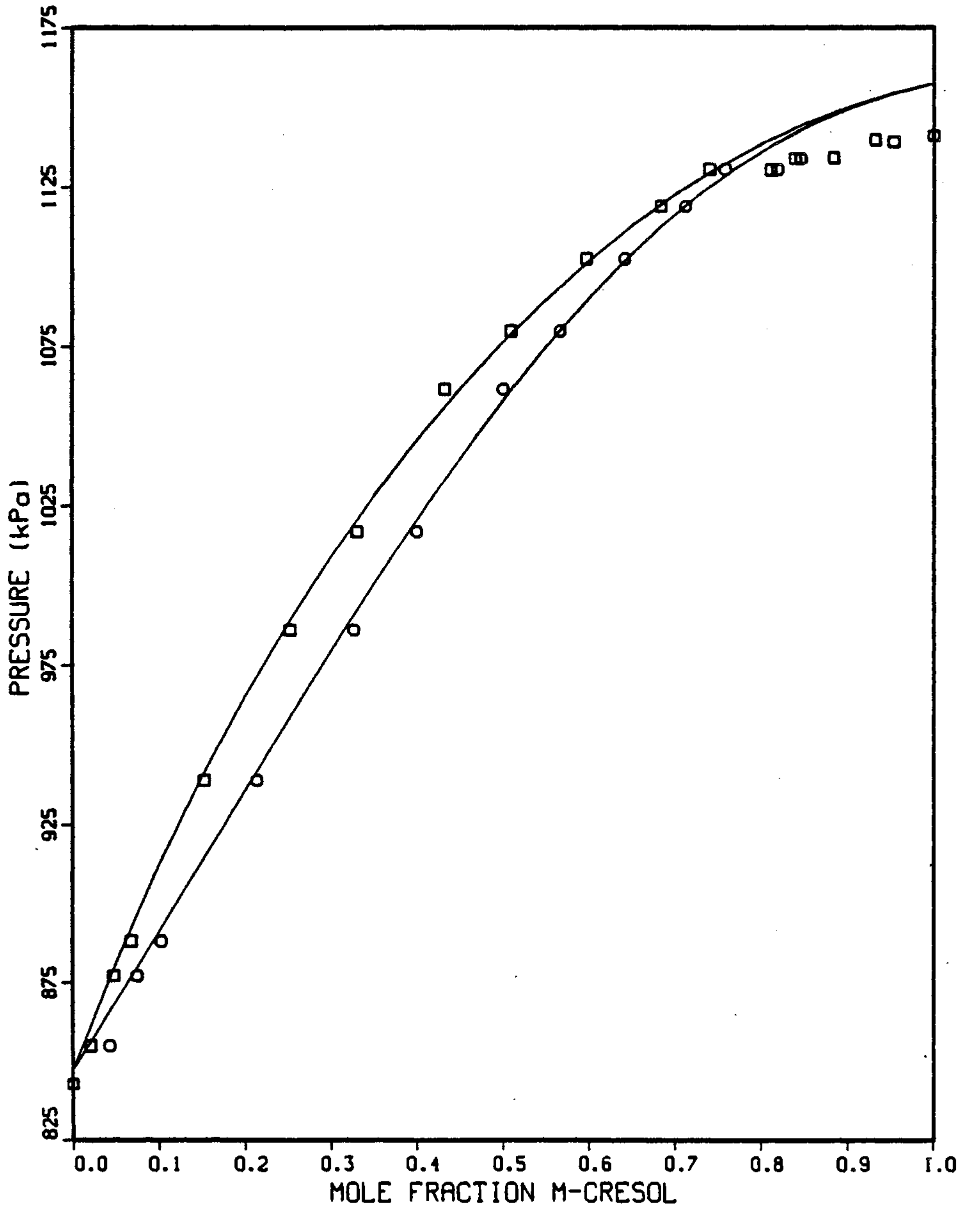

FIGURE 53
M-CRESOL/TETRALIN 250°C ISOTHERM
PRED=YSRK, (A+C's)

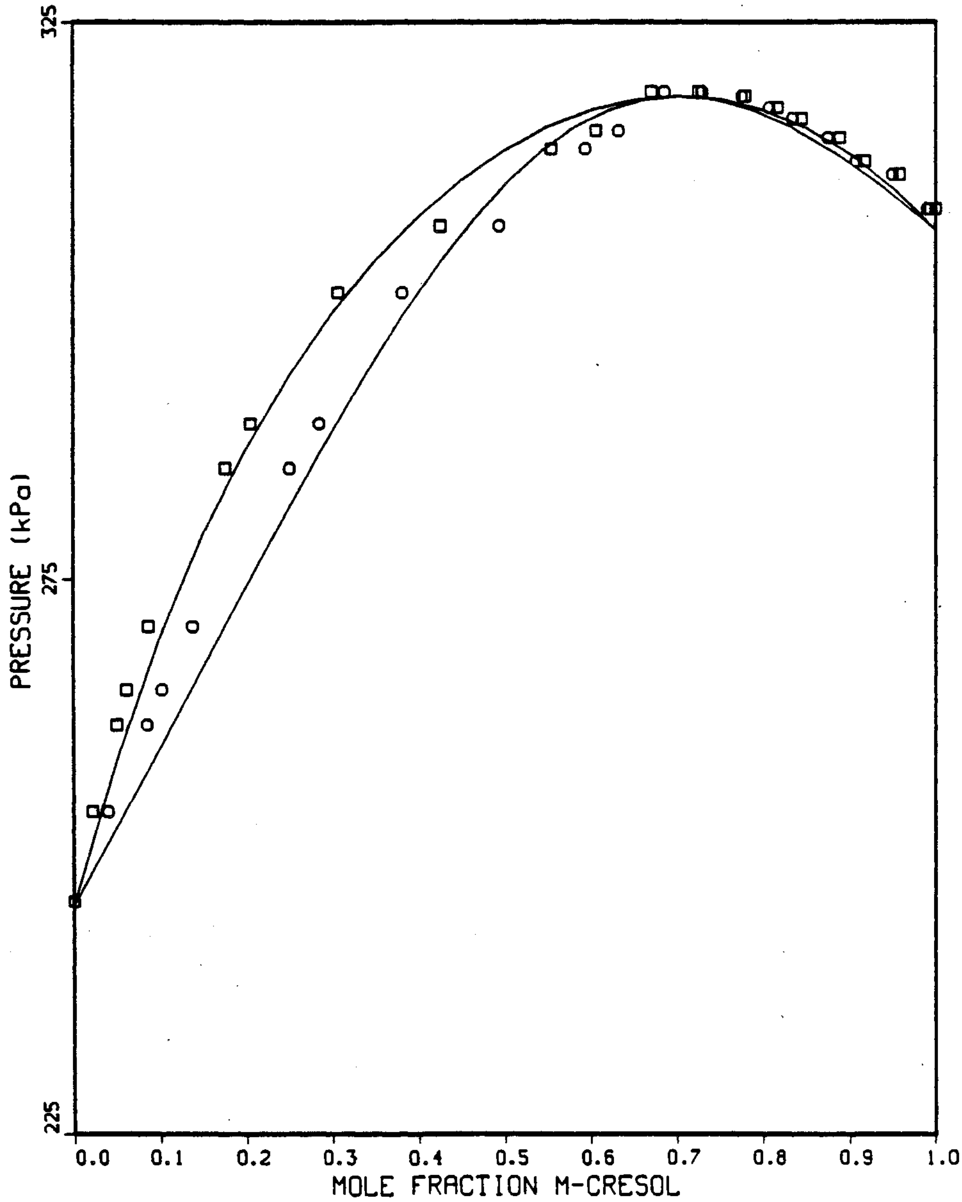

FIGURE 54
M-CRESOL/TETRALIN 325°C ISOTHERM
PRED=YSRK, (A+C's)

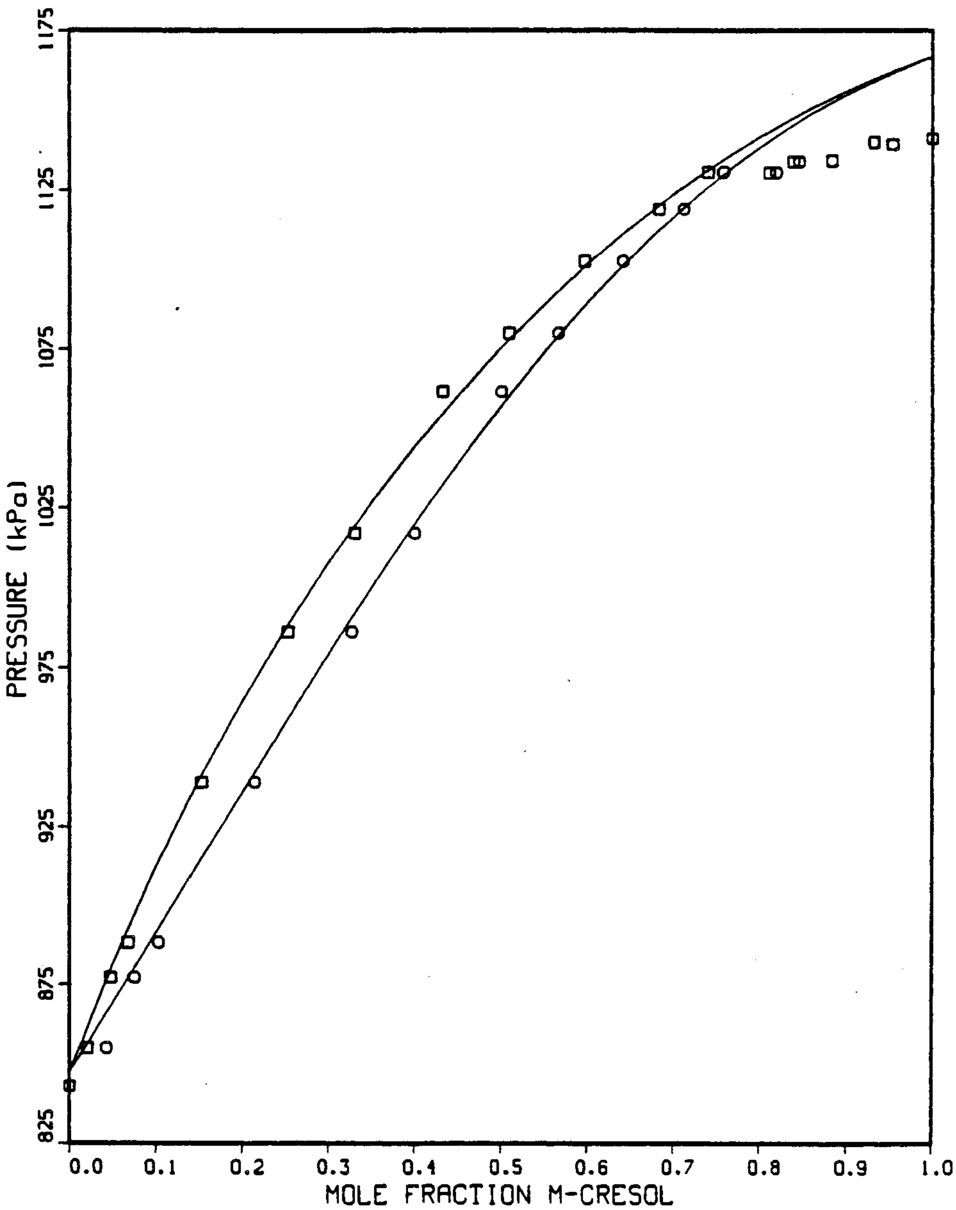

FIGURE 55
M-CRESOL/QUINOLINE 250°C ISOTHERM
PRED=SRK, SIMPLE

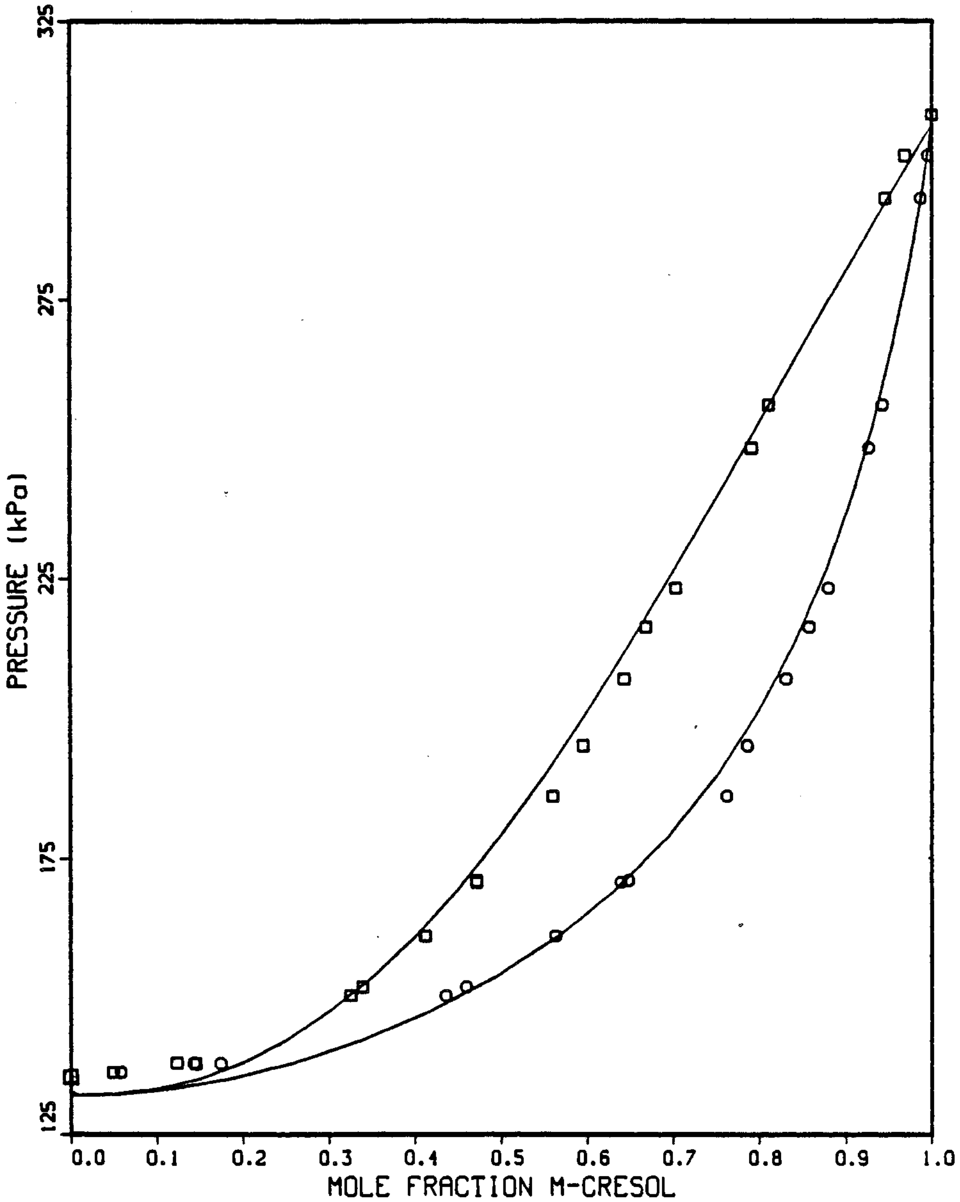

FIGURE 56

M-CRESOL/QUINOLINE 325°C ISOTHERM
PRED=SRK, SIMPLE

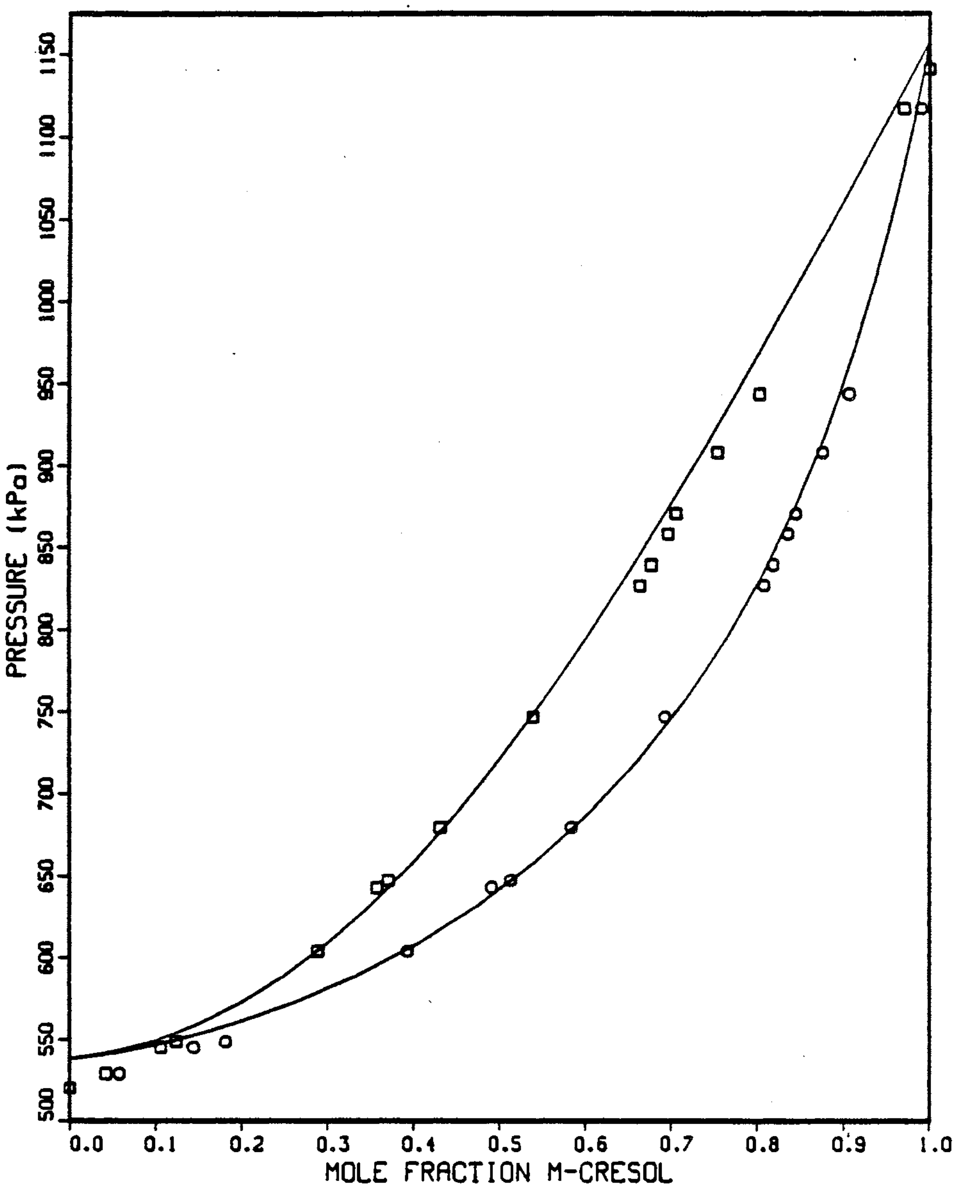

FIGURE 57
M-CRESOL/QUINOLINE 250°C ISOTHERM
PRED=SRK, (A+B/T)

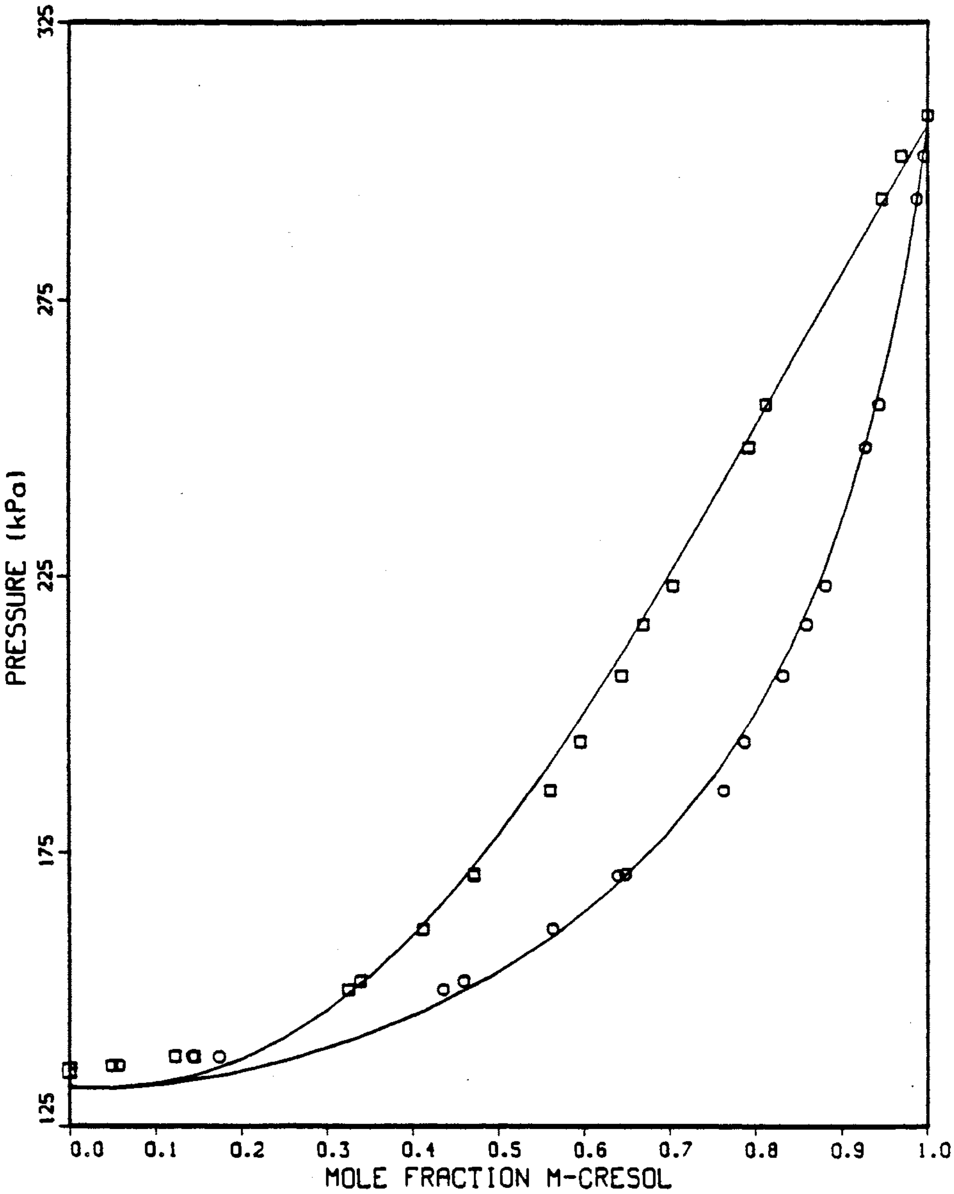

FIGURE 58
M-CRESOL/QUINOLINE 325°C ISOTHERM
PRED=SRK, (A+B/T)

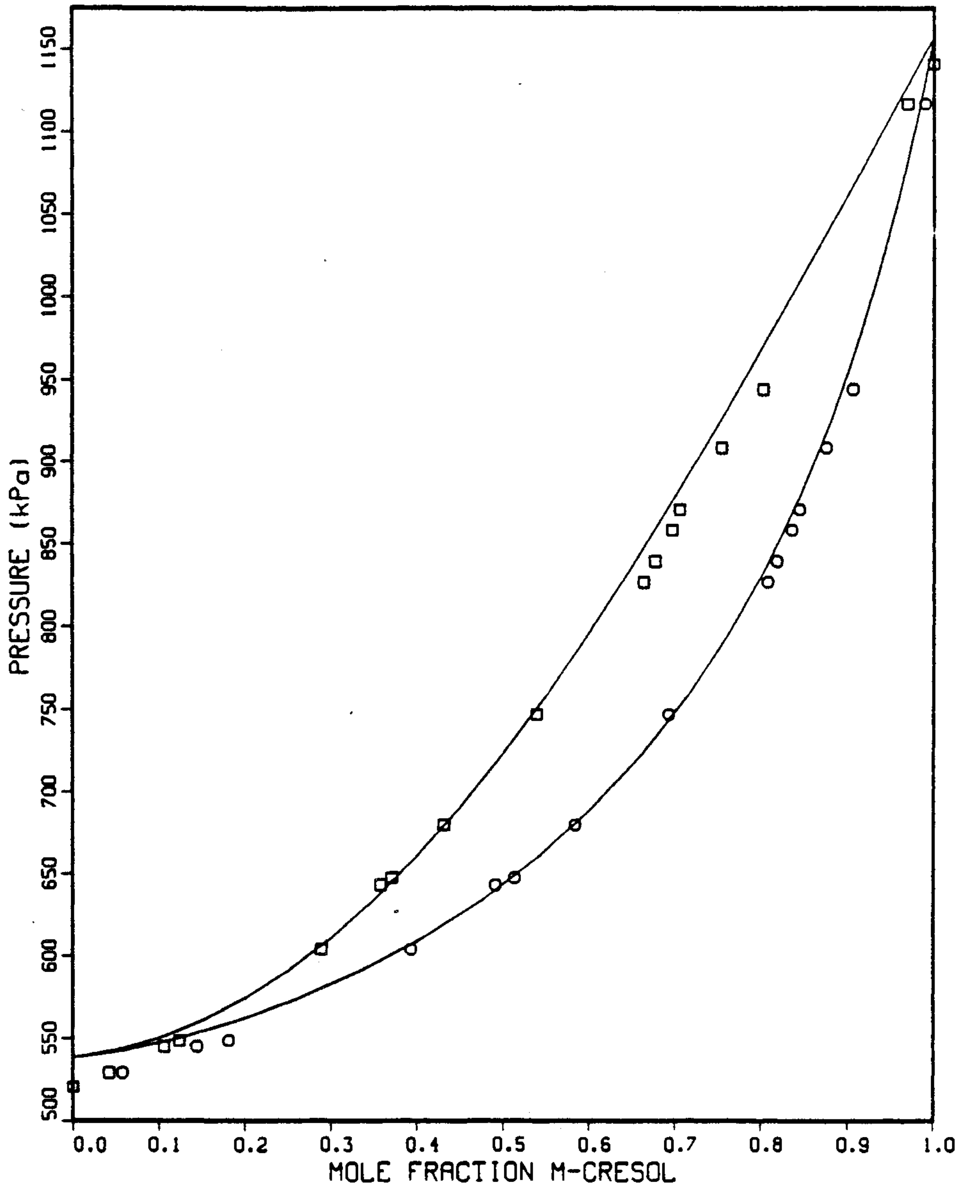

FIGURE 59
M-CRESOL/QUINOLINE 250°C ISOTHERM
PRED=SRK, (A-B/V)

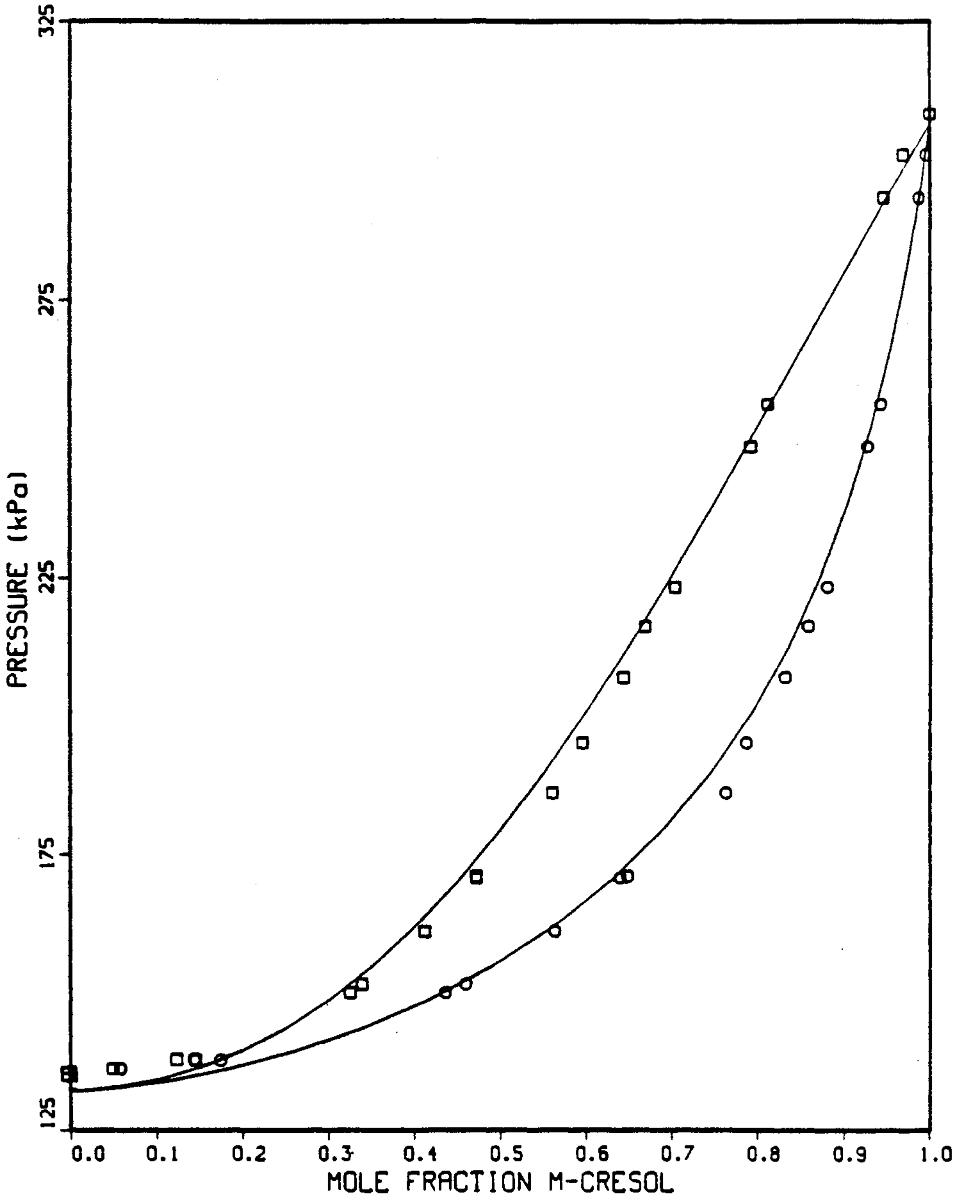

FIGURE 60
M-CRESOL/QUINOLINE 325°C ISOTHERM
PRED=SRK, (A-B/V)

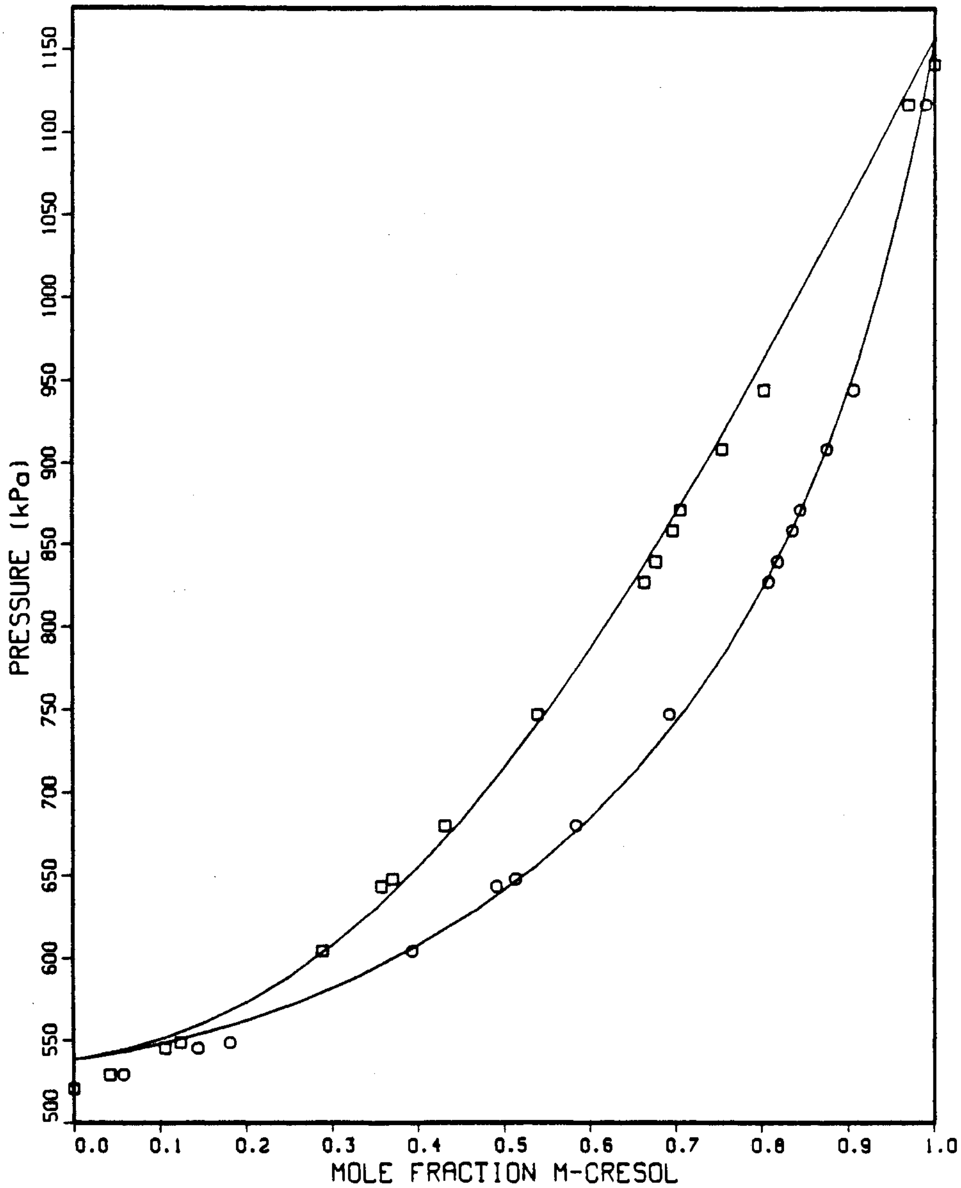

FIGURE 61
M-CRESOL/QUINOLINE 250°C ISOTHERM
PRED=SRK, (A-B/VRT)

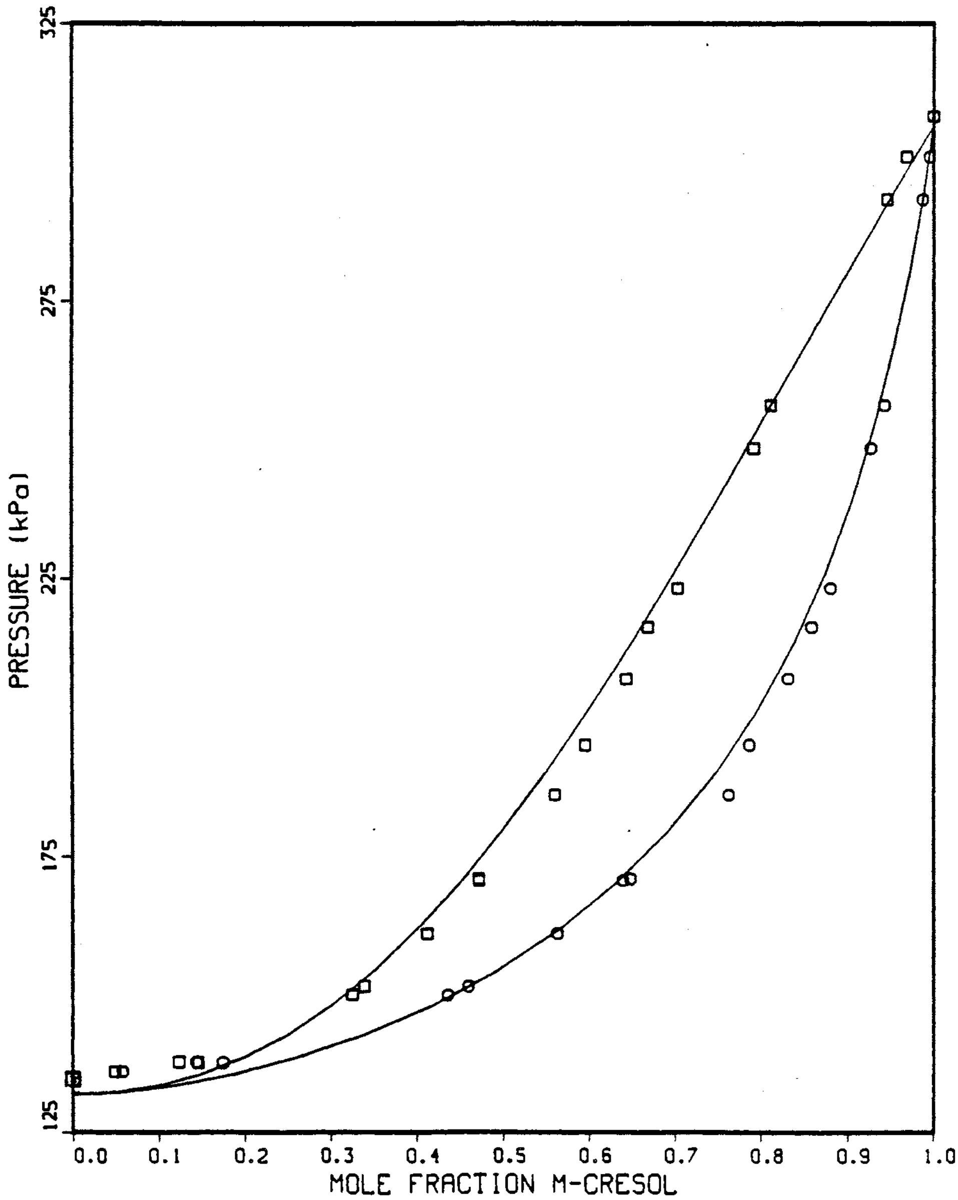

FIGURE 62
M-CRESOL/QUINOLINE 325°C ISOTHERM
PRED=SRK, (A-B/VRT)

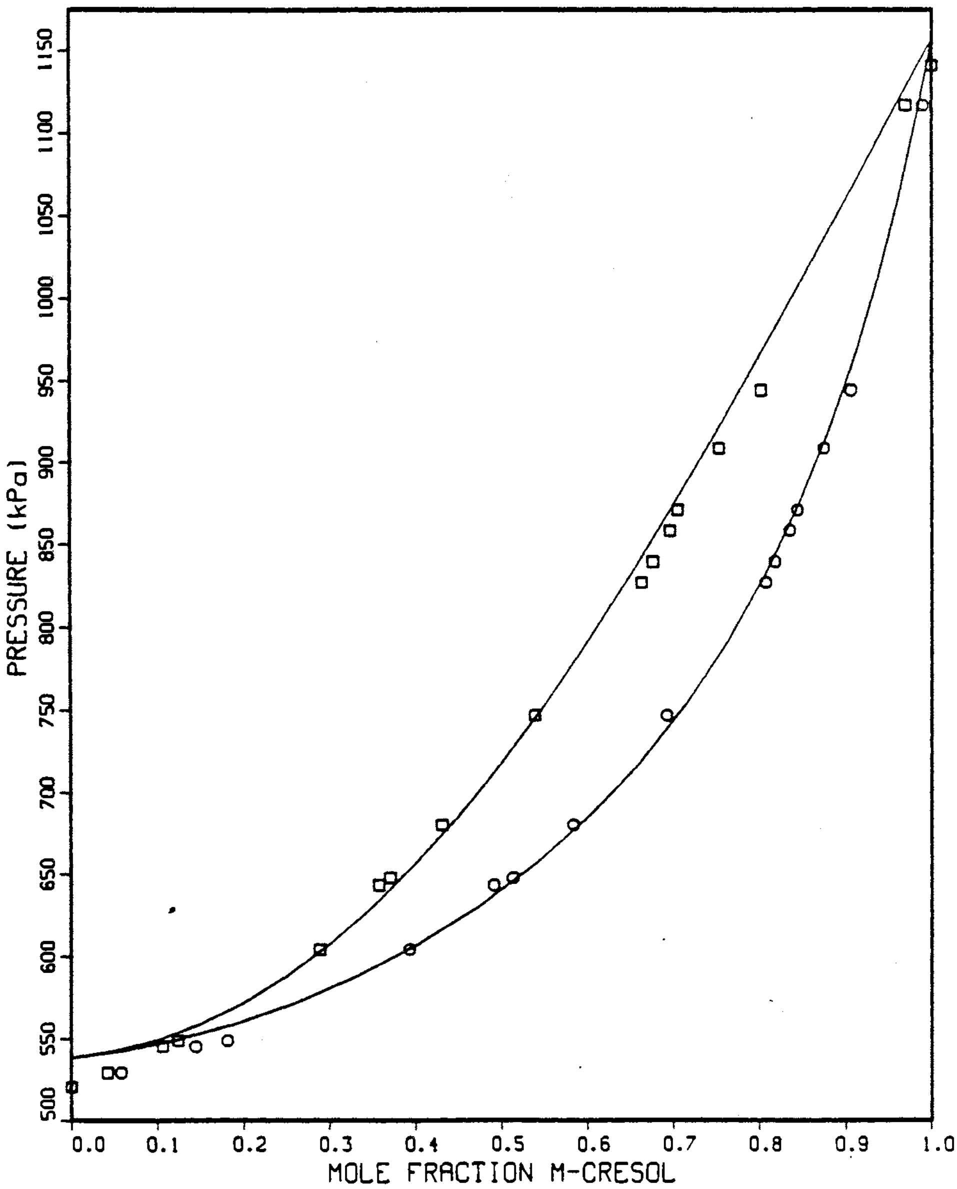

FIGURE 63
M-CRESOL/QUINOLINE 250°C ISOTHERM
PRED=SRK, (A+C's)

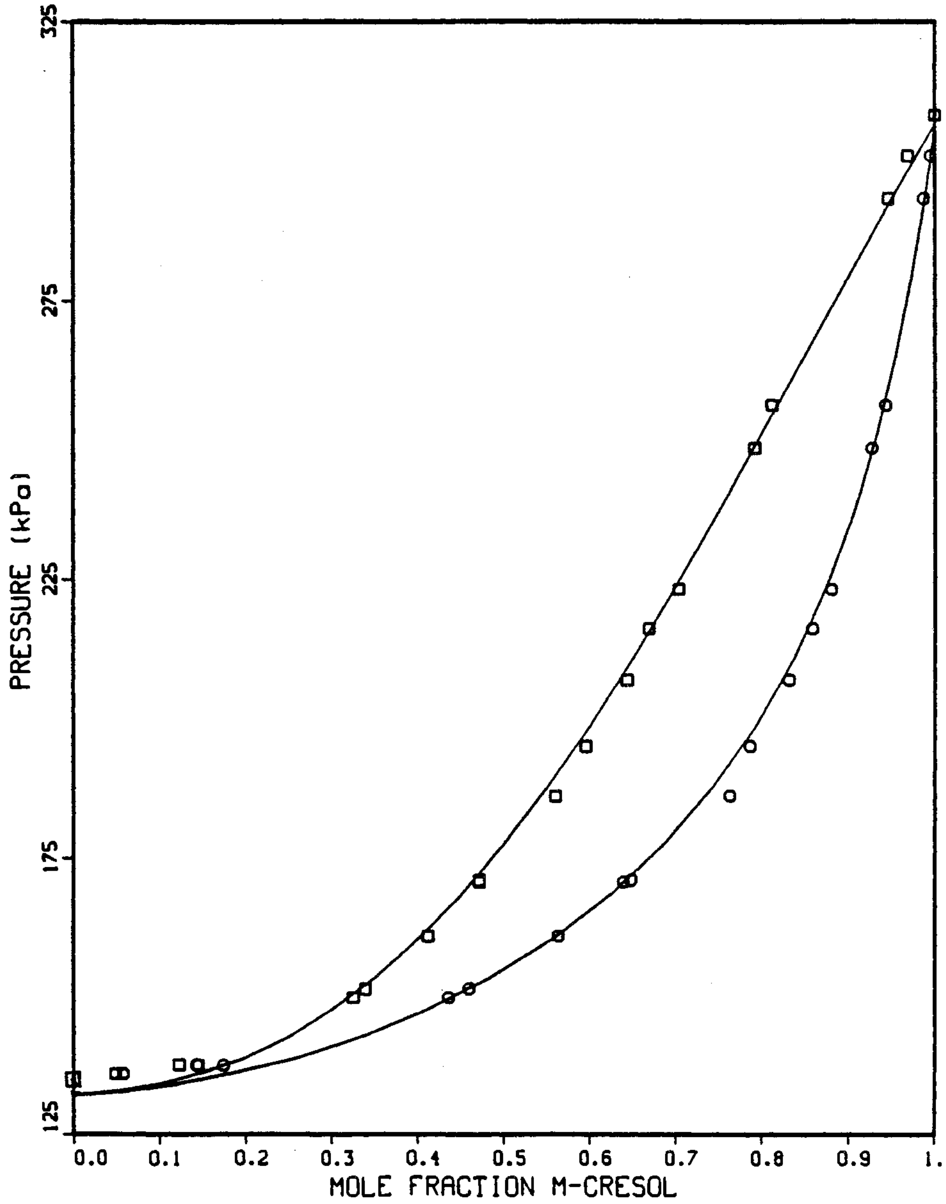

FIGURE 64
M-CRESOL/QUINOLINE 325°C ISOTHERM
PRED=SRK, (A+C's)

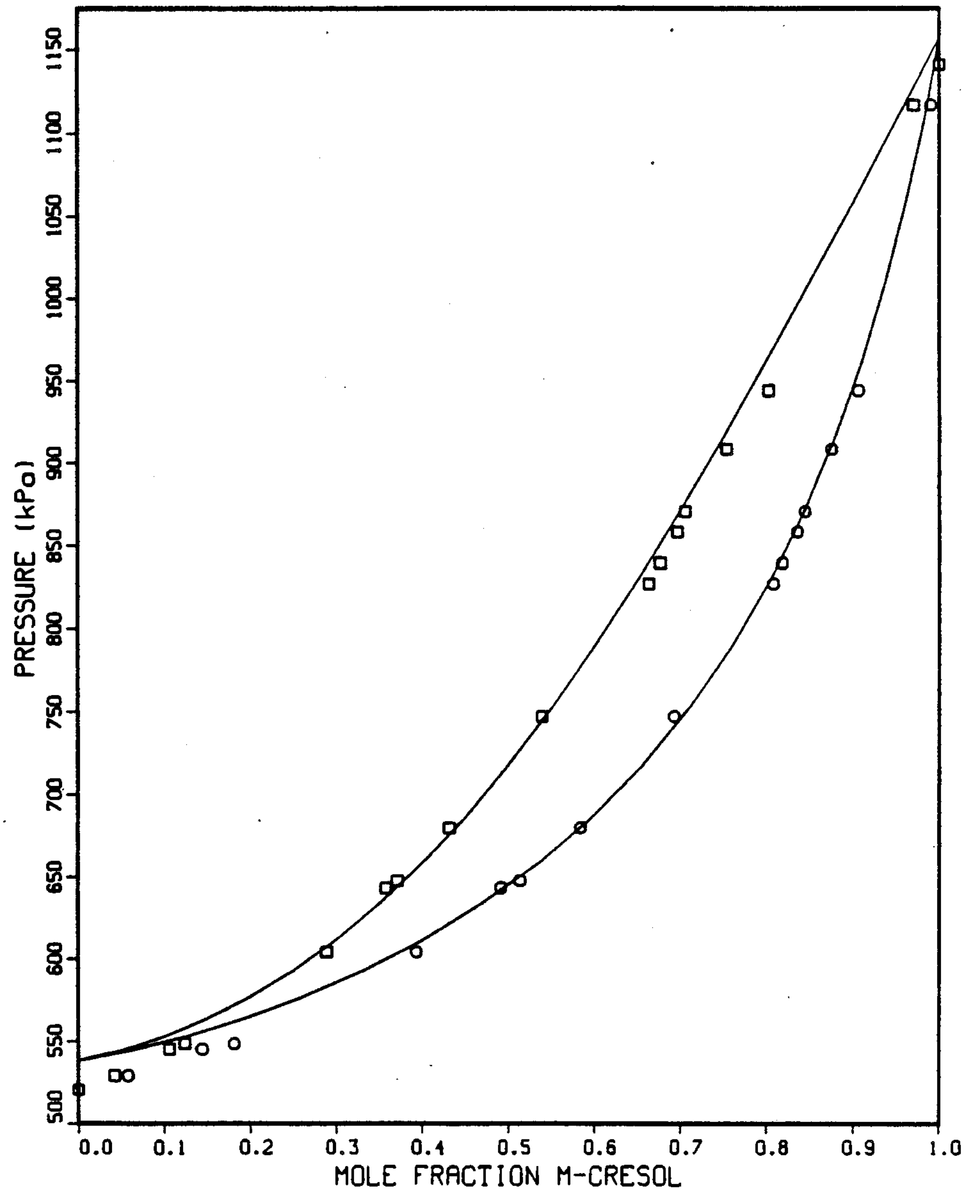

FIGURE 65
M-CRESOL/QUINOLINE 250°C ISOTHERM
PRED=YSRK, (A+C's)

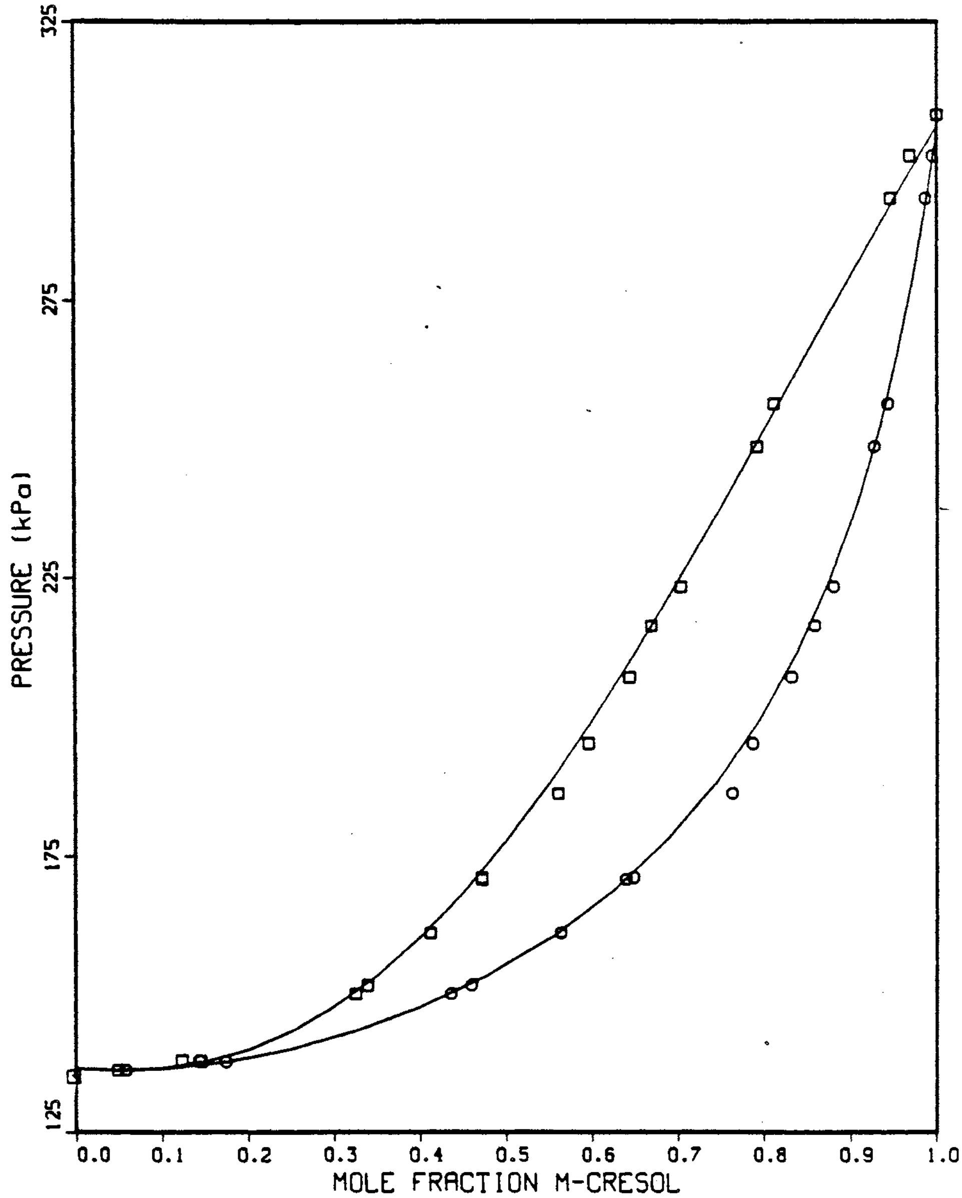

FIGURE 66

M-CRESOL/QUINOLINE 325°C ISOTHERM
PRED=YSRK, (A+C's)

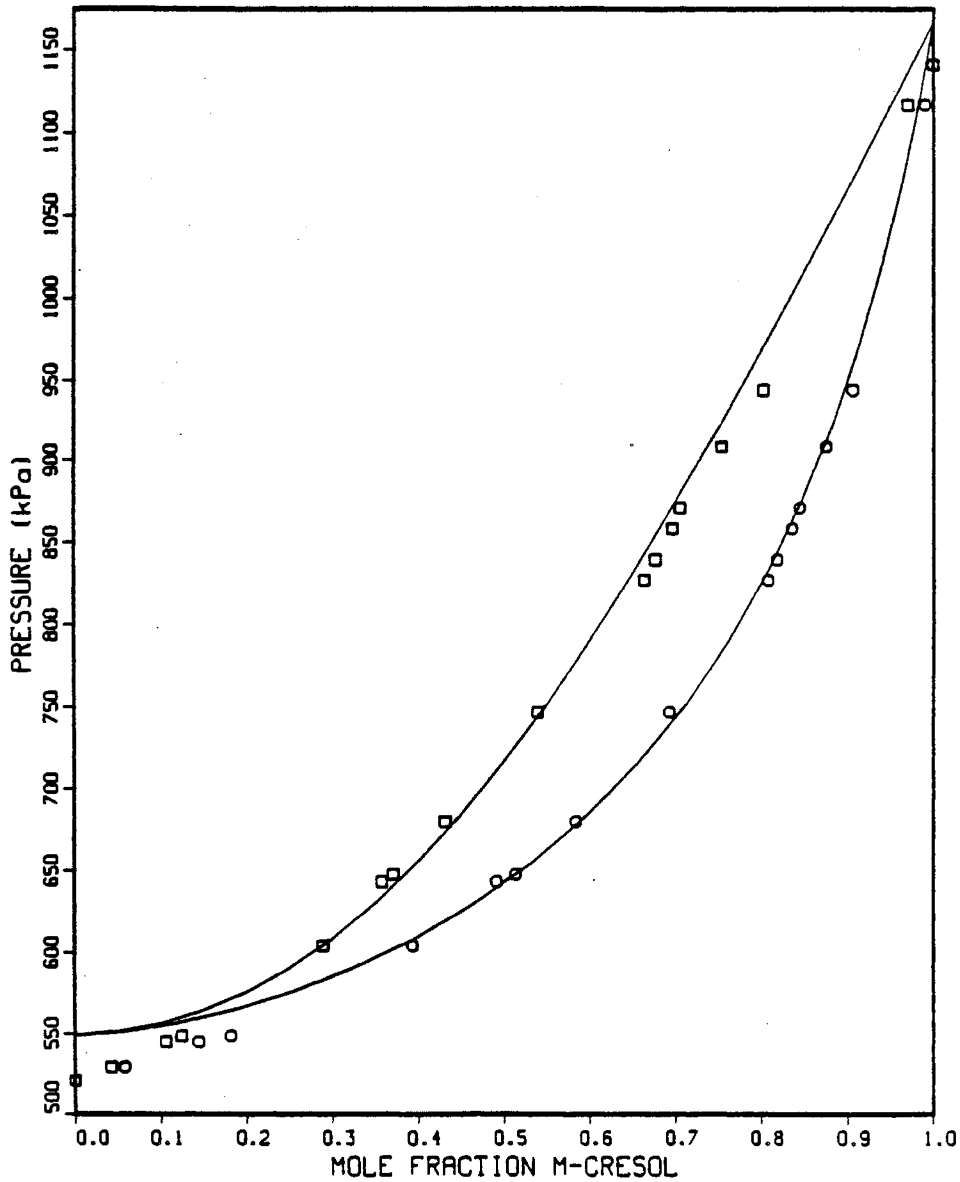

Looking at the overall results, all models using the SRK equation of state predicted the phase behavior of all three binaries well within an absolute percent standard deviation of 5% for both pressure and vapor composition. Certainly for industrial use, almost all of these models would be adequate. Therefore, when discussing the differences between the models, there is a relatively small range for improvement. When a model performed poorly, many times it was a result of poor vapor pressure predictions rather than the mixing rule used. In fact, even the simple interaction parameter would have performed very well if the EOS had been capable of predicting the correct vapor pressures. The YSRK equation of state with any mixing rule did not perform as well as the SRK equation. This was to be expected since all of the VLE data are in the reduced temperature range of 0.7 where the SRK equation of state is forced to fit the experimental vapor pressures.

For two of the systems, tetralin/quinoline and m-cresol/tetralin, model 5 (Luedecke mixing rule) was shown to be statistically superior to all of the other models. For the m-cresol/quinoline system, model 5 gave only a slightly better representation of the data than did the other models. However, even the simple k_{ij} interaction parameter gave a reasonably good prediction of m-cresol/quinoline with the major discrepancies most likely due to errors in vapor pressure predictions. Obviously, if a simple model does well, the more sophisticated model cannot show much improvement.

The results of the other models, using the SRK equation, are quite interesting. In almost all cases, the models appear to be not statistically different. It is interesting that the inclusion of a temperature, volume, or temperature and volume dependency did not improve the models. In viewing the graphs, it appears that these added dependencies altered the shapes of the curves but did not represent the data any better. It is most likely that since the data were over a relatively narrow temperature range (75°C) and were at high temperatures, the benefits of the temperature or volume dependencies may not be apparent.

These results can also allow some conclusions to be drawn about the Luedecke mixing rule. Models 2-4 each have a different functional dependency (volume, temperature, or volume and temperature) yet none show statistical superiority. These same dependencies are also present in the Luedecke mixing rule and are considered to be primary reasons for the superior predictive capabilities of the mixing rule. If this were truly the case, then models 2-4 should show increased modeling abilities. There are three major distinctions between models 2-4 and model 5: (1) model 5 has a cubic compositional dependency whereas models 1-4 are only quadratic, (2) unlike models 1-4, the second term in model 5 is not multiplied by a_{ij} which has a built-in temperature dependency, and (3) model 5 has one additional parameter.

In an attempt to determine the reason for the superiority of the Luedecke mixing rule, another mixing rule was studied briefly. The form of the mixing rule was $k_{ij} = A + B/T - C/v$. This mixing rule has the same quadratic compositional dependency as models 2-4 and all three parameters are multiplied by a_{ij}. Essentially, this model closely resembles models 2-4, yet has a third parameter. This model (model 7) was tested on the m-cresol/tetralin and the tetralin/quinoline binaries. The m-cresol/quinoline binary was not used since statistically there was little difference between any of the models. The s^2 value for model 7 was 10 for m-cresol/tetralin and 19 for tetralin/quinoline. When an F test was used to compare model 7 to all other models for both systems, model 7 was statistically superior to models 1-4 at almost a 99% confidence level; however, model 5 and model 7 were shown to be not statistically different.

Model 7 has the compositional, volume, and temperature dependencies of models 1-4 yet has an additional parameter. A logical conclusion is that (for these data) the most significant aspect of model 7 is the additional parameter. A further conclusion may be drawn that since models 5 and 7 are not statistically different, the main improvement of model 5 is the additional parameter rather than the functional form.

The above conclusion has additional support. Looking at the simple k_{ij} prediction for tetralin/quinoline (Figure 32), it can be seen that the model qualitatively follows the experimental data, but an error of almost 4% in the quinoline vapor pressure prediction prevents a quantitative result. However, looking at the model 5 prediction for the same system (Figure 41) it can be seen that this model fits the data quite well. Notice that model 5 quickly corrects for the bad quinoline vapor pressure prediction by putting a bend in the model to bring it back in line with the data. This is not a thermodynamic phenomenon, but a result of "fitting" the data rather than predicting the phase behavior. It is interesting to see that an additional parameter has almost completely modeled the data, even to the point of correcting for error in vapor pressure predictions by the EOS.

There are advantages and disadvantages to using a model that fits the data in the manner of model 5. Firstly, if the model is used for design purposes in the temperature region of the experimental data, then the model would be quite useful since it models the data very well. There is little extra computational difficulty in fitting three parameters over two, especially if a method such as the maximum likelihood algorithm is used. Caution should be used however, if one type of data is used to predict another thermodynamic property.

If experimental data are fit at one region and the model is to be used to predict the behavior in another region; using the Luedecke mixing rule (model 5) might not be advantageous. If the model corrects for poor vapor predictions or poor data, then extending the model to other temperature regions could cause significant errors. To illustrate this problem, data for the m-cresol/tetralin and the m-cresol/quinoline systems between temperatures of 150 and 200°C (recently published by Krevor et al. (1986)) were compared to predictions by models 1-5. Since these were predictions and not fits, the s^2 values were not available; therefore, the absolute percent standard deviations between the calculated and predicted values (ΔP and Δy) are presented in Tables 22-23. It can be seen that some of the

TABLE 22

MODEL PREDICTION OF M-CRESOL/TETRALIN

COMPARISON WITH KREVOR, et. al.

150-195°C

EOS	Model	ΔP(%)	Δy(%)
SRK	k_{ij}	1.03	3.22
SRK	A+B/T	4.02	6.70
SRK	A-B/v	1.73	1.58
SRK	A-B/vRT	1.92	2.06
SRK	A+C's	4.95	6.50
YSRK	k_{ij}	2.48	1.67

TABLE 23

MODEL PREDICTION OF M-CRESOL/QUINOLINE

COMPARISON WITH KREVOR, et. al.

160 - 200°C

EOS	Model	ΔP(%)	Δy(%)
SRK	k_{ij}	4.03	19.61
SRK	A+B/T	3.82	15.86
SRK	A-B/v	4.22	25.12
SRK	A-B/vRT	4.43	24.28
SRK	A+C's	3.57	21.7
YSRK	k_{ij}	3.08	10.71

predictions for m-cresol/tetralin are not bad; however, model 5 performs less well than most other models. In fact, it appears that the simple k_{ij} model predicts the phase behavior the best. Figures 67-72 present the predictions versus the experimental data for m-cresol/tetralin. Graphically, it appears that the simple k_{ij} performs better than most others and certainly model 5 is one of the least accurate.

The m-cresol/quinoline predictions are extremely poor. This is unusual given the reasonably good results for the m-cresol/tetralin predictions. When the m-cresol/quinoline data from this investigation were fit, the models had little statistical difference and all models performed well. Figures 73-77 present the predictions and the experimental data.

Since the interaction paramters were fit to a relatively small temperature range (75°C) it was thought that a better fit could be obtained if the range were extended. The m-cresol/tetralin system was fit over the temperature range 150-325°C using a combination of data from Krevor and from this investigation. The m-cresol/quinoline data was fit over the temperature range 160-325°C. It was attempted to use even amounts of data over the entire range in order not to bias one region over another.

FIGURE 67

M-CRESOL/TETRALIN COMPARISON WITH KREVOR, et al.
PRED=SRK, SIMPLE

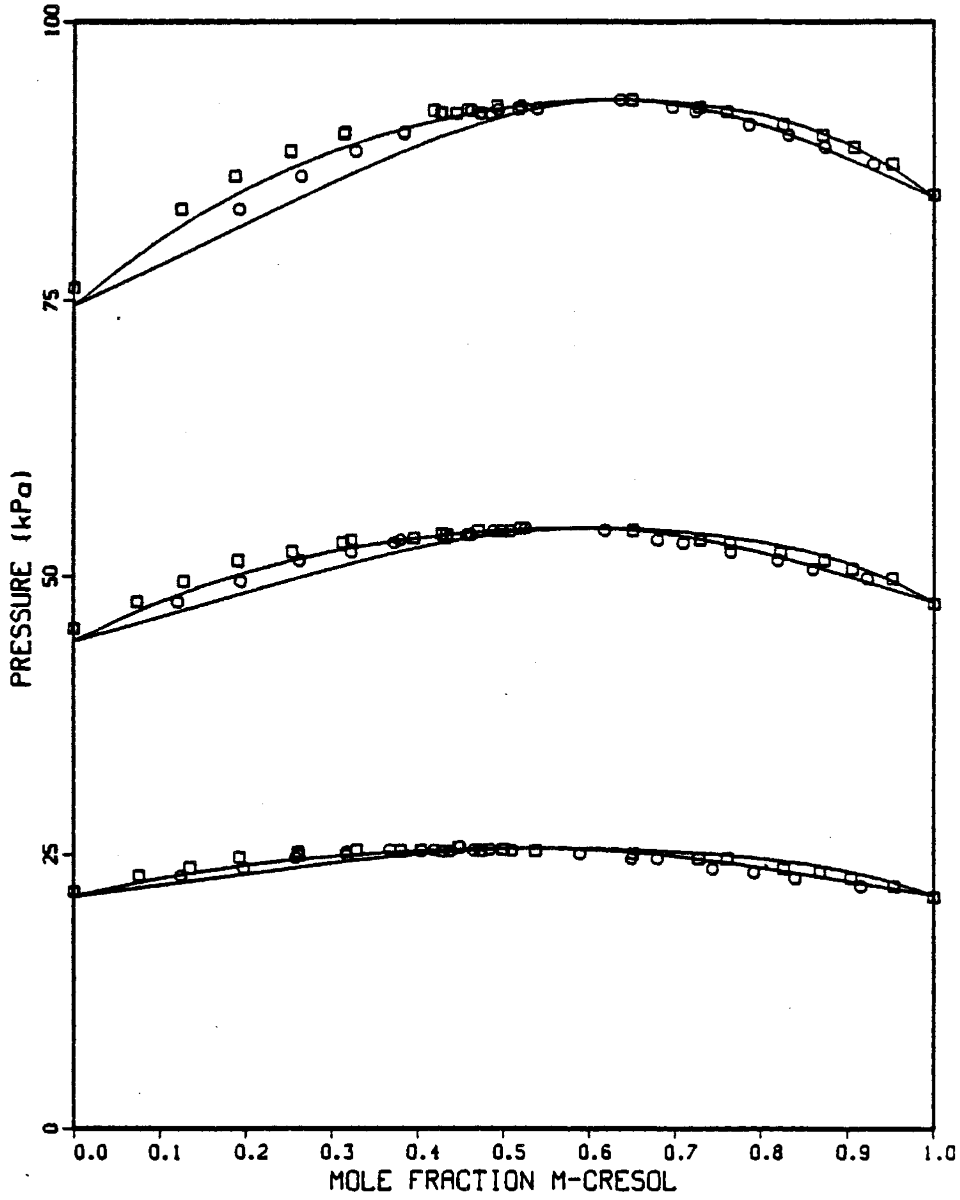

FIGURE 68

M-CRESOL/TETRALIN COMPARISON WITH KREVOR, et al.
PRED=SRK, (A+B/T)

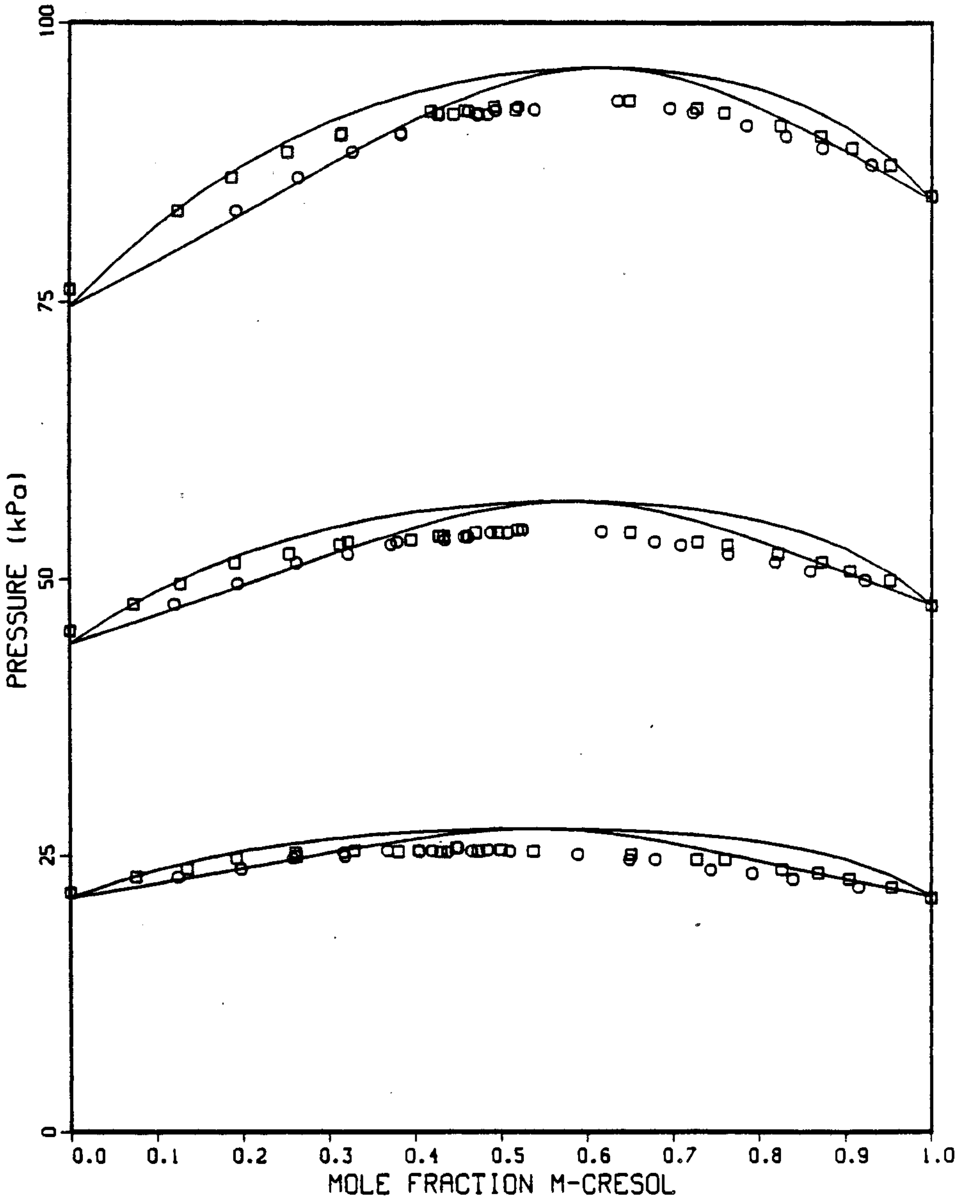

FIGURE 69

M-CRESOL/TETRALIN COMPARISON WITH KREVOR, et al.
PRED=SRK, (A-B/V)

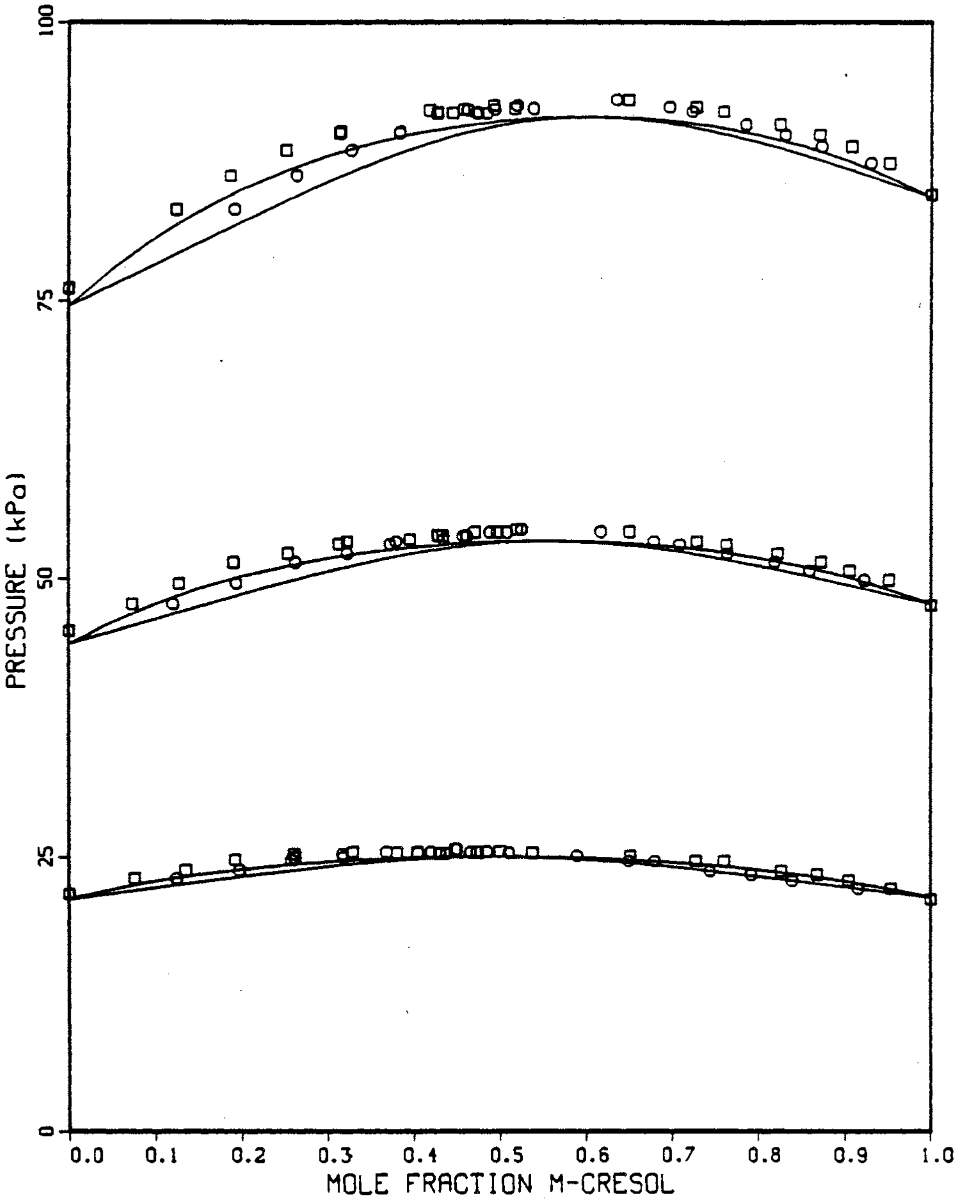

FIGURE 70

M-CRESOL/TETRALIN COMPARISON WITH KREVOR, et al.
PRED=SRK, (A-B/VRT)

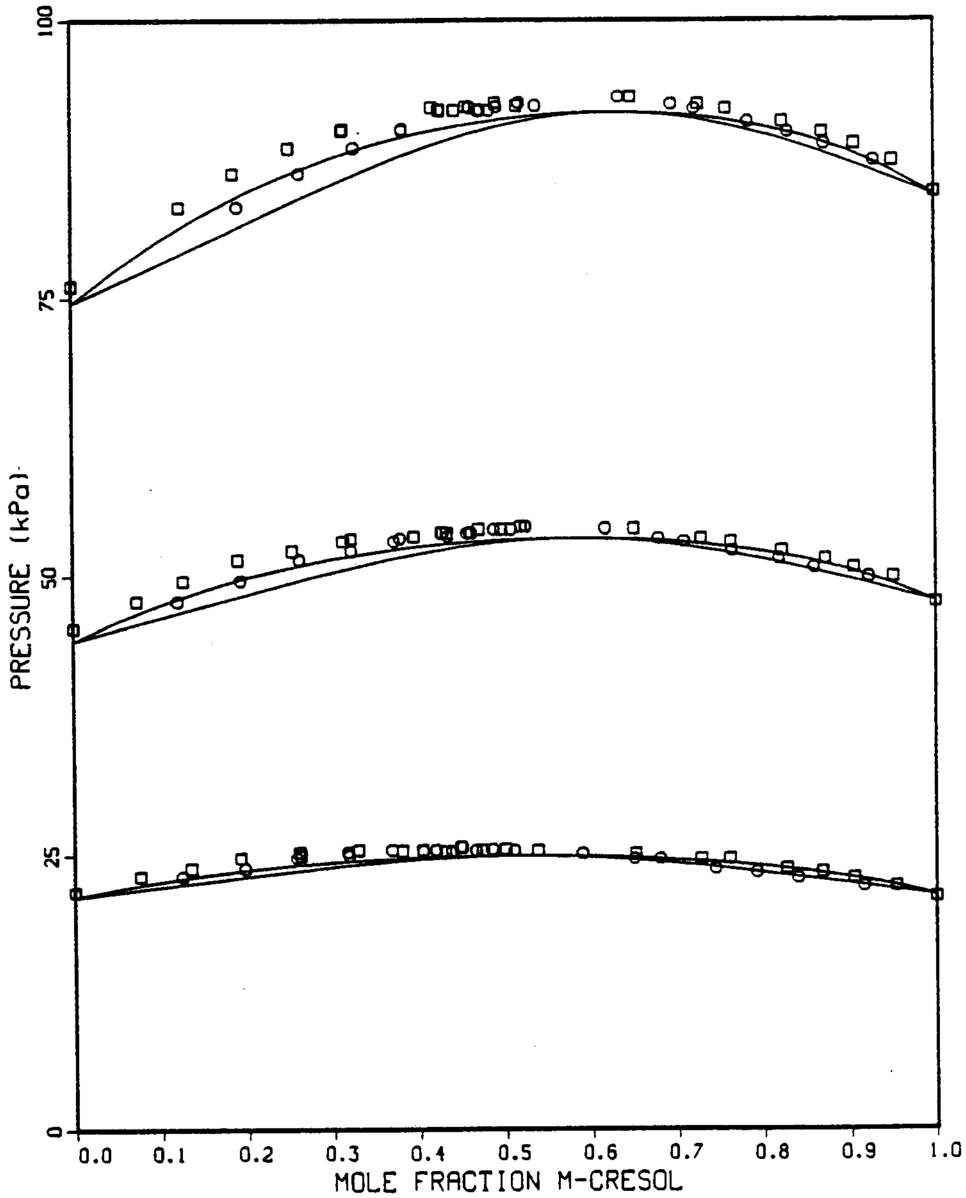

FIGURE 71

M-CRESOL/TETRALIN COMPARISON WITH KREVOR, et al.
PRED=SRK, (A+C's)

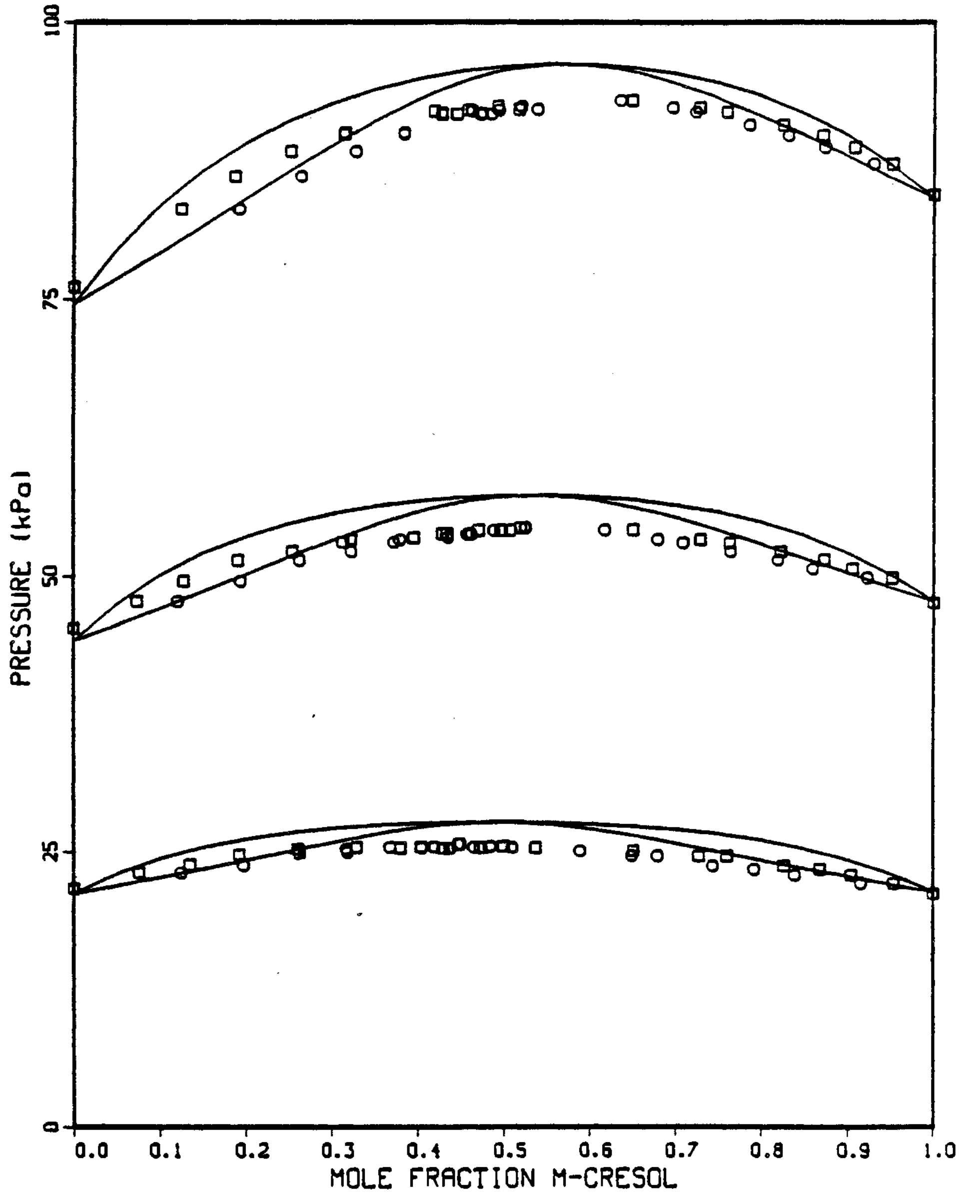

FIGURE 72

M-CRESOL/TETRALIN COMPARISON WITH KREVOR, et al.
PRED=YSRK, (A+C's)

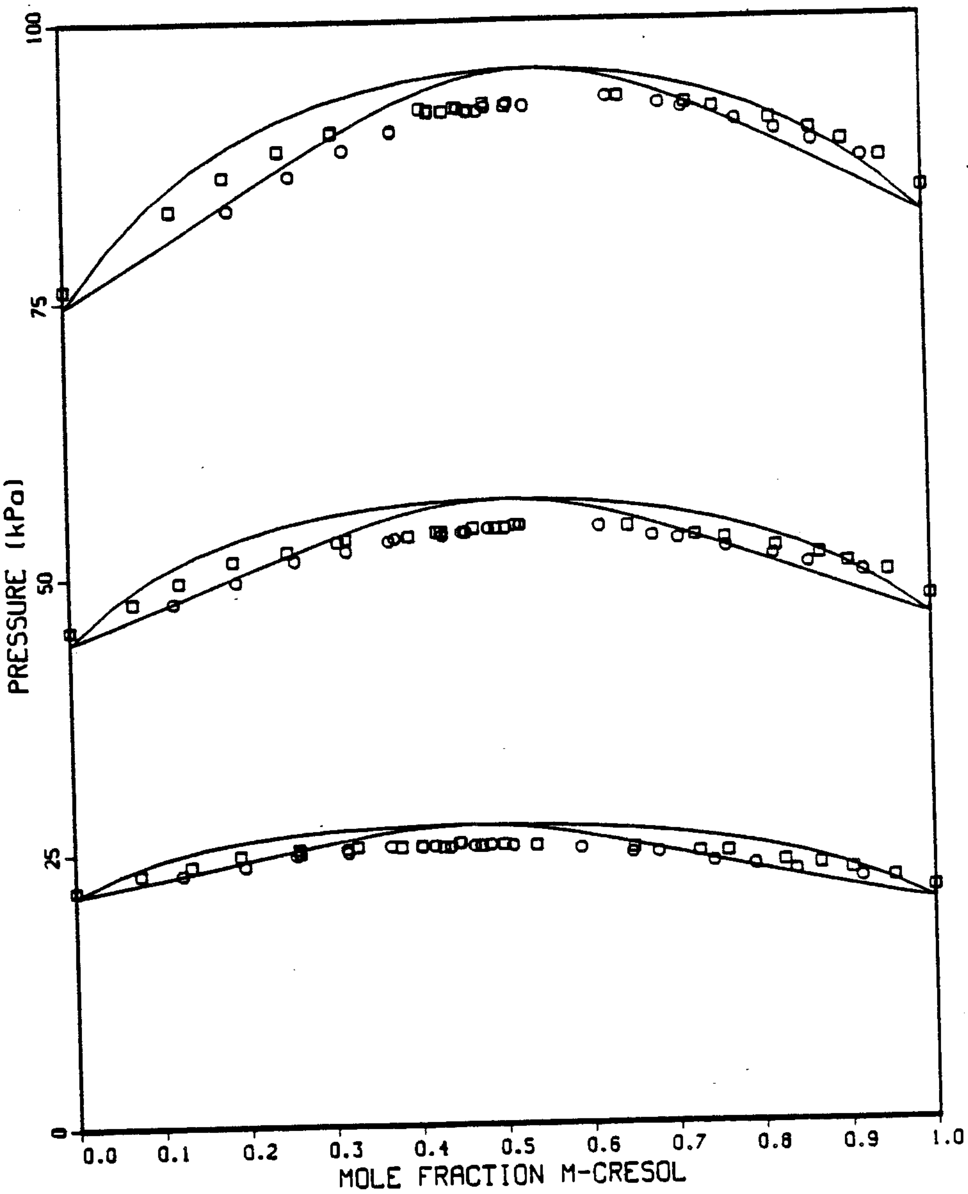

FIGURE 73

M-CRESOL/QUINOLINE COMPARISON WITH KREVOR, et al.
PRED=SRK, SIMPLE

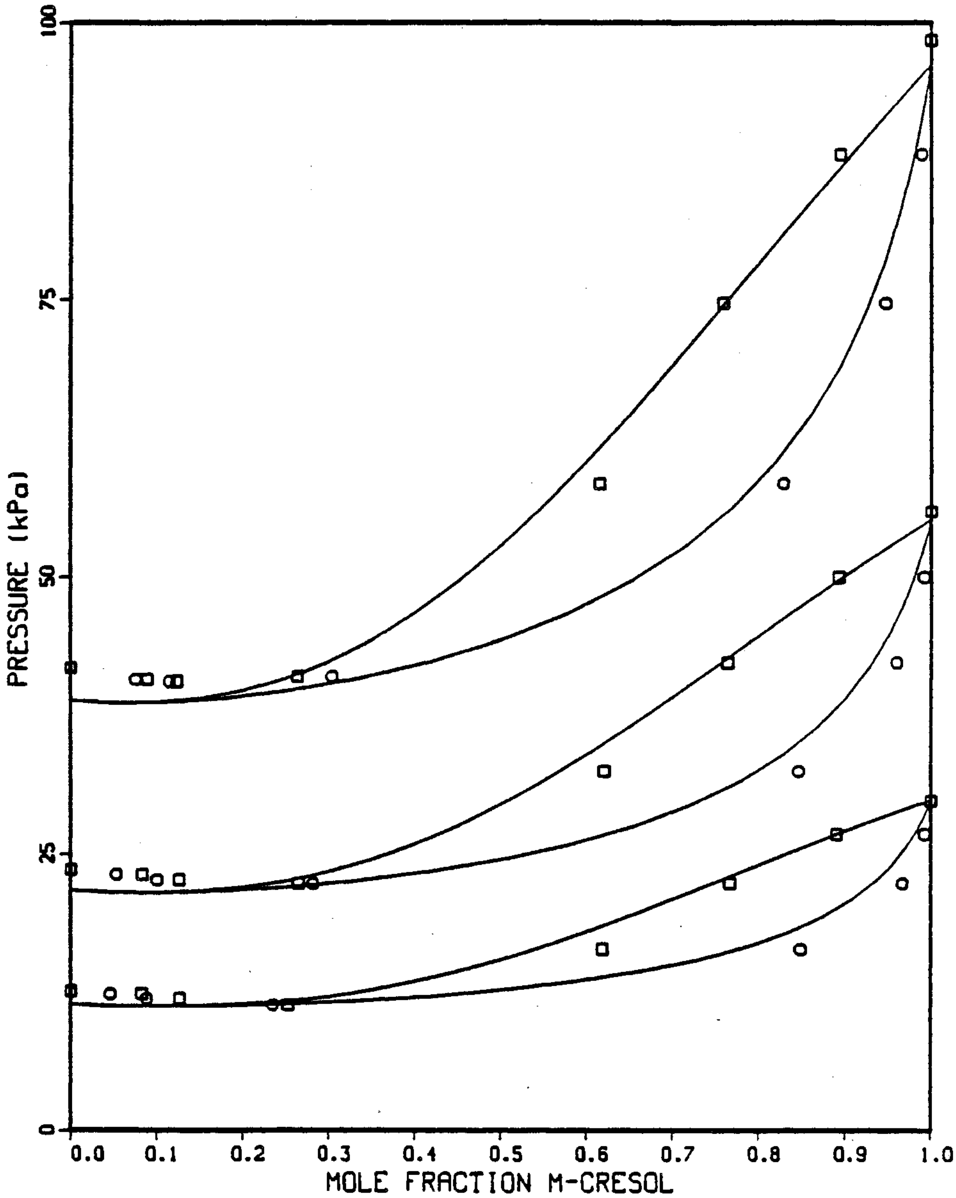

FIGURE 74

M-CRESOL/QUINOLINE COMPARISON WITH KREVOR, et al.
PRED=SRK, (A-B/V)

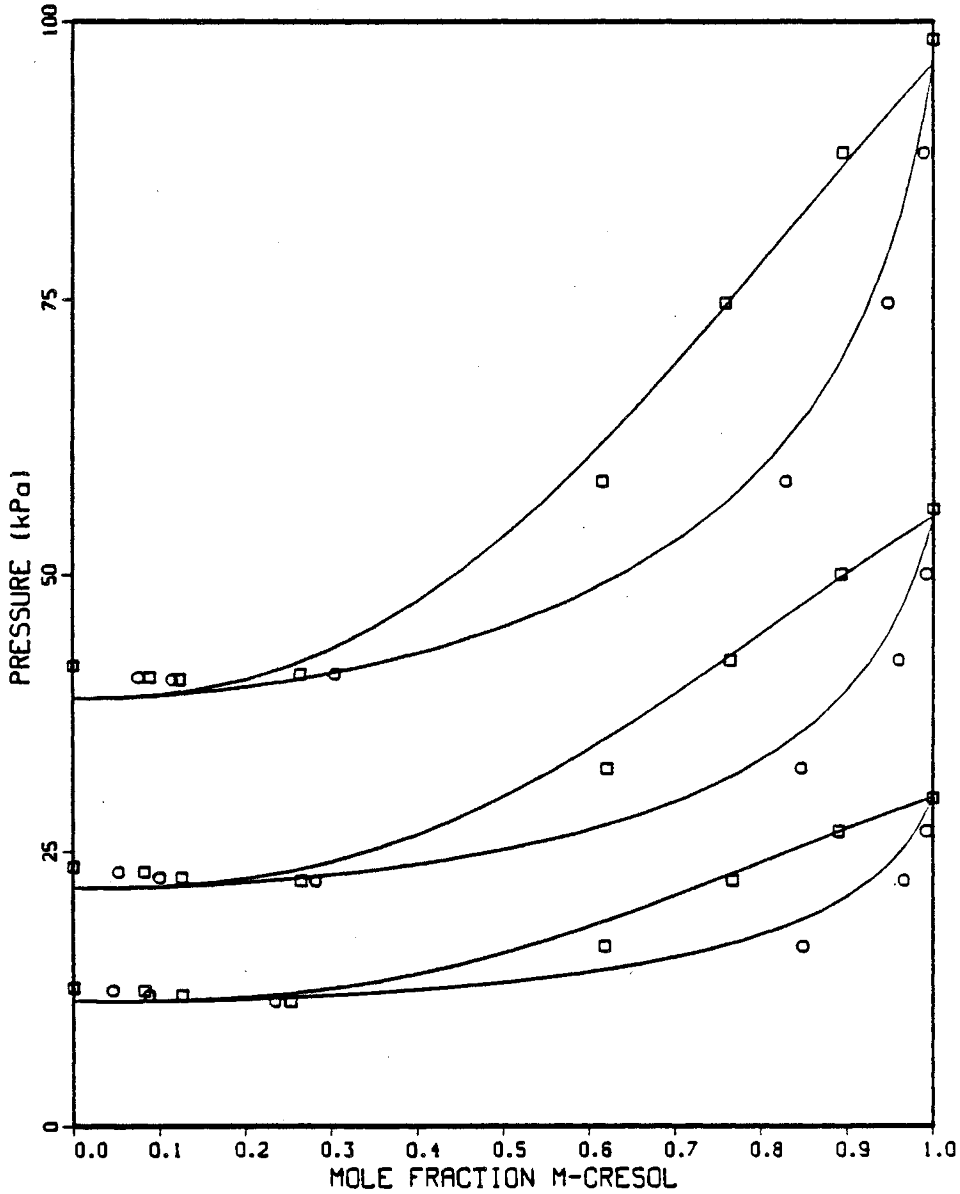

FIGURE 75

M-CRESOL/QUINOLINE COMPARISON WITH KREVOR, et al.
PRED=SRK, (A-B/VRT)

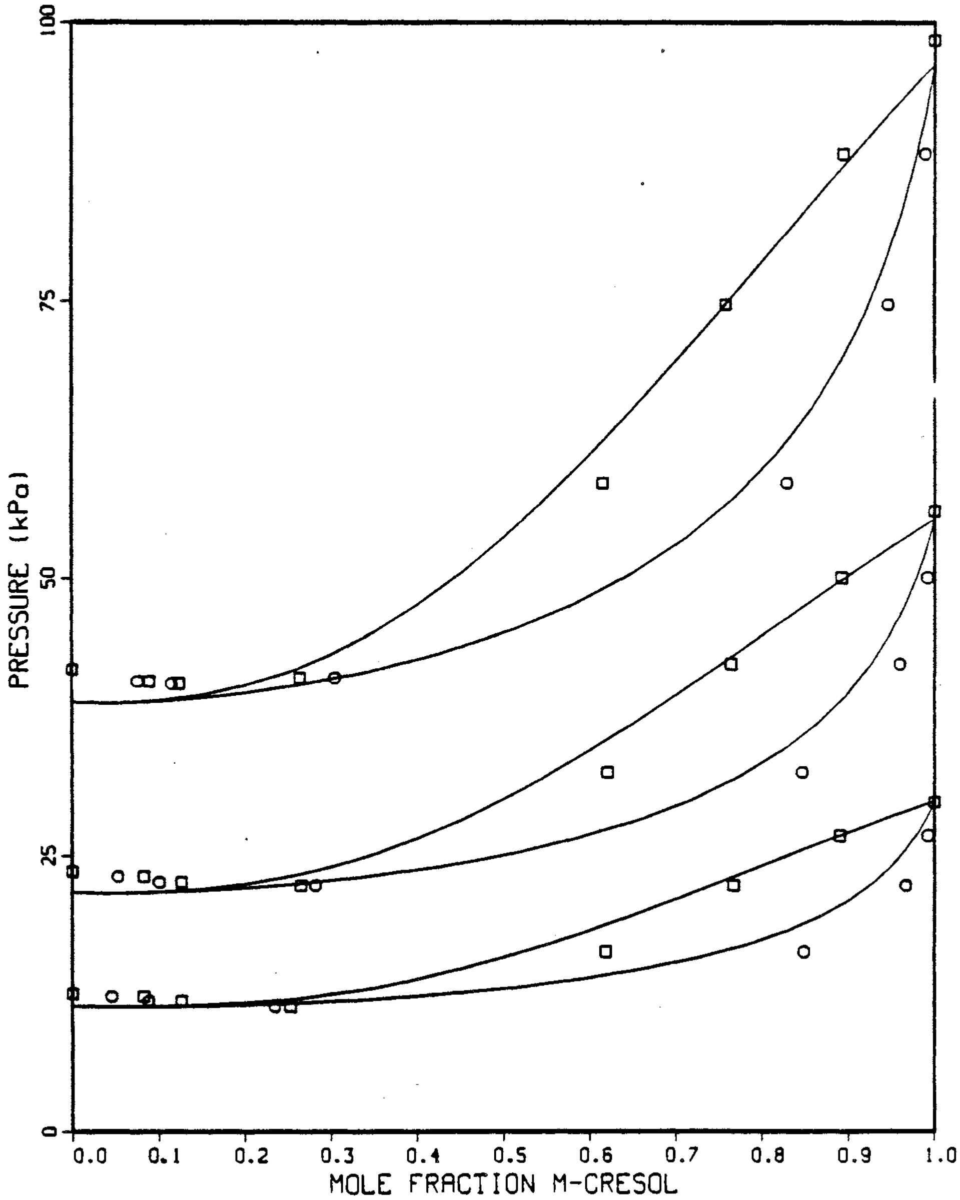

FIGURE 76

M-CRESOL/QUINOLINE COMPARISON WITH KREVOR, et al.
PRED=SRK, (A+C's)

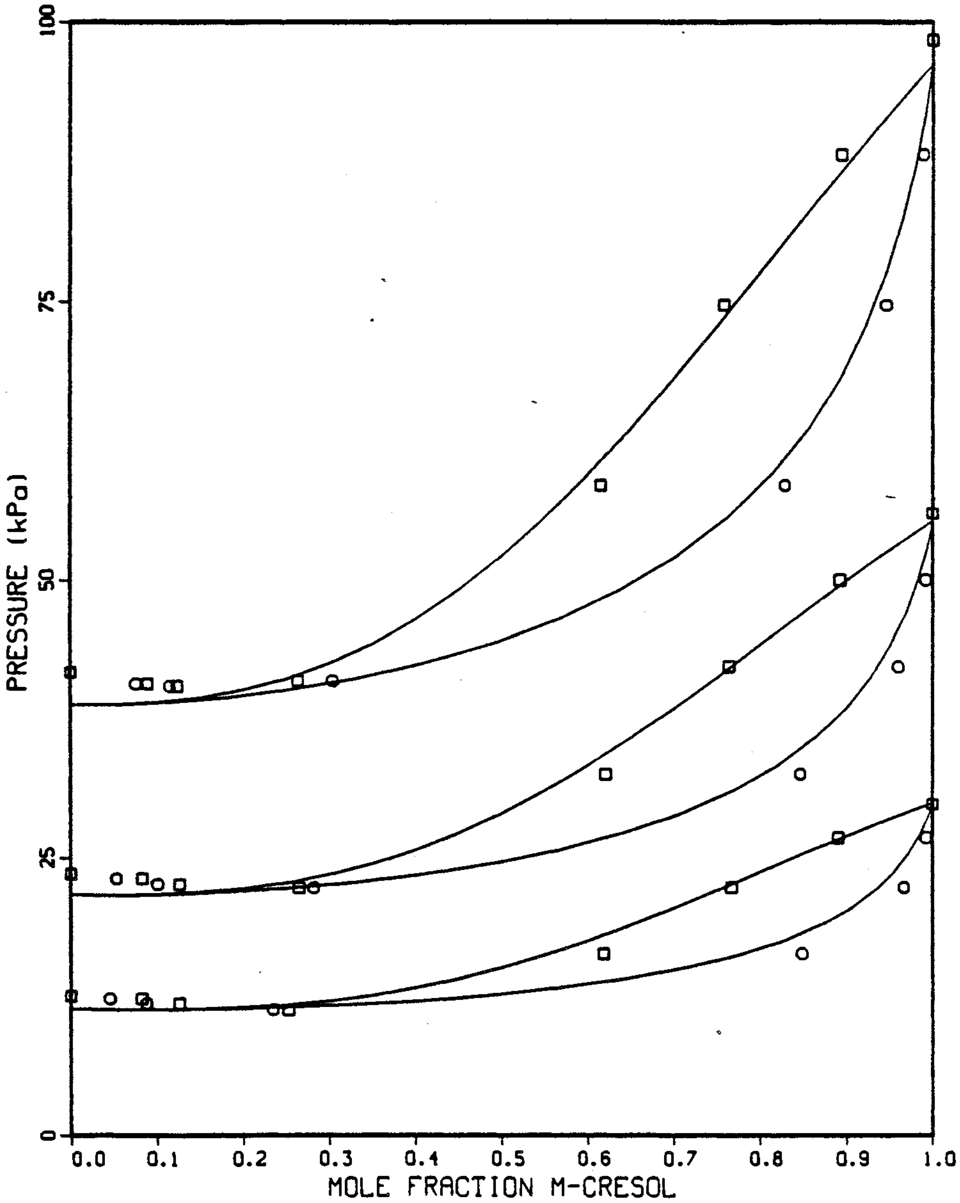

FIGURE 77

M-CRESOL/QUINOLINE COMPARISON WITH KREVOR, et al.
PRED=YSRK, (A+C's)

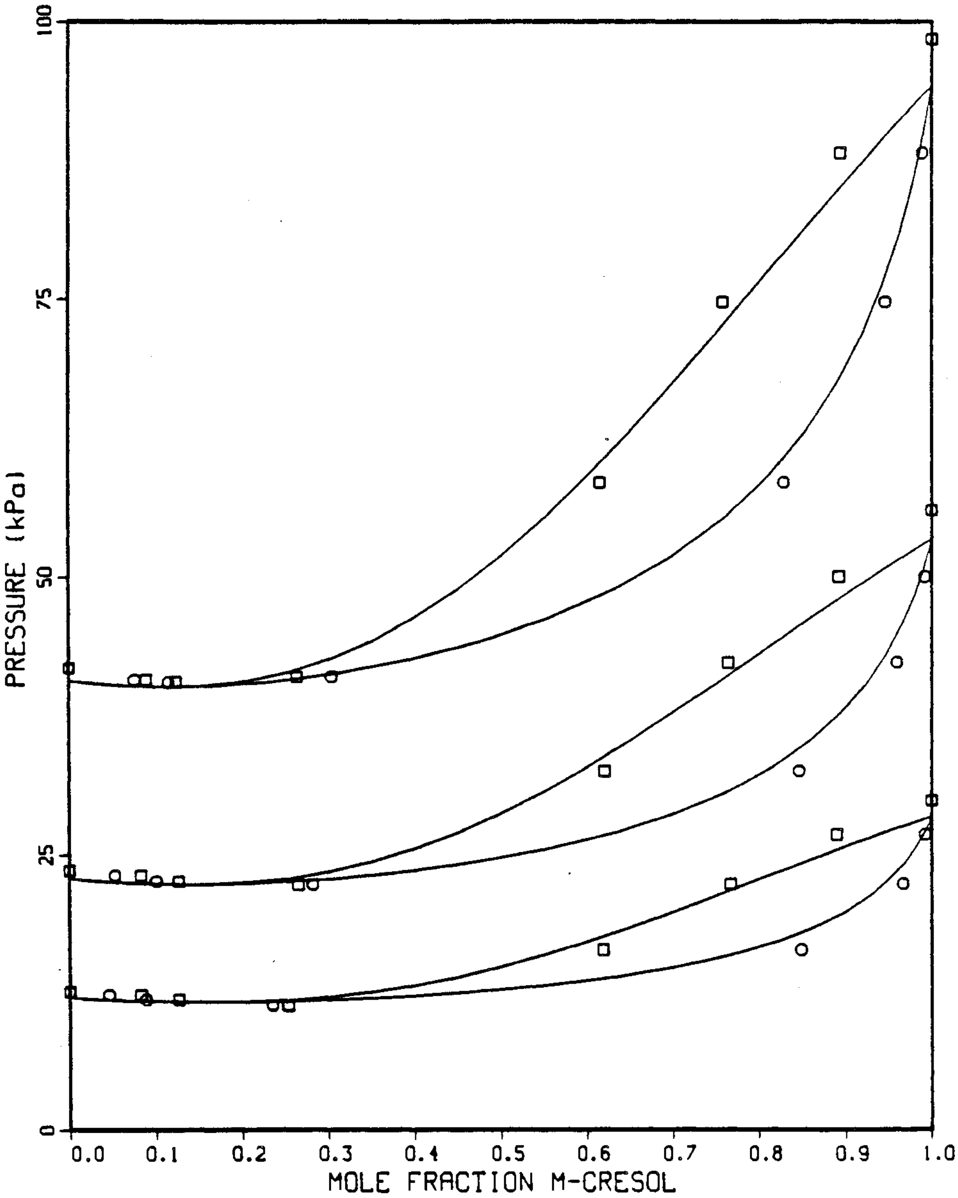

The results are presented in Tables 24-25 and the new interaction parameters are presented in Tables 26-27. Two values of the absolute percent deviations are presented, one for Krevor's data and one for the data from this investigation. For m-cresol/tetralin, model 5 predicted the data better than the other models by a confidence level of 99% and the ΔP and Δy values are lower than the predictions in Table 22. For m-cresol/quinoline, again model 5 is better than the other models with a confidence level of 99%. The absolute percent deviations for this system have decreased but are still very high for Krevor's data. This is quite unusual since the fit is reasonably good for the data from this research. This may indicate inconsistencies between the two data sets and cast some doubt upon Krevor's data. The YSRK equation of state in combination with the simple k_{ij} interaction parameter is shown to perform statistically better than the SRK with a k_{ij} interaction parameter for the m-cresol/quinoline system. The vapor pressures for quinoline are better predicted in the lower region by the YSRK than the SRK. Notice that while there is a significant statistical difference between the two equations of state for the simple interaction parameter, no statistical difference is apparent between the equations of state for the more complex model 5 mixing rule. This is a

TABLE 24

COMPARISON OF THERMODYNAMIC MODELS

M-CRESOL/TETRALIN AT 150 - 325°C

i	EOS	Model	s^2	α_{i1}	α_{i2}	α_{i3}	α_{i4}	α_{i5}	ΔP(%)	Δy(%)	
1	SRK	k_{ij}	46.3	---					1.05	3.16	Krevor
									0.99	1.29	This inv.
2	SRK	A+B/T	47.0	ns	---						
3	SRK	A-B/v.	27.8	95	95	---					
4	SRK	A-B/vRT	40.3	ns	ns	90-95	---				
5	SRK	A+C's	19.1	99.9	99.9	90	99.9	---	0.57	2.10	Krevor
									0.83	1.61	This inv.
6	YSRK	A+C's	30.4	---	---	---	---	95	0.87	2.49	Krevor
									0.82	1.12	This inv.

1 = simple interaction parameter
2 = temperature dependent interaction parameter
3 = Holder et al. (1986)
4 = modification of Holder mixing rule
5 = Luedecke et al. (1985)

ns = significantly less than a 90% confidence level

TABLE 25

COMPARISON OF THERMODYNAMIC MODELS

M-CRESOL/QUINOLINE AT 160 - 325°C

i	EOS	Model	s^2	α_{i1}	α_{i2}	α_{i3}	α_{i4}	α_{i5}	ΔP(%)	Δy(%)	
1	SRK	k_{ij}	137	---					3.90	15.10	Krevor
									1.30	3.10	This inv.
2	SRK	A+B/T	119	ns	---						
3	SRK	A-B/v	139	ns	ns	---					
4	SRK	A-B/vRT	129	ns	ns	<90	---				
5	SRK	A+C's	95	90	<90	90	<90	---	3.50	12.80	Krevor
									1.20	1.70	This inv.
	YSRK	k_{ij}	76	95	90-95	95	95	ns	3.02	6.13	Krevor
									1.10	3.30	This inv.
	YSRK	A+C's	81	95	90-95	95	95	ns	3.04	8.04	Krevor
									1.22	3.84	This inv.

1 = simple interaction parameter
2 = temperature dependent interaction parameter
3 = Holder et al. (1986)
4 = modification of Holder mixing rule
5 = Luedecke et al. (1985)
ns = significantly less than a 90% confidence level

TABLE 26

INTERACTION PARAMETERS

M-CRESOL/TETRALIN 150-325°C

EOS	Model	Parameters		
SRK	k_{ij}	A = 3.80E-2		
SRK	A+B/T	A = 3.84E-2	B = -.1896	
SRK	A-B/v	A = .1020	B = 22.902	
SRK	A-B/vRT	A = 5.89E-2	B = 28911982	
SRK	A+C's	A = 4.13E-2	C_{12} = 1.04E-2	C_{21} = -3.90E-3
YSRK	A+C's	A = 1.93E-3	C_{12} = -2.00E-2	C_{21} = -2.18E-2

The values of C_{12} and C_{21} are normalized by $a_i(Tc)^2$

TABLE 27

INTERACTION PARAMETERS

M-CRESOL/QUINOLINE 160-325°C

EOS	Model	Parameters		
SRK	k_{ij}	A = -8.73E-2		
SRK	A+B/T	A = -2.38E-2	B = -32.482	
SRK	A-B/v	A = -7.26E-2	B = 4.389	
SRK	A-B/vRT	A = -5.72E-2	B = 37781921	
SRK	A+C's	A = 1.03E-2	C_{12} = 6.62E-2	C_{21} = 4.10E-2
YSRK	A+C's	A = -3.89E-2	C_{12} = 3.31E-2	C_{21} = 2.41E-2
YSRK	k_{ij}	A = -9.13E-2		

The values of C_{12} and C_{21} are normalized by $a_i(Tc)^2$

further indication that model 5 is correcting for poor vapor pressure predictions and results in fitting the data rather than predicting phase behavior.

Except for model 3 for the m-cresol/tetralin system, there was no statistical difference between models 1-4. The temperature range that the models were fit over was 175°C. The statistical tests may lead to the conclusion that a much wider temperature range is required before the expected temperature or volume dependencies become significant or that these data are at temperatures where the strong interactions are not as significant.

In conclusion, for these systems and temperature ranges, the Luedecke mixing rule was found to be far superior to all other models. In most cases, two parameter models were shown to be not statistically different indicating that temperature or volume dependencies did not significantly alter the performance of the models. This is most likely due to the narrow temperature range over which the models were fit and/or the high temperatures at which the data were obtained. The single most significant aspect of the models that enhanced the ability to fit the data was the addition of a third parameter. It is believed that the addition of a third parameter in the mixing rule allowed the model to overfit the data. The overfitting resulted in the three parameter mixing rule (model 5) modeling not only thermodynamic phenomena but also poor vapor pressure predictions by the EOS and possible inconsistencies in the data. For these reasons, when the three parameter mixing rule was used to predict phase behavior at other temperatures, it performed poorly in comparison to the simple k_{ij} interaction parameter (model 1).

In the final analysis, if a model is fit to a set of data and used in the same region as the data, then the three parameter mixing rule has a statistical advantage over all of the other models. If however, the model is to be used to predict phase behavior in other temperature regions, then the three parameter mixing rule may perform poorly in comparison to a more simple model. Errors in vapor pressure predictions were the most significant error in the models; obviously, the equations of state still require more work.

The maximum likelihood method was found to be not only extremely useful in fitting complex models to experimental data but also provided valuable statistical information by which models could be compared. Considering the current controversy in fitting interaction parameters and the inconclusive methods of comparing models; the maximum likelihood method should be promoted as the standard in phase behavior modeling.

CONCLUSIONS

To achieve the primary goal of advancing the knowledge of phase behavior at elevated temperatures and pressures of non-ideal compounds, an experimental program was developed for obtaining VLE data. In addition, unique VLE data were obtained for three non-ideal compounds, and currently proposed models were evaluated using the VLE data obtained.

A high temperature and pressure flow vapor liquid equilibria apparatus was redesigned. The equipment operates at temperatures up to 325°C and pressures up to 10 MPa and is capable of maintaining equilibrium for a period up to thirty minutes which ensures constant compositions throughout the system. The equipment was modified to allow temperature control to within +/- 0.1 K; to maintain a constant phase boundary level; and to permit safe operating conditions. The equipment was evaluated against published VLE data for the methanol/ethanol system at 100 and 140°C.

Analytical techniques were developed for the particular compounds studied in this research using a gas chromatograph. Due to inherent limitations in gas chromatography, tedious procedures were employed to ensure analytical results to within +/- .001 mole fraction. In addition, all samples were purified to 99.9% + and were monitored to maintain sample integrity.

Binary phase behavior data were obtained for the compounds m-cresol, quinoline, and tetralin at four isotherms, 250, 275, 300, and 325°C. The m-cresol/quinoline binary exhibits a high boiling azeotrope that disappears with increasing temperature. The m-cresol/tetralin system exhibits a low boiling azeotrope at the lower isotherms that also disappears with increasing temperature. The tetralin/quinoline system is more of an ideal system. Vapor pressure measurements for these compounds agreed well with most published values as well as vapor pressures from a complementary calorimetry program also at the Colorado School of Mines, Flanigan (1986).

In the process of obtaining these data a major difficulty was identified, which is the drastic effect that minute traces of water can have on these measurements. When working with polar, hydrogen bonding compounds, extreme care must be taken to remove all water and to isolate the samples from the atmosphere.

The data obtained in this research were used to study some of the currently proposed phase behavior models. Two equations of state and five mixing rules were evaluated with these data. To facilitate this study, a sophisticated statistical program was written to fit interaction parameters as well as provide information on the ability of the model to fit the data. This program was based on the maximum likelihood method extended to permit the use of implicit constraints as is required in VLE modeling.

While the YSRK equation of state modeled the vapor pressures of the polar compounds better in low temperature regions, the SRK equation of state performed better in the temperature region where these data were located. For these systems, at temperatures between 250 and 325°C, temperature or volume functional dependencies were not found to significantly affect the performance of the model. The major contributing factor to the modeling capabilities of a mixing rule was found to be the addition of a third fitting parameter. A mixing rule with three parameters was capable of not only modeling the experimental data but also attempted to correct for poor vapor pressure predictions by the equation of state. The three parameter mixing rule was shown not to predict phase behavior as well as more simple models when extrapolated to lower temperatures and compared to experimental data. The most significant improvement needed is the further development of the equations of state to provide better vapor pressure predictions.

RECOMMENDATIONS

In reviewing the work in this thesis, areas for future work became apparent. For the development of more sophisticated models for phase behavior, a logical database needs to be established. A conclusion from this research was that data need to be obtained over wide temperature ranges. Data over a narrow temperature range may lead to wrong conclusions concerning temperature or volume dependencies. To enhance the study of non-ideality, compounds should be chosen which are non-ideal because of size or polarity. Compounds which have both a large size and polarity make it difficult to separate the two effects.

This research indicates that the equations of state still need refinement to provide better vapor pressure predictions. Many of the models qualitatively predicted the shape of the phase diagram; however, poor vapor pressure predictions prevented more quantitative representations.

One of the major recommendations for correlational development would be to establish an industrial and research standard for fitting experimental data to models. Currently various methods are in use, some of which are better than others. The variety of fitting methods leads to a lack of communication between researchers; results in subjective and sometimes erroneous conclusions concerning the predictive capabilities of proposed models; and typically does not use all of the experimentally measured variables available. The proposed standard is the maximum likelihood method as proposed by Anderson (1978) and as modified in this thesis. The obvious advantages of this method are that it:

(1) Uses all experimental data including experimental errors.

(2) Provides a true statistical fit while remaining relatively simple to understand.

(3) Provides valuable information concerning the ability of the model to fit the data.

(4) Allows different models to be compared on a statistical basis.

(5) Provides information concerning the interrelationships and errors associated with the fitted parameters.

When comparing models, a better criterion may be a method similar to the weighted sum of squared used for the maximum likelihood method. The weighting factors would be based upon the experimental precision of the data. This should eliminate the discrepancies that were found in using absolute percent standard deviations.

For the experimental program the following recommendation are made:

(1) The in-line bayonet heater should be replaced with a smaller wattage heater. This may increase the performance of the Bayley controller as well as decreasing the safety hazard.

(2) The piping in the system should be decreased as much as possible to reduce the overall volume of the system so that equilibrium can be achieved more rapidly. This will also require less chemicals which have proven to be quite expensive in some cases.

(3) The current feed tank is vastly oversized. Replacing it with a smaller glass cylinder would reduce the volume and allow the vapor and liquid flowrates to be visually monitored.

(4) A GC should be obtained that is equipped with a thermal conductivity dectector (TCD) so that the water content of the samples can be monitored. A reasonable solution would be to use an older GC that is no longer in service.

REFERENCES CITED

Ambrose, D., Sprake, C.H.S., and Townsend, R., 1975. Thermodynamic Properties of Organic Oxygen Compounds", Journal of Chemical Thermodynamics, 7:185-190.

Anderson, T.F., Abrams, D.S., and Grens, E.A., 1978. "Evaluation of Parameters for Nonlinear Thermodynamic Models", AIChE Journal, 24:20-29.

Brusset, H., Gaynes, J., 1953. Comp. Rend., 236:1563.

Butcher, K.L., and Robinson, W.I., 1966. "High Pressure Liquid-Vapour Equilibrium Data", Journal of Applied Chemistry, 16:289.

Chao, J., Lin, C.T., and Chung, T.H., 1983. "Vapor Pressure of Coal Chemicals", J. Phys. Chem. Ref. Data, 12:1033-1063.

CRC Handbook of Chemistry and Physics, 56th edition. 1975-76. CRC Press: Cleveland, Ohio.

Eatough, D.J., Wolfley, S.L., Dungan, L.J., Lewis, E.A., and Hansen, L.D., 1986. "Thermodynamics of Molecular Interactions in Model Coal.", Energy and Fuels, submitted.

Eubank, T., Kim, E.S., Holste, J.C., and Hall, K.R., 1985. "The Effect of Impurities Upon Pure Component Thermophysical Properties", presented at the 9th Symposium on Thermophysical Properties, Boulder, Co., June 23-27.

Engineering Sciences Data Unit, 1977. "Vapor Pressures and Critical Points of Liquids" XI: Heterocyclic Nitrogen Compounds", Engineering Sciences Data Item Number 77019.

Flanigan, D., 1983. Enthalpy Measurements of the m-Cresol /Quinoline System. Thesis 2810, M.S., Colorado School of Mines.

Flanigan, D., 1986. Ph.D. Thesis 3305, Colorado School of Mines

Flanigan, D.A., and Yesavage, V.F., 1986. "Enthalpy of Tetralin Between 291 and 655 K and at Pressures 10 MPa", J. Chem. Thermodynamics, 18:563-569.

Flanigan, D.A., Yesavage, V.F., and Kidnay, A.J., 1986. "Enthalpy of m-Cresol Between 291 and 655 K and at Pressures of 207 and 690 kPa", J. Chem. Thermodynamics, 18:563-569.

Glaser, F., Ruland, H., 1957. Untersuchungen uber Dampfdruckkurven and Kritishe Daten einger Technisch Wichtiger Organischer Substanzen", Chemie Ing. Techn., 12:772-775.

Gmehling, J., Onken, U., Arlt, W., 1982. Vapor-Liquid Equilibrium Data Collection, Chemistry Data Series, Dechema, West Germany.

Goldblum, K. F., Martin, R. W., and Young, R. B. 1947. "Vapor Pressure Data for the Phenols", Industrial and Engineering Chemistry, 39:1471-1476.

Gray, J.A., Wilson, G.M., Brody, C.J.,Cunning, J.R., Freeman, J.R., 1981. "Select Physical, Chemical, and Thermodynamic Properties of Narrow Boiling Range Coal Liquids," paper presented at AIChE 1981 Annual Meeting, New Orleans, LA, Nov. 8-12.

Holder, G.D., and Mohamed, R.S., 1986. "High Pressure Phase Behavior in Systems Containing CO_2 and Heavier Compounds with Similar Vapor Pressures", Presented at the AIChE Meeting, New Orleans, La.

Kara, M; Sung, S; Klinzing, G.E.; and Chiang, S.H. Fuel, 1981, 60, 633-634.

Katayama, H., Harada, Y., 1984. "Vapor Pressure Measurments of Tetralin at Reduced Pressures", J. Chem. Eng. Data, 29:373-375.

Kobayashi, R., 1978. "Phase and Volumetric Equilibrium in Coal Hydrogenation System," Annual Report for April 1977 - March 1978, DOE Contract No. E(49-18)-2334.

Kobayashi, R., Nov. 1979. "Physical Properties of Coal Liquids," Electrical Power Research Institute, AF-1209, Research Project 633-1, Interim Report.

Krevor, D.H., Lam, F.W., and Prausnitz, J.M., 1986. "Vapor-

Liquid Equilibria for Model Mixtures of Coal-Derived Liquids. 2. Binary Systems with Bicyclic and High-Boiling Fluids", J. Chem. Eng. Data, 31:353-357.

Lekhova, G.B., Kushner, T.M., Kharlampovick, G.D., and Serafimov, L.A., 1971. Russian Journal of Physical Chemistry, 45:11.

Lin, C.T., Young, F.K., Brule, M.R., Lee, L.L., Starling K.E., and Chao, J., 1980. "Data Bank for Synthetic Fuels: Part 2. Properties and Constants for 161 One- and Two-Ring Coal Chemicals", Hydrocarbon Processing, 117-123.

Lin, H.M., Kim, H., Leet, W.A. and Chao, K.C., 1985. Ind. Eng. Chem. Fundam., 24: 2,260.

Luedecke, D.; Prausnitz, J.M., 1985. "Phase Equilibria for Strongly Nonideal Mixtures from an Equation of State with Density-Dependent Mixing Rules," Fluid Phase Equilibria, 22, 1-19.

Maczynski, A., Maczynska, Q., 1965. Bull. Acad. Pl. Scl., Ser. Sci. Chim., 13:299

Mansoori, G.A., and Benmekki, E.H., 1986. "Accurate Vaporizing Gas Drive Minimum Miscibility Pressure Prediction", SPE Paper 15677 for the 61st Annual Technical Conference, New Orleans, La.

Mathias, P.M., and Stein, F.P., Sept. 1983. "Enthalpy Studies", United States Department of Energy, Contract No. DE-AC05-78-OR-03054.

Nasir, P., Hwang, S. C., Kobayashi, R., 1980. J. Chem. Eng. Data 25:298.

Natarajan, G., Viswanath, D.S., 1985. "Enthalpy of Vaporization and Vapor Pressure of Benzene, Toluene, p-Xylene, and Tetralin between 1 and 16 bar", J. Chem. Eng. Data, 30:137-140.

Neter, J., Wasserman, W., Kutner, M.H., 1985. Applied Linear Statistical Models, Richard D. Irwin, Inc., Homewood, Illinois.

Niesen, V., 1981. M.S. Thesis 2582 , Colorado School of Mines.

Niesen, V.G., Palavra, A., Kidnay, A.J., and Yesavage, V.F., 1986. "An Apparatus for Vapor-Liquid Equilibrium at Elevated Temperatures and Pressures and Selected Results for the Water/Ethanol and Methanol/Ethanol Systems", Fluid Phase Equilibria, to be published.

Prausnitz, J.M., Lichtenhaler, R.N., and de Azevedo, E.G., 1986. Molecular Thermodynamics of Fluid Phase Equilibria, Prentice-Hall, Inc., New Jersey

Reid, R. C., Prausnitz, J. M., and Sherwood, T. K. 1977. The Properties of Gases and Liquids, 3rd edition. McGraw-Hill: New York.

Sandarusi, J., 1984. M.S. Thesis 2859, Colorado School of Mines.

Sebastian, H.M., Simnick, J.J., Lin, H., and Chao, K., 1978. "Gas-Liquid Equilibrium in Mixtures of Hydrogen and Quinoline". Journal of Chemical and Engineering Data. 234:305-307.

Sharma, R., 1980. Enthalpy Measurements for a Coal Derived Naphtha and Middle Distillate and Characterization of Coal Liquids for Their Extent of Association, Thesis 2318, Ph.D., Colorado School of Mines.

Simnick, J.J., Lawson, C.C., Lin, H.M., and Chao, K.C., 1977. "Vapor-Liquid Equilibrium of Hydrogen'Tetralin System at Elevated Temperatures and Pressures", AIChE Journal, 23:469-476.

Skaates, J.M., and Kay, W.B., 1964. Chem. Eng. Sci. 19:431.

Soave, G., 1972. "Equilibrium Constants from a Modified Redlich-Kwong Equation of State", Chemical Engineering Science, 27:1197-1203.

Soave, G.S., 1979. Int. Chem. Engng. Symp. Ser. No. 56, 1.2/1.

Soave, G.S., 1980. Chem. Eng. Sci., 35:1725-1729.

Starling, K.E., 1983. "Development of a Thermodynamic Properties Correlation Framework for the Coal Conversion Industry," Final Report, Contract DE-FG22-80PC30249.

Stull, D.R., 1947. "Vapor Pressure of Pure Substances, Organic Compounds", Industrial and Engineering Chemistry, 39:517,540.

Van De Rostyne, C., and Prausnitz, J.M., 1980. "Vapor Pressures of Some Nitrogen-Containing, Coal-Derived Liquids", J. Chem. Eng. Data., 25:1-3.

Wilson, G.M., Johnston, R.H., Hwang, S.C., Tsonopoulos, C. 1981. "Volatility of Coal Liquids of High Temperatures and Pressures," Ind. Eng. Chem. Process Des. Dev., 20:94.

Yesavage, V.F., 1986. "An Approach for Extending Van der Waals Equations of State for Polar, Hydrogen Bonding Fluids Applied to The Soave Equation of State", accepted Fluid Phase Equilibria.

Zudkevitch, D., 1982. "Impact of Thermodynamic & Fluid Properties Data Uncertainties on Design and Economics of Separation Operations",The Encyclopedia of Chemical Processing and Design, McKetta, J.J., (ed.), 14:466-467.

APPENDIX A

PROCEDURES FOR THE VLE APPARATUS

Operating Procedure for the VLE Apparatus

The following operating procedure was found to work well for a binary system and posed no serious safety hazards.

Start-up Procedure

1.) Open vents on the feed tank.

2.) Fill the feed tank with approximately one liter of fluid through the funnel on the feed tank. Close the valve after all the fluid has entered the tank to prevent the fluid from being exposed to the atmosphere.

3.) Open the micrometering valve on the vapor line slightly. It is best not to adjust this valve once a vapor flow rate is established that allows a stable operation.

4.) Prime the pump by turning the pump on and opening the valve just past the outlet of the pump. Increase the pump setting to approximately 300. After a short period of time the pump will prime itself. Collect fluid from the purge line until a steady flow rate is established. Close the valve. Watch the outlet pressure gauge located just past the outlet of the pump. When the pressure begins to rise, quickly decrease the pump setting to 100. If the pump is primed properly, a pump stroke will be apparent on the gauge. The pressure of the gauge should not be above 200 psi (1400 kPa). If the pressure is substantially above this value then the system may have become plugged or the fluid may be extremely viscous. If appears that the system is plugged, then refer to step 5 in the Troubleshooting Procedure.

The pump setting may need to be adjusted depending upon the fluid being studied. A reasonable flow rate is on the order of 120 mls/min.

5.) Allow the pump to run until fluid has filled the equilibrium cell. Purge the differential pressure indicator (DPI) cell by allowing fluid to flow through the U tube attached to the lower chamber of the DPI cell until all of the air has been removed.

6.) Open the valves to the Heise pressure gauges located on the front control panel. This will allow the gauges to adjust to atmospheric pressure.

7.) Turn on the water to the vapor and liquid heat exchangers. The valves are located above the work bench in the lab. The flow rate on the liquid line heat exchanger should be low enough to prevent it from overflowing. The vapor line heat exchanger requires a high water flow rate.

8.) Turn the air on to the fluidized sand bath. A pressure of 20 psi is required at the regulator located above the work bench. A flow rate of 100 scfh (as indicated by the rotameter on the front panel) was found to be satisfactory. A pneumatic safety switch prevents the fluidized sand bath heaters from being turned on without an adequate air supply.

9.) Turn the Keithley multimeter on, the multimeter should be allowed to warm-up for several hours before it is used.

10.) Set the oven controls to the desired operating temperature. The controls are located on the windowed side of the oven. The main power switch is located on the front control panel.

11.) Set the fluidized sand bath temperature through the Omega temperature controller located on the front panel. The main power switch for the fluidized sand bath and the controller are located on the front panel. For the fluids studied in this investigation, typically a temperature of 50°C above the desired operating temperature was required for the sand bath. The desired situation is to have the fluid leaving the fluidized sand bath at a temperature of 1-2°C below the desired operating temperature.

12.) Partially close the micrometering valve on the liquid line. This valve will need to be adjusted during the warm-up period to keep the fluid in the liquid phase.

13.) Allow the equipment to warm up to the desired temperature. This should take between 2-4 hours. If the temperature is not increasing substantially, check the flow rate. Too low a flow rate will lead to a low heat transfer coefficient and retard heat transfer. Also, check the water coil to the fluidized sand bath (used for cool down), if the water to this coil is left on, the system may never heat up to temperature.

As long as the vapor valve is open, there is little chance of the system overpressurizing. However, the equipment should be closely monitored. Under no circumstances should the Bayley controller to the in-line bayonet heater be turned on during the warm-up period. The bayonet heater is the single most hazardous piece of equipment in the apparatus. The equipment should not be unattended while the Bayley controller is on.

During the warm-up period, the fluid needs to be kept in the liquid phase. If a vapor phase begins to appear in the equilibrium cell, increase the pressure of the system by closing the micrometering valve on the liquid line until the vapor phase disappears.

14.) While the equipment is warming up, adjust the Heise gauges to read 0 psi (0 kPa) when open to the atmosphere. Close the valves to the gauges that will not be required. Increase the nitrogen pressure to slightly above the estimated pressure of the system using the regulator on the nitrogen tank. Turn on the null indicator located on the front panel. The needle should be pegged to the left, indicating that the system pressure is higher than the pressure on the gauges. Open the valves on the front panel labeled "Nitrogen Inlet." Slowly increase the nitrogen pressure until the needle on the null indicator reads zero. If too much nitrogen is added, it can be vented through the valve labeled "vent." Once an adequate amount of nitrogen has been added, close all the inlet and vent valves tightly. Push in the black knob located underneath the hand pump. The hand pump can now be used to make small adjustments on the nitrogen pressure.

15.) When the temperature of the fluid is about 5 °C above the desired temperature, the liquid line micrometering valve should be opened slowly until two phases can be seen in the equilibrium cell. When the valve is opened the pressure is reduced to allow two phases to form. The temperature of the fluid will drop substantially during this process. This is due to the extra heat load put on the fluidized sand bath to provide the heat of vaporization for the fraction of the fluid that is vaporized.

16.) The liquid line micrometering valve should be adjusted until a stable phase boundary is established inside the equilibrium cell.

17.) During the time that the stable phase boundary is being obtained, the Bayley controller for the inline bayonet heater should be turned on. To do this, the 10 turn set-point adjustment knob on the Bayley should be turned to zero. Turn on the main power switch located on the Bayley controller. If the needle on the power indicator gauge rapidly moves to 100% (right) and then back to 0% (left) then the controller is functioning properly. Increase the setting on the set-point adjustment knob until the controller starts supplying power to the heater as indicated by the power indicator gauge. The bayonet heater should only be used to smooth out the temperature fluctuations of the fluidized sand bath. Good temperature control will not be obtained if the bayonet heater is required to input too much power. See item 2 in the Troubleshooting Procedure for further details.

18.) Both the micrometering valve on the liquid line and the Bayley controller will have to be adjusted simultaneously to bring the equipment to equilibrium. The two phase boundary needs to be relatively stable with little adjustments required.

19.) Equilibrium conditions will have to be maintained for 30 minutes. That is, the temperature will have to be within +/- 0.1 K, the phase boundary must be relatively constant inside the equilibrium cell, and the pressure must be stable to within the accuracy of the gauge being used. (See equipment description for the gauge accuracy).

20.) Once the equilibrium conditions have been maintained for 30 minutes, record the resistance reading on the Keithley multimeter (temperature) and the pressure reading on the Heise gauge (the null indicator must be at zero for this to be the correct pressure reading). Flush the vapor and liquid collection lines until about 10-15 mls are removed from each. Collect the samples into small vials. Once again record the resistance and pressure readings.

21.) After the point is taken, it must be decided if the composition is going to be changed of if another point will be taken at the same composition but at a new temperature. From past experience, it was found that the optimal method was to take data at two isotherms for one composition. For example, a point was taken at the lower isotherm, then the temperature was raised and another data point was taken. The composition was then changed by adding one component of the binary while the equipment was still running. After restabilization (one or more hours) a new data point was taken at the same isotherm. The temperature was lowered to the lower isotherm and another point was taken. This zigzag approach worked well for minimizing the volume of fluids used, the operation time required and also the amount of time needed for GC analysis of the samples. This last reason is due to the fact that the samples from the two isotherms were close enough together in composition that the same standards could be used for both in the GC analyses, thus eliminating half of the standards required.

22.) If the temperature is to be changed, then the liquid micrometering valve is partially closed to increase the pressure to return the system back to the liquid phase.

23.) Turn off the Bayley controller.

24.) Return to step 13 and repeat the procedure through step 20.

25.) If the composition is to be changed, first turn off the Bayley controller.

26.) Add one component of the binary system being studied to the feed tank. At the same time, remove an equal amount of fluid from the vapor or liquid stream (whichever has the highest concentration of the component being diluted).

27.) Partially close the liquid line valve until only a liquid phase is present. Allow the equipment to run for at least one hour to ensure good mixing. Return to step 13 and proceed as before. Watch the pressure during the 30 minute equilibrium time. If the pressure changes more than the precision of the pressure gauge, then the system is not yet well mixed.

Shutdown Procedure

1.) Turn off the Bayley controller.

2.) Turn off the fluidized sand bath and oven at the main control panel.

3.) Partially close the liquid line to bring the system back to the liquid phase only.

4.) Open the oven door to allow the contents to cool quickly.

5.) Open the valve on the water line to the cooling coil in the fluidized sand bath.

6.) Pull the knob below the hand pump out and open the nitrogen vent valve to release the nitrogen pressure on the Heise gauges. Leave these valves open to allow the gauges to return to atmospheric pressure.

7.) Turn off the null indicator.

8.) Allow the pump to run until the fluid and the fluidized sand bath temperatures are below the boiling point of the lowest boiling compound.

9.) Turn off the pump.

10.) Turn off all power switches on the front panel.

11.) Turn off the water to the heat exchangers.

12.) Close vents on the feed tank.

Troubleshooting Procedure

The following problems occurred during the development and operation of the equipment. This is a complex system where many variables must be balanced to achieve good overall stability. This section attempts to describe the interrelationships between flow rates, temperature control, liquid level control and numerous other variables.

1.) A constant overall flow rate must be provided by the pump. The present pump is quite adequate and is very easy to maintain and repair. The major problem was that at times the pump would lose its prime on the oil side. This resulted in a continually decreasing flow rate and caused very poor control. Refer to the pump manual for priming instructions.

2.) The fluidized sand bath must be operated so that it provides almost all of the heat required. The inline bayonet heater should only be used to smooth out the fluctuations of the sand bath. If the bayonet heater is used too much, the surrounding fluid will instantly vaporize and will create bumping of the fluid inside the cell as well as extremely poor temperature control. It is possible that the heater could cause the surrounding fluid to coke and plug the system.

In the last week of operation it was realized that the bayonet heater was oversized for the system, so that the Bayley controller could not perform as well as possible. The current heater is 250 watts, it is believed that a much smaller heater would significantly increase the performance of the Bayley controller.

3.) It is extremely difficult to operate the equipment at a high vapor flow rate, the heat load is too great for the fluidized sand bath. This is especially evident at the higher temperatures. Also, a compound with a high heat of vaporization will require a lower vapor flow rate for stable operation.

4.) An unstable liquid level can be caused by plugging of the strainers or the micrometering valve on the liquid line.

5.) A low overall flow rate can result in the fluidized sand bath heat exchanger coil coking up. In this case, overpressurization occurs causing the pressure relief device to rupture. In addition, a loss of flow due to a power failure will invariably coke up the coil. The coking can also occur over a period of time and can be observed as a gradual increase in pressure drop. As the coke is deposited, the rate of heat transfer will decrease inside the coil.

If the coil becomes plugged the coil must be replaced by removing first the sand and then the coil. The operator has the option of using the same size tubing (1/8") and length (20') or can change the dimensions to increase or decrease the pressure drop as desired.

6.) A high flow rate will cause bumping of the fluid as it enters the cell and create pressure fluctuations. Only a narrow range of flow rates will give stable operations. These flow rates must be chosen based on experience and the fluid being studied.

7.) The oven will shut off if the temperature goes above 350°C. To restart the oven a switch on the oven control panel must be reset.

Safety Precautions

Several important precautions should be taken during the operation of this equipment to ensure a safe environment. These precautions are listed below.

1.) This equipment operates at high temperatures and pressures. In a very short period of time the pressure can build up to 1600 psi and vent through the rupture disk. The most likely reasons for the pressure building up to hazardous levels are: (a) the coil inside the fluidized sand bath cokes up, or (b) the vapor line valve is closed. Unfortunately, the seal on the cell will leak before the rupture disk vents. This allows flammable fluid to be released inside the oven. In the past, the fluid did not ignite but toxic fumes were produced, requiring the area to be evacuated.

The simplest way of preventing this from happening is to never leave the equipment unattended and never completely close the vapor line valve. This equipment was operated for over a year without any hazardous situations occurring because these two procedures were strictly followed.

2.) Another important safety procedure is to never leave the inline bayonet heater on unless the equipment is being equilibrated for a data point. If the flow is stopped for some reason, the controller will turn on and stay on. Since there is no flow, the heat cannot be removed from the surrounding area and a rupture may occur in the tubing. This has never happened on this equipment but has occurred on a similar apparatus.

A similar situation may occur if the fluidized sand bath is shutoff but not the Bayley controller. The controller will try and maintain the temperature that it is set for and will continue to heat. The surrounding tubing will glow cherry red and may rupture to release toxic fumes.

3.) During the operation of the equipment, the air flow rate should be periodically checked. In the past, the air flow rate has been cut off unexpectedly. If this happens the bed should be cooled off as quickly as possible by turning on the cooling water and increasing the fluid flow rate to remove the heat from the bed. If the air is turned off, the heaters automatically shut off but the hot sand subsides and the heat cannot be removed. This will invariably lead to plugging of the fluidized sand bath heat exchanger coil and overpressurization of the entire system.

4.) A power outage can be a serious problem when operating at high temperatures. If flow is stopped for even a short period of time the fluidized sand bath heat exchanger will coke. Upon return of the power, the pump will start pumping and the system will overpressurize.

5.) The equilibrium cell will seal up to 1500 psi (10500 kPa) however, due to temperature cycling the bolts will loosen and leakage of toxic fumes may occur. The bolts should be checked on a frequent basis. In addition, the equipment has been shown to operate with noxious fluids without significant quantities of fumes being released into the atmosphere. If fumes are being released then typically a fitting inside of the oven is not properly tightened.

APPENDIX B

EFFECTS OF WATER CONTAMINATION

To estimate the effects of water on the pressure measurements, the following derivation was used.

Starting with the equilibrium constraints, the following equation can be written:

$$f_i^v = f_i^l \tag{1}$$

which can be written in terms of fugacity coefficients and activity coefficients as:

$$\phi_i^v y_i P = \gamma_i x_i P_i^s \phi_i^s \tag{2}$$

Since the pressure is low, ideal gas is assumed which allows ϕ_i^v and ϕ_i^s to equal 1. Therefore,

$$\gamma_i = y_i P / x_i P_i^s \tag{3}$$

For an infinite dilution activity coefficient, the same equation may be written as:

$$\gamma_i^\infty \simeq \left.\frac{dy_i}{dx_i}\right|_{x=0} \frac{P}{P_i^s} \tag{4}$$

Let water be component 2 and let the other compound (quinoline or m-cresol) be component 1. Therefore, for component 1 and component 2 the following equations can be written:

$$dy_2/dx_2 = \gamma_2^{\infty} P_2^s / P \tag{5}$$

$$y_1 P = \gamma_1 x_1 P_1^s \tag{6}$$

Since the water is in infinite dilution, the activity coefficient of quinoline can be assumed to be equal to 1. Equation 6 can be rewritten as:

$$P = (1-x_2) P_1^s / (1-y_2) \tag{7}$$

By substracting P_1^s from each side of equation 7 and rearranging, the following equation can be written:

$$\frac{P - P_1^s}{P_1^s} = \frac{(y_2/x_2 - 1)x_2}{(1 - y_2 x_2/x_2)} \simeq \frac{(dy_2/dx_2 - 1)x_2}{(1 - (dy_2/dx_2)x_2)} \tag{8}$$

substituting equation 4 into equation 8 and assuming that the total pressure in equation 4 can be approximated by the vapor pressure of quinoline, then

$$\frac{P - P_1^s}{P_1^s} = \frac{(\gamma_2^{\infty} P_2^s / P_1^s - 1)x_2}{(1 - \gamma_2^{\infty} P_2^s x_2 / P_1^s)} \tag{9}$$

If it is assumed that the infinite dilution activity coefficient for water is not a function of temperature, then equation 9 can be used to determine the effects of water on the vapor pressure of component 1 at different temperatures.

APPENDIX C

COMPUTER PROGRAMS

```
C       THIS PROGRAM EMPLOYS AN IMPLICIT CONSTRAINT MAXIMUM
C       LIKELIHOOD  ALGORITHM  FOR  DETERMINING  PARAMETERS
C       FROM EXPERIMENTAL DATA FOR ONE CONSTRAINT
C***********************************************************
        PARAMETER NN =16, KK = 1, LL = 1, NK =16
        IMPLICIT REAL*8 (A-H,P-Z)
        CHARACTER*20 FILN1,FILN2,FILN3,FILN4,FILN5,FILN6,FILN7,FILN8
        1,FILN9,FILN10,FILN11
        REAL*8 YM(NN),XM(NK),PAR(LL),EVX(NK),EVY(NN),EVXSQ(NK),
        1EVYSQ(NN),EVXD(NK,NK),EVYD(NN,NN),EVXDI(NK,NK),DFX(NN,NK),
        1DFP(NN,LL),DFXT(NK,NN),DFPT(LL,NN),DELXM(NK),DELYM(NN),
        1DUM(NN,NK),DUM2(NN,NN),TAU(NN,NN),DUM3(NN,NN),DUM3I(NN,NN),
        1DUM4(LL,NN),DUM5(LL,NN),DUM6(LL,LL),DUM7(LL,NN),DUM8(LL,NN),
        1DUM9(LL,NN),DUM10(NN),DUM11(NN), DELPN(LL),DUMM1(NK,NN),
        1DUMM2(NK,NN),DUMM3(NK,NN),DUMM4(NN),DUMM5(NN),DUMM6(NN),
        1DUMM7(NN),DELXN(NK),DEN(NN,NN),XR(NK),YR(NN),DUMMY(NN),
        1DELX(NK),DELY(NN),YC(NN),DIF(NN),DFYM(NN,NN),DFYMI(NN,NN),
        1DFXM(NN,NK),DFPM(NN,LL),FX(NK),FY(NN),FR(NN),FP(NN),
        1YDUM(NN,1),YDUM2(NN,1),YDUM3(NN,1),YDUM4(NN,1),YDUM5(NN,1),
        1YDUM6(NN,1),YDUM7(NN,1),DELYN(NN),XRN(NK)

        IT=0
        SSQ=0
        ITMX=100

        DO 33 I=1,NN
                DO 34 J=1,NN
                        IF(J.EQ.I) THEN
                        DEN(I,J)=1.
                        ELSE
                        DEN(I,J)=0.
                        ENDIF
34              CONTINUE
33      CONTINUE
        TYPE*,'ENTER THE TOLERANCE LIMIT'
        ACCEPT*,SSTL

        TYPE*,'ENTER THE FILENAME CONTAINING THE DEPENDENT VARIABLE,NN'
        READ(5,1)FILN1
1       FORMAT(A20)
        TYPE*,'ENTER THE FILENAME CONTAINING THE INDEPENDENT VARIABLES,
        1NK'
        READ(5,1)FILN2
        TYPE*,'ENTER THE FILENAME CONTAINING PARAMETER ESTIMATES,LL'
        READ(5,1)FILN3
        TYPE*,'ENTER THE FILENAME CONTAINING THE VARIANCES FOR THE
        1INDEPENDENT VARIABLES,NK'
```

```
      READ(5,1)FILN4
      TYPE*,'ENTER THE FILENAME CONTAINING THE VARIANCES FOR THE
     1 DEPENDENT VARIABLE,NN'
      READ(5,1)FILN5

      OPEN(UNIT=10,FILE=FILN1,STATUS='OLD')
      OPEN(UNIT=20,FILE=FILN2,STATUS='OLD')
      OPEN(UNIT=30,FILE=FILN3,STATUS='OLD')
      OPEN(UNIT=40,FILE=FILN4,STATUS='OLD')
      OPEN(UNIT=50,FILE=FILN5,STATUS='OLD')
C
      TYPE*,'ENTER THE CRITICAL TEMPERATURE, PRESSURE AND ACENTRIC
     1FACTOR FOR THE COMPOUND IN KELVIN AND KPA'
      ACCEPT*,TC,PC,ACCN

C     READ IN DEPENDENT VARIABLE
C
      READ(10,*,END=101) (YM(I),I=1,NN)
C     READ IN INDEPENDENT VARIABLES
C
101   READ(20,*,END=102) (XM(I),I=1,NK)
C
C     READ IN PARAMETER ESTIMATES
C
102   READ(30,*,END=103) (PAR(I),I=1,LL)
C
C     READ IN VARIANCES FOR INDEPENDENT VARIABLES
C
103   READ(40,*,END=104) (EVX(I),I=1,NK)
C
C     READ IN VARIANCES FOR DEPENDENT VARIABLE
C
104   READ(50,*,END=105) (EVY(I),I=1,NN)
C
C     SET INITIAL TRUE VALUES TO MEASURED VALUES
105   DO 10 I=1,NN
            YR(I)=YM(I)
10    CONTINUE
      DO 20 I=1,NK
            XR(I)=XM(I)
20    CONTINUE
C
C     SQUARE AND INVERT VARIANCES EVX AND EVY, CREATE DIAG MATRICES
C
      DO 30 I=1,NK
            EVXSQ(I)=1./EVX(I)**2
30    CONTINUE
```

```
      DO 40 I=1,NN

            EVYSQ(I)=1./EVY(I)**2
40    CONTINUE
      CALL DIAG(EVXSQ,NK,EVXD)
      CALL DIAG(EVYSQ,NN,EVYD)
C
C     CALCULATE THE INVERSE OF EVXD
C
      CALL DIAGINV(NK,NK,EVXD,EVXDI)
C
C     CALCULATE FUNCTIONS AND DERIVATIVES
150   IT=IT+1

      CALL FUNC(XR,PAR,YR,DFXM,DFPM,DFYM,FR,
      1NN,LL,KK,NK,TC,PC,ACCN,FP,FY,FX,IT)


C     CALCULATE INITIAL MINIMIZING FUNCTION
      IF(IT.EQ.1)THEN
      CALL SUM(SSQ,XR,YR,EVXSQ,EVYSQ,YM,XM,NN,NK,LL,KK)
      ENDIF



C     CALCULATE DFX,DFP,DELYM
      CALL DIAGINV(NN,NN,DFYM,DFYMI)
      CALL MATMULT(DFYMI,FR,YDUM,NN,NN,1)
      CALL MATSUB(YR,YDUM,YDUM2,NN,1)

      DO 90 I=1,NN
            DELYM(I)=YDUM2(I,1)-YM(I)

90    CONTINUE

      CALL MATMULT(DFYMI,DFXM,DFX,NN,NN,NK)
      CALL NEG(DFX,DFX,NN,NK)

      CALL MATMULT(DFYMI,DFPM,DFP,NN,NN,LL)
      CALL NEG(DFP,DFP,NN,LL)

C
C     CALCULATE TRANSPOSE OF DERIVATIVES
C
      DO 50 I=1,NN
            DO 60 J=1,NK
                  DFXT(J,I)=DFX(I,J)
60          CONTINUE
```

```
50      CONTINUE
        DO 70 I=1,NN
                DO 80 J=1,LL
                        DFPT(J,I)=DFP(I,J)
80              CONTINUE
70      CONTINUE
C
C       CALCULATE DELXM
C
        DO 100 I=1,NK
                DELXM(I)=XR(I)-XM(I)
100     CONTINUE

C       CALCULATE TAU(NN,NN)DIAG MATRIX

        CALL MATMULT(DFX,EVXDI,DUM,NN,NK,NK)
        CALL MATMULT(DUM,DFXT,DUM2,NN,NK,NN)
        CALL MATMULT(DUM2,EVYD,TAU,NN,NN,NN)


C       CALCULATE (DEN+TAU)**-1

        CALL MATADD(DEN,TAU,DUM3,NN,NN)
        CALL DIAGINV(NN,NN,DUM3,DUM3I)


C       CALCULATE DELP

        CALL MATMULT(DFPT,EVYD,DUM4,LL,NN,NN)
        CALL MATMULT(DUM4,DUM3I,DUM5,LL,NN,NN)
        CALL MATMULT(DUM5,DFP,DUM6,LL,NN,LL)
        CALL SYMINV(DUM6,LL,IRR)
        CALL MATMULT(DUM6,DFPT,DUM7,LL,LL,NN)
        CALL MATMULT(DUM7,EVYD,DUM8,LL,NN,NN)
        CALL MATMULT(DUM8,DUM3I,DUM9,LL,NN,NN)
        CALL MATMULT(DFX,DELXM,DUM10,NN,NK,1)
        CALL MATSUB(DELYM,DUM10,DUM11,NN,1)
        CALL MATMULT(DUM9,DUM11,DELPN,LL,NN,1)

C       MAKE DELPN NEGATIVE

        DO 91 I=1,LL
                DELPN(I)=-DELPN(I)
91      CONTINUE
```

```
C         CALCULATE DELXN

          CALL MATMULT(EVXDI,DFXT,DUMM1,NK,NK,NN)
          CALL MATMULT(DUMM1,EVYD,DUMM2,NK,NN,NN)
          CALL MATMULT(DUMM2,DUM3I,DUMM3,NK,NN,NN)
          CALL MATMULT(DFP,DELPN,DUMM4,NN,LL,1)
          CALL MATMULT(DFX,DELXM,DUMM5,NN,NK,1)
          CALL MATSUB(DELYM,DUMM5,DUMM6,NN,1)
          CALL MATADD(DUMM6,DUMM4,DUMMY,NN,1)
          CALL MATMULT(DUMM3,DUMMY,DELXN,NK,NN,1)

C         MAKE DELXN NEGATIVE

          DO 110 I=1,NK
                 DELXN(I)=-DELXN(I)
110       CONTINUE


C         CALCULATE NEW ESTIMATES OF PARAMETERS AND X AND Y

          DO 120 I=1,LL
                 PAR(I)=DELPN(I)+PAR(I)
          TYPE*,'PAR,DELPN',PAR(I),DELPN(I)
120       CONTINUE

          DO 130 I=1,NK
                 XRN(I)=DELXN(I) + XM(I)
                 DELX(I)=XRN(I)-XR(I)
                 XR(I)=XRN(I)

130       CONTINUE

C         CALCULATE NEW GUESS OF YR(I)

          CALL MATMULT(DFPM,DELPN,YDUM3,NN,LL,1)
          CALL MATMULT(DFXM,DELX,YDUM4,NN,NK,1)
          CALL MATADD(FR,YDUM4,YDUM5,NN,1)
          CALL MATADD(YDUM5,YDUM3,YDUM6,NN,1)
          CALL MATMULT(DFYMI,YDUM6,YDUM7,NN,NN,1)
          CALL NEG(YDUM7,DELYN,NN,1)

          DO 141 I=1,NN
                 YR(I)=DELYN(I) + YR(I)

141       CONTINUE
```

```
C       CALCULATE THE MINIMIZING FUNCTION

        CALL SUM(SSQN,XR,YR,EVXSQ,EVYSQ,YM,XM,NN,NK,LL,KK)

C       CHECK FOR CONVERGENCE

        DIFF=(SSQ-SSQN)/SSQN
        TYPE*,'DIFF',DIFF
        TYPE*,'SSQ,SSQN',SSQ,SSQN
        IF(ABS(DIFF).LT.SSTL)GO TO 200
        SSQ=SSQN

        IF(IT.LT.ITMX)GO TO 150
        TYPE*,'NUMBER OF INTERATIONS GREATER THAN ITMX'
        GO TO 1000

200     TYPE*,'ENTER FILENAME FOR CALCULATED VALUES'
        READ(5,1)FILN8
        OPEN(UNIT=80,FILE=FILN8,STATUS='NEW')
        DO 21 I=1,NN
        WRITE(80,*),'TEMPC',XR(I),'PRESC',YR(I)
21      CONTINUE

        WRITE(80,*),'                                  '
        WRITE(80,*),'PARAMETER',PAR(1)
        WRITE(80,*),'                                  '
        WRITE(80,*),'CRITICAL TEMP, PRESS, AND ACENTRIC FACTOR'
        WRITE(80,*),TC,PC,ACCN

        CALL VP(XM,YM,TC,PC,ACCN,PAR(1),NN,YC,NK)
        TYPE*,'ENTER FILENAME FOR VAPOR PRESSURES WITH MEASURED TEMP'
        READ(5,2) FILN9
        OPEN(UNIT=90,FILE=FILN9,STATUS='NEW')
2       FORMAT(A15)
        ABSDIF=0.0
        DO 23 I=1,NN
        DIF(I) = ((YC(I)-YM(I))/YM(I))*100
        ABSDIF=ABSDIF + ABS(DIF(I))

        WRITE(90,*),'TEMP',XM(I),'PERCENT DIF',DIF(I)
        WRITE(90,*),'MEAS PRES',YM(I),'CALC PRES',YC(I)
        WRITE(90,*),'                                            '
23      CONTINUE
        WRITE(90,*),'TC',TC,'PC',PC
        WRITE(90,*),'ACENTRIC FACTOR',ACCN,'POLAR PAR',PAR(1)
        ABSDIF=ABSDIF/NN
```

```
      WRITE(90,*),' AVERAGE PERCENT DEVIATION',ABSDIF

      TYPE*,'ENTER THE A DIFFERENT ACCENTRIC FACTOR AND
     1 POLAR PARAMETER'
      ACCEPT*,ACC,POL
      CALL VP(XM,YM,TC,PC,ACC,POL,NN,YC,NK)
      TYPE*,'ENTER FILENAME FOR VAPOR PRESSURES FOR SRK'
      READ(5,2)FILN11
      OPEN(UNIT=110,FILE=FILN11,STATUS='NEW')
      ABSDIF=0.0
      DO 22 I=1,NN
      DIF(I) = ((YC(I)-YM(I))/YM(I))*100
      ABSDIF=ABSDIF + ABS(DIF(I))
      WRITE(110,*),'TEMP',XM(I),' PERCENT DIF',DIF(I)
      WRITE(110,*),'MEAS PRES',YM(I),'CALC PRES',YC(I)
      WRITE(110,*),'
22    CONTINUE
      WRITE(110,*),'TC',TC,'PC',PC
      WRITE(110,*),'ACENTRIC FACTOR',ACC,'POLAR PAR',POL
      ABSDIF=ABSDIF/NN
      WRITE(110,*),' AVERAGE PERCENT DEVIATION',ABSDIF
1000  STOP
      END


      SUBROUTINE NEG(S,SN,N,K)
      REAL*8 S(N,K),SN(N,K)
      DO 10 I=1,N
              DO 20 J=1,K
                      SN(I,J)=-S(I,J)
20            CONTINUE
10    CONTINUE
      RETURN
      END

      SUBROUTINE DIAG(S,N,W)
      REAL*8 W(N,N),S(N)
      DO 11 I=1,N
              DO 21 J=1,N
                      IF (J.EQ.I) THEN
                      W(I,J)=S(I)
                      ELSE
                      W(I,J)=0
                      ENDIF
21            CONTINUE
11    CONTINUE
      RETURN
      END
```

```
      SUBROUTINE DIAGINV(N,K,W,WI)
      REAL*8 W(N,K),WI(N,K)
      DO 31 I=1,N
              DO 41 J=1,K
                      IF (J.EQ.I) THEN
                      WI(I,J)=1./W(I,J)
                      ELSE
                      WI(I,J)=0
                      ENDIF
41            CONTINUE
31    CONTINUE
      RETURN
      END


      SUBROUTINE MATMULT(A,U,T,M,N,P)
      INTEGER P
      REAL*8 T(M,P),A(M,N),U(N,P)

C     T(M,P)=A(M,N)*U(N,P)

      DO 10 I=1,M
              DO 20 KKJ=1,P
                      T(I,KKJ)=0
20            CONTINUE
10    CONTINUE
      DO 30 I=1,M
              DO 40 KKJ=1,P
                      DO 50 K=1,N
                              T(I,KKJ)=A(I,K)*U(K,KKJ)+T(I,KKJ)
50                    CONTINUE
40            CONTINUE
30    CONTINUE
      RETURN
      END


      SUBROUTINE MATADD(A,B,C,M,N)

C     C(M,N)=A(M,N)+B(M,N)

      REAL*8 A(M,N),B(M,N),C(M,N)
      DO 10 I=1,M
              DO 20 J=1,N
                      C(I,J)=A(I,J)+B(I,J)
20            CONTINUE
```

```
10      CONTINUE
        RETURN
        END


        SUBROUTINE MATSUB(A,B,C,M,N)
C       C(M,N)=A(M,N)-B(M,N)

        REAL*8 A(M,N),B(M,N),C(M,N)
        DO 10 I=1,M
                DO 20 J=1,N
                        C(I,J)=A(I,J)-B(I,J)
20              CONTINUE
10      CONTINUE
        RETURN
        END


        SUBROUTINE SYMINV(A,N,IRR)
C       INVERTS A SYMMETRIC MATRIX A(N,N), THE MATRIX TO BE INVERTED
C       IS DESTROYED AND ULTIMATELY CONTAINS THE INVERSE
C       IRR IF THE FAILURE PARAMETER WHEN NO INVERSE CAN BE FOUND
C       REFERENCE "COMPUTER CALCULATIONS FOR MULTICOMPONENT VL
C       AND LLE", PRAUSNITZ,J, PRENTICE-HALL ,1980

        REAL*8 A(N,N),P(50),Q(50)
        INTEGER R(50)
        IRR=0
        DO 10 I=1,N
10      R(I)=1
        DO 150 I=1,N
        BIG=0.
        DO 40 J=1,N
        TEST=ABS(A(J,J))
        IF (TEST-BIG) 40,40,20
20      IF (R(J)) 160,40,30
30      BIG=TEST
        K=J
40      CONTINUE
        IF(BIG.LT.1.E-19) GO TO 160
        R(K)=0
        Q(K)=1./A(K,K)
        P(K)=1.
```

```
      A(K,K)=0.0
      KP1=K+1
      KM1=K-1
      IF(KM1) 160,80,50
50    DO 70 J=1,KM1
              P(J)=A(J,K)
              Q(J)=A(J,K)*Q(K)
              IF(R(J)) 160,70,60
60    Q(J)=-Q(J)
70    A(J,K)=0.
80    IF(K-N)90,130,160
90    DO 120 J=KP1,N
      P(J)=A(K,J)
      IF (R(J)) 160,100,110
100   P(J)=-P(J)
110   Q(J)=-A(K,J)*Q(K)
120   A(K,J)=0.
130   DO 140 J=1,N
      DO 140 K=J,N
      A(J,K)=A(J,K)+P(J)*Q(K)
140   A(K,J)=A(J,K)
150   CONTINUE
      RETURN
160   IRR=1
      RETURN
      END


      SUBROUTINE SUM(SSQ1,XR1,YR1,EVXSQ1,EVYSQ1,YM1,XM1,NN1,NK1
      1,LL1,KK1)
      IMPLICIT REAL*8 (A-H,P-Z)
      REAL*8 XR1(NK1),YR1(NN1),EVXSQ1(NK1),EVYSQ1(NN1),YM1(NN1
      1),XM1(NK1)

      SSQ1=0
      DO 10 I=1,NK1
              SSQ1=SSQ1+(XR1(I)-XM1(I))**2*EVXSQ1(I)

10    CONTINUE
      DO 20 I=1,NN1
              SSQ1=SSQ1+(YR1(I)-YM1(I))**2*EVYSQ1(I)

20    CONTINUE
      RETURN
      END
C
```

```
      SUBROUTINE FUNC(XR1,PAR1,YR1,DFXM,DFPM,DFYM,FR,
     1NN1,LL1,KK1,NK1,TC,PC,ACCN,DFP,DFY,DFX,IT)

C     THIS PROGRAM CALCULATES  THE DERIVATIVES REQUIRED FOR
      THE MAXIMUM LIKELIHOOD PROGRAM

      IMPLICIT REAL*8 (A-H,P-Z)
      PARAMETER R=8314.41,C=.45
      REAL*8 XR1(NK1),PAR1(LL1),YR1(NN1),DFXM(NN1,NK1),DFPM(NN1,LL1),
     1DFYM(NN1,NN1),DFP(NN1),DFY(NN1),DFX(NK1),FR(NN1)

      IF(IT.EQ.1)THEN
      CALL VP(XR1,YR1,TC,PC,ACCN,PAR,NN1,YR1,NK1)
      ENDIF


      DO 30 I=1,NN1
      IF(YR1(I).LT.0)YR1(I)=.0000000001
      CALL FUGC(XR1(I),PAR1(1),TC,PC,ACCN,FUGL,FUGV,YR1(I))

      FR(I)=FUGV-FUGL
      TYPE*,'FUGV-FUGL',FR(I)

C     DERIVATIVE OF F WRT Y

      Y=YR1(I)*.998
      CALL FUGC(XR1(I),PAR1(1),TC,PC,ACCN,FUGL,FUGV,Y)
      FY2N=FUGV-FUGL

      Y=YR1(I)*.999
      CALL FUGC(XR1(I),PAR1(1),TC,PC,ACCN,FUGL,FUGV,Y)
      FY1N=FUGV-FUGL

      Y=YR1(I)*1.001
      CALL FUGC(XR1(I),PAR1(1),TC,PC,ACCN,FUGL,FUGV,Y)
      FY1=FUGV-FUGL

      Y=YR1(I)*1.002
      CALL FUGC(XR1(I),PAR1(1),TC,PC,ACCN,FUGL,FUGV,Y)
      FY2=FUGV-FUGL


      DFY(I)=(2*FY2N - 16*FY1N + 16*FY1 - 2*FY2)/(24*YR1(I)*.001)

C     DERIVATIVE F WRT X

      X=XR1(I)*.998
      CALL FUGC(X,PAR1(1),TC,PC,ACCN,FUGL,FUGV,YR1(I))
```

```
      FX2N=FUGV-FUGL

      X=XR1(I)*.999
      CALL FUGC(X,PAR1(1),TC,PC,ACCN,FUGL,FUGV,YR1(I))
      FX1N=FUGV-FUGL

      X=XR1(I)*1.001
      CALL FUGC(X,PAR1(1),TC,PC,ACCN,FUGL,FUGV,YR1(I))
      FX1=FUGV-FUGL

      X=XR1(I)*1.002
      CALL FUGC(X,PAR1(1),TC,PC,ACCN,FUGL,FUGV,YR1(I))
      FX2=FUGV-FUGL


      DFX(I)=(2*FX2N - 16*FX1N + 16*FX1 - 2*FX2)/(24*XR1(I)*.001)

C     DERIVATIVE OF F WRT PAR

      DPAR=PAR1(1)*.998
      CALL FUGC(XR1(I),DPAR,TC,PC,ACCN,FUGL,FUGV,YR1(I))
      FP2N=FUGV-FUGL

      DPAR=PAR1(1)*.999
      CALL FUGC(XR1(I),DPAR,TC,PC,ACCN,FUGL,FUGV,YR1(I))
      FP1N=FUGV-FUGL

      DPAR=PAR1(1) *1.001
      CALL FUGC(XR1(I),DPAR,TC,PC,ACCN,FUGL,FUGV,YR1(I))
      FP1=FUGV-FUGL

      DPAR=PAR1(1) *1.002
      CALL FUGC(XR1(I),DPAR,TC,PC,ACCN,FUGL,FUGV,YR1(I))
      FP2=FUGV-FUGL


      DFP(I)=(2*FP2N - 16*FP1N + 16*FP1 - 2*FP2)/(24*PAR1(1)*.001)


30    CONTINUE


C     CREATE MATRICES OUT OF DERIVATIVES DFP SHOULD BE A
C     NN X LL MATRIX.  DFY SHOULD BE A NN X NN DIAG MATRIX
C     AND DFX SHOULD BE A NN X NK DIAG MATRIX. NOTE: CURRENTLY
C     NK=NN SINCE ONLY ONE INDEPENDENT PARAMETER
```

```
      DO 31 I=1,NN1

      DO 44 J=1,LL1

      DFPM(I,J)=DFP(I)
44    CONTINUE

      DO 45 J=1,NN1

      IF(J.EQ.I)THEN
      DFYM(I,J)=DFY(I)
      DFXM(I,J)=DFX(I)
      ELSE
      DFYM(I,J)=0
      DFXM(I,J)=0
      ENDIF
45    CONTINUE
31    CONTINUE

      RETURN
      END

      SUBROUTINE FUGC(T,PAR1,TC,PC,ACCN,FUGL,FUGV,P)

C     THIS PROGRAM CALCULATES FUGACITY COEFFICIENTS

      PARAMETER R=8314.41,C=.45
      IMPLICIT REAL*8 (A-H,P-Z)


C     CALCULATE SRK SMALL  B (SMB) AND A(TC) (ATC)
C     R IS THE GAS CONSTANT AND TC AND PC ARE THE CRITICAL PROPERTIES
C     ACCN IS THE ACENTRIC FACTOR FOR THE NONPOLAR COMPOUND

      SMB=0.08664*R*TC/PC
      ATC=0.42747*R**2.*TC**2./PC

C     CALCULATE THE FUGACITY COEFFICIENT (FUGV) IN THE VAPOR PHASE

C     CALCULATE THE ALPHA OF THE NONPOLAR COMPOUND (ALPHAN)

      ALPHAN=(1. + (0.48 + 1.574*ACCN-0.176*(ACCN)**2.)*(1.-(T/
     1TC)**0.5))**2.

C     CALCULATE THE PARAMETER PART OF A

      PARA=1. + PAR1*DEXP(-PAR1**C)-PAR1*DEXP(-(PAR1*
```

```
     1TC/T)**C)
C    CALCULATE SMALL "A" (SMA) IN THE SRK
     SMA=ATC*ALPHAN*PARA
C    CALCULATE CAPITAL A AND B
     A=SMA*P/(R**2.*T**2.)
     B=SMB*P/(R*T)
C    SET COEFFICIENTS FOR THE CUBIC SOLVER
     D=-1
     E=(A-B-B**2)
     F=-(A*B)
     CALL VCUB(D,E,F,ZV,-1)
     TYPE*,'ZV',ZV
C    NOW CALCULATE FUGACITY COEFFICIENT IN THE VAPOR PHASE (FUGV)
     FUGV=DEXP(ZV-1.-DLOG(ZV-B)-(A/B)*DLOG((ZV+B)/ZV))
C    CALCULATE THE FUGACITY COEFFICIENT IN THE LIQUID PHASE (FUGL)
     CALL VCUB(D,E,F,ZL,1)
     TYPE*,'ZL',ZL
C    CALCULATE THE LIQUID PHASE FUGACITY COEFFICIENT (FUGL)
     FUGL=DEXP(ZL-1.-DLOG(ZL-B) - (A/B)*DLOG((ZL+B)/ZL))

     RETURN
     END
C
C    CUBIC SOLVER
C
     SUBROUTINE VCUB(D,E,F,Z,ID)
C    SUBPROGRAM FOR SOLVING A CUBIC EQUATION OF THE FORM:
C    Z**3 +D*Z**2+ E*Z + F=0.0
C    WHERE D,E, AND F ARE CONSTANTS
     IMPLICIT REAL*8(A-H,P-Z)
     G=(3.*E-D*D)/3.
     H=-(9.*D*E-27.*F-2*D*D*D)/27.
     IF((G**3)/27. +H*H/4..LE.0.)GO TO 10
     S=-H/2. + DSQRT(G**3/27. + H*H/4.)
```

```
      TT=-H/2. - DSQRT(G**3/27. + H*H/4.)
      IF(S)5,6,6
5     S=-((-S)**(1./3.))
      GO TO 7
6     S=S**(1./3.)
7     IF(TT)8,9,9
8     TT=-(-TT)**(1./3.)
      GO TO 15
9     TT=(TT)**(1./3.)
C     SINGLE REAL ROOT
15    Z=S+TT-D/3.
      GO TO 40
C     THERE ARE THREE ROOTS.
10    THETA=(DACOS(-.5*H/DSQRT(-G**3/27.)))/3.
      Z1=2.*DSQRT(-G/3.)*DCOS(THETA)
      Z2=2.*DSQRT(-G/3.)*DCOS(THETA+2.0943951)
      Z3=2.*DSQRT(-G/3.)*DCOS(THETA+ 4.1887902)
C     DECIDING WHICH TO CHOOSE
      IF(ID)20,30,30
C     TAKE LARGEST ROOT FOR VAPOR VOLUME.
20    Z=DMAX1(Z1,Z2,Z3)-D/3.
      GO TO 40
C     TAKE SMALLEST ROOT FOR LIQUID VOLUME.
30    Z=DMIN1(Z1,Z2,Z3)-D/3.
      IF(Z.LT.0)Z=.000000001
      DO 31 I=1,20
      ZN=Z-(Z**3+D*Z**2+E*Z+F)/(3.*Z**2+2.*Z*D+E)
      IF(ABS((ZN-Z)/Z).LT..00000001)GO TO 40
31    Z=ZN
40    RETURN
      END


      SUBROUTINE VP(XM,YM,TC,PC,ACCN,PAR,NN,YC,NK)

C     THIS IS A PROGRAM FOR CALCULATING VAPOR PRESSURES

      IMPLICIT REAL*8(A-H,P-Z)
      REAL*8 XM(NK),YM(NN),YC(NN)

      DO 10 I=1,NN

              P=YM(I)

9     CALL FUGACITY(XM(I),P,TC,PC,ACCN,PAR,FUGLI,FUGVI)

      PN=P*FUGLI/FUGVI
```

```
        IF (ABS(PN-P).LT..001) THEN
        YC(I)=PN
        GO TO 10
        ELSE

        P=PN
        GO TO 9
        ENDIF
10      CONTINUE

        RETURN
        END

        SUBROUTINE FUGACITY(T,P,TC,PC,ACCN,PAR,FUGL,FUGV)
        PARAMETER R=8314.41,C=.45
        IMPLICIT REAL*8 (A-H,P-Z)

C       CALCULATE SRK SMALL  B (SMB) AND A(TC) (ATC)
C       R IS THE GAS CONSTANT AND TC AND PC ARE THE CRITICAL PROPERTIES
C       ACCN IS THE ACENTRIC FACTOR FOR THE NONPOLAR COMPOUND

        SMB=0.08664*R*TC/PC
        ATC=0.42747*R**2.*TC**2./PC

C       CALCULATE THE ALPHA OF THE NONPOLAR COMPOUND (ALPHAN)

        ALPHAN=(1. + (0.48 + 1.574*ACCN-0.176*(ACCN)**2.)*(1.-(T/
        1TC)**0.5))**2.

C       CALCULATE THE PARAMETER PART OF A

        PARA=1. + PAR*DEXP(-PAR**C)-PAR*DEXP(-(PAR*
        1TC/T)**C)

C       CALCULATE SMALL "A" (SMA) IN THE SRK

        SMA=ATC*ALPHAN*PARA

C       CALCULATE CAPITAL A AND B

        A=SMA*P/(R**2.*T**2.)

        B=SMB*P/(R*T)

C       SET COEFFICIENTS FOR THE CUBIC SOLVER
```

```
      D=-1
      E=(A-B-B**2)
      F=-(A*B)

      CALL VCUB(D,E,F,ZV,-1)

C     NOW CALCULATE FUGACITY COEFFICIENT IN THE VAPOR PHASE (FUGV)

      FUGV=DEXP(ZV-1.-DLOG(ZV-B)-(A/B)*DLOG((ZV+B)/ZV))

C     CALCULATE THE FUGACITY COEFFICIENT IN THE LIQUID PHASE (FUGL)

C     CALL CUBIC SOLVER

      CALL VCUB(D,E,F,ZL,1)

C     CALCULATE THE LIQUID PHASE FUGACITY COEFFICIENT (FUGL)

      FUGL=DEXP(ZL-1.-DLOG(ZL-B) - (A/B)*DLOG((ZL+B)/ZL))

      RETURN
      END
```

```
C       THIS PROGRAM EMPLOYS AN IMPLICIT CONSTRAINT MAXIMUM
C       LIKELIHOOD ALGORITHM FOR DETERMINING PARAMETERS FOR
C       TWO CONSTRAINTS
C*************************************************************
        PARAMETER NN =100, KK = 2, LL = 3, NK =200
        IMPLICIT REAL*8 (A-H,P-Z)
        CHARACTER*20 FILN1,FILN2,FILN3,FILN4,FILN5,FILN6,FILN7,FILN8,
        1FILN9,FILN10,FILN11

        REAL*8 YM(NN),XM(NK),PAR(LL),EVX(NK),EVY(NN),EVXSQ(NK),
        1EVYSQ(NN),EVXD(NK,NK),EVYD(NN,NN),EVXDI(NK,NK),DFX(NN,NK),
        1DFP(NN,LL),DFXT(NK,NN),DFPT(LL,NN),DELXM(NK),DELYM(NN),
        1DUM(NK,NN),DUM1(NK,NK),DUM2(NK,NN),DUM3(NK,NK),
        1DUM4(NK,NK),D(NK,NK),RDUM(NK,NN),RDUM1(NK,LL),RDUM2(NK,NN),
        1RDUM3(NK,LL),R(NK,LL),RT(LL,NK),TDUM(LL,NN),TDUM1(LL,LL),
        1TDUM2(LL,NN),TDUM3(LL,LL),T(LL,LL),UDUM(LL,1),UDUM1(LL,1),
        1U(LL,1),QDUM(NK,1),QDUM1(NK,1),QDUM2(NK,1),QDUM3(NK,1),
        1Q(NK,1),D1UM(LL,NK),D2UM(LL,LL),D3UM(LL,LL),D4UM(LL,1),
        1D5UM(LL,1),DELPN(LL),D6UM(NK,1),D7UM(NK,1),DELXN(NK),
        1XR(NK),YR(NN),ZM(NN),EVZ(NN),EVZSQ(NN),EVZD(NN,NN),DGX(NN,NK),
        1DGP(NN,LL),DGXT(NK,NN),DGPT(LL,NN),ZR(NN),DELZM(NN),
        1CDFX(NN,NK),CDFP(NN,LL),CDGX(NN,NK),CDGP(NN,LL),CDFZ(NN,NN)
        1,CDGZ(NN,NN),CDFY(NN,NN),CDGY(NN,NN),CDFZI(NN,NN),AA(NN,NN),
        1AAI(NN,NN),UUUI(NN,NN),DELZN(NN),DELYN(NN),DFR(NN),DGR(NN),
        1CDFYI(NN,NN),FR(NN),GR(NN),AA1(NN,NN),AA2(NN,NN),AA3(NN,NN),
        1AA4(NN,NN),AA5(NN,NN),AA6(NN,1),AA7(NN,1),AA8(NN,1),
        1AA9(NN,NN),AA10(NN,NK),AA11(NN,NK),AA12(NN,NN),AA13(NN,LL),
        1AA14(NN,LL),AA0(NN,NN),AA15(NN,1),AA16(NN,1),AA17(NN,1)
        1,AA18(NN,1),AA19(NN,NK),AA20(NN,NK),AA21(NN,NK),AA22(NN,LL),
        1AA23(NN,LL),AA24(NN,LL),DELY1(NN,1),DELY2(NN,1),DELY3(NN,1),
        1ZZZ1(NN,1),BBB1(NN,1),BBB2(NN,1),BBB(NN,1),YYY(NN,1),
        1XXX(NN,1),ZZZ(NN,1),PART(LL),XRT(NK),ZRT(NN),YRT(NN)

        IT=0

        ITMX=100


        TYPE*,'**************CAUTION, IF THE NUMBER OF DATA PTS
        1  TIMES THE NUMBER OF INDEPENDENT VARIABLES EXCEEDS 150,
        1 CHANGE THE MATRIX DIMENSIONS IN THE SUBROUTINE SYMINV'

        TYPE*,'ENTER THE TOLERANCE LIMIT'
        ACCEPT*,SSTL

        TYPE*,'ENTER THE LIMITING FACTOR'
        ACCEPT*,V
```

```
      TYPE*,'ENTER THE FILENAME CONTAINING THE DEPENDENT VARIABLE Y
      1,NN'
      READ(5,1)FILN1
1     FORMAT(A20)
      TYPE*,'ENTER THE FILENAME CONTAINING THE DEPENDENT VARIABLE Z
      1,NN'
      READ(5,1)FILN9
      TYPE*,'ENTER THE FILENAME CONTAINING THE INDEPENDENT VARIABLES,
      1NK'
      READ(5,1)FILN2
      TYPE*,'ENTER THE FILENAME CONTAINING PARAMETER ESTIMATES,LL'
      READ(5,1)FILN3
      TYPE*,'ENTER THE FILENAME CONTAINING THE VARIANCES FOR THE
      1INDEPENDENT VARIABLES,NK'
      READ(5,1)FILN4
      TYPE*,'ENTER THE FILENAME CONTAINING THE VARIANCES FOR THE
      1DEPENDENT VARIABLE Y ,NN'
      READ(5,1)FILN5
      TYPE*,'ENTER THE FILENAME CONTAINING THE VARIANCES FOR THE
      1DEPENDENT VARIABLE Z ,NN'
      READ(5,1)FILN10

      TYPE*,'ENTER THE CRITICAL TEMPERATURE, CRITICAL PRESSURE,
      1ACCENTRIC FACTOR, AND POLAR PARAMETER FOR COMPONENT 1 IN
      1THE UNITS  K AND KPA'
      ACCEPT*,TC1,PC1,ACCN1,RP1
      TYPE*,TC1,PC1,ACCN1,RP1
      TYPE*,'ENTER THE CRITICAL TEMPERATURE,CRITICAL PRESSURE,
      1ACCENTRIC FACTOR, AND POLAR PARAMETER FOR COMPONENT 2 IN
      1THE UNITS K AND KPA'
      ACCEPT*,TC2,PC2,ACCN2,RP2
      TYPE*,TC2,PC2,ACCN2,RP2

      OPEN(UNIT=10,FILE=FILN1,STATUS='OLD')
      OPEN(UNIT=20,FILE=FILN2,STATUS='OLD')
      OPEN(UNIT=30,FILE=FILN3,STATUS='OLD')
      OPEN(UNIT=40,FILE=FILN4,STATUS='OLD')
      OPEN(UNIT=50,FILE=FILN5,STATUS='OLD')
      OPEN(UNIT=90,FILE=FILN9,STATUS='OLD')
      OPEN(UNIT=100,FILE=FILN10,STATUS='OLD')

C     READ IN DEPENDENT VARIABLES Y AND Z

      READ(10,*,END=99) (YM(I),I=1,NN)
99    READ(90,*,END=101) (ZM(I),I=1,NN)
```

```
C       READ IN INDEPENDENT VARIABLES

101     READ(20,*,END=102) (XM(I),I=1,NK)

C       READ IN PARAMETER ESTIMATES

102     READ(30,*,END=103) (PAR(I),I=1,LL)

C       READ IN VARIANCES FOR INDEPENDENT VARIABLES

103     READ(40,*,END=104) (EVX(I),I=1,NK)

C       READ IN VARIANCES FOR DEPENDENT VARIABLE Y AND Z

104     READ(50,*,END=105) (EVY(I),I=1,NN)
105     READ(100,*,END=106) (EVZ(I),I=1,NN)

C       SET INITIAL TRUE VALUES TO MEASURED VALUES

106     DO 10 I=1,NN
                YR(I)=YM(I)
                ZR(I)=ZM(I)
10      CONTINUE
        DO 20 I=1,NK
                XR(I)=XM(I)
20      CONTINUE

C       SQUARE AND INVERT VARIANCES EVX AND EVY, CREATE DIAG MATRICES

        DO 30 I=1,NK
                EVXSQ(I)=1./EVX(I)**2
30      CONTINUE
        DO 40 I=1,NN
                EVYSQ(I)=1./EVY(I)**2
                EVZSQ(I)=1./EVZ(I)**2
40      CONTINUE
        CALL DIAG(EVXSQ,NK,EVXD)
        CALL DIAG(EVYSQ,NN,EVYD)
        CALL DIAG(EVZSQ,NN,EVZD)

C       CALCULATE THE INVERSE OF EVXD

        CALL DIAGINV(NK,NK,EVXD,EVXDI)

C       CALCULATE FUNCTIONS AND DERIVATIVES

150     IT=IT+1
```

```
      CALL FUNC(XR,PAR,YR,ZR,NN,LL,KK,NK,TC1,TC2,FR,GR,PC1,PC2,
     1ACCN1,ACCN2,RP1,RP2,CDFX,CDFP,CDGX,CDGP,CDFZ,CDGZ,
     1CDFY,CDGY,IT)

      IF(IT.EQ.1)THEN
      CALL SUM(SSQ,XR,YR,ZR,EVXSQ,EVYSQ,EVZSQ,YM,XM,ZM,NN,
     1NK,LL,KK)
      ELSE
      CONTINUE
      ENDIF

C     CALCULATE THE GROUPS OF DERIVATIVES GIVEN IN ANDERSON'S
C     ARTICLE AS SMALL f AND SMALL g

C     FOR THE DERIVATIVES OF f THE INVERTED TERM IS AAI
C     (CDGY - CDGZ*CDFZI*CDFY)**-1

151   CALL DIAGINV(NN,NN,CDFZ,CDFZI)
      CALL MATMULT(CDGZ,CDFZI,AA,NN,NN,NN)
      CALL MATMULT(AA,CDFY,AA3,NN,NN,NN)
      CALL MATSUB(CDGY,AA3,AA4,NN,NN)
      CALL DIAGINV(NN,NN,AA4,AAI)

C     CALCULATE fr (DFR)

      CALL MATMULT(CDGZ,CDFZI,AA5,NN,NN,NN)
      CALL MATMULT(AA5,FR,AA6,NN,NN,1)
      CALL MATSUB(GR,AA6,AA7,NN,1)
      CALL MATMULT(AAI,AA7,AA8,NN,NN,1)
      CALL MATSUB(YR,AA8,DFR,NN,1)

C     CALCULATE fx (DFX)

      CALL MATMULT(CDGZ,CDFZI,AA9,NN,NN,NN)
      CALL MATMULT(AA9,CDFX,AA10,NN,NN,NK)
      CALL MATSUB(CDGX,AA10,AA11,NN,NK)
      CALL MATMULT(AAI,AA11,DFX,NN,NN,NK)
      CALL NEG(DFX,DFX,NN,NK)

C     CALCULATE ftheta (DFP)

      CALL MATMULT(CDGZ,CDFZI,AA12,NN,NN,NN)
      CALL MATMULT(AA12,CDFP,AA13,NN,NN,LL)
      CALL MATSUB(CDGP,AA13,AA14,NN,LL)
      CALL MATMULT(AAI,AA14,DFP,NN,NN,LL)
      CALL NEG(DFP,DFP,NN,LL)
```

```
C       CALCULATE DERIVATIVES OF FUNCTION G

C       FOR THE DERIVATIVES OF G THE INVERTED TERM IS MATRIX UUUI
C       (CDGZ - CDGY*CDFYI*CDFZ)**-1

        CALL DIAGINV(NN,NN,CDFY,CDFYI)
        CALL MATMULT(CDFYI,CDFZ,AA0,NN,NN,NN)
        CALL MATMULT(CDGY,AA0,AA1,NN,NN,NN)
        CALL MATSUB(CDGZ,AA1,AA2,NN,NN)
        CALL DIAGINV(NN,NN,AA2,UUUI)

C       CALCULATE gr (DGR)

        CALL MATMULT(CDFYI,FR,AA15,NN,NN,1)
        CALL MATMULT(CDGY,AA15,AA16,NN,NN,1)
        CALL MATSUB(GR,AA16,AA17,NN,1)
        CALL MATMULT(UUUI,AA17,AA18,NN,NN,1)
        CALL MATSUB(ZR,AA18,DGR,NN,1)

C       CALCULATE gx (DGX)

        CALL MATMULT(CDFYI,CDFX,AA19,NN,NN,NK)
        CALL MATMULT(CDGY,AA19,AA20,NN,NN,NK)
        CALL MATSUB(CDGX,AA20,AA21,NN,NK)
        CALL MATMULT(UUUI,AA21,DGX,NN,NN,NK)
        CALL NEG(DGX,DGX,NN,NK)


C       CALCULATE gtheta (DGP)

        CALL MATMULT(CDFYI,CDFP,AA22,NN,NN,LL)
        CALL MATMULT(CDGY,AA22,AA23,NN,NN,LL)
        CALL MATSUB(CDGP,AA23,AA24,NN,LL)
        CALL.MATMULT(UUUI,AA24,DGP,NN,NN,LL)
        CALL NEG(DGP,DGP,NN,LL)


C       CALCULATE TRANSPOSE OF DERIVATIVES

        CALL TRANS(DFX,DFXT,NN,NK)
        CALL TRANS(DGX,DGXT,NN,NK)
        CALL TRANS(DFP,DFPT,NN,LL)
        CALL TRANS(DGP,DGPT,NN,LL)

C       CALCULATE DELXM AND DELYM

        DO 90 I=1,NN
                DELYM(I)=(YR(I)-YM(I))
```

```
              DELZM(I)=(ZR(I)-ZM(I))
90       CONTINUE

         DO 100 I=1,NK
              DELXM(I)=XR(I)-XM(I)
100      CONTINUE

C        CALCULATE MATRIX D

         CALL MATMULT(DFXT,EVYD,DUM,NK,NN,NN)
         CALL MATMULT(DUM,DFX,DUM1,NK,NN,NK)
         CALL MATMULT(DGXT,EVZD,DUM2,NK,NN,NN)
         CALL MATMULT(DUM2,DGX,DUM3,NK,NN,NK)
         CALL MATADD(EVXD,DUM1,DUM4,NK,NK)
         CALL MATADD(DUM4,DUM3,D,NK,NK)

C        INVERT MATRIX D

         CALL SYMINV (D,NK,IRR)

C        CALCULATE MATRIX R

         CALL MATMULT (DFXT,EVYD,RDUM,NK,NN,NN)
         CALL MATMULT(RDUM,DFP,RDUM1,NK,NN,LL)
         CALL MATMULT(DGXT,EVZD,RDUM2,NK,NN,NN)
         CALL MATMULT(RDUM2,DGP,RDUM3,NK,NN,LL)
         CALL MATADD(RDUM1,RDUM3,R,NK,LL)
         CALL TRANS(R,RT,NK,LL)

C        CALCULATE MATRIX T

         CALL MATMULT(DFPT,EVYD,TDUM,LL,NN,NN)
         CALL MATMULT(TDUM,DFP,TDUM1,LL,NN,LL)
         CALL MATMULT(DGPT,EVZD,TDUM2,LL,NN,NN)
         CALL MATMULT(TDUM2,DGP,TDUM3,LL,NN,LL)
         CALL MATADD(TDUM1,TDUM3,T,LL,LL)

C        CALCULATE MATRIX U

         CALL MATMULT(TDUM,DELYM,UDUM,LL,NN,1)
         CALL MATMULT(TDUM2,DELZM,UDUM1,LL,NN,1)
         CALL MATADD(UDUM,UDUM1,U,LL,1)

C        CALCULATE MATRIX Q

         CALL MATMULT(EVXD,DELXM,QDUM,NK,NK,1)
         CALL MATMULT(RDUM,DELYM,QDUM1,NK,NN,1)
         CALL MATMULT(RDUM2,DELZM,QDUM2,NK,NN,1)
```

```
      CALL MATADD(QDUM,QDUM1,QDUM3,NK,1)
      CALL MATADD(QDUM3,QDUM2,Q,NK,1)

C     CALCULATE DELPN

      CALL MATMULT(RT,D,D1UM,LL,NK,NK)
      CALL MATMULT(D1UM,R,D2UM,LL,NK,LL)
      CALL MATSUB(T,D2UM,D3UM,LL,LL)
      CALL SYMINV(D3UM,LL,IRR)
      CALL MATMULT(D1UM,Q,D4UM,LL,NK,1)
      CALL MATSUB(U,D4UM,D5UM,LL,1)
      CALL MATMULT(D3UM,D5UM,DELPN,LL,LL,1)
      CALL NEG(DELPN,DELPN,LL,1)


C     CALCULATE DELXN

      CALL MATMULT(R,DELPN,D6UM,NK,LL,1)
      CALL MATADD(Q,D6UM,D7UM,NK,1)
      CALL MATMULT(D,D7UM,DELXN,NK,NK,1)
      CALL NEG(DELXN,DELXN,NK,1)

C     CALCULATE NEW ESTIMATES OF PARAMETERS AND X AND Y AND Z

      DO 120 I=1,LL
              PAR(I)=V*DELPN(I) +PAR(I)
120   CONTINUE

      DO 130 I=1,NK
              XR(I)=V*DELXN(I) + XR(I)

130   CONTINUE

C     CALCULATE DELZN
      CALL MATSUB(DGR,ZR,YYY,NN,1)
      CALL MATMULT(DGP,DELPN,XXX,NN,LL,1)
      CALL MATMULT(DGX,DELXN,ZZZ,NN,NK,1)
      CALL MATADD(YYY,ZZZ,ZZZ1,NN,1)
      CALL MATADD(ZZZ1,XXX,DELZN,NN,1)

C     CALCULATE DELYN

      CALL MATSUB(DFR,YR,BBB,NN,1)
      CALL MATMULT(DFP,DELPN,BBB1,NN,LL,1)
      CALL MATMULT(DFX,DELXN,BBB2,NN,NK,1)
      CALL MATADD(BBB,BBB1,DELY1,NN,1)
      CALL MATADD(DELY1,BBB2,DELYN,NN,1)
```

```
      DO 140 I=1,NN
             ZR(I)=V*DELZN(I) + ZR(I)
             YR(I)=V*DELYN(I) + YR(I)

140   CONTINUE

      CALL SUM(SSQN,XR,YR,ZR,EVXSQ,EVYSQ,EVZSQ,YM,XM,ZM,NN,
      1NK,LL,KK)


      DIFF=(SSQ-SSQN)/SSQN
      TYPE*,'DIFF',DIFF
      TYPE*,'SSQ,SSQN',SSQ,SSQN
      IF(IT.EQ.5)THEN
      TYPE*,'ENTER LIMITING FACTOR'
      ACCEPT*,V
C     TYPE*,'CHANGED LIMITING FACTOR TO .5'
      ENDIF
      IF(ABS(DIFF).LT.SSTL)GO TO 200

      SSQ=SSQN

      IF(IT.LT.ITMX)GO TO 150
      TYPE*,'NUMBER OF INTERATIONS GREATER THAN ITMX'
      GO TO 200
C

200   S=SSQ/(NN-LL)
      TYPE*,'ENTER FILENAME FOR OUTPUT'
      READ(5,1)FILN6

      OPEN(UNIT=60,FILE=FILN6,STATUS='NEW')

      WRITE(60,*)'CRITICAL PROPERTIES OF COMP 1',TC1,PC1,ACCN1,RP1
      WRITE(60,*)'CRITICAL PROPERTIES OF COMP 2',TC2,PC2,ACCN2,RP2
      WRITE(60,*)'PARAMETERS ALPHA',PAR(1),'C12',PAR(2),'C21',PAR(3)
      WRITE(60,*)'S=SSQ/(N-L)',S
      DO  I=1,NN
      WRITE(60,*)'                TCALC               TMEAS
      1               PCALC               PMEAS'

      WRITE(60,2)XR(2*I-1),XM(2*I-1),YR(I),YM(I)

      WRITE(60,*)'                XCALC               XMEAS
      1               YCALC               YMEAS'
      WRITE(60,3)XR(2*I),XM(2*I),ZR(I),ZM(I)
      WRITE(60,*)'                                           '
      ENDDO
```

```
2       FORMAT(4F20.2)
3       FORMAT(4F20.5)
1000    STOP
        END

C
        SUBROUTINE TRANS(W,WT,N,K)
        REAL*8 W(N,K),WT(K,N)
                DO 121 I=1,N
                DO 122 J=1,K
                        WT(J,I)=W(I,J)
122             CONTINUE
121     CONTINUE
        RETURN
        END

        SUBROUTINE NEG(S,SN,N,K)
        REAL*8 S(N,K),SN(N,K)
        DO 10 I=1,N
                DO 20 J=1,K
                        SN(I,J)=-S(I,J)
20      CONTINUE
10      CONTINUE
        RETURN
        END

        SUBROUTINE MULT(S,N,K,C)
        REAL*8 S(N,K)
        DO 10 I=1,N
                DO 20 J=1,K
                        S(I,J)=C*S(I,J)
20      CONTINUE
10      CONTINUE
        RETURN
        END

        SUBROUTINE DIAG(S,N,W)
        REAL*8 W(N,N),S(N)
        DO 11 I=1,N
                DO 21 J=1,N
                        IF (J.EQ.I) THEN
                        W(I,J)=S(I)
                        ELSE
                        W(I,J)=0
```

```
                 ENDIF
21           CONTINUE
11      CONTINUE
        RETURN
        END
C
C
C
        SUBROUTINE DIAGINV(N,K,W,WI)
        REAL*8 W(N,K),WI(N,K)
        DO 31 I=1,N
                DO 41 J=1,K
                        IF (J.EQ.I) THEN
                        WI(I,J)=1./W(I,J)
                        ELSE
                        WI(I,J)=0
                        ENDIF
41              CONTINUE
31      CONTINUE
        RETURN
        END
C
C
C
        SUBROUTINE MATMULT(A,U,T,M,N,P)
        INTEGER P
        REAL*8 T(M,P),A(M,N),U(N,P)
C
C       T(M,P)=A(M,N)*U(N,P)
C
        DO 10 I=1,M
                DO 20 KKJ=1,P
                        T(I,KKJ)=0
20              CONTINUE
10      CONTINUE
        DO 30 I=1,M
                DO 40 KKJ=1,P
                        DO 50 K=1,N
                                T(I,KKJ)=A(I,K)*U(K,KKJ)+T(I,KKJ)
50                      CONTINUE
40              CONTINUE
30      CONTINUE
        RETURN
        END
C
C
C
        SUBROUTINE MATADD(A,B,C,M,N)
```

```
C
C       C(M,N)=A(M,N)+B(M,N)
C
        REAL*8 A(M,N),B(M,N),C(M,N)
        DO 10 I=1,M
                DO 20 J=1,N
                        C(I,J)=A(I,J)+B(I,J)
20              CONTINUE
10      CONTINUE
        RETURN
        END
C
C
C
        SUBROUTINE MATSUB(A,B,C,M,N)
C
C       C(M,N)=A(M,N)-B(M,N)
C
        REAL*8 A(M,N),B(M,N),C(M,N)
        DO 10 I=1,M
                DO 20 J=1,N
                        C(I,J)=A(I,J)-B(I,J)
20              CONTINUE
10      CONTINUE
        RETURN
        END
C
C
C
        SUBROUTINE SYMINV(A,N,IRR)
C
C       INVERTS A SYMMETRIC MATRIX A(N,N), THE MATRIX TO BE INVERTED
C       IS DESTROYED AND ULTIMATELY CONTAINS THE INVERSE
C       IRR IF THE FAILURE PARAMETER WHEN NO INVERSE CAN BE FOUND
C       REFERENCE "COMPUTER CALCULATIONS FOR MULTICOMPONENT VL
C       AND LLE", PRAUSNITZ,J, PRENTICE-HALL ,1980
C
        IMPLICIT REAL*8 (A-H,P,Q,S-Z)
        REAL*8 A(N,N),P(150),Q(150)
        INTEGER R(150)
        IRR=0
        DO 10 I=1,N
10      R(I)=1
        DO 150 I=1,N
        BIG=0.
        DO 40 J=1,N
        TEST=ABS(A(J,J))
        IF (TEST-BIG) 40,40,20
```

```
20      IF (R(J)) 160,40,30
30      BIG=TEST
        K=J
40      CONTINUE
        IF(BIG.LT.1.E-19) GO TO 160
        R(K)=0
        Q(K)=1./A(K,K)
        P(K)=1.
        A(K,K)=0.0
        KP1=K+1
        KM1=K-1
        IF(KM1) 160,80,50
50      DO 70 J=1,KM1
                P(J)=A(J,K)
                Q(J)=A(J,K)*Q(K)
                IF(R(J)) 160,70,60
60      Q(J)=-Q(J)
70      A(J,K)=0.
80      IF(K-N)90,130,160
90      DO 120 J=KP1,N
        P(J)=A(K,J)
        IF (R(J)) 160,100,110
100     P(J)=-P(J)
110     Q(J)=-A(K,J)*Q(K)
120     A(K,J)=0.
130     DO 140 J=1,N
        DO 140 K=J,N
        A(J,K)=A(J,K)+P(J)*Q(K)
140     A(K,J)=A(J,K)
150     CONTINUE
        RETURN
160     IRR=1
        RETURN
        END
C
C
C
        SUBROUTINE SUM(SSQ1,XR1,YR1,ZR1,EVXSQ1,EVYSQ1,EVZSQ1,
        1YM1,XM1,ZM1,NN1,NK1,LL1,KK1)
        IMPLICIT REAL*8 (A-H,P-Z)
        REAL*8 XR1(NK1),YR1(NN1),EVXSQ1(NK1),EVYSQ1(NN1),YM1(NN1
        1),XM1(NK1),ZR1(NN1),EVZSQ1(NN1),ZM1(NN1)

        SSQ1=0
        DO 10 I=1,NK1
                SSQ1=SSQ1+(XR1(I)-XM1(I))**2*EVXSQ1(I)

10      CONTINUE
```

```
      DO 20 I=1,NN1
            SSQ1=SSQ1+(YR1(I)-YM1(I))**2*EVYSQ1(I)
            SSQ1=SSQ1+(ZR1(I)-ZM1(I))**2*EVZSQ1(I)
20    CONTINUE
      RETURN
      END


      SUBROUTINE FUNC(XR1,PAR1,YR1,ZR1,NN1,LL1,KK1,NK1,TC1,
      1TC2,FR,GR,PC1,PC2,ACCN1,ACCN2,RP1,RP2,DFX,DFP,DGX,DGP,
      1DFZ,DGZ,DFY,DGY,IT)
      PARAMETER C=.45,R=8314.41
      IMPLICIT REAL*8 (A-H,M,P-Z)
      REAL*8 XR1(NK1),PAR1(LL1),YR1(NN1),DFX(NN1,NK1),DFP(NN1,LL1)
      1,ZR1(NN1),DGX(NN1,NK1),DGP(NN1,LL1),DFY(NN1,NN1),DGY(NN1,NN1),
      1DGZ(NN1,NN1),DFZ(NN1,NN1),FR(NN1),GR(NN1)



      DO 30 I=1,NN1

C     CALCULATE THE REDUCED TEMPERATURES

      XRT=XR1(2*I-1)
      XRX=XR1(2*I)
      XR2=1-XRX
      ZRZ=ZR1(I)
      ZR2=1-ZRZ
      TR1=XRT/TC1
      TR2=XRT/TC2

      IF(IT.EQ.1)THEN

      CALL INITGUESS(XRT,XR2,XRX,ZRZ,ZR2,PAR1,YR1(I),TC1,TC2,PC1,
      1PC2,ACCN1,ACCN2,RP1,RP2)
      XR1(2*I)=XRX
      ZR1(I)=ZRZ


      ELSE
      CONTINUE
      ENDIF


C     CALCULATE THE FUNCTIONS F AND G
```

```
      CALL FUGC(XRT,XR2,XRX,ZRZ,ZR2,PAR1(1),YR1(I),TC1,TC2,
     1PC1,PC2,ACCN1,ACCN2,RP1,RP2,
     1FUGV1I,FUGV2I,FUGL1I,FUGL2I,PAR1(2),PAR1(3))

      FR(I)=XRX*FUGL1I-ZRZ*FUGV1I
      GR(I)=XR2*FUGL2I-ZR2*FUGV2I
      TYPE*,'FR(I),GR(I)',FR(I),GR(I)

C     CALCULATE THE DERIVATIVES WRT PARAMETERS (CURRENTLY SET FOR 1
C     PARAMETER)

      DO 44 J=1,LL1

      IF(J.EQ.1)THEN

      DPAR=PAR1(1)*.998

      CALL FUGC(XRT,XR2,XRX,ZRZ,ZR2,DPAR,YR1(I),TC1,TC2,PC1,PC2,ACCN1
     1,ACCN2,RP1,RP2,FUGV1,FUGV2,FUGL1,FUGL2,PAR1(2),PAR1(3))

      F2N=XRX*FUGL1-FUGV1*ZRZ
      G2N=XR2*FUGL2-FUGV2*ZR2

      DPAR=PAR1(1)*.999

      CALL FUGC(XRT,XR2,XRX,ZRZ,ZR2,DPAR,YR1(I),TC1,TC2,PC1,PC2,ACCN1
     1,ACCN2,RP1,RP2,FUGV1,FUGV2,FUGL1,FUGL2,PAR1(2),PAR1(3))

      F1N=XRX*FUGL1-FUGV1*ZRZ
      G1N=XR2*FUGL2-FUGV2*ZR2

      DPAR=PAR1(1)*1.001

      CALL FUGC(XRT,XR2,XRX,ZRZ,ZR2,DPAR,YR1(I),TC1,TC2,PC1,PC2,ACCN1
     1,ACCN2,RP1,RP2,FUGV1,FUGV2,FUGL1,FUGL2,PAR1(2),PAR1(3))

      F1=XRX*FUGL1-FUGV1*ZRZ
      G1=XR2*FUGL2-FUGV2*ZR2

      DPAR=PAR1(1)*1.002

      CALL FUGC(XRT,XR2,XRX,ZRZ,ZR2,DPAR,YR1(I),TC1,TC2,PC1,PC2,ACCN1
     1,ACCN2,RP1,RP2,FUGV1,FUGV2,FUGL1,FUGL2,PAR1(2),PAR1(3))

      F2=XRX*FUGL1-FUGV1*ZRZ
      G2=XR2*FUGL2-FUGV2*ZR2
```

```
      DFP(I,J)=(2*F2N -16*F1N + 16*F1 - 2*F2)/(24*PAR1(1)*.001)
      DGP(I,J)=(2*G2N - 16*G1N + 16*G1 - 2*G2)/(24*PAR1(1)*.001)

      ELSE

C     DERIVATIVE WRT TO SECOND PARAMETER

      IF(J.EQ.2)THEN

      DPAR=PAR1(2)*.998

      CALL FUGC(XRT,XR2,XRX,ZRZ,ZR2,PAR1(1),YR1(I),TC1,TC2,PC1,PC2,ACCN1
     1,ACCN2,RP1,RP2,FUGV1,FUGV2,FUGL1,FUGL2,DPAR,PAR1(3))

      F2N=XRX*FUGL1-FUGV1*ZRZ
      G2N=XR2*FUGL2-FUGV2*ZR2

      DPAR=PAR1(2)*.999

      CALL FUGC(XRT,XR2,XRX,ZRZ,ZR2,PAR1(1),YR1(I),TC1,TC2,PC1,PC2,ACCN1
     1,ACCN2,RP1,RP2,FUGV1,FUGV2,FUGL1,FUGL2,DPAR,PAR1(3))

      F1N=XRX*FUGL1-FUGV1*ZRZ
      G1N=XR2*FUGL2-FUGV2*ZR2

      DPAR=PAR1(2)*1.001

      CALL FUGC(XRT,XR2,XRX,ZRZ,ZR2,PAR1(1),YR1(I),TC1,TC2,PC1,PC2,ACCN1
     1,ACCN2,RP1,RP2,FUGV1,FUGV2,FUGL1,FUGL2,DPAR,PAR1(3))

      F1=XRX*FUGL1-FUGV1*ZRZ
      G1=XR2*FUGL2-FUGV2*ZR2

      DPAR=PAR1(2)*1.002

      CALL FUGC(XRT,XR2,XRX,ZRZ,ZR2,PAR1(1),YR1(I),TC1,TC2,PC1,PC2,ACCN1
     1,ACCN2,RP1,RP2,FUGV1,FUGV2,FUGL1,FUGL2,DPAR,PAR1(3))

      F2=XRX*FUGL1-FUGV1*ZRZ
      G2=XR2*FUGL2-FUGV2*ZR2


      DFP(I,J)=(2*F2N -16*F1N + 16*F1 - 2*F2)/(24*PAR1(2)*.001)
      DGP(I,J)=(2*G2N - 16*G1N + 16*G1 - 2*G2)/(24*PAR1(2)*.001)

      ELSE

C     DERIVATIVE WRT TO THIRD PARAMETER
```

```
          DPAR=PAR1(3)*.998

          CALL FUGC(XRT,XR2,XRX,ZRZ,ZR2,PAR1(1),YR1(I),TC1,TC2,PC1,PC2,ACCN1
          1,ACCN2,RP1,RP2,FUGV1,FUGV2,FUGL1,FUGL2,PAR1(2),DPAR)

          F2N=XRX*FUGL1-FUGV1*ZRZ
          G2N=XR2*FUGL2-FUGV2*ZR2

          DPAR=PAR1(3)*.999

          CALL FUGC(XRT,XR2,XRX,ZRZ,ZR2,PAR1(1),YR1(I),TC1,TC2,PC1,PC2,ACCN1
          1,ACCN2,RP1,RP2,FUGV1,FUGV2,FUGL1,FUGL2,PAR1(2),DPAR)

          F1N=XRX*FUGL1-FUGV1*ZRZ
          G1N=XR2*FUGL2-FUGV2*ZR2

          DPAR=PAR1(3)*1.001

          CALL FUGC(XRT,XR2,XRX,ZRZ,ZR2,PAR1(1),YR1(I),TC1,TC2,PC1,PC2,ACCN1
          1,ACCN2,RP1,RP2,FUGV1,FUGV2,FUGL1,FUGL2,PAR1(2),DPAR)

          F1=XRX*FUGL1-FUGV1*ZRZ
          G1=XR2*FUGL2-FUGV2*ZR2

          DPAR=PAR1(3)*1.002

          CALL FUGC(XRT,XR2,XRX,ZRZ,ZR2,PAR1(1),YR1(I),TC1,TC2,PC1,PC2,ACCN1
          1,ACCN2,RP1,RP2,FUGV1,FUGV2,FUGL1,FUGL2,PAR1(2),DPAR)

          F2=XRX*FUGL1-FUGV1*ZRZ
          G2=XR2*FUGL2-FUGV2*ZR2


          DFP(I,J)=(2*F2N -16*F1N + 16*F1 - 2*F2)/(24*PAR1(3)*.001)
          DGP(I,J)=(2*G2N - 16*G1N + 16*G1 - 2*G2)/(24*PAR1(3)*.001)

          ENDIF
          ENDIF

44        CONTINUE

C         INPUT THE DERIVATIVE OF THE FUNCTION WRT TO THE INDEPENDENT
C         VARIABLES HERE.
C         PUT INTO AN NN BY NK MATRIX WITH THE ELEMENTS ON THE DIAGONAL
          DO 38 J=1,NK1
                  DFX(I,J)=0
```

```
            DGX(I,J)=0
38      CONTINUE

        DO 40 J=1,NK1

        IF (J.EQ.(2*I-1)) THEN

C       CALCULATE THE DERIVATIVE OF THE FUGACITY COEFFICIENT WRT TEMP

        DXRT=XRT-.02

        CALL FUGC(DXRT,XR2,XRX,ZRZ,ZR2,PAR1(1),YR1(I),TC1,TC2,
        1PC1,PC2,ACCN1,ACCN2,RP1,RP2,FUGV1,FUGV2,FUGL1,FUGL2,
        1PAR1(2),PAR1(3))

        FT2N=XRX*FUGL1-FUGV1*ZRZ
        GT2N=XR2*FUGL2-FUGV2*ZR2


        DXRT=XRT-.01

        CALL FUGC(DXRT,XR2,XRX,ZRZ,ZR2,PAR1(1),YR1(I),TC1,TC2,
        1PC1,PC2,ACCN1,ACCN2,RP1,RP2,FUGV1,FUGV2,FUGL1,FUGL2,
        1PAR1(2),PAR1(3))

        FT1N=XRX*FUGL1-FUGV1*ZRZ
        GT1N=XR2*FUGL2-FUGV2*ZR2

        DXRT=XRT+.01

        CALL FUGC(DXRT,XR2,XRX,ZRZ,ZR2,PAR1(1),YR1(I),TC1,TC2,
        1PC1,PC2,ACCN1,ACCN2,RP1,RP2,FUGV1,FUGV2,FUGL1,FUGL2,
        1PAR1(2),PAR1(3))

        FT1=XRX*FUGL1-FUGV1*ZRZ
        GT1=XR2*FUGL2-FUGV2*ZR2


        DXRT=XRT+.02

        CALL FUGC(DXRT,XR2,XRX,ZRZ,ZR2,PAR1(1),YR1(I),TC1,TC2,
        1PC1,PC2,ACCN1,ACCN2,RP1,RP2,FUGV1,FUGV2,FUGL1,FUGL2,
        1PAR1(2),PAR1(3))

        FT2=XRX*FUGL1-FUGV1*ZRZ
        GT2=XR2*FUGL2-FUGV2*ZR2

        DFX(I,J)=(2*FT2N - 16*FT1N + 16*FT1 - 2*FT2)/(24*.01)
```

```
DGX(I,J)=(2*GT2N - 16*GT1N + 16*GT1 - 2*GT2)/(24*.01)

IF(XRX.LT..9998)THEN

DXRX=XRX*.998
DXR2=1-DXRX

CALL FUGC(XRT,DXR2,DXRX,ZRZ,ZR2,PAR1(1),YR1(I),TC1,TC2,
1PC1,PC2,ACCN1,ACCN2,RP1,RP2,FUGV1,FUGV2,FUGL1,FUGL2,
1PAR1(2),PAR1(3))

FX2N=DXRX*FUGL1-FUGV1*ZRZ
GX2N=DXR2*FUGL2-FUGV2*ZR2


DXRX=XRX*.999
DXR2=1-DXRX

CALL FUGC(XRT,DXR2,DXRX,ZRZ,ZR2,PAR1(1),YR1(I),TC1,TC2,
1PC1,PC2,ACCN1,ACCN2,RP1,RP2,FUGV1,FUGV2,FUGL1,FUGL2,
1PAR1(2),PAR1(3))

FX1N=DXRX*FUGL1-FUGV1*ZRZ
GX1N=DXR2*FUGL2-FUGV2*ZR2

DXRX=XRX*1.001
DXR2=1-DXRX

CALL FUGC(XRT,DXR2,DXRX,ZRZ,ZR2,PAR1(1),YR1(I),TC1,TC2,
1PC1,PC2,ACCN1,ACCN2,RP1,RP2,FUGV1,FUGV2,FUGL1,FUGL2,
1PAR1(2),PAR1(3))

FX1=DXRX*FUGL1-FUGV1*ZRZ
GX1=DXR2*FUGL2-FUGV2*ZR2

DXRX=XRX*1.002
DXR2=1-DXRX

CALL FUGC(XRT,DXR2,DXRX,ZRZ,ZR2,PAR1(1),YR1(I),TC1,TC2,
1PC1,PC2,ACCN1,ACCN2,RP1,RP2,FUGV1,FUGV2,FUGL1,FUGL2,
1PAR1(2),PAR1(3))

FX2=DXRX*FUGL1-FUGV1*ZRZ
GX2=DXR2*FUGL2-FUGV2*ZR2

DFX(I,J+1)=(2*FX2N - 16*FX1N + 16*FX1 - 2*FX2)/(24*XRX*.001)
DGX(I,J+1)=(2*GX2N - 16*GX1N + 16*GX1 - 2*GX2)/(24*XRX*.001)
```

```
ELSE

DXRX=XRX*.9998
DXR2=1-DXRX

CALL FUGC(XRT,DXR2,DXRX,ZRZ,ZR2,PAR1(1),YR1(I),TC1,TC2,
1PC1,PC2,ACCN1,ACCN2,RP1,RP2,FUGV1,FUGV2,FUGL1,FUGL2,
1PAR1(2),PAR1(3))

FX2N=DXRX*FUGL1-FUGV1*ZRZ
GX2N=DXR2*FUGL2-FUGV2*ZR2


DXRX=XRX*.9999
DXR2=I-DXRX

CALL FUGC(XRT,DXR2,DXRX,ZRZ,ZR2,PAR1(1),YR1(I),TC1,TC2,
1PC1,PC2,ACCN1,ACCN2,RP1,RP2,FUGV1,FUGV2,FUGL1,FUGL2,
1PAR1(2),PAR1(3))

FX1N=DXRX*FUGL1-FUGV1*ZRZ
GX1N=DXR2*FUGL2-FUGV2*ZR2

DXRX=XRX*1.0001
DXR2=1-DXRX

CALL FUGC(XRT,DXR2,DXRX,ZRZ,ZR2,PAR1(1),YR1(I),TC1,TC2,
1PC1,PC2,ACCN1,ACCN2,RP1,RP2,FUGV1,FUGV2,FUGL1,FUGL2,
1PAR1(2),PAR1(3))

FX1=DXRX*FUGL1-FUGV1*ZRZ
GX1=DXR2*FUGL2-FUGV2*ZR2

DXRX=XRX*1.0002
DXR2=1-DXRX

CALL FUGC(XRT,DXR2,DXRX,ZRZ,ZR2,PAR1(1),YR1(I),TC1,TC2,
1PC1,PC2,ACCN1,ACCN2,RP1,RP2,FUGV1,FUGV2,FUGL1,FUGL2,
1PAR1(2),PAR1(3))

FX2=DXRX*FUGL1-FUGV1*ZRZ
GX2=DXR2*FUGL2-FUGV2*ZR2

DFX(I,J+1)=(2*FX2N - 16*FX1N + 16*FX1 - 2*FX2)/(24*XRX*.0001)
DGX(I,J+1)=(2*GX2N - 16*GX1N + 16*GX1 - 2*GX2)/(24*XRX*.0001)
```

```
      ENDIF
      ELSE

      CONTINUE
      ENDIF

40    CONTINUE

C     DERIVATIVES WRT PRESSURE

      DO 41 J=1,NN1

      IF(J.EQ.I)THEN

      P=YR1(I)*.998

      CALL FUGC(XRT,XR2,XRX,ZRZ,ZR2,PAR1(1),P,TC1,TC2,PC1,PC2,ACCN1
     1,ACCN2,RP1,RP2,FUGV1,FUGV2,FUGL1,FUGL2,PAR1(2),PAR1(3))

      FP2N=XRX*FUGL1-FUGV1*ZRZ
      GP2N=XR2*FUGL2-FUGV2*ZR2

      P=YR1(I)*.999

      CALL FUGC(XRT,XR2,XRX,ZRZ,ZR2,PAR1(1),P,TC1,TC2,PC1,PC2,ACCN1
     1,ACCN2,RP1,RP2,FUGV1,FUGV2,FUGL1,FUGL2,PAR1(2),PAR1(3))

      FP1N=XRX*FUGL1-FUGV1*ZRZ
      GP1N=XR2*FUGL2-FUGV2*ZR2

      P=YR1(I)*1.001

      CALL FUGC(XRT,XR2,XRX,ZRZ,ZR2,PAR1(1),P,TC1,TC2,PC1,PC2,ACCN1
     1,ACCN2,RP1,RP2,FUGV1,FUGV2,FUGL1,FUGL2,PAR1(2),PAR1(3))

      FP1=XRX*FUGL1-FUGV1*ZRZ
      GP1=XR2*FUGL2-FUGV2*ZR2

      P=YR1(I)*1.002

      CALL FUGC(XRT,XR2,XRX,ZRZ,ZR2,PAR1(1),P,TC1,TC2,PC1,PC2,ACCN1
     1,ACCN2,RP1,RP2,FUGV1,FUGV2,FUGL1,FUGL2,PAR1(2),PAR1(3))

      FP2=XRX*FUGL1-FUGV1*ZRZ
      GP2=XR2*FUGL2-FUGV2*ZR2

      DFY(I,J)=(2*FP2N - 16*FP1N + 16*FP1 - 2*FP2)/(24*YR1(I)*.001)
      DGY(I,J)=(2*GP2N - 16*GP1N + 16*GP1 - 2*GP2)/(24*YR1(I)*.001)
```

```
C       DERIVATIVE WRT TO VAPOR COMPOSITION

        IF(ZRZ.LT..9998)THEN

        Z=ZRZ*.998
        Z2=1-Z

        CALL FUGC(XRT,XR2,XRX,Z,Z2,PAR1(1),YR1(I),TC1,TC2,
        1PC1,PC2,ACCN1,ACCN2,RP1,RP2,FUGV1,FUGV2,FUGL1,FUGL2,
        1PAR1(2),PAR1(3))

        FZ2N=XRX*FUGL1-FUGV1*Z
        GZ2N=XR2*FUGL2-FUGV2*Z2

        Z=ZRZ*.999
        Z2=1-Z

        CALL FUGC(XRT,XR2,XRX,Z,Z2,PAR1(1),YR1(I),TC1,TC2,
        1PC1,PC2,ACCN1,ACCN2,RP1,RP2,FUGV1,FUGV2,FUGL1,FUGL2
        1,PAR1(2),PAR1(3))

        FZ1N=XRX*FUGL1-FUGV1*Z
        GZ1N=XR2*FUGL2-FUGV2*Z2

        Z=ZRZ*1.001
        Z2=1-Z

        CALL FUGC(XRT,XR2,XRX,Z,Z2,PAR1(1),YR1(I),TC1,TC2,
        1PC1,PC2,ACCN1,ACCN2,RP1,RP2,FUGV1,FUGV2,FUGL1,FUGL2
        1,PAR1(2),PAR1(3))

        FZ1=XRX*FUGL1-FUGV1*Z
        GZ1=XR2*FUGL2-FUGV2*Z2

        Z=ZRZ*1.002
        Z2=1-Z

        CALL FUGC(XRT,XR2,XRX,Z,Z2,PAR1(1),YR1(I),TC1,TC2,
        1PC1,PC2,ACCN1,ACCN2,RP1,RP2,FUGV1,FUGV2,FUGL1,FUGL2
        1,PAR1(2),PAR1(3))

        FZ2=XRX*FUGL1-FUGV1*Z
        GZ2=XR2*FUGL2-FUGV2*Z2


        DFZ(I,J)=(2*FZ2N - 16*FZ1N + 16*FZ1 - 2*FZ2)/(24*ZRZ*.001)
        DGZ(I,J)=(2*GZ2N - 16*GZ1N + 16* GZ1 - 2*GZ2)/(24*ZRZ*.001)
```

```
ELSE

Z=ZRZ*.9998
Z2=1-Z

CALL FUGC(XRT,XR2,XRX,Z,Z2,PAR1(1),YR1(I),TC1,TC2,
1PC1,PC2,ACCN1,ACCN2,RP1,RP2,FUGV1,FUGV2,FUGL1,FUGL2
1,PAR1(2),PAR1(3))

FZ2N=XRX*FUGL1-FUGV1*Z
GZ2N=XR2*FUGL2-FUGV2*Z2

Z=ZRZ*.9999
Z2=1-Z

CALL FUGC(XRT,XR2,XRX,Z,Z2,PAR1(1),YR1(I),TC1,TC2,
1PC1,PC2,ACCN1,ACCN2,RP1,RP2,FUGV1,FUGV2,FUGL1,FUGL2
1,PAR1(2),PAR1(3))

FZ1N=XRX*FUGL1-FUGV1*Z
GZ1N=XR2*FUGL2-FUGV2*Z2

Z=ZRZ*1.0001
Z2=1-Z

CALL FUGC(XRT,XR2,XRX,Z,Z2,PAR1(1),YR1(I),TC1,TC2,
1PC1,PC2,ACCN1,ACCN2,RP1,RP2,FUGV1,FUGV2,FUGL1,FUGL2,
1PAR1(2),PAR1(3))

FZ1=XRX*FUGL1-FUGV1*Z
GZ1=XR2*FUGL2-FUGV2*Z2

Z=ZRZ*1.0002
Z2=1-Z

CALL FUGC(XRT,XR2,XRX,Z,Z2,PAR1(1),YR1(I),TC1,TC2,
1PC1,PC2,ACCN1,ACCN2,RP1,RP2,FUGV1,FUGV2,FUGL1,FUGL2,
1PAR1(2),PAR1(3))

FZ2=XRX*FUGL1-FUGV1*Z
GZ2=XR2*FUGL2-FUGV2*Z2


DFZ(I,J)=(2*FZ2N - 16*FZ1N + 16*FZ1 - 2*FZ2)/(24*ZRZ*.0001)
DGZ(I,J)=(2*GZ2N - 16*GZ1N + 16*GZ1 - 2*GZ2)/(24*ZRZ*.0001)

ENDIF
```

```
      ELSE
      DFZ(I,J)=0
      DGZ(I,J)=0
      DFY(I,J)=0
      DGY(I,J)=0
      ENDIF
41    CONTINUE


30    CONTINUE

      RETURN
      END


      SUBROUTINE FUGC(T,X2,X,Y,Y2,GAMMA,P,TC1,TC2,PC1,PC2,ACCN1,
     1ACCN2,RP1,RP2,FUGV1,FUGV2,FUGL1,FUGL2,C12,C21)
      PARAMETER CC=.45,R=8314.41
      IMPLICIT REAL*8 (A-H,M,P-Z)

C     THIS SUBROUTINE CALCULATES THE FUGACITIES IN THE LIQUID AND
C     VAPOR PHASES
C
C     CALCULATE SRK SMALL  B (SMB) AND A(TC) (ATC)
C     R IS THE GAS CONSTANT AND TC AND PC ARE THE CRITICAL PROPERTIES
C     ACCN IS THE ACENTRIC FACTOR FOR THE NONPOLAR COMPOUND

      SMB1=0.08664*R*TC1/PC1
      SMB2=0.08664*R*TC2/PC2
      ATC1=0.42747*R**2.*(TC1**2.)/PC1
      ATC2=0.42747*R**2.*(TC2**2.)/PC2
      TR1=T/TC1
      TR2=T/TC2
      M1=0.48 + 1.574*ACCN1 - 0.176*(ACCN1**2.)
      M2=0.48 + 1.574*ACCN2 - 0.176*(ACCN2**2.)

      ALPHAN1=(1.+M1*(1.-TR1**.5))**2
      ALPHAN2=(1.+M2*(1.-TR2**.5))**2

C     CALCULATE THE PARAMETER PART OF SMALL A
```

```
      PARA1=1.+RP1*EXP(-RP1**CC) - RP1*EXP(-(RP1*TC1
     1/T)**CC)
      PARA2=1.+RP2*EXP(-RP2**CC) - RP2*EXP(-(RP2*TC2
     1/T)**CC)

      SMA1=ATC1*ALPHAN1*PARA1
      SMA2=ATC2*ALPHAN2*PARA2


C     CALCULATE THE FUGACITY COEFFICIENT IN THE LIQUID PHASE (FUGL)

      SMAM=X**2*SMA1 + X2**2*SMA2 + 2*X*X2*(SMA1*SMA2)**.5*
     1(1-GAMMA)
      SMBM=SMB1*X +SMB2*X2
      SMCM=2*X*X2*(X*C12*ATC1**2 + X2*C21*ATC2**2)/(R*T)

C     CALCULATE CAPITAL A AND B AND C

      A=SMAM*P/(R**2*T**2)

      B=SMBM*P/(R*T)

      C=SMCM*P**2/(R*T)**3

C     CALCULATE COEFFICIENTS FOR QUARTIC SOLVER

      D=-1
      E=(A-B-B**2)
      F=-(A*B-C)
      G=-B*C

C     CALL QUARTIC SOLVER

      CALL VQUARTIC(B,D,E,F,G,ZL,1)


C     CALCULATE THE LIQUID PHASE FUGACITY COEFFICIENT (FUGL)

      FUGL1=DEXP( SMB1*P/(R*T*(ZL-B)) - SMB1*A/(SMBM*(ZL+B))
     1 - (C/X + 2*X*X2*C12*ATC1**2*P**2/(R*T)**4)/(ZL*B)
     1  + SMB1*C*(B+2*ZL)/(SMBM*B*ZL*(ZL+B))
     1 -DLOG(ZL-B)
     1 + DLOG(1+B/ZL)*(-(2*X*SMA1 + 2*X2*(SMA1*SMA2)**.5*(1-GAMMA))
     1/(SMBM*R*T) + (SMB1/SMBM)*(A/B - 2*C/B**2) + (C/(B**2*X)+
     1 2*X*X2*C12*ATC1**2/(SMBM**2*R**2*T**2))))
```

```
      FUGL2=DEXP(SMB2*P/(R*T*(ZL-B)) - SMB2*A/(SMBM*(ZL+B))
      1 - (C/X2 + 2*X*X2*C21*ATC2**2*P**2/(R*T)**4)/(ZL*B)
      1  + SMB2*C*(B+2*ZL)/(SMBM*B*ZL*(ZL+B))
      1 -DLOG(ZL-B)
      1 + DLOG(1+B/ZL)*(-(2*X2*SMA2 + 2*X*(SMA1*SMA2)**.5*(1-GAMMA))
      1/(SMBM*R*T) + (SMB2/SMBM)*(A/B - 2*C/B**2) + (C/(B**2*X2) +
      1 2*X*X2*C21*ATC2**2/(SMBM**2*R**2*T**2))))

C     FOR THE VAPOR PHASE

      SMAM=Y**2*SMA1 + Y2**2*SMA2 + 2*Y*Y2*(SMA1*SMA2)**.5*
      1(1-GAMMA)
      SMBM=SMB1*Y +SMB2*Y2
      SMCM=2*Y*Y2*(Y*C12*ATC1**2 + Y2*C21*ATC2**2)/(R*T)

C     CALCULATE CAPITAL A AND B

      A=SMAM*P/(R**2*T**2)

      B=SMBM*P/(R*T)

      C=SMCM*P**2/(R*T)**3

C     CALCULATE COEFFICIENTS FOR QUARTIC SOLVER

      D=-1
      E=(A-B-B**2)
      F=-(A*B -C)
      G=-B*C

      CALL VQUARTIC(B,D,E,F,G,ZV,-1)

C     NOW CALCULATE FUGACITY COEFFICIENT IN THE VAPOR PHASE (FUGV)

      FUGV1=DEXP(SMB1*P/(R*T*(ZV-B)) - SMB1*A/(SMBM*(ZV+B))
      1 - (C/Y + 2*Y*Y2*C12*ATC1**2*P**2/(R*T)**4)/(ZV*B)
      1  + SMB1*C*(B+2*ZV)/(SMBM*B*ZV*(ZV+B))
```

```
     1 -DLOG(ZV-B)
     1 + DLOG(1+B/ZV)*(-(2*Y*SMA1 + 2*Y2*(SMA1*SMA2)**.5*(1-GAMMA))
     1/(SMBM*R*T) + (SMB1/SMBM)*(A/B - 2*C/B**2) +
     1 C/(B**2*Y) +2*Y*Y2*C12*ATC1**2/(SMBM**2*(R*T)**2)))

      FUGV2=DEXP(SMB2*P/(R*T*(ZV-B)) - SMB2*A/(SMBM*(ZV+B))
     1 - (C/Y2 + 2*Y*Y2*C21*ATC2**2*P**2/(R*T)**4)/(ZV*B)
     1 + SMB2*C*(B+2*ZV)/(SMBM*B*ZV*(ZV+B))
     1 -DLOG(ZV-B)
     1 + DLOG(1+B/ZV)*(-(2*Y2*SMA2 + 2*Y*(SMA1*SMA2)**.5*(1-GAMMA))
     1/(SMBM*R*T) + (SMB2/SMBM)*(A/B - 2*C/B**2) +
     1 C/(B**2*Y2) + 2*Y*Y2*C21*ATC2**2/(SMBM**2*(R*T)**2)))




      RETURN
      END
C
C     QUARTIC SOLVER
C
      SUBROUTINE VQUARTIC(B,D,E,F,G,ZZ,ID)
      IMPLICIT REAL*8 (A-H,P-Z)
      REAL*8 Z(4)

C     CALL CUBIC SOLVER TO SOLVE THE RESOLVENT CUBIC EQUATION
C     Z**3 - E*Z**2 +(D*F - 4*G)*Z - D**2*G + 4*E*G - F**2=0

      DD=-E
      EE=(D*F - 4*G)
      FF=-D**2*G + 4*E*G - F**2

C     GET ANY REAL ROOT TO THE CUBIC EQUATION

      CALL VCUB(DD,EE,FF,V,-1)

C     CALCULATE R

      R=(D**2/4 - E + V)

      IF(ABS(R).LT..00000000001)THEN

      R=R**.5
```

```
P=(3*D**2/4 - 2*E + 2*(V**2 - 4*G)**.5)

Q=(3*D**2/4 - 2*E - 2*(V**2 - 4*G)**.5)

IF(P.GT.0)THEN

        P=P**.5
        Z(1)=-D/4 + R/2 +P/2
        Z(2)=-D/4 + R/2 -P/2

ELSE

        Z(1)=-1
        Z(2)=-1

ENDIF

IF(Q.GT.0)THEN

        Q=Q**.5
        Z(3)=-D/4 - R/2 +Q/2
        Z(4)=-D/4 - R/2 - Q/2

ELSE

        Z(3)=-1
        Z(4)=-1
ENDIF

ELSE

R=R**.5

P=(3*D**2/4 - R**2 - 2*E + (4*D*E - 8*F - D**3)/(R*4))

Q=(3*D**2/4 - R**2 - 2*E - (4*D*E - 8*F - D**3)/(R*4))

IF(P.GT.0)THEN

        P=P**.5
        Z(1)=-D/4 + R/2 +P/2
        Z(2)=-D/4 + R/2 -P/2

ELSE

        Z(1)=-1
        Z(2)=-1
```

```
      ENDIF

      IF(Q.GT.O)THEN

              Q=Q**.5
              Z(3)=-D/4 - R/2 +Q/2
              Z(4)=-D/4 - R/2 - Q/2

      ELSE

              Z(3)=-1
              Z(4)=-1
      ENDIF


      ENDIF

      DO I=1,4
      IF(ID.EQ.1.AND.Z(I).LT.B)Z(I)=99999999
      ENDDO

      IF(ID.EQ.1)THEN
      ZZ=DMIN1(Z(1),Z(2),Z(3),Z(4))
      ELSE
      ZZ=DMAX1(Z(1),Z(2),Z(3),Z(4))
      ENDIF

      RETURN
      END


      SUBROUTINE VCUB(D,E,F,Z,ID)
C     SUBPROGRAM FOR SOLVING A CUBIC EQUATION OF THE FORM:
C     Z**3 +D*Z**2+ E*Z + F=0.0
C     WHERE D,E, AND F ARE CONSTANTS
      IMPLICIT REAL*8(A-H,P-Z)
      G=(3.*E-D*D)/3.
      H=-(9.*D*E-27.*F-2*D*D*D)/27.

      IF((G**3)/27. +H*H/4..LE.0.)GO TO 10
      S=-H/2. + DSQRT(G**3/27. + H*H/4.)
      TT=-H/2. - DSQRT(G**3/27. + H*H/4.)
      IF(S)5,6,6
5     S=-((-S)**(1./3.))
      GO TO 7
6     S=S**(1./3.)
7     IF(TT)8,9,9
```

```
8       TT=-(-TT)**(1./3.)
        GO TO 15
9       TT=(TT)**(1./3.)
C       SINGLE REAL ROOT
15      Z=S+TT-D/3.
        GO TO 40
C       THERE ARE THREE ROOTS.
10      THETA=(DACOS(-.5*H/DSQRT(-G**3/27.)))/3.
        Z1=2.*DSQRT(-G/3.)*DCOS(THETA)
        Z2=2.*DSQRT(-G/3.)*DCOS(THETA+(2./3.)*3.141592654)
        Z3=2.*DSQRT(-G/3.)*DCOS(THETA+ (4./3.)*3.141592654)
C       DECIDING WHICH TO CHOOSE
        IF(ID)20,30,30
C       TAKE LARGEST ROOT FOR VAPOR VOLUME.
20      Z=DMAX1(Z1,Z2,Z3)-D/3.
        GO TO 40
C       TAKE SMALLEST ROOT FOR LIQUID VOLUME.
30      Z=DMIN1(Z1,Z2,Z3)-D/3.
        IF(Z.LT.0)Z=.000001
        DO 31 I=1,20
        ZN=Z-(Z**3+D*Z**2+E*Z+F)/(3.*Z**2+2.*Z*D+E)
        IF(ABS((ZN-Z)/Z).LT..00001)GO TO 40
31      Z=ZN
40      RETURN
        END


        SUBROUTINE INITGUESS(XRT,XR2,XRX,ZRZ,ZR2,PAR,POLD,TC1,TC2,PC1,
        1PC2,ACCN1,ACCN2,RP1,RP2)
        PARAMETER C=.45,R=8314.41
        IMPLICIT REAL*8 (A-H,M,P-Z)
        REAL*8 PAR(3)



29      IT=IT+1

        ZR2=1-ZRZ


        CALL FUGC(XRT,XR2,XRX,ZRZ,ZR2,PAR(1),POLD,TC1,TC2,
        1PC1,PC2,ACCN1,ACCN2,RP1,RP2,FUGV1,FUGV2,FUGL1,FUGL2,
        1PAR(2),PAR(3))
        FR=XRX*FUGL1 - ZRZ*FUGV1
        GR=XR2*FUGL2 - ZR2*FUGV2

        IF(ZRZ.GT..98)THEN
```

```
      ZRZN=1-(FUGL2*XR2/FUGV2)
      PNEW=((POLD*FUGL1*XRX)/(FUGV1*ZRZN))*.05 + .95*POLD
      ELSE
      ZRZN=FUGL1*XRX/FUGV1
      PNEW=(POLD*FUGL2*XR2/(FUGV2*(1-ZRZN)))*.05 + .95*POLD
      ENDIF

      IF(ZRZN.GT.1)THEN
      ZRZN=1.0
      GO TO 1001
      ENDIF

      IF((ABS(FR).LT..00001.AND.ABS(GR).LT..00001).AND.(PNEW-POLD.LT.
     1 .001))THEN
      TYPE*,'FR,GR',FR,GR
1001  POLD=PNEW
      ZRZ=ZRZN
      TYPE*,'PNEW',PNEW,'ZRZN',ZRZN
      GO TO 1000
      ELSE

      POLD=PNEW
      ZRZ=ZRZN
      IF(IT.EQ.200)THEN
      TYPE*,'ITERATIONS GREATER THAN 200 FOR P,Y1',PNEW,ZRZ
      GO TO 1000
      ELSE
      GO TO 29
      ENDIF
      ENDIF

1000  RETURN
      END
```

```
C       THIS PROGRAM CALCULATES BINARY PHASE BEHAVIOR BY HOLDING TEMPE-
        RATURE AND LIQUID COMPOSITIONS CONSTANT AND CALCULATING PRESSURE
        AND VAPOR COMPOSITIONS
C**********************************************************************
        PARAMETER NN =69, KK = 2, LL = 3, NK =138
        IMPLICIT REAL*8 (A-H,P-Z)
        CHARACTER*20 FILN1,FILN2,FILN3,FILN4,FILN5,FILN6,FILN7,FILN8,
        1FILN9,FILN10,FILN11

        REAL*8 YM(NN),XM(NK),XR(NK),YR(NN),ZM(NN),ZR(NN),DIFFP(NN),
        1DIFFY(NN)
C
        TYPE*,'***********CAUTION*********** THIS PROGRAM CALCULATES
        1 VLE FOR DENSITY DEPENDENT MIXING RULES ONLY IN THE FORM
        1 DESCRIBED BY LUEDECKE AND PRAUSNITZ
        1'


        TYPE*,'ENTER THE FILENAME CONTAINING THE PRESSURE IN KPA'
        READ(5,1)FILN1
1       FORMAT(A20)
        TYPE*,'ENTER THE FILENAME CONTAINING THE VAPOR COMPOSITION'
        READ(5,1)FILN9
        TYPE*,'ENTER THE FILENAME CONTAINING THE TEMPERATURE AND
        1 LIQUID COMPOSITION ALTERNATING'
        READ(5,1)FILN2

        TYPE*,'ENTER THE CRITICAL TEMPERATURE, CRITICAL PRESSURE,
        1 ACENTRIC FACTOR, AND POLAR PARAMETER FOR COMPONENT 1 IN
        1 THE UNITS  K AND KPA'
        ACCEPT*,TC1,PC1,ACCN1,RP1
        TYPE*,TC1,PC1,ACCN1,RP1

        TYPE*,'ENTER THE CRITICAL TEMPERATURE,CRITICAL PRESSURE,
        1 ACENTRIC FACTOR, AND POLAR PARAMETER FOR COMPONENT 2 IN
        1 THE UNITS K AND KPA'
        ACCEPT*,TC2,PC2,ACCN2,RP2
        TYPE*,TC2,PC2,ACCN2,RP2

        TYPE*,'ENTER THE INTERACTION PARAMETERS GAMMA,C12,C21'

        ACCEPT*,GAMMA,C12,C21
        TYPE*,GAMMA,C12,C21

        OPEN(UNIT=10,FILE=FILN1,STATUS='OLD')
        OPEN(UNIT=20,FILE=FILN2,STATUS='OLD')
        OPEN(UNIT=90,FILE=FILN9,STATUS='OLD')
```

```
C
C       READ IN DEPENDENT VARIABLES Y AND Z
C
        READ(10,*,END=99) (YM(I),I=1,NN)
99      READ(90,*,END=101) (ZM(I),I=1,NN)

C       READ IN INDEPENDENT VARIABLES

101     READ(20,*,END=102) (XM(I),I=1,NK)

C       SET INITIAL TRUE VALUES TO MEASURED VALUES
102     DO  I=1,NN
                YR(I)=YM(I)
                ZR(I)=ZM(I)
        ENDDO

        DO  I=1,NK
                XR(I)=XM(I)
        ENDDO


        CALL FUNC(XR,YR,ZR,NN,LL,KK,NK,TC1,
        1TC2,PC1,PC2,ACCN1,ACCN2,RP1,RP2,GAMMA,C12,C21)


        TYPE*,'ENTER THE OUTPUT FILE NAME'
        READ(5,1)FILN10
        OPEN(UNIT=100,FILE=FILN10,STATUS='NEW')

        ABSDIFY=0.0
        ABSDIFP=0.0
        DO I=1,NN
                DIFFY(I)=(ZR(I)-ZM(I))*100/ZM(I)
                ABSDIFY=ABSDIFY +ABS(DIFFY(I))
                DIFFP(I)=(YR(I)-YM(I))*100/YM(I)
                ABSDIFP=ABSDIFP + ABS(DIFFP(I))
        ENDDO
                ABSDIFY=ABS(ABSDIFY)/NN
                ABSDIFP=ABS(ABSDIFP)/NN
        DO I=1,NN
        WRITE(100,2)XM(2*I-1),XM(2*I)
        WRITE(100,*)'  PMEAS.    PCALC.     DIFF P'
        WRITE(100,4)YM(I),YR(I),DIFFP(I)
        WRITE(100,*)'  YMEAS.    YCALC.     DIFF Y'
        WRITE(100,3)ZM(I),ZR(I),DIFFY(I)
        WRITE(100,*)'
2       FORMAT(' TEMPERATURE, LIQUID COMPOSITION',F10.2,F10.5)
3       FORMAT(3F10.5)
```

```
4       FORMAT(3F10.2)
        WRITE(100,*)'                                         '
        ENDDO

        WRITE(100,*)'COMPONENT 1 PROPERTIES, TC,PC,ACENTRIC FACTOR,
        1 POLAR PARAMETER'
        WRITE(100,*)TC1,PC1,ACCN1,RP1
        WRITE(100,*)'                                         '
        WRITE(100,*)'COMPONENT 2 PROPERTIES, TC,PC,ACENTRIC FACTOR,
        1 POLAR PARAMETER'
        WRITE(100,*)TC2,PC2,ACCN2,RP2
        WRITE(100,*)'                                         '
        WRITE(100,*)'ABSOLUTE DIFF IN PRESSURE',ABSDIFP
        WRITE(100,*)'ABSOLUTE DIFF IN Y',ABSDIFY
        WRITE(100,*)'INTERACTION PARAMETERS FOR PRAUSRULES'
        WRITE(100,*)'GAMMA',GAMMA,'C12',C12,'C21',C21

        TYPE*,'ENTER THE OUTPUT FILE NAME FOR PXY DATA'
        READ(5,1)FILN11
        OPEN(UNIT=110,FILE=FILN11,STATUS='NEW')
        DO I=1,NN
        WRITE(110,*)YR(I),XR(2*I),ZR(I)
        ENDDO
        WRITE(110,*)'COMPONENT 1 PROPERTIES, TC,PC,ACENTRIC FACTOR,
        1 POLAR PARAMETER'
        WRITE(110,*)TC1,PC1,ACCN1,RP1
        WRITE(110,*)'                                         '
        WRITE(110,*)'COMPONENT 2 PROPERTIES, TC,PC,ACENTRIC FACTOR,
        1 POLAR PARAMETER'
        WRITE(110,*)TC2,PC2,ACCN2,RP2
        WRITE(110,*)'                                         '
        WRITE(110,*)'INTERACTION PARAMETERS FOR PRAUSRULES'
        WRITE(110,*)'GAMMA',GAMMA,'C12',C12,'C21',C21

C       TYPE*,'ENTER THE OUTPUT FILE NAME FOR PY DATA'
C       READ(5,1)FILN3
C       OPEN(UNIT=30,FILE=FILN3,STATUS='NEW')
C       DO I=1,NN
C       WRITE(110,*)ZR(I),YM(I)
C       ENDDO

        STOP
        END

        SUBROUTINE FUNC(XR1,YR1,ZR1,NN1,LL1,KK1,NK1,TC1,
        1TC2,PC1,PC2,ACCN1,ACCN2,RP1,RP2,GAMMA,C12,C21)
```

```
      PARAMETER C=.45,R=8314.41
      IMPLICIT REAL*8 (A-H,M,P-Z)
      REAL*8 XR1(NK1),YR1(NN1),ZR1(NN1)

      DO 30 I=1,NN1
      TYPE*,'I',I
C     CALCULATE THE REDUCED TEMPERATURES
      XRT=XR1(2*I-1)
      TR1=XRT/TC1
      TR2=XRT/TC2
      POLD=YR1(I)
      XRX=XR1(2*I)
      ZRZ=ZR1(I)
      XR2=1-XRX
      IT=0

29    IT=IT+1

      ZR2=1-ZRZ

      CALL FUGC(XRT,XR2,XRX,ZRZ,ZR2,POLD,TC1,TC2,
     1PC1,PC2,ACCN1,ACCN2,RP1,RP2,FUGV1,FUGV2,FUGL1,FUGL2
     1,GAMMA,C12,C21)
      FR=XRX*FUGL1 - ZRZ*FUGV1
      GR=XR2*FUGL2 - ZR2*FUGV2

      IF(ZRZ.GT..90)THEN
      ZRZN=1-(FUGL2*XR2/FUGV2)
      PNEW=((POLD*FUGL1*XRX)/(FUGV1*ZRZN))*.05 + .95*POLD
      ELSE
      ZRZN=FUGL1*XRX/FUGV1
      PNEW=(POLD*FUGL2*XR2/(FUGV2*(1-ZRZN)))*.1 + .9*POLD
      ENDIF


      IF((ABS(FR).LT..00001.AND.ABS(GR).LT..00001).AND.(PNEW-POLD.LT.
     1 .001))THEN
      TYPE*,'FR,GR',FR,GR


1001  YR1(I)=PNEW
      ZR1(I)=ZRZN
      TYPE*,'PNEW',PNEW,'ZRZN',ZRZN
      GO TO 30
      ELSE
      POLD=PNEW
      ZRZ=ZRZN
```

```
      IF(IT.EQ.200)THEN
      TYPE*,'ITERATIONS GREATER THAN 200 FOR P,Y1',PNEW,ZRZ
      GO TO 1000
      ELSE
      GO TO 29
      ENDIF
      ENDIF

30    CONTINUE

1000  RETURN
      END


      SUBROUTINE FUGC(T,X2,X,Y,Y2,P,TC1,TC2,PC1,PC2,ACCN1,
     1ACCN2,RP1,RP2,FUGV1,FUGV2,FUGL1,FUGL2,GAMMA,C12,C21)
      PARAMETER CC=.45,R=8314.41
      IMPLICIT REAL*8 (A-H,M,P-Z)


C     THIS SUBROUTINE CALCULATES THE FUGACITIES IN THE LIQUID AND
C     VAPOR PHASES
C
C     CALCULATE SRK SMALL  B (SMB) AND A(TC) (ATC)
C     R IS THE GAS CONSTANT AND TC AND PC ARE THE CRITICAL PROPERTIES
C     ACCN IS THE ACENTRIC FACTOR FOR THE NONPOLAR COMPOUND


      SMB1=0.08664*R*TC1/PC1
      SMB2=0.08664*R*TC2/PC2
      ATC1=0.42747*R**2.*(TC1**2.)/PC1
      ATC2=0.42747*R**2.*(TC2**2.)/PC2
      TR1=T/TC1
      TR2=T/TC2
      M1=0.48 + 1.574*ACCN1 - 0.176*(ACCN1**2.)
      M2=0.48 + 1.574*ACCN2 - 0.176*(ACCN2**2.)

      ALPHAN1=(1.+M1*(1.-TR1**.5))**2
      ALPHAN2=(1.+M2*(1.-TR2**.5))**2

C     CALCULATE THE PARAMETER PART OF SMALL A

      PARA1=1.+RP1*EXP(-RP1**CC) - RP1*EXP(-(RP1*TC1
     1/T)**CC)
      PARA2=1.+RP2*EXP(-RP2**CC) - RP2*EXP(-(RP2*TC2
     1/T)**CC)
```

```
      SMA1=ATC1*ALPHAN1*PARA1
      SMA2=ATC2*ALPHAN2*PARA2

C     CALCULATE THE FUGACITY COEFFICIENT IN THE LIQUID PHASE (FUGL)

      SMAM=X**2*SMA1 + X2**2*SMA2 + 2*X*X2*(SMA1*SMA2)**.5*
     1(1-GAMMA)
      SMBM=SMB1*X +SMB2*X2
      SMCM=2*X*X2*(X*C12*ATC1**2 + X2*C21*ATC2**2)/(R*T)

C     CALCULATE CAPITAL A AND B AND C

      A=SMAM*P/(R**2*T**2)

      B=SMBM*P/(R*T)

      C=SMCM*P**2/(R*T)**3

C     CALCULATE COEFFICIENTS FOR QUARTIC SOLVER

      D=-1
      E=(A-B-B**2)
      F=-(A*B-C)
      G=-B*C

C     CALL QUARTIC SOLVER

      CALL VQUARTIC(B,D,E,F,G,ZL,1)

C     CALCULATE THE LIQUID PHASE FUGACITY COEFFICIENT (FUGL)

      FUGL1=DEXP( SMB1*P/(R*T*(ZL-B)) - SMB1*A/(SMBM*(ZL+B))
     1 - (C/X + 2*X*X2*C12*ATC1**2*P**2/(R*T)**4)/(ZL*B)
     1  + SMB1*C*(B+2*ZL)/(SMBM*B*ZL*(ZL+B))
     1 -DLOG(ZL-B)
     1 + DLOG(1+B/ZL)*(-(2*X*SMA1 + 2*X2*(SMA1*SMA2)**.5*(1-GAMMA))
     1/(SMBM*R*T) + (SMB1/SMBM)*(A/B - 2*C/B**2) + (C/(B**2*X)+
     1 2*X*X2*C12*ATC1**2/(SMBM**2*R**2*T**2))))

      FUGL2=DEXP(SMB2*P/(R*T*(ZL-B)) - SMB2*A/(SMBM*(ZL+B))
     1 - (C/X2 + 2*X*X2*C21*ATC2**2*P**2/(R*T)**4)/(ZL*B)
     1  + SMB2*C*(B+2*ZL)/(SMBM*B*ZL*(ZL+B))
     1 -DLOG(ZL-B)
```

```
     1 + DLOG(1+B/ZL)*(-(2*X2*SMA2 + 2*X*(SMA1*SMA2)**.5*(1-GAMMA))
     1/(SMBM*R*T) + (SMB2/SMBM)*(A/B - 2*C/B**2) + (C/(B**2*X2) +
     1 2*X*X2*C21*ATC2**2/(SMBM**2*R**2*T**2))))

C    FOR THE VAPOR PHASE

     SMAM=Y**2*SMA1 + Y2**2*SMA2 + 2*Y*Y2*(SMA1*SMA2)**.5*
     1(1-GAMMA)
     SMBM=SMB1*Y +SMB2*Y2
     SMCM=2*Y*Y2*(Y*C12*ATC1**2 + Y2*C21*ATC2**2)/(R*T)

C    CALCULATE CAPITAL A AND B

     A=SMAM*P/(R**2*T**2)

     B=SMBM*P/(R*T)

     C=SMCM*P**2/(R*T)**3

C    CALCULATE COEFFICIENTS FOR QUARTIC SOLVER

     D=-1
     E=(A-B-B**2)
     F=-(A*B -C)
     G=-B*C

     CALL VQUARTIC(B,D,E,F,G,ZV,-1)

C    NOW CALCULATE FUGACITY COEFFICIENT IN THE VAPOR PHASE (FUGV)

     FUGV1=DEXP(SMB1*P/(R*T*(ZV-B)) - SMB1*A/(SMBM*(ZV+B))
     1 - (C/Y + 2*Y*Y2*C12*ATC1**2*P**2/(R*T)**4)/(ZV*B)
     1  + SMB1*C*(B+2*ZV)/(SMBM*B*ZV*(ZV+B))
     1 -DLOG(ZV-B)
     1 + DLOG(1+B/ZV)*(-(2*Y*SMA1 + 2*Y2*(SMA1*SMA2)**.5*(1-GAMMA))
     1/(SMBM*R*T) + (SMB1/SMBM)*(A/B - 2*C/B**2) +
     1 C/(B**2*Y) +2*Y*Y2*C12*ATC1**2/(SMBM**2*(R*T)**2)))

     FUGV2=DEXP(SMB2*P/(R*T*(ZV-B)) - SMB2*A/(SMBM*(ZV+B))
     1 - (C/Y2 + 2*Y*Y2*C21*ATC2**2*P**2/(R*T)**4)/(ZV*B)
     1 + SMB2*C*(B+2*ZV)/(SMBM*B*ZV*(ZV+B))
     1 -DLOG(ZV-B)
     1 + DLOG(1+B/ZV)*(-(2*Y2*SMA2 + 2*Y*(SMA1*SMA2)**.5*(1-GAMMA))
     1/(SMBM*R*T) + (SMB2/SMBM)*(A/B - 2*C/B**2) +
```

```
      1 C/(B**2*Y2) + 2*Y*Y2*C21*ATC2**2/(SMBM**2*(R*T)**2)))

        RETURN
        END

C       QUARTIC SOLVER

        SUBROUTINE VQUARTIC(B,D,E,F,G,ZZ,ID)

        IMPLICIT REAL*8 (A-H,P-Z)
        REAL*8 Z(4)

C       CALL CUBIC SOLVER TO SOLVE THE RESOLVENT CUBIC EQUATION
C       Z**3 - E*Z**2 +(D*F - 4*G)*Z - D**2*G + 4*E*G - F**2=0

        DD=-E
        EE=(D*F - 4*G)
        FF=-D**2*G + 4*E*G - F**2

C       GET ANY REAL ROOT TO THE CUBIC EQUATION

        CALL VCUB(DD,EE,FF,V,-1)

C       CALCULATE R

        R=(D**2/4 - E + V)

        IF(ABS(R).LT..00000000001)THEN

        R=R**.5

        P=(3*D**2/4 - 2*E + 2*(V**2 - 4*G)**.5)

        Q=(3*D**2/4 - 2*E - 2*(V**2 - 4*G)**.5)

        IF(P.GT.0)THEN

                P=P**.5
                Z(1)=-D/4 + R/2 +P/2
                Z(2)=-D/4 + R/2 -P/2

        ELSE
```

```
        Z(1)=-1
        Z(2)=-1

ENDIF

IF(Q.GT.0)THEN

        Q=Q**.5
        Z(3)=-D/4 - R/2 +Q/2
        Z(4)=-D/4 - R/2 - Q/2

ELSE

        Z(3)=-1
        Z(4)=-1
ENDIF

ELSE

R=R**.5

P=(3*D**2/4 - R**2 - 2*E + (4*D*E - 8*F - D**3)/(R*4))

Q=(3*D**2/4 - R**2 - 2*E - (4*D*E - 8*F - D**3)/(R*4))

IF(P.GT.0)THEN

        P=P**.5
        Z(1)=-D/4 + R/2 +P/2
        Z(2)=-D/4 + R/2 -P/2

ELSE

        Z(1)=-1
        Z(2)=-1

ENDIF

IF(Q.GT.0)THEN

        Q=Q**.5
        Z(3)=-D/4 - R/2 +Q/2
        Z(4)=-D/4 - R/2 - Q/2

ELSE

        Z(3)=-1
        Z(4)=-1
```

```
      ENDIF

      ENDIF

      DO I=1,4
      IF(ID.EQ.1.AND.Z(I).LT.B)Z(I)=99999999
      ENDDO

      IF(ID.EQ.1)THEN
      ZZ=DMIN1(Z(1),Z(2),Z(3),Z(4))
      ELSE
      ZZ=DMAX1(Z(1),Z(2),Z(3),Z(4))
      ENDIF

      RETURN
      END

      SUBROUTINE VCUB(D,E,F,Z,ID)
C     SUBPROGRAM FOR SOLVING A CUBIC EQUATION OF THE FORM:
C     Z**3 +D*Z**2+ E*Z + F=0.0
C     WHERE D,E, AND F ARE CONSTANTS
      IMPLICIT REAL*8(A-H,P-Z)
      G=(3.*E-D*D)/3.
      H=-(9.*D*E-27.*F-2*D*D*D)/27.

      IF((G**3)/27. +H*H/4..LE.0.)GO TO 10
      S=-H/2. + DSQRT(G**3/27. + H*H/4.)
      TT=-H/2. - DSQRT(G**3/27. + H*H/4.)
      IF(S)5,6,6
5     S=-((-S)**(1./3.))
      GO TO 7
6     S=S**(1./3.)
7     IF(TT)8,9,9
8     TT=-(-TT)**(1./3.)
      GO TO 15
9     TT=(TT)**(1./3.)
C     SINGLE REAL ROOT
15    Z=S+TT-D/3.
      GO TO 40
C     THERE ARE THREE ROOTS.
10    THETA=(DACOS(-.5*H/DSQRT(-G**3/27.)))/3.
      Z1=2.*DSQRT(-G/3.)*DCOS(THETA)
      Z2=2.*DSQRT(-G/3.)*DCOS(THETA+(2./3.)*3.141592654)
      Z3=2.*DSQRT(-G/3.)*DCOS(THETA+ (4./3.)*3.141592654)
C     DECIDING WHICH TO CHOOSE
      IF(ID)20,30,30
```

```
C       TAKE LARGEST ROOT FOR VAPOR VOLUME.
20      Z=DMAX1(Z1,Z2,Z3)-D/3.
        GO TO 40
C       TAKE SMALLEST ROOT FOR LIQUID VOLUME.
30      Z=DMIN1(Z1,Z2,Z3)-D/3.
        IF(Z.LT.0)Z=.000001
        DO 31 I=1,20
        ZN=Z-(Z**3+D*Z**2+E*Z+F)/(3.*Z**2+2.*Z*D+E)
        IF(ABS((ZN-Z)/Z).LT..00001)GO TO 40
31      Z=ZN
40      RETURN
        END
```

APPENDIX D

NOMENCLATURE

NOMENCLATURE

For Phase Equilibria

P = pressure

P_c = critical pressure

P_i^s = vapor pressure of component i

R = gas constant

R_p = polar parameter as described by Yesavage (1986)

T = temperature

T_c = critical temperature

T_r = reduced temperature, T/T_c

a = attractive term of the EOS

a_i = attractive term of the EOS for component i

b = repulsive term of the EOS

b_i = replusive term of the EOS for component i

f_i^l = fugacity of component i in the liquid phase

f_i^v = fugacity of component i in the vapor phase

k_{ij} = interaction parameter

v = volume

x_i = liquid composition of component i

y_i = vapor composition of component i

ϕ_i^l = liquid phase fugacity coefficient of component i

ϕ_i^v = fugacity coefficient of component i in the vapor phase

γ_i = activity coefficient of component i

γ_i^∞ = infinite dilution activity coefficient

ω = acentric factor

ω_n = acentric factor for the non-polar homomorph

For Maximum Likelihood Method

X = vector consisting of the independent variables

Y = vector consisting of one of the dependent variables

Z = vector consisting of one of the dependent variables

Θ = vector of parameters

γ = matrix of the variances for vector X

λ = diagonal matrix of variances for vector Y

δ = diagonal matrix of variances for vector Z

σ = variance of the experimental measurement

ν = degreee of freedom, N-L

α_{ij} = confidence level of model i compared to model j